The Dissertation Committee for Srijith Balakrishnan
certifies that this is the approved version of the following dissertation:

METHODS FOR RISK AND RESILIENCE EVALUATION IN INTERDEPENDENT INFRASTRUCTURE NETWORKS

Committee:

Zhanmin Zhang, Supervisor

Randy Machemehl

Stephen Boyles

Lu Gao

METHODS FOR RISK AND RESILIENCE EVALUATION IN INTERDEPENDENT INFRASTRUCTURE NETWORKS

by

Srijith Balakrishnan

DISSERTATION

Presented to the Faculty of the Graduate School of

The University of Texas at Austin

in Partial Fulfillment

of the Requirements

for the Degree of

DOCTOR OF PHILOSOPHY

THE UNIVERSITY OF TEXAS AT AUSTIN

August 2020

In the memory of my father.

"By failing to prepare, you are preparing to fail."

–Benjamin Franklin

Acknowledgments

This dissertation has enormously benefited from the support, patience, and guidance of the following individuals without which this dissertation would not have come to its fruition. I am deeply indebted to them.

I would like to start by extending my deepest gratitude to my supervisor Prof. Zhanmin Zhang for his relentless and thorough support throughout my doctoral research. Prof. Zhang provided me complete freedom in my research and has been a wonderful mentor whenever I needed help. I would like to express my sincere appreciation to my doctoral committee members–Prof. Randy Machamehl, Prof. Stephen Boyles, and Prof. Lu Gao–for their insightful comments and suggestions towards my doctoral research. Prof. Boyles has been also a great friend and trainer. I am extremely grateful to Dr. Michael R. Murphy of the Center of Transportation Research at The University of Texas at Austin who employed me throughout my doctoral research and provided valuable and detailed insights on my research. He has been always a great listener and I have learned a lot about leadership from him.

My strongest supporters during my Ph.D. have been my parents and my brother. Even while battling cancer, my father encouraged me to continue my research and never allowed my studies to be affected by his hardships.

My friends– Praveen Vayalamkuzhi, Srinath Mahesh, Kyle Bathgate, and

Trinh Hoang– provided extremely helpful comments and insights on my dissertation and several of my journal articles.

I would like to acknowledge the graduate coordinators of the civil engineering department– Caitlan Leigh Zilligen, Lisa Macias, Velma Vela, and Kathryn McWilliams– for their prompt assistance to resolve several administrative issues I encountered in the last four years.

I will always cherish the wonderful company, support, and encouragement of my friends in transportation engineering division– Stefanos Politis, Gopindra Sivakumar Nair, John Collier, Murthy Krishna Gurumurthy, Natalia Zuniga Garcia, Cesar Yahia, Oscar Daniel Galvis Arce, Mohammed Al-Amin, Jingran Sun, Yang Xu, Antonio Perez, Priyadarshan, Carlin Liao, Aditya Karanam, Taehoon Lim, Pragun Vinayak, Vineeth Dharmapalan, and Zhe Han, among others. I am grateful to ITE/ITS/WTS student chapters for providing opportunities to get involved in various social and technical events within transportation engineering.

I would also like to mention a few names outside the Civil Engineering department who made Austin a home away from home– Vaidyanathan Sethuraman, Arjun Anand, Rituparna Samanta, Ashwin Harikumar, Kiran Venugopal, Bharathwaj Sankaran, Kurian Abraham, Mahesh Srinivasan, Harish Potti, Soumik Das, and Arathi Issac.

I am extremely grateful to my master's thesis supervisor at the Indian Institute of Technology Madras– Prof. R. Sivanandan– for being an amazing mentor even today.

Several friends from my high school and college– Jithin Kudiyirikal, Nideesh Nirmal, Sanjay Radhakrishnan, Sheetal Patil Barge, Sonu Mathew, Juby Joy, Sruthi Gopal, and Vinaya Prakash – have been very supportive and encouraging.

Finally, I thank the Almighty for reinforcing my belief in myself whenever there were roadblocks in my research.

METHODS FOR RISK AND RESILIENCE EVALUATION IN INTERDEPENDENT INFRASTRUCTURE NETWORKS

Srijith Balakrishnan, Ph.D.
The University of Texas at Austin, 2020

Supervisor: Zhanmin Zhang

Urban infrastructure plays a key role in the structure and dynamics of every city. Besides ensuring the sustainability of communities and businesses, high-quality infrastructure services are crucial for generating jobs and attracting capital investments. Modern infrastructure systems are highly interconnected to enhance efficiency and safety of operations; however, the interconnections increase the risks of cascading failures during extreme events, such as natural disasters, acts of terrorism, and pandemics. Not only are the normal operations interrupted during such events, but prolonged operational disruptions in infrastructure services also have debilitating effects on emergency response and economic recovery in affected regions. With the emergence of new threats and intensifying climate change, the resilience of infrastructure systems has become a necessity rather than a choice for our cities.

As with any resource allocation problem, potential resilience investments require identifying priorities and evaluating project alternatives. Appropriate resilience indicators can be used to rank and prioritize infrastructure components and

systems as well as to evaluate the efficacy of resilience interventions. The dissertation proposes five indicator-based methodological frameworks to assist decision-makers in analyzing the intrinsic risks and resilience in large-scale interdependent infrastructure networks.

For generic interdependent networks, an agent-based simulation approach is adopted. In this approach, the interdependent network is modeled as a weighted bi-directed network where nodes represent infrastructure components and links denote the interconnections. For evaluating the risks of cascading failures and the network's resilience, a hybrid risk measure based on the well-known Inoperability Input-Output Model (IIM) using expert judgments is developed. In the process, to handle the issue of epistemic uncertainty associated with subjective infrastructure dependency data, a method based on possibility theory is also proposed. Later, the hybrid risk measure is extended to develop two resilience indexes for quantifying the criticality and susceptibility of infrastructure components and ranking algorithms are presented. In addition, the hybrid risk measure is combined with socio-economic characteristics obtained from census data to develop a priority index to quantify the risks of cascading failures in various urban communities.

With regard to infrastructure-specific networks, the dissertation developed infrastructure ranking and prioritization methods for two distinct transportation systems, specifically road networks, and marine port systems, based on empirical disaster data. For characterizing the resilience of road networks, the dissertation proposed three indicators based on the concepts of resilience triangle and extreme travel time observations. The dissertation combined time series decom-

position techniques with anomaly detection algorithms to segregate disaster effects from normal traffic patterns. For characterizing the risks of natural hazards to port systems, the dissertation employed disaster impact data along with international trade data and identified the ports with the highest risks.

Table of Contents

List of Tables

List of Figures

Chapter 1

Introduction

Cities, since their inception, have been exposed to various external shocks and stresses, such as natural disasters, military invasions, and pandemics. Such events not only resulted in the loss of life but also led to serious consequences on the socio-economic fronts. Over the centuries, many cities learned from past adversities and developed various strategies to minimize the traditional disaster risks on the communities, physical infrastructure, economic systems, and environment. However, the scope of threats and hazards that cities face today are more severe and have far-reaching consequences than before. Emerging threats, such as cyber-attacks and climate crisis, are some prominent additions to the list of potential hazards that every city should be prepared for in the 21st century (Shackelford, 2015; White, George, Boult, & Chow, 2016). Furthermore, the impacts of disasters are compounded by changes in the built environment and the fast-paced urbanization (Chmutina, Ganor, & Bosher, 2014). This is particularly true in low- and middle-income countries, where cities witness rapid urbanization due to migration of people from rural areas in search of better living conditions and job opportunities (Wang, Lin, Glendinning, & Xu, 2018).

Paradoxically, the cities in the low- and middle-income countries are more

vulnerable to disasters, and the consequences are disproportionately high among vulnerable populations in those countries (The World Bank, 2009). Nevertheless, the intensifying climate crisis and other emerging threats are global concerns and every country needs to be prepared to withstand such extreme events. The resilience of infrastructure systems is particularly important because of their enormous role in the evolution of urban dynamics in cities. As infrastructure systems become more interdependent, the infrastructure disruptions will become more expensive (Brown, Beyeler, & Barton, 2004; Rinaldi, Peerenboom, & Kelly, 2001). Therefore, immediate realignment of development goals and incorporation of resilience criteria in the current infrastructure management practices and urban development frameworks are necessary for enabling cities to prepare for future extreme events.

1.1 Research Background

1.1.1 The role of cities in the 21st century

The industrial revolution, which started in Europe in the 18th century and later spread to other parts of the world, marked the beginning of urbanization. As a result, traditional economies based on primary activities, such as agriculture, forestry, and mining, paved the way for industrial production followed by services (Satterthwaite, McGranahan, & Tacoli, 2010). This led to a sizable fraction of rural populations migrating to cities in search of better jobs. As of 2018, 55% of the global population (4.2 billion) lives in urban areas and this number is expected to reach 68% (6.7 billion) by 2050 (Figure 1.1).

Urbanization is considered to be an essential stage in the transformation of

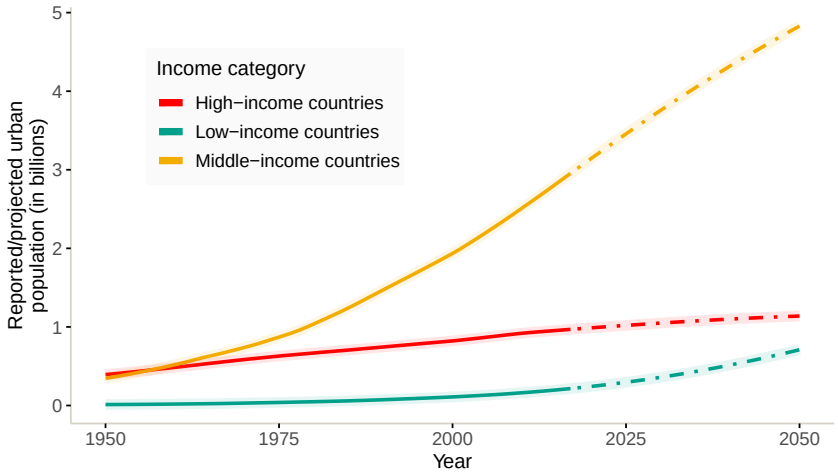

Figure 1.1: World urban population growth projections (Data from Ritchie and Rose (2018))

the national economy of every country. It is proven that a higher percentage of urbanization is associated with higher per capita income (pci) of countries (Henderson, 2010). Cities continue to develop new capital markets, incentivize new economic activities, and generate high-quality jobs. As a result, today, cities generate 80% of the world's Gross Domestic Product (GDP).

In addition to job creation, cities have themselves transformed into hubs for technology innovation and laboratories for urban experiments. The emergence of cities has not only catered to the interests of the urban population but also facilitated the linkages between the rural economies and international markets. The continued efforts to maintain and upgrade public infrastructure, impart universal healthcare and education, and reform legal and governance systems have further accelerated the growth of cities and have become a blueprint for emerging urban areas to follow.

1.1.2 Infrastructure and cities

Among various urban systems, infrastructure services have the most definitive impact on the evolution of cities. Proper planning and design of infrastructure services, such as transportation, telecommunications, water and sanitation, energy, and healthcare, determine the future form, structure, and dynamics of cities (Camagni, Gibelli, & Rigamonti, 2002; Chandra & Thompson, 2000). In the literature, terms such as infrastructure systems, critical infrastructures, lifelines, etc. are quite common, and used interchangeably to denote the most vital infrastructure systems for day-to-day functions in the urban regions. Chang (2016) defined infrastructure systems as the set of "assets, networks, and systems in the built environment that provide essential services for social and economic activities." Infrastructure systems are highly interconnected. The interconnections are known as interdependencies, which refer to the flow of services and goods within the urban infrastructure network. It is because of interconnections that the smooth functioning of each of the critical infrastructure systems, and dependent communities and other infrastructure systems are facilitated.

Infrastructure systems, such as highways, are crucial for every economic activity in cities. Infrastructure systems form the lifelines of cities (O'Rourke, 2007) around which all the other urban systems, including economies and communities, are built on. Urban land use development and economic activities are heavily reliant on access to essential infrastructure services. For this reason, urban planners and policymakers have always used infrastructure development as a catalyst to attract more private sector investments (Y. Song, 2012). In addition to fostering economic

growth, equitable spending on urban infrastructure in cities could also contribute to the social progress of underprivileged communities, manage population growth, and reduce poverty (Cui & Sun, 2019; Guild, 2000). Social infrastructure such as healthcare, education, and law enforcement improve livability in urban neighborhoods and can bring inclusive development in the long-term.

While urban infrastructure can cater to the development goals of cities, it is also true that their poor design and management can worsen urban issues. Urban infrastructure systems, once built, may be too rigid for redevelopment in the future, especially because each of the systems is intertwined with others. This has been one of the pressing issues faced by developing countries where inadequate and obsolete infrastructure systems have resulted in a variety of urban woes, including traffic congestion, poor air quality, and the creation of slums. Efforts for a complete overhaul of urban infrastructure in such countries are often met with political, legal, and financial obstructions.

1.1.3 Infrastructure resilience: A necessity rather than a choice

The increasing relevance and inevitability of infrastructure services in cities also comes with a cost. While investing in infrastructure is a widely accepted solution to tackle urban issues, the possibility of unanticipated disruptions caused by extreme events, such as hurricanes, earthquakes, and floods, was not given adequate importance until recently. Physical damages and operational disruptions to infrastructure systems caused by extreme events cost billions of dollars and resulted in significant loss of life (Ritchie & Roser, 2014; Smith & Katz, 2013). Figure 1.2

presents the year-wise global deaths and direct economic loss due to natural disasters between 1990 and 2017.

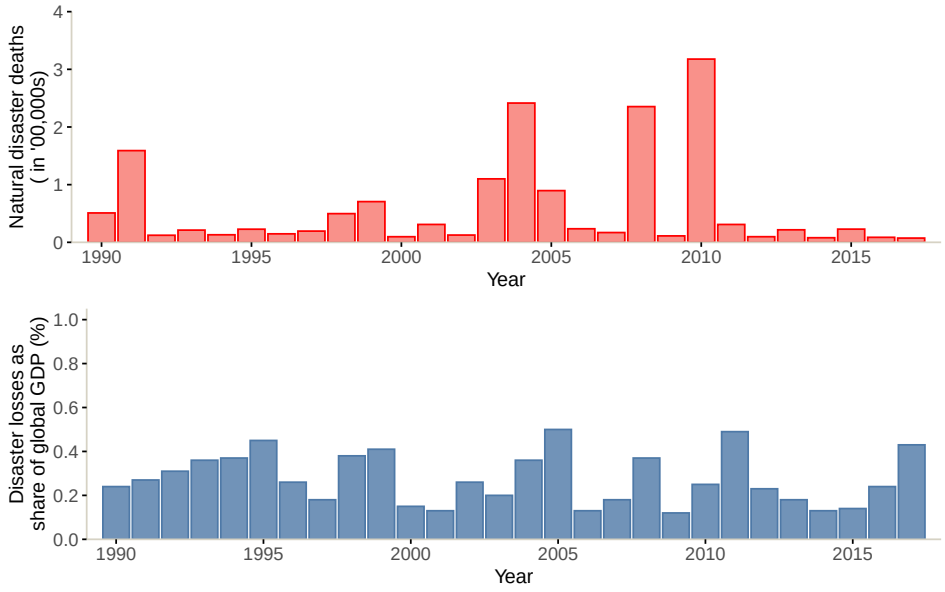

Figure 1.2: Global deaths and economic impacts from natural disasters (Data from Ritchie and Roser (2014))

In addition to the direct losses, failure of a system could further trigger the failure of dependent systems due to the networked structure of urban infrastructure systems, and consequently cause widespread disruptions in public utility services. The economic, social, health, and environmental consequences of infrastructure failures (Table 1.1) resulting from extreme events are not limited to the area directly affected. Rather, the consequences often scale up to the communities and economic sectors that are not at direct exposure to such events (Ouyang, 2014). For instance, the 2003 Northeast Blackout occurred due to the breakdown of a few high voltage transmission lines in Cleveland-Akron area and subsequent failure of alarm systems

Table 1.1: Indirect/cascading effects of infrastructure failures and disruptions (Chang, 2016)

Category	Impacts of infrastructure disruptions
Economic	• Revenue loss for infrastructure agencies due to downtime • Reduction in productivity or complete closure of dependent infrastructure sectors and businesses • Additional expenses for restoration of failed infrastructure systems
Social	• Mass evacuation or migration • Rise in violence • Food insecurity • Political instability • Reduced efficiency of emergency response and mitigation
Health	• Potential fatalities and inuries from physical failure of infrastructures • Technological disasters such as fire events and chemical accidents • Pollution of natural resources • Epidemics/pandemics and helath hazards due to deteriorated essential services
Environmental	• Contamination of natural resources and pollution • Destabilization of ecological systems

to detect the incident, leading to overburdening of other parallel power lines and resulting in a cascade of failures in southeastern Canada and eight northeastern states in the United States. The blackout affected 50 million consumers, led to at least 11 deaths, and incurred an overall economic cost of $6.4 billion (Minkel, 2008). A more recent example of the interdependent effects of disasters is the ongoing global slowdown caused by the Novel Coronavirus (COVID-19). The pandemic not only incapacitated healthcare infrastructure systems but also disrupted a large share of global and regional supply chains. The economic cost of the pandemic to the global economy is estimated to be in the order of trillions of dollars (Nicola et al., 2020).

The potential threats to infrastructure systems have also diversified over the years. Though the initial discussions on infrastructure resilience were focused on

natural disasters such as earthquakes (Bruneau et al., 2003), later, its scope was extended to a broad range of other hazard categories including terrorist attacks (Apostolakis & Lemon, 2005; Boin & Smith, 2006), cyber-attacks (Cardenas et al., 2009), climate change (Linnenluecke, Griffiths, & Winn, 2012; Panteli & Mancarella, 2017), and natechs (natural disaster-induced technological disasters) (Cruz, Kajitani, & Tatano, 2015). Aging infrastructure and increasing demand for infrastructure services due to urbanization will also accentuate the impacts of disasters.

Historically, the strategy to reduce the impacts of disasters on infrastructure systems was to enhance physical protection and asset hardening (or in other words, improve system robustness) (Turnquist & Vugrin, 2013; Vugrin, Warren, & Ehlen, 2011); however, the emergence of new and more intense hazards and threats compelled policy-makers to think beyond the physical strength of infrastructure systems. The shift from infrastructure robustness to infrastructure resilience was also fueled by the scale of societal and economic costs of indirect effects of infrastructure disruptions. Today, infrastructure resilience is viewed as a collective term for all system qualities, which may be either intrinsic to the system or could be enhanced through proper interventions, that enable systems to absorb unexpected shocks, speed up recovery, and adapt to minimize impacts from future shocks.

The concept of infrastructure resilience is heavily influenced by the concept of ecological resilience introduced by Holling (1973). In his seminal paper, Holling defined resilience as the ability of ecological populations to absorb external shocks and still exist. Holling suggested that the persistence of relationships in an affected ecological system was more important than the consistency of its behavior. This

is particularly true in the case of interdependent infrastructure systems where each component function is significantly dependent on the operations of other components.

The formal definition of infrastructure system resilience was introduced by Bruneau et al. (2003) which is stated as "the ability of a system to reduce the chances of a shock, to absorb a shock if it occurs and to recover quickly after a shock". Since then, several studies attempted to define infrastructure resilience and its characteristics. Table 1.2 presents some of the prominent definitions found in the literature. These definitions, though tailored to address specific resilience objectives, have two common elements – ability to absorb external shocks, and to respond and recover rapidly, while adapting to emerging external conditions is also cited many times in the wake of climate crisis concerns.

Table 1.2: Definitions of infrastructure resilience

Study	Infrastructure resilience definition
Y. Y. Haimes (2009)	"the ability of the system to withstand a major disruption within acceptable degradation parameters and to recover within an acceptable time and composite costs and risks."
National Infrastructure Advisory Council (2010)	"ability to reduce the magnitude and/or duration of disruptive events."
Vugrin et al. (2011)	"ability to efficiently reduce both the magnitude and duration of the deviation from targeted system performance levels."
The White House (2013)	"the ability of infrastructure systems or components to endure potential external shocks, and to recover quickly and adapt to changing external conditions."
Alderson, Brown, and Carlyle (2015)	"the ability of a system to adapt its behavior to maintain continuity of function (or operations) in the presence of disruptions"

The concept of infrastructure resilience has been there in existence since

the 1850s. However, it was only in the aftermath of September 11, 2001, World Trade Center Attacks that infrastructure resilience received enhanced attention from policy-makers, governments, and the private sector (National Infrastructure Advisory Council, 2010). There was a paradigm shift from robustness (ability to absorb shocks) to other characteristics of infrastructure systems that influence their disaster response and quick recovery. Furthermore, the new emphasis was not restricted to the resilience of individual systems but was extended to minimize the aggregate impacts on interdependent infrastructure networks spanning larger geographical and administrative regions.

The research on infrastructure resilience received a further boost with the President's Policy Directive 21 (The White House, 2013) which identified 16 major infrastructure sectors that are critical to the economy and security of the United States. Today, efforts are in place for improving individual infrastructure resilience due to the advancements in communication, control, and sensing technologies. On the other hand, the increased dependence of infrastructure systems on others for their operations has led to more uncertainty over the impacts of known disasters and emerging threats. Therefore, identifying such extreme events and evaluating the network-wide vulnerabilities and capabilities are essential to adopt measures that would help cities to contain the consequences of infrastructure failures and minimize the network-wide effects through resilience measures, such as inbuilt system redundancies and temporary supply mechanisms. Given the emergence of new threats and how extreme events could impair urban dynamics, it is highly imperative for both public and private sectors to incorporate resilience criteria in infrastructure-

related decision-making. Advocating for investing in infrastructure resilience, a recent study by the World Bank and the Global Facility for Disaster Reduction and Recovery (GFDRR) estimated a net benefit of $4.2 trillion with $4 in returns for every $1 spent on resilient infrastructure in disaster-prone regions (Hallegatte, Rentschler, & Rozenberg, 2019).

1.1.4 Managing infrastructure risks and the need for resilience indicators

The broad objective of resilience interventions in infrastructure systems is to reduce the overall risks (both direct and indirect) from unanticipated events (Y. Y. Haimes, 2009; Zio, 2016). Therefore, assessing the effectiveness of resilience interventions is determined by the reduction in disaster risks to the infrastructure systems. Most of the frameworks for assessing resilience in infrastructure systems are based on the well-known relationship connecting hazard[1], exposure[2], vulnerability[3], and risk[4], as shown in Figure 1.3.

The risk is considered a function of hazard intensity, exposure of system components to the hazard, and intrinsic vulnerabilities associated with system com-

[1]Hazard is defined as a process, phenomenon, or human activity that may cause loss of life, injury or other health impacts, property damage, social and economic disruption or environmental degradation UNISDR (2015)

[2]The situation of people, infrastructure, housing, production capacities and other tangible human assets located in hazard-prone areas UNISDR (2015)

[3]The conditions determined by physical, social, economic, and environmental factors or processes which increase the susceptibility of an individual, a community, assets or systems to the impacts of hazards UNISDR (2015)

[4]The potential loss of life, injury, or destroyed or damaged assets which could occur to a system, society, or a community in a specific period of time, determined probabilistically as a function of hazard, exposure, vulnerability and capacity UNISDR (2015)

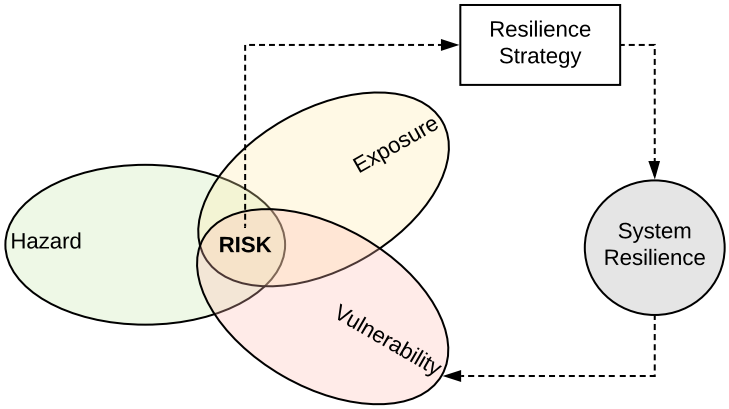

Figure 1.3: Relationship among hazard, exposure, vulnerability and system resilience (adapted from Cardona et al. (2012))

ponents. The vulnerabilities are determined by the resilience capabilities of the system. The resilience of a system improves with the adoption of strategies that reduce the system component vulnerabilities and thereby the hazard risks to the infrastructure systems. Thus, resilience enhancement is a continuous and incremental process. Resilience assessments help infrastructure agencies to identify and prioritize critical or weak components, evaluate the progress of the adopted resilience measures, and fine-tune them to achieve desired resilience in the system.

Quantification of the resilience of an infrastructure system is a crucial stage in every resilience assessment framework. Resilience quantification methods consist of three steps:

1. Definition of resilience properties of infrastructure systems and networks.

2. Modeling the cascading/interdependent effects of infrastructure failures.

3. Quantification of infrastructure resilience using appropriate metrics or indicators.

Defining and characterizing the resilience properties of a system can be helpful in systematic investigation and quantification of the infrastructure resilience. Among the several classifications of resilience properties, the 4 R's framework (robustness, redundancy, resourcefulness, and rapidity) (Bruneau et al., 2003) and the three-pillar framework (absorptive capacity, adaptive capacity, and restorative capacity) (Vugrin et al., 2011) are most commonly adopted.

The 4 R's framework, proposed suggested that infrastructure resilience can be represented using the following four dimensions (properties), namely, robustness (ability to endure a given level of stress, shock or demand without consequences on its level of functioning), redundancy (ability to satisfy its functional requirements and achieve stated goals by substituting its elements of the system itself in the event of a disruption, degradation or loss of functionality), resourcefulness (ability to recognize failures, prioritize restoration activities, and mobilize resources during conditions that threaten to disrupt the functions of the system), and rapidity (capacity to recognize problems and mobilize resources to contain and avoid further losses due to external stress promptly).

In the three-pillar framework, the resilience properties are classified into absorptive capacity (ability to absorb impacts of system shocks and minimize consequences), adaptive capacity (ability to self-organize for recovery and minimize future risks from similar disasters), and restorative capacity (ability to be repaired

or restored easily).

Once the resilience capabilities and capacities of individual infrastructure components/systems are identified and modeled, the next step in the evaluation of network resilience is to model the consequences of infrastructure disruptions on the whole network. This is a challenging task due to the presence of a wide range of interdependencies among infrastructure systems. The presence of interdependencies makes an infrastructure network a complex "system of systems" (Eusgeld, Nan, & Dietz, 2011; Mostafavi, 2018). For the convenience of modeling, Rinaldi et al. (2001) categorized the infrastructure interdependencies into four categories: physical-, geographic-, cyber-, and logical interdependencies. Ouyang (2014) identified and classified infrastructure network models into five broad categories, namely empirical-, system dynamics based-, agent based-, economic theory based-, and network-based approaches. A detailed review of the above methods can be found in Section 2.2.1 of Chapter 2.

In the next step, the resilience of the individual infrastructure system and the network can be quantified. The concept of resilience triangle is widely used for resilience quantification. The concept of the 'resilience triangle" was first introduced by Bruneau et al. (2003) to quantify the resilience of social and infrastructure systems against earthquakes. Figure 1.4 presents the concept of the resilience triangle and relates it to the four properties of resilient systems as described in the 4 R's framework.

Suppose $Q(t)$ is the performance measure which reflects the extent to which a given objective is fulfilled by the infrastructure node over time and an external

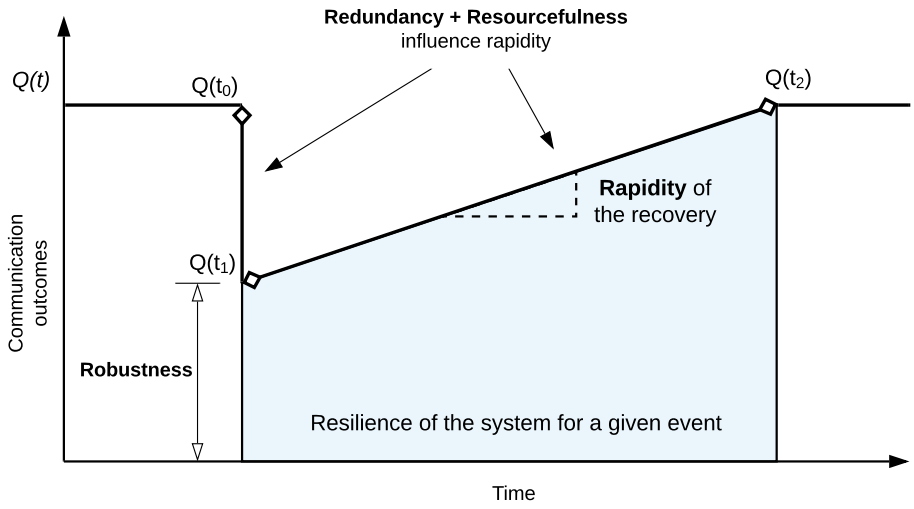

Figure 1.4: Resilience triangle for communication systems and its relationship to the four dimensions of system resilience based on Bruneau et al. (2003) and illustrated by Franz et al. (2018)

shock occurs at t_0. As a result, the performance measure of the infrastructure system drops and reaches a stable performance level, $Q(t_j)$. Due to restoration and recovery efforts after the event, the system performance slowly attains its original performance level at t_2. This is the most generalized model for a system's performance during a disaster. Bruneau et al. (2003) defined the area loss of resilience of the system (assuming that the initial performance level is 100) as shown in Equation 1.1.

$$R = \int_{t_0}^{t_2} (Q(t_0) - Q(t)dt) \tag{1.1}$$

On the contrary, the resilience of the system can be obtained as the area under the curve (Cimellaro, Tinebra, Renschler, & Fragiadakis, 2016). The significance of this framework is that it is simple, intuitive and defines the relationship to

the 4 R's (as illustrated in Figure 1.4). Many modifications for resilience quantification using the resilience triangle has happened over the years to address various technical issues with it, such as its incapability to distinguish fast and slow recovery processes (Bocchini & Frangopol, 2012) and incapability to distinguish between various time scales (Frangopol & Bocchini, 2011).

The quantification of infrastructure risks and resilience requires suitable metrics and indicators. The metrics and indicators quantitatively measure the direct (physical and operational) and indirect effects (interdependent, societal, and economic) of infrastructure disruptions. Appropriate resilience indicators can not only be used for ranking and prioritization of infrastructure components but also be effectively used for measuring and evaluating the resilience of infrastructure systems (Henry & Emmanuel Ramirez-Marquez, 2012; Nan & Sansavini, 2017; K. Zhao, Kumar, Harrison, & Yen, 2011). The resilience indicators also help in monitoring the trends in infrastructure networks, such as the intensity of extreme events and common failure causes, and for validating the resilience compliance of infrastructure systems and networks with standards and regulations (European Network and Information Security Agency, 2010). Figure 1.5 illustrates the role of resilience indicators in resilience-related decision making. The resilience indicators can be broadly classified into three, namely, graph-based indicators, performance-based indicators, and hybrid indicators. A detailed discussion of the various resilience indicators used in the literature is provided in Section 3.2 in Chapter 3.

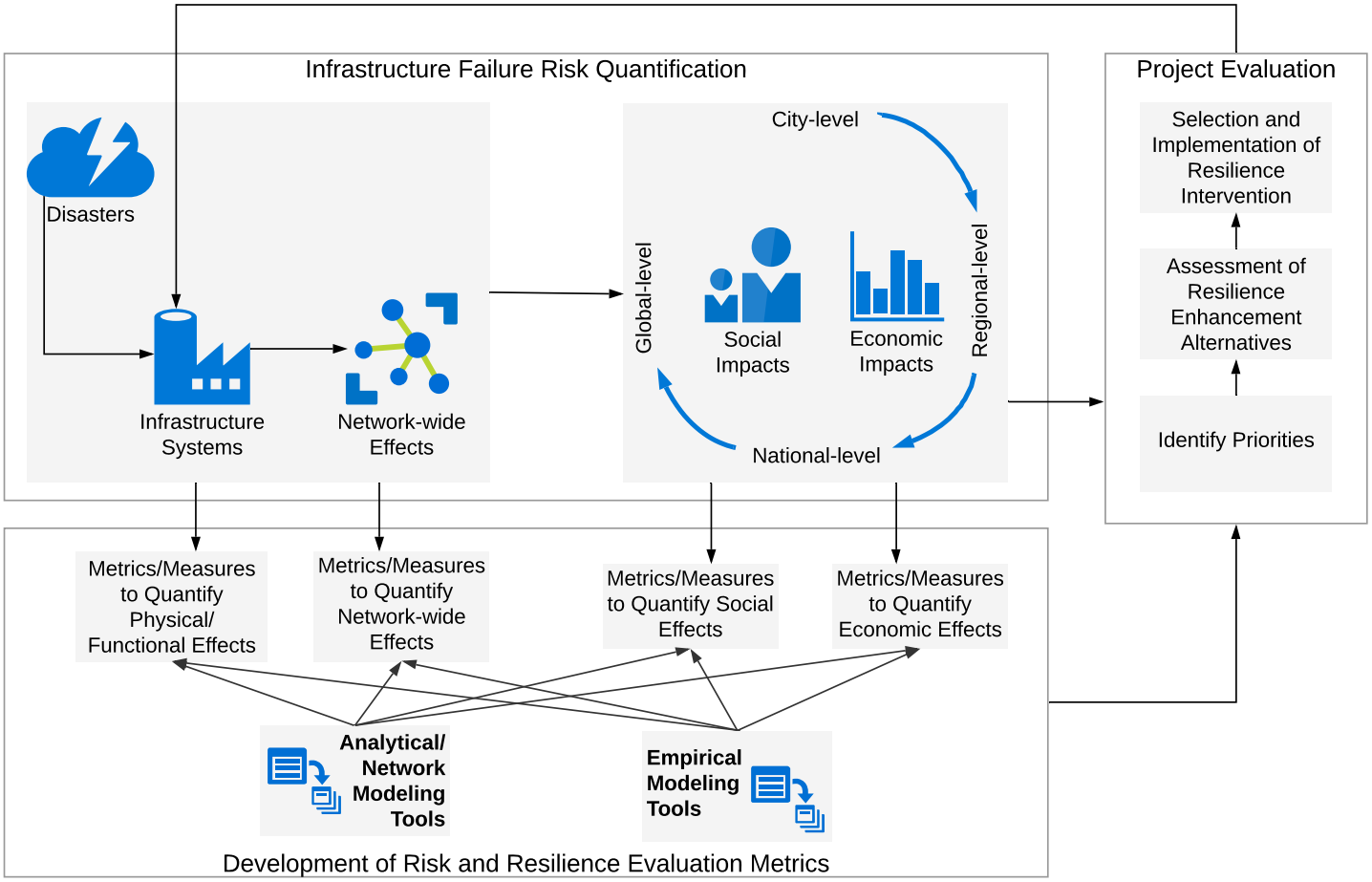

Figure 1.5: Framework for Enhancing Resilience in Interdependent Infrastructure Networks

1.2 Problem Statement

Infrastructure-related resilience investments are dependent on budgetary constraints like any other resource allocation problem. Common optimization methods for enhancing resilience could be computationally expensive or insufficient due to the presence of complex interdependencies in the network. Furthermore, the unique operational characteristics of the component systems also contribute to the complexity. A more actionable approach is to prioritize the infrastructure components for implementing resilience enhancement programs so that the desired level of network resilience can be achieved under the given constraints. However, the concept of network-level resilience with regard to infrastructure systems is still not clear. While resilience metrics specific to certain infrastructure systems have been developed in the past, the development of indicators for estimating risks and measuring resilience in large-scale interdependent infrastructure networks remains a sparsely researched domain.

Developing effective indicators and metrics for evaluating risks and resilience in interdependent infrastructure networks require addressing several challenges with regard to modeling cascading or interdependent effects of infrastructure failures. Some of the pertinent issues are presented below.

- Urban infrastructure systems are increasingly becoming interdependent for improving their performance, operational efficiency, and safety. The interdependencies among infrastructure systems could be physical, cyber, geographical, or logical in nature. The increasing number of such interdependencies

make modeling cascading or interdependent effects of infrastructure system more complex.

- Urban infrastructure systems vary considerably in their physical, functional, and organizational characteristics. Mathematical representation of some of the characteristics that influence infrastructure risks and resilience is difficult.

- Level of technology adoption for sensing and control of infrastructure varies across infrastructure systems within a single urban network. Therefore, a modeling approach that may be suitable for one infrastructure system may not be appropriate for another.

- Even in most developed countries, there is a lack of coordination among various infrastructure agencies within a geographical region. Sharing of quantitative data related to infrastructure operations and dependencies are often under stringent regulations or are discouraged due to security-, or business concerns. Therefore, availability of operational data is a pertinent issue in infrastructure interdependency modeling.

- Each agency could have multiple conflicting or competing resilience objectives which may not be easily captured by the existing operational interdependency models.

Hence, it is highly imperative to develop network-risk assessment models and resilience indicators under various data and modeling constraints to serve a

wide range of infrastructure agencies and other stakeholders. Such models and indicators would help decision-makers in incorporating resilience criteria in existing infrastructure development and management methodologies or develop methodologies for resilience-oriented intervention strategies.

1.3 Research Objectives and Scope

The primary objective of the dissertation research is to propose indicator-based methodological frameworks for risk and resilience analysis of interdependent infrastructure networks and apply them for ranking and prioritization of network components. Two types of indicator-based methodologies are proposed to address the above objective, namely, graph-based and empirical (data-driven) methodologies. The graph-based methodologies are proposed to address the issue of infrastructure prioritization when quantitative data on infrastructure interdependencies are unavailable. The data-driven methodologies, on the other hand, rely on metrics and indicators developed using historical data to evaluate the disaster risks and impacts on infrastructure systems. Furthermore, this research will also investigate the possibility of incorporating societal and economic impacts of infrastructure disruptions in the infrastructure prioritization problem. Infrastructure systems are designed and built to cater to the needs of urban communities and economies. Therefore, such an approach is hypothesized to produce more effective resilience-related decisions.

The specific objective of the dissertation research are as follows:

1. Identify and record the various frameworks, models, and metrics used for risk and resilience evaluation in interdependent infrastructure networks by conducting a comprehensive literature review. Enlist their advantages and limitations in ranking and prioritizing infrastructure network components for resilience interventions. The findings from the literature review will be used to develop appropriate methodological frameworks to address the identified research gaps.

2. Develop a methodological framework and a risk measure to quantify the network-wide impacts of infrastructure failures using linguistic descriptions of interdependencies instead of quantitative data. Address the issue of epistemic uncertainties resulting from the use of imprecise information in the interdependency model.

3. Propose a methodological framework to identify the most critical and most susceptible infrastructure components (nodes and links) in a network. Construct appropriate node-level, system-level, and network-level resilience indicators to represent the criticality and susceptibility of components against random and targeted extreme events. Propose algorithms to quantify the criticality and susceptibility of infrastructure components.

4. Develop a methodological framework and resilience indicator to identify most-affected communities in an urban region by combining infrastructure disruption data with socio-economic data.

5. Propose a methodological framework to quantify the operational and economic risks posed by infrastructure shutdowns using historical disaster data. Rank the infrastructure components based on the direct operational and economic risks, and the affected economic sectors based on the indirect economic risks.

6. Develop a methodological framework and appropriate resilience metrics to quantify disaster impacts and identify most affected infrastructure components using historical data. Demonstrate the application of the metrics to quantify the resilience of the infrastructure system to a historical disaster event.

7. Conduct case studies to demonstrate the applicability of the proposed methodological frameworks and resilience indicators. Identify and report the advantages and limitations of the proposed methodologies based on the findings from the case studies.

1.4 Organization of the Dissertation

As discussed before, the dissertation focuses on two broad categories of methodologies for evaluating the risks and resilience in large-scale interdependent infrastructure networks, namely, graph-based methodologies and empirical methodologies. These methodologies are intended to address the issue of infrastructure prioritization when quantitative interdependency data is unavailable. In the first part of the dissertation, three chapters (Chapters 2–4) are included which deals with

generic infrastructure networks as follows:

- In Chapter 2, a hybrid risk measure based on the well-known Inoperability Input-Output Model (IIM) is presented for evaluating infrastructure networks with a lack of interdependency data. The indicator uses subjective information from expert judgments instead of quantitative data for simulating the interdependent effects of infrastructure failures. A case study is conducted on the simplified Great Britain gas and electricity network to identify the most-affected infrastructure nodes due to a hypothetical energy shortage event.
- In Chapter 3, the hybrid resilience indicator presented in Chapter 2 is used to develop two resilience indices, namely, node criticality index and node susceptibility index. The chapter also presents methods based on the resilience indices to prioritize infrastructure components (nodes and links) for implementing resilience-related interventions. A case study based on the simplified Austin infrastructure network is conducted to demonstrate the applicability of the resilience indexes.
- In Chapter 4, a methodology is presented to prioritize urban regions that are vulnerable to large-scale utility disruptions by combining the interdependent effects of infrastructure failures with social vulnerability. For this purpose, a priority index is introduced by combining the hybrid risk indicator with the socioeconomic characteristics of affected communities. The proposed methodology is demonstrated using the simplified Austin infrastructure network and socio-demographic information of census tracts in Austin.

In the second part of the dissertation, methods are presented for evaluating the risk and resilience in infrastructure systems for which historical data regarding failure events are available (Chapters 5-6).

- In Chapter 5, an analysis framework is introduced to predict the functional and economic risks posed by natural disasters to infrastructure systems. The case study investigates the hurricane risks to the Texas ports and its impact to the various sectors in the U.S. economy.
- In Chapter 6, an analysis framework is presented for investigating the resilience of infrastructure systems against historical disasters (natural or man-made). The case study investigates the traffic conditions on the Houston freeway network during- and after Hurricane Harvey and develops the resilience triangle.

Figure 1.6 summarizes the focuses in each chapter concerning the impacts on infrastructure (direct or interdependent), communities, and economy. Throughout this dissertation, direct impacts refer to the functional and physical disruptions resulting from the direct exposure of the infrastructure systems to disasters. The network-wide impacts are the interdependent effects of local infrastructure failures arising from the coupling between various infrastructure components in an urban network. The societal and economic impacts of such infrastructure failures are also considered in the comparison.

Part	Chapters	Generic or infrastructure-specific	Graph-based or Empirical	Type of effects modeled or analyzed			
				Direct effects	Network-wide effects	Societal impacts	Economic impacts
Part I	**Chapter 2:** A Hybrid Risk Measure for Interdependent Infrastructure Networks Using Imprecise Dependency Information	**Generic**	**Graph-based**	✗	✓	✗	✗
	Chapter 3: Development of a Resilience Enhancement Scheme Using the Hybrid Risk Measure: Introducing Criticality and Susceptibility Indicators			✗	✓	✗	✗
	Chapter 4: Application of the Hybrid Risk Measure for Identifying Vulnerable Communities and Economic Centers			✗	✓	✓	✗
Part II	**Chapter 5:** Evaluation of the Functional and Economic Risks Posed by Natural Hazards to Infrastructure Systems: A Case Study of the Texas Ports	**Infrastructure-specific**	**Empirical**	✓	✓	✗	✓
	Chapter 6: Mapping Resilience of Infrastructure Systems Using Historical Data: A Case Study of Houston Freeway Network During Hurricane Harvey			✓	✓	✗	✗

Figure 1.6: Organization of the main chapters in the dissertation and the respective focus areas

Chapter 2

A Hybrid Risk Measure for Interdependent Infrastructure Networks Using Imprecise Dependency Information[1]

2.1 Introduction

Modeling failures in interdependent infrastructure networks requires extensive data related to the various interdependencies existing among the component infrastructure systems. While topological information can be easily obtained through GIS tools, identifying and modeling interdependencies at the network-level is still a challenge, unless system-level data related to dependencies are available. The data related to infrastructure interdependencies are unavailable due to three major reasons:

- Data on infrastructure network components and interdependencies are not readily available due to security and business concerns.
- System-level interdependency data are not maintained in some infrastructure networks with a lower level of technology adoption.

[1] based on Balakrishnan, S., and Z. Zhang. 2020, A Methodology to Analyze Interdependent Effects of Infrastructure Failures Using Imprecise Dependency Information, *Sustainable and Resilient Infrastructure*, https://doi.org/10.1080/23789689.2020.1735836.

- Interdependencies are not only function in nature, but also organizational, logical, etc. which may not be captured by existing functional models.

When quantitative data on system operation is unavailable (which is the case in most of the infrastructure networks), an alternative is to collect the required information from experts in the relevant field. However, expert judgments are based on a person's experience, belief, and knowledge, and therefore are vague, imprecise, and subjective which could potentially cause epistemic uncertainties in the model. Anchoring on the primary issue of inadequate interdependency data availability, this chapter attempts to address the following objectives:

1. Develop a hybrid risk measure and methodological framework for evaluating the interdependent effects of infrastructure node failures by combining the principles of existing network models, economic models, and agent-based models, related to infrastructure vulnerability assessment.

2. Model the interdependencies between infrastructure systems using expert judgments and conduct a simulation-based analysis of network-wide effects of infrastructure failures.

3. Present a method to address the issue of epistemic uncertainties associated with the imprecise nature of expert judgments on infrastructure interdependencies.

In this chapter, the simulation approach develops three different probability distributions of infrastructure dependencies for capturing the resulting imprecision

in estimated network-wide effects: a pair of lower- and upper bound distributions, and a most-likely distribution. Possibility theory is used to develop the bounding distributions for the network-wide effects, whereas probability theory is used to derive the most-likely distribution from the linguistic dependency values. The methodology is then used to investigate the response of the well-known simplified Great Britain gas and electricity network against a hypothetical infrastructure failure scenario. In addition, this chapter also presents a sensitivity analysis to demonstrate the effect of imprecision of dependencies on the estimates of network-wide impacts.

This chapter is organized as follows: Section 2.2 provides an overview of the various infrastructure network vulnerability assessment models and their limitations, and the common mathematical models for handling epistemic uncertainties; Section 2.3 presents the detailed methodology adopted; Section 2.4 discusses the results of the application of the methodology on a simplified infrastructure network; and Section 2.5 summarizes the major findings of the study.

2.2 Literature Review

Estimation of disaster vulnerability is of utmost interest to a wide range of institutions and stakeholders who are directly involved in urban infrastructure development and management. Though the objectives of each of the stakeholders vary, the estimation of disaster vulnerability of infrastructure systems is a critical stage in accomplishing those objectives. For example, the various levels of governments and emergency management agencies, such as the Federal Emergency

Management Agency (FEMA), are interested in vulnerability assessment so that public funding for future infrastructure expansion and management projects could be aligned with the national disaster resilience goals (Malalgoda, Amaratunga, & Haigh, 2013; Ye et al., 2016). However, from the perspective of business entities belonging to various sectors, assessment of infrastructure vulnerabilities is required to formulate alternate plans for business continuity during large-scale infrastructure disruptions (W. Lam, 2002) and to make strategic investment decisions for a region (Hiles, 2010). Table 2.1 presents a comprehensive list of major stakeholders who are interested in quantifying disaster vulnerabilities of infrastructure systems.

Vulnerability assessment models specific to infrastructure systems can be broadly classified into two categories, namely, the direct vulnerability models (catastrophe models) and the indirect (interdependent) vulnerability models. Direct vulnerability models focus on an infrastructure node or a set of nodes that are under direct exposure to a given disaster event, whereas, indirect vulnerability models focus on larger infrastructure systems and networks with due consideration to the interdependencies among them.

Since the focus of the current research is limited to the interdependent effects of infrastructure failures, further discussions are focused on those models used for assessing the vulnerabilities due to interdependencies in infrastructure networks.

Table 2.1: Infrastructure systems stakeholders and their interests in disaster vulnerability assessment

Stakeholder	Examples	Need for estimation of disaster vulnerability of infrastructure systems
Governments and policymakers	Local, state and federal governments, emergency management agencies, etc.	• Align critical infrastructure investment and protection plans with disaster risk reduction goals (Malalgoda et al., 2013; Ye et al., 2016).
Global financial institutions and intergovernmental organizations	World Bank, United Nations, etc.	• Provide organizational and technical assistance to governments for resilience building and infrastructure investments (GFDRR, 2017; The World Bank, 2015).
Infrastructure agencies	Water supply, electricity, sewage collection, etc.	• Develop mitigation plans and strategies (Cavdaroglu, Hammel, Mitchell, Sharkey, & Wallace, 2013; McDaniels, Chang, Cole, Mikawoz, & Longstaff, 2008). • Risk informed infrastructure planning, protection and management (Department of Homeland Security, 2016; Willis et al., 2016).
Emergency managers	Fire and safety, military, civil defense, etc.	• Emergency response, evacuation plans and essential services restoration (Castillo, 2014; Warner & Gordon, 2009).
Insurance industry	Munich Re, Swiss Re, etc.	• Formulate and implement disaster insurance plans for clients such as local governments, private sectors, etc. (Kunreuther, Michel-Kerjan, & Tonn, 2016)
Business enterprises	Retail sector, financial sector, IT sector, etc.	• Identify operational risks and formulate alternative plans for business continuity during critical infrastructure failures (W. Lam, 2002). • Make decisions on strategic investments in a region (Hiles, 2010).
Urban planners	Land use planners and town planners	• Establish land use regulations and building codes, and for future infrastructure development to prevent consequences of disasters (Saunders & Kilvington, 2016).
Non-governmental organizations	Local citizen groups, international aid organizations, etc.	• Build capacity of communities and housing infrastructure to cope up with infrastructure disruptions (Benson, Myers, & Twigg, 2001; Fitzpatrick & Molloy, 2014).

2.2.1 Interdependency models for quantifying indirect effects of disasters on infrastructure networks

The presence of interdependencies makes an infrastructure network a complex "system of systems" (Eusgeld et al., 2011; Mostafavi, 2018). For the convenience of modeling, Rinaldi et al. (2001) categorized the infrastructure interdependencies into four categories: physical-, geographic-, cyber-, and logical interdependencies. Ouyang and Wang (2015) suggested that even though the presence of infrastructure interdependencies enhances the operational efficiency of component systems in the network, they can also increase the system vulnerability. An external hazard or internal technical failure of an infrastructure system could trigger the failure of its dependent systems, degrading its functional efficiency. Many models have been established to quantify the interdependent effects of failures on infrastructure networks. Ouyang (2014) identified and classified such models into five broad categories, namely empirical-, system dynamics based-, agent based-, economic theory based-, and network-based approaches.

Empirical models use databases of historical infrastructure failures and resultant effects for identifying frequencies of failures and accidents, analyzing the strength of interdependencies among infrastructure systems and risk analysis of infrastructure disruption (Chou & Tseng, 2010; Luiijf, Nieuwenhuijs, Klaver, van Eeten, & Cruz, 2009; Mendonça & Wallace, 2006).

System dynamics models consist of feedback loops to capture the relationships between events and system components, whereas, the stock and flows represent the flow of resources and information within the system. Using system dy-

namics, the aggregate response of the whole system under different scenarios can be simulated (Pasqualini & Witkowski, 2005; Powell, DeLand, & Samsa, 2008; Santella, Steinberg, & Parks, 2009).

Economic theory-based models are largely dominated by the input-output model and its variants. Y. Haimes and Jiang (2001) introduced the static inoperability input-output model (IIM) in order to model the interdependent effects of infrastructure failures on other infrastructure systems. The IIM models underwent further modifications and, subsequently, the advantages of other modeling techniques were incorporated (Oliva, Panzieri, & Setola, 2010, 2011).

Agent-based modeling (ABM) is a bottom-up approach to model complex systems consisting of numerous components that interact with each other based on well-defined logical rules and class characteristics (Helbing & Balietti, 2013). Critical infrastructure systems are often viewed as complex adaptive systems (Eusgeld et al., 2011; Rinaldi et al., 2001), for which ABM techniques have been effectively implemented (Nilsson & Darley, 2006; Tesfatsion, 2003).

The network-based models use graph theory to model the interdependencies among infrastructure systems. Graph theory enables the analyst to view infrastructure units as nodes and the logical or resource-based interdependencies as links (Dunn, Fu, Wilkinson, & Dawson, 2013). Graph-theoretic models are convenient as they can efficiently model the spatial and functional aspects of interdependencies in infrastructure networks (Holden, Val, Burkhard, & Nodwell, 2013; Patterson, 2005; Praks, Kopustinskas, & Masera, 2017; Svendsen & Wolthusen, 2007).

2.2.2 Treatment of imprecise model parameters in quantification of risks

Most of the models discussed in the previous section require interdependency data to model infrastructure networks accurately. However, in most cities, though topological netowork data can be easily obtained, the data related to interdependencies in large-scale interdependent infrastructure networks are not easily obtained, especially the data pertaining to interdependencies. Even if dependency data are available, constructing large-scale sophisticated infrastructure network models for capturing real-world infrastructure operations and responses is computationally expensive and challenging. In such circumstances, subjective information obtained from experts is commonly used for the development and validation of models. The subjective nature of model components gives rise to epistemic uncertainties in the interdependency values, which need to be properly addressed in the model. For handling epistemic uncertainties, several tools, such as probability theory, probability bound analysis, random sets and possibility theory, have been proposed in the past (Zio & Pedroni, 2013). In this subsection, some basic principles of probability theory, fuzzy set theory, and possibility theory are discussed, as they are relevant to the present chapter.

2.2.2.1 Probability theory

Probability theory is a common tool for modeling both aleatory and epistemic uncertainties due to the flexibility it provides for interpretation. According to the frequentist notion, probability is the relative frequency of occurrence of an event if the experiment is repeated an infinite number of times.

When data for constructing probability distributions are not available, they are often elicited from experts familiar with the problem under consideration. A number of theories have been proposed to deal with subjective probabilities in engineering, such as evidence theory, interval probabilities, p-boxes, fuzzy probabilities, etc. (Beer, Ferson, & Kreinovich, 2013).

2.2.2.2 Fuzzy set theory

Epistemic uncertainty originates from imprecise data, such as linguistic expressions. Fuzzy set theory (Zadeh, 1965) is a rigorous mathematical theory that enables models to deal with subjectivity and uncertainty in natural language. Fuzzy set theory becomes handy when information related to model parameters are elicited from subject matter experts, which are based on their experience and knowledge. Given a universal set X, a fuzzy subset A of X is characterized by a membership function $\mu_A(x)$ which denotes the grade of membership of x in A. The membership function maps elements in X to a real number in the interval [0,1]. A membership value of 1 denotes that the element is surely in the set A; a membership value of zero suggests that the element does not belong to A, and any value between 0 and 1 represents partial membership. Many risk assessment models use fuzzy numbers, a special case of fuzzy sets, to represent the vagueness of model parameters (Oliva et al., 2011). A fuzzy number, $\tilde{A}$ is defined as follows:

$$\tilde{A} = \{x, \mu_A(x)\} \tag{2.1}$$

and is a normal convex fuzzy set. Fuzzy numbers can model ordered linguistic variables such as *very small*, *small*, *medium*, *high*, etc., thereby make use of expert

judgments to define real-life situations without the need of a large amount of data. Another advantage is that the fuzzy number simulation does not assume independence or dependence between variables.

2.2.2.3 Possibility theory

Possibility theory was introduced by Zadeh (1999) to handle the imprecision intrinsic to the natural language. Possibility theory is based on set functions, which makes it comparable to probability theory. However, possibility theory introduces a pair of dual set functions, namely possibility and necessity measures, to represent real-world scenarios using partial information. The possibility distribution π is a mapping of $x \in X$ to a real number in the interval [0,1]. If $\pi(x) = 1$, the state x is totally possible, and if $\pi(x) = 0$, the state x is impossible. Possibility theory assumes that unless there is evidence to reject a hypothesis, it is still possible. The possibility and necessity measures, denoted by $\Pi(A)$ and $N(A)$, can be derived from possibility distribution π as follows:

$$\begin{aligned} \Pi(A) &= \sup_{x \in A} \pi(x) \\ N(A) &= \inf_{x \notin A} 1 - \pi(x) \end{aligned} \tag{2.2}$$

Possibility theory offers the flexibility of converting a fuzzy number corresponding to a parameter into necessity and possibility measures. The possibility and the necessary measures in combination can be used for reasoning with extreme probabilities, which is useful when quantitative data is not available (Dubois, 2006). Zadeh (1965) suggested that the possibility distribution π coincides with the membership function μ_F of a fuzzy subset F of U. Later, several studies (Dubois, Kerre,

Mesiar, & Prade, 2000; Liu & Liu, 2002; Lodwick, 2012) demonstrated that a fuzzy number A (as defined in Equation 2.1) can be considered as an envelope of a family of probability measures P_A enclosed by possibility and necessity measures. This can be mathematically defined as follows:

$$P_A = \{P|\Pi_A(X) = \sup_{x \in X} \mu_A(x) \geq prob(X)\} = \{P|N_A(X) = \inf_{x \notin X} 1 - \mu_A(x) \leq prob(X)\} \tag{2.3}$$

where $X = (-\infty,\ x]$. The necessity measure can be considered the lower bound of the family of probability distributions representing an imprecise parameter, whereas, the possibility measure corresponds to the upper bound of the same.

2.2.3 Gaps in the literature

The review of the literature revealed that though there exists a wide range of infrastructure interdependency models, a majority of them require extensive data related to the interconnections between various infrastructure components. While there are models such as the fuzzy-inoperability infrastructure models (Fuzzy-IIM) proposed in the past (Oliva et al., 2011; Setola, De Porcellinis, & Sforna, 2009) for incorporating the expert judgments related to infrastructure dependencies, their applications were restricted to aggregate level modeling and did not provide any methods for integration with aleatory uncertainties. This aspect is critical because, in large-scale infrastructure networks, both uncertainties need to be handled properly to ensure the desired level of resilience against external shocks. In addition, the topological characteristics such as the presence of redundancies in large-scale infrastructure networks were also not considered in such models.

2.3 Methodology

The methodological framework adopted for the present chapter is illustrated in Figure 2.1. The urban infrastructure network is modeled as a set of nodes and links, where nodes represent the various infrastructure system components and links are the interdependencies among them. For example, power plants, water treatment plants, hospitals, etc. constitute the nodes in the network, whereas, the flow of resources, such as electricity and water, and flow of services, such as healthcare, between nodes are represented by the links. The topography of infrastructure networks is obtained from available databases and web mapping services, whereas, the interdependency models are constructed using expert opinions and judgments. Finally, a hazard is initiated in the network (leading to failure of the node(s) under consideration), and the network performance under various scenarios (best-, worst-, and most-likely cases) are simulated and analyzed. The following subsections discuss the various stages of the methodology in detail.

2.3.1 Modeling infrastructure network

An urban infrastructure network can be simplified into a directed graph Ω, where the nodes are infrastructure facilities that produce or consume resources and services, and the connecting links are the medium through which the resources are transported, and can be represented as follows.

$$G_{\Omega} = (N_{\Omega}, D_{\Omega}) \tag{2.4}$$

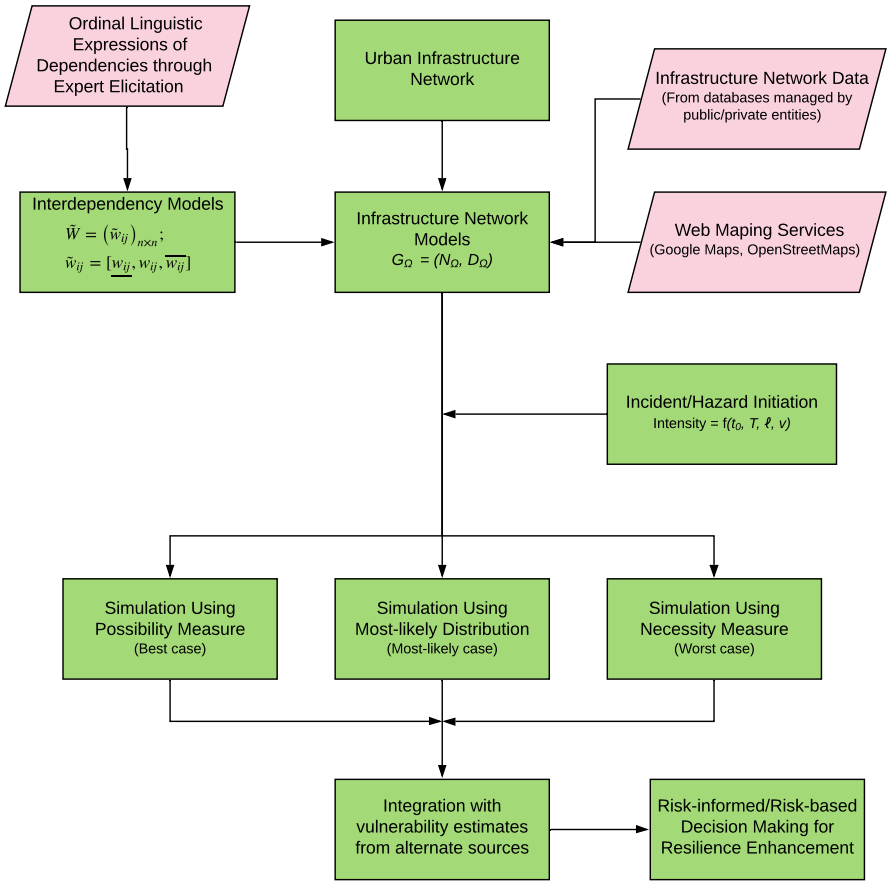

Figure 2.1: Methodological framework adopted for simulating interdependent vulnerabilities in infrastructure networks

where G_Ω is the infrastructure network model, N_Ω is the set of infrastructure nodes and D_Ω is the set of connections among the nodes based on resource or service flow. As already indicated, there could be several types of infrastructure systems (represented as κ: $\kappa(j) = r \in R$) with associated attributes which define their physical and functional characteristics. Each infrastructure node may be dependent on other infrastructure nodes for their functioning. Hence, the presence of connection

between nodes j, $k \in N_\Omega$ (j dependent on k) can be represented as $d_{jk} \in D_\Omega$.

Whether j is directly connected to k is dependent on two important factors – their corresponding infrastructure class ($\kappa(j)$ and $\kappa(k)$), and the extent of the service area of k. If there exists both d_{jk} as well as d_{jk}, the nodes are said to be mutually dependent or interdependent.

2.3.2 Modeling interdependencies and dependencies

Determining the presence of dependencies and interdependencies among infrastructure nodes alone may not be sufficient to evaluate the aggregate impacts of a hazard on the network under consideration. Consider that j is a node under consideration and its degree of failure needs to be assessed. The degree of failure is the same as the reduction in performance of the node under consideration, given another node fails (assuming the node does not have an alternate mechanism to negate the effect of infrastructure disruption on its functionality). The node j gets resources and services from n other nodes represented by a set $K : \ k \in K$. Assuming that the failure of j can happen due to the failure of one or more nodes in K_j or as a direct result of the external event itself (denoted by H), the degree of failure of j is a function of degrees of failure of nodes in K and the degrees of failure of j due to the external event H. Hence, the degree of failure of node j as a function of direct and interdependent effects of H is given by,

$$\Gamma(j) = f_{k \in K}\left(\Gamma(k), \Gamma(j|k), \Gamma(j|H)\right) \tag{2.5}$$

where $\Gamma(k)$ the degree of failure of k, $\Gamma(j|k)$ the degree of failure of j given k fails completely, $\Gamma(j|H)$ the degree of failure of j due to the direct impact of hazard H, and $f_k(\cdot)$ is the function defining $\Gamma(j)$.

When there are redundant links in the network, infrastructure node j may have access to the same resource or service from multiple nodes belonging to the same infrastructure family. In such a case, the infrastructure nodes may be capable of switching the dependee nodes based on their performance levels. This is particularly usual in several grid-based infrastructure networks, such as electric networks, where electricity may be rerouted through alternate feeders if the main feeder fails. Then, it could be assumed that the set of nodes that provide resources to j at a specific time K_j^* may dynamically change during an extreme event, depending on the performance reduction in the network. It can be assumed that at any point in time, node j would depend on the node with the minimum performance reduction among all the available redundant nodes belonging to an infrastructure family ($r \in R$). If so, Equation 2.5 can be rewritten as follows:

$$\Gamma(j) = f_{k \in K_j^*}\left(\Gamma(k), \Gamma(j|k), \Gamma(j|H)\right) \tag{2.6}$$

where $K_j^* = \bigcup_{r \in R} \text{argmin}_{k \in K_i^r} \Gamma(k)$. At the same time, the performance reduction of the dependee nodes $k \in L_k^*$ can be modeled as a function of their respective dependee nodes $L_k^* \ni l$ as in Equation 2.6, i.e, $\Gamma(k) = f_{l \in L_k^*}\left(\Gamma(l), \Gamma(k|l), \Gamma(k|H)\right)$. The dependee node set of k may contain node j, which then forms an interdependency.

Under circumstances when the above function $f_k(\cdot)$ is not known, the degree of failure of j can take any value between the following two bounds.

$$\max_{k \in K_j^*} \left[\Gamma(j|k) \times \Gamma(k)),\ \Gamma(j|H)\right] \leq \Gamma(j) \leq \min \left[1, \sum_{k \in K^*(j)} \left[\Gamma(j|k) \times \Gamma(k)\right] + \Gamma(j|H)\right] \tag{2.7}$$

When there is no information on the combined effects of partial or complete failure of multiple nodes in K_j^*, the lower and upper bounds of $\Gamma(j)$ could be calculated. The upper bound of the cumulative impacts is obtained when it is assumed that the effect of the failure of each node k on j are non-overlapping, whereas, the lower bound is obtained when it is assumed that all such individual effects are overlapping with each other. Equation 2.7 is analogous to the Boole-Frèchet inequality for logical disjunction (Boole, 1854). If the lower and upper bounds are deducted from the maximum performance of one, the upper and lower bounds of performance levels of the node can be obtained, respectively. By adopting the higher bound for the degree of failure, the inaccuracies arising from the assumptions of non-independence or independence among the impacts of failure events could be handled. However, the drawback of this approximation is that it could lead to conservative estimates for degrees of node failures.

In this chapter, a dependency is defined as the degree of failure of a node given another node it depends on for a particular resource or service fails and is denoted by w_{jk}.

$$w_{jk} = \Gamma(j|k) \tag{2.8}$$

Also, the hazard induced impact on node j is represented by ι_j^H.

$$\iota_j^H = \Gamma(j|H) \tag{2.9}$$

If both w_{jk} and w_{kj} are non-zero, then it is called an interdependency. Unfortunately, dependencies, as defined above, are difficult to derive quantitatively due to inadequate interdependency data. Alternatively, information on dependencies could be obtained from the subject experts using standard elicitation methods. A sizable number of studies have delineated the methodologies for elicitation of model parameters from experts (Cooke & Goossens, 2004; Setola et al., 2009; Usher & Strachan, 2013). To handle the epistemic uncertainty of the parameters, each of the linguistic dependency values is characterized using a minimum possible value, a mode, and a maximum possible value.

Equation 2.4 defines the structure of the infrastructure network model. However, the degree of dependencies among various nodes vary depending on the infrastructure types. The interdependency model $\tilde{W}$ is a set of imprecise dependency values in the range of [0, 1] mapped against every d_{jk} that exists in the network. For the present chapter, a triangular fuzzy number is generated for each of the linguistic dependency value using the minimum, the mode, and the maximum values. Mathematically,

$$\tilde{w}_{jk} = \tilde{w}_{\kappa(j)\kappa(k)} \iff \exists d_{jk}, \tag{2.10}$$

where $\tilde{w}_{jk} \in \tilde{W}$ is the fuzzy dependency value of j on k, $\tilde{w}_{\kappa(j)\kappa(k)}$, is the fuzzy

dependency value for infrastructure type $\kappa(j)$ dependent on $\kappa(k)$.

$$\tilde{w}_{\kappa(j)\kappa(k)} = [\underline{w_{\kappa(j)\kappa(k)}}, w_{\kappa(j)\kappa(k)}, \overline{w_{\kappa(j)\kappa(k)}}] \tag{2.11}$$

where $\underline{w_{\kappa(j)\kappa(k)}}$ represents the minimum value, $w_{\kappa(j)\kappa(k)}$ the mode, and $\overline{w_{\kappa(j)\kappa(k)}}$ the maximum value of the dependency.

In many cases, multiple experts may be involved in the fuzzy number elicitation process. In such cases, disagreement among the experts may occur regarding the shape of the membership function. There are several aggregation techniques available to deal with such scenarios (Cheng, 2004; Hsi-Mei Hsu & Chen-Tung Chen, 1996).

2.3.3 Modeling hazards and consequences

The United Nations Office for Disaster Risk Reduction (UNISDR, 2015) defines a hazard as "a potentially damaging physical event, phenomenon or human activity that may cause the loss of life or injury, property damage, social and economic disruption or environmental degradation." Threats and hazards which pose risks to infrastructure systems are broadly classified into three categories by the U.S. Department of Homeland Security (2013), namely, natural hazards, technological, and human-caused. For a reasonable prediction of the interdependent effects due to hazard-induced infrastructure failures on the infrastructure network, defining hazard intensity, its characteristics of propagation, and possible state changes on affected infrastructure node(s) in the hazard model are crucial. In the present chapter, it is assumed that all infrastructure nodes and links are insulated from internal fail-

ures since the focus of this chapter is to model the sudden changes in infrastructure networks induced by external hazards and not the natural deterioration process of infrastructure components.

For the present chapter, the agent-based framework presented by Oliva et al. (2010) for modeling the propagation of hazard induced node failures in infrastructure networks is adapted in order to incorporate the network redundancies and the uncertainties in dependency values.

Consider a disruptive event H occurring at point p and affects a certain geographical area $\omega \subset \Omega$. The direct impact of the hazard on a node j is given by the following equation.

$$\iota_H^j = g(\iota_0, T, \ell_{jp}, v) \quad : \quad 0 \leq \iota_H^j \leq 1; j \in \omega \tag{2.12}$$

where ι_0 is the initial intensity of the hazard at the point of occurrence, T is the time of occurrence of hazard, ℓ_{jp} is the distance between the node and the point of occurrence of the hazard, and v is the speed of propagation of the impact of the hazard. There could be other characteristics as well to define the impact of the hazard, which is not within the scope of this chapter.

If the performance level of j at time $t < T$ is $P_j(0) : 0 \leq P_j(0) \leq 100$, and given the performance of infrastructure nodes on which j is dependent remains the same, the performance of the node j at any time t is given by,

$$P_j(t) = \begin{cases} P_j(0) & \text{if } t - T < \frac{\ell_{jp}}{v} \\ P_j(0) - \iota_j^H & \text{if } t - T \geq \frac{\ell_{jp}}{v} \end{cases} \tag{2.13}$$

The equation suggests that the performance of the nodes affected by the direct impact of the event remains at a normal level until the event directly impact it.

At the same time, the performance level reduction in nodes in the network would subsequently affect those infrastructure nodes which are dependent on them to function. However, if there are redundant links, the failure of one dependee node may be compensated by those redundant connections. The reduction in performance of a node is propagated to those nodes which depend on it for functioning within a very short period (based on the speed of flow of the resource or service). This is under the assumption that all nodes are incapable of handling a shortage in resources without external supply. Considering the effect of interdependencies along with the direct impact due to the hazard, Equation 2.13 can be modified as follows:

$$P_j(t) = \max\left(0, P_j(0) - \left[\sum_{k^* \in K_j^*(t)} \left(P_{k^*}(0) - P_{k^*}(t - \Delta t)\right) \tilde{w}_{jk^*}\right] - \rho_j \iota_j^H\right) : 0 \leq P_j(t) \leq 1, \tag{2.14}$$

where Δt is the time step in the simulation, $K_j^*(t)$ is the set of dependee nodes of j with the highest performance level corresponding to each infrastructure system $r \in R$ in the previous iteration, $\tilde{w}_{jk^*}$ is the dependency of node j on node k^*, ρ_j is the indicator variable with value 1 if $t - T > \frac{\ell_{jp}}{\nu}$, and 0 otherwise, and ι_j^H is the degree of impact of extreme event H on node j. The performance loss of a node j at any time t is given by $P_j(0) - P_j(t)$.

Equation 4.4 gives a simulation framework and measure to evaluate the di-

rect and indirect effects of H on the network performance at a given time. Figure 2.2 illustrates the simulated performance time line of a typical infrastructure node impacted by an extreme event using the presented model.

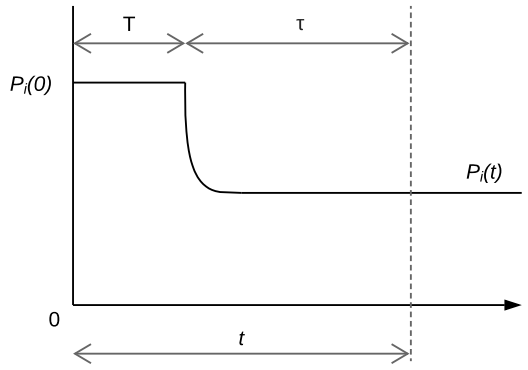

Figure 2.2: Typical performance timeline of an infrastructure node after impacted by an extreme event, considering both direct and interdependent effects

2.3.4 Simulation of interdependent effects

Three different scenarios, namely, best-, worst-, and most-likely cases of network performance, were considered. The most-likely case is simulated using the most-likely distribution of linguistic dependency values based on probability theory. The best- and the worst cases are simulated using the possibility and necessity measures corresponding to the linguistic dependency values based on possibility theory. All the three distributions were constructed from the membership functions of ordinal linguistic expressions of dependencies.

2.3.4.1 Transformation technique to convert membership functions into most likely probability distributions

The most-likely distribution is constructed based on the assumption that the minimum, mode, and maximum values of interdependency values elicited from an expert reflect the person's experience, knowledge, and belief about the dependencies between the infrastructure systems. In such a case, the analyst can interpret that the expert believes that the highest frequency of dependency (between two nodes) he/she would observe is for the mode value and there is no possibility of observing a value less than the minimum or greater than the maximum for the dependency. The most-likely distribution reflects the above interpretation of imprecise dependency variable and can be modeled as follows.

Suppose, the linguistic expression of the conditional degree of failure (dependency) of an infrastructure node j given infrastructure node k is completely failed can be represented by a fuzzy number $\tilde{w}_{jk}$ as follows:

$$\tilde{w}_{jk} = \{(x, \mu_{\tilde{w}_{jk}}(x)) | x \in [0, 1]\} \tag{2.15}$$

where $\mu_{\tilde{w}_{jk}}$ is the membership function corresponding to the imprecise description of the dependency value. The membership function can be considered as a convex function of x, represented by $\phi(x)$, in the range [0, 1] as follows:

$$\mu_{\tilde{w}_{jk}}(x) = \phi(x) : x \in [0, 1] \tag{2.16}$$

Then, the area function of the membership curve can be obtained as follows:

$$\Phi(x) = \int_0^x \phi(x)dx : x \in [0,1] \tag{2.17}$$

In order to obtain the cumulative probability distribution from the membership function, the area function can be normalized using the total area under $\phi(x)$ as follows:

$$F(x) = \frac{\int_0^x \phi(x)dx}{\int_0^1 \phi(x)dx} \tag{2.18}$$

$F(x)$ satisfies all the conditions of cumulative probability distributions ($0 \leq F(x) \leq 1$, $F(x_{min}) = 0$, and $F(x_{max}) = 1$). The transformation technique is illustrated in Figure 2.3. $F(x)$ can be considered as the prior distribution of the dependency value. The idea behind simulation using probability theory is that if the interdependent effects of the same node failure are simulated a large number of times based on the dependency distribution constructed using expert judgments, the resultant distribution of the network performance will reflect the epistemic uncertainties in the model.

2.3.4.2 Necessity and possibility measures based on possibility theory

The upper- and lower probability bounds of the linguistic dependencies can be constructed from the corresponding membership functions (Equation 2.15) using the possibility theory. In a quantitative setting, the possibility and necessity measures of infrastructure dependencies (derived using possibility theory) can be interpreted as upper and lower probabilities corresponding to the values those de-

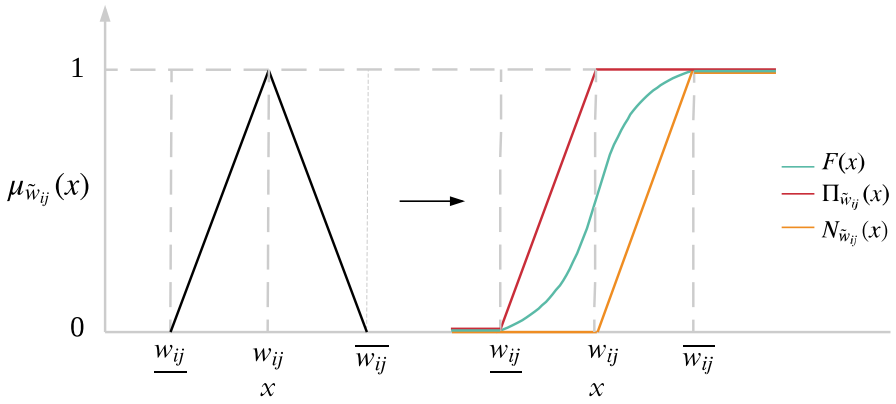

Figure 2.3: Transformation of fuzzy dependency value into most-likely distribution along with necessity and possibility measures

pendencies can take. The possibility and necessity measures (Figure 2.3) of dependencies are calculated as follows:

$$\Pi_{\tilde{w_{jk}}}(X) = \begin{cases} \mu_{\tilde{w}_{jk}}(x) & \text{if } \underline{w_{jk}} \leq x \leq w_{jk} \\ 0 & \text{if } x < \underline{w_{jk}} \\ 1 & \text{if } x > w_{jk} \end{cases} \tag{2.19}$$

$$N_{\tilde{w_{jk}}}(X) = \begin{cases} 1 - \mu_{\tilde{w}_{jk}}(x) & \text{if } w_{jk} \leq x \leq \overline{w_{jk}} \\ 0 & \text{if } x < w_{jk} \\ 1 & \text{if } x > \overline{w_{jk}} \end{cases} \tag{2.20}$$

where $\mu_{w_{jk}}(x)$ is the membership function of A ; $\mu_{w_{jk}}$, $x \in$ [0,1].

2.3.4.3 Agent-based simulation algorithm

The possibility and necessity measures and the most-likely distribution for infrastructure interdependencies were used to simulate the best-, worst-, and most-likely network performance scenarios, respectively. For every simulation run m, a dependency value $\hat{w}_{jk}^{m}$ was drawn from the respective distributions using Monte-

Carlo simulation by fixing the value of cumulative probability. In this way, it was ensured that the model only captures the epistemic component of uncertainty. The network-wide effects under different combinations of dependency values were simulated using agent-based models constructed based on the interdependency model presented in Equation 2.13. Each simulation was continued until the performance difference in each node in two consecutive time-steps was less than 0.001. The simulations were repeated for each scenario to obtain corresponding network performance distributions. The algorithm used for implementing the agent-based model for a single simulation run for a given scenario is presented in Algorithm 1.

2.4 Model Implementation and Results

2.4.1 Description of infrastructure network

For demonstrating the method presented in this chapter, a case study was conducted on well-known Great Britain (GB) gas and electricity network (Figure 2.4. The infrastructure components considered in the integrated GB electricity and gas networks are the bus bars, gas pipeline nodes, gas compressors, and gas storage units (storage tanks or terminals). The case study demonstrates how the proposed metric can be used to quantify the interdependent effects on both the electricity and the gas networks due to a hypothetical event of a sudden 50% shortage in gas supply to the gas-based power plants in the GB networks.

The GB electricity network consists of 29 bus bars, 47 transmission lines, and 148 electric generators (National Grid, 2014). Each bus bar has access to a unique combination of energy sources, including wind turbines, pump storage

Algorithm 1 Pseudo-code for simulating interdependent effects of infrastructure node failures on the urban network

simTime = number of time-steps for one simulation run (initial value of 1)
maxPerfChange = maximum node-level performance difference compared to previous iteration (initial value 0)
errorTolerance = criterion for termination of simultion (1e-04)
agentClasses[] = index(of all infrastructure classes)
agentDependencies[] = index(of dependencies of the infrastructure class)
define the membership functions of each agentDependencies[] and corresponding cumulative distributions (best, worst, most-likely)
for $i = 0$ to $agentClasses.length$ **do**
    for $j = 0$ to $agentDependencies.length$ **do**
        select the scenario for simulation (best, worst or most-likely)
        generate random value of cumulative density [0,1]
        calculate corresponding dependency value using inverse transformation method for the given scenario
    end for
end for
agents[] = index(of all infrastructure nodes belonging to an infrastructure class)
while *maxPerfChange* $\geq$ *errorTolerance* **do**
    for $i = 0$ to $agentClasses.length$ **do**
        for $j = 0$ to $agents.length$ **do**
            update the current list of dependee nodes for the agent
            generate current performance value for the agent
        end for
    end for
    compute *maxPerfChange*
    $simTime$ += 1
end while

plants, nuclear plants, hydroelectric plants, coal plants, and natural gas plants. The details regarding the energy sources at each bus bar and the interconnections between the bus bars were retrieved from Bukhsh and McKinnon (2013). A bidirectional relationship was considered between the connected bus bars, implying that electric power can be transmitted through the bus lines in both directions depending

upon the fluctuations in the demand.

For modeling the GB gas network, the simplified GB gas network introduced by Ameli, Qadrdan, and Strbac (2017); Qadrdan, Chaudry, Wu, Jenkins, and Ekanayake (2010) was adopted. The network consists of 63 nodes (21 compressors, 29 pipeline nodes, 13 terminals/storage facilities), and 54 gas pipelines. A bidirectional relationship was assigned between each of the gas node pairs which was physically linked by a pipeline, assuming that the flow of gas can be reversed by the compressors.

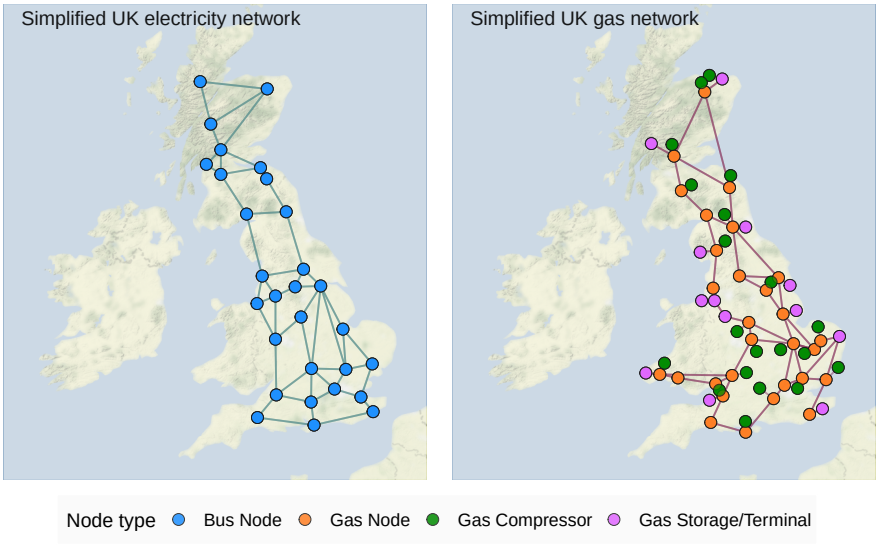

Figure 2.4: Simplified UK electricity and gas infrastructure networks (Map tiles by Stamen Design, under CC BY 3.0. Data by OpenStreetMap, under ODbL)

As far as the interconnections between the gas and electricity networks, the pipeline nodes, compressors, and the storage facilities are dependent on the bus bars for electric power. The details regarding the bus nodes on which each of the gas network components was dependent on were retrieved from Qadrdan et al. (2010).

On the other hand, the bus bars are also dependent on the nearest gas pipe nodes for fuel (this is approximated since gas plants receive fuel from the gas distribution network).

The linguistic dependencies between the network components were assigned based on levels of dependencies (influence) presented by Setola et al. (2009). The linguistic dependencies were converted to the numerical scale using the influence table and the values are presented in Table 2.2. For example, a value of 0.5 indicates that the event will cause the infrastructure component unable to provide the required resources to the dependent nodes. With regard to the imprecision in the dependency values, the base scenario considered a higher value of ± 0.2 (a maximum support width of 0.2+0.2 = 0.4 for fuzzy dependency values) compared to those suggested by Setola et al. (2009).

Table 2.2: Assumed degree of dependencies between infrastructure systems for the case study (based on the definitions by Oliva et al. (2011))

Node type	Gas Node	Gas Storage	Gas Compressor	Bus Node
Gas Node	0.1	0.5	0	0.3
Gas Storage	0.3	0	0	0
Gas Compressor	0.3	0.3	0	0
Bus Node	0.1	0.05	0.5	0.2

2.4.2 Simulation results and discussion

The agent-based infrastructure model was developed using the R-statistical software. To demonstrate the methodology for vulnerability assessment using the proposed methodology, Algorithm 1 was implemented on the integrated GB gas and electricity network assuming that there was a sudden 50% shortfall in gas supply to

the gas power plants. While the necessity and possibility measures of performance loss are not influenced by the number of simulations, the most-likely distribution may be affected by it.

In order the to calculate the required number of simulations for achieving desired confidence interval for the mean with respect to the most-likely distribution, the two-stage absolute precision method was used.

$$N(\epsilon) = \min \left\{ n : n \geq \frac{t^2_{n-1,\alpha} S^2(n_0)}{\epsilon^2}, n \in \mathbf{Z}_+ \right\} \tag{2.21}$$

where $N(\epsilon)$ is the number of simulations required for a precision of ϵ; $t_{n-1,\alpha}$ is the student-t quantile, $S(n_0)$ is the standard deviation corresponding to initial n_0 simulations.

The values of $N(\epsilon)$ for each of the infrastructure node types were calculated by fixing $\epsilon = 0.001$, $n_0 = 1000$, and $\alpha = 0.05$. The minimum number of required simulations obtained for gas nodes, gas compressors, gas storage/terminals and bus nodes are 340, 40, 443 and 49, which are considerably lower than the initial number of simulations ($n_0 = 1000$). Therefore, 1000 simulations were implemented in each case for developing the cumulative performance loss distributions. Each simulation run elapsed until change in every node in two consecutive time steps for the simulation was at least 0.001.

2.4.2.1 Timeline of infrastructure failure propagation

Figure 2.5 presents the mean system performance degradation of all the infrastructure node types over time due to a deficit in natural gas supply. The colors

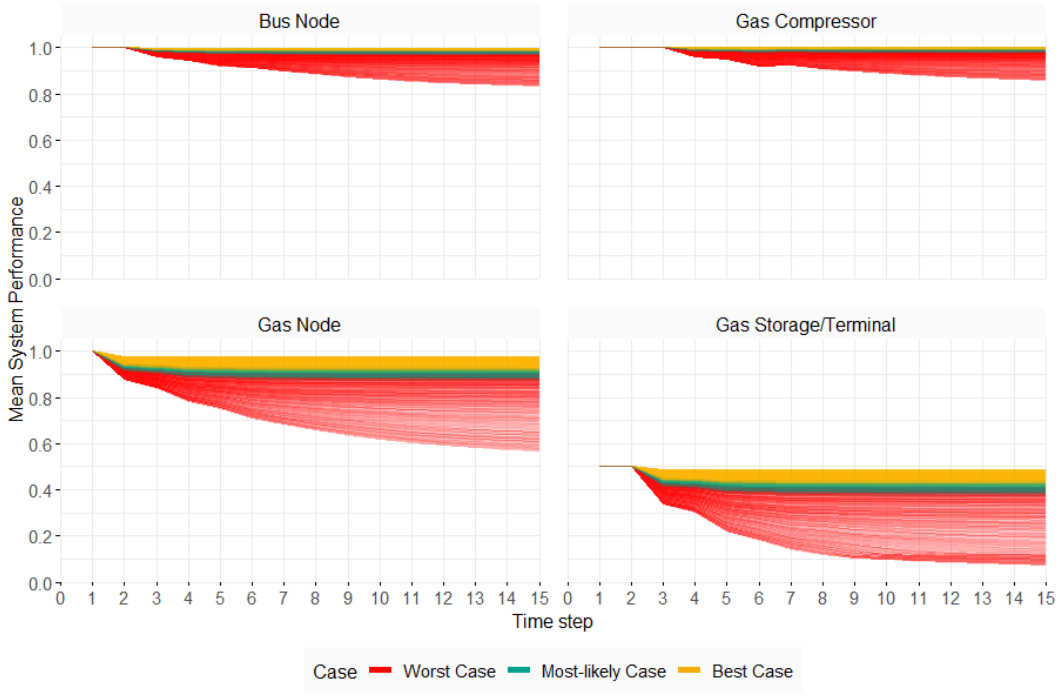

Figure 2.5: Simulation results: Progression of mean network performance of infrastructure systems after the network underwent shortage in gas supply during the first 15 time steps

represent the three distinct scenarios (best-, worst- and most-likely cases) considered in a simulation. Each line corresponds to a single simulation. At the start of each simulation, the performance of gas storage is reduced from one to 0.5, indicating a 50% shortage in gas supply, and the failure is reflected in the performance of all other dependent infrastructure systems causing a string of cascading failures in the entire network. This can be observed in all three cases. However, mean system performance distributions at every time-step are significantly different from one another. This is intuitive because possibility measures of dependencies were used for simulating the best case, necessity measures for the worst case, and the most-likely

distribution for the most-likely case.

There is a significant variation in the rate at which each infrastructure system performance degrades as well. In the best-case scenario, it can be observed that there is no considerable reduction in the performance of infrastructure systems after the initial few time-steps, which means that the further accumulation of interdependent effects is negligible. In the worst - scenario, the performance reduction is steeper in all infrastructure nodes, which decays over time. As expected, in the most likely case, the degradation in the performance of infrastructure systems is at a rate intermediate of the best- and the worst-case.

2.4.2.2 Best, worst and most-likely scenarios

Table 2.3 presents the details of the best-, worst-, and most-likely distributions of the degraded mean system performance levels at the end of simulations for various infrastructure components in the network due to the initial 50% shortage in gas supply to the gas-based power plants.

In all the three cases, the most affected node type is the gas storage/terminals (including direct and interdependent effects). According to the best case distribution, the degraded mean performance of the gas storage/terminals could be between 42% and 49% (1% to 8% performance due to interdependencies) with a mean value of 46% and as per the worst-case distribution, the same is estimated to be between 8% and 40% (10% to 42% performance loss due to interdependencies) with a mean of 29%. The variance of worst-case distributions of all infrastructure node types is higher because the simulations assume higher probabilities for stronger dependen-

Table 2.3: Simulation results: Quantiles corresponding to the mean degraded performance estimated using best-, worst-, and most-likely case distributions

Case	Infrastructure Node type	Cumulative impact of 50% gas shortage					
		0th	25th	50th	75th	100th	Mean
Best Case	Bus Node	0.9834	0.9904	0.9941	0.9961	0.9983	0.9930
	Gas Compressor	0.9899	0.9947	0.9970	0.9982	0.9994	0.9962
	Gas Node	0.9087	0.9328	0.9514	0.9606	0.9748	0.9475
	Gas Storage/Terminal	0.4170	0.4445	0.4642	0.4734	0.4855	0.4594
Most-likely Case	Bus Node	0.9694	0.9781	0.9803	0.9825	0.9883	0.9801
	Gas Compressor	0.9760	0.9851	0.9873	0.9890	0.9935	0.9869
	Gas Node	0.8688	0.8952	0.9014	0.9101	0.9273	0.9020
	Gas Storage/Terminal	0.3763	0.4026	0.4084	0.4187	0.4389	0.4089
Worst Case	Bus Node	0.8388	0.9182	0.9540	0.9724	0.9808	0.9394
	Gas Compressor	0.8635	0.9357	0.9667	0.9816	0.9880	0.9534
	Gas Node	0.5767	0.7458	0.8294	0.8765	0.9005	0.7993
	Gas Storage/Terminal	0.0788	0.2091	0.3179	0.3778	0.4073	0.2864

cies between the infrastructure node based on the necessity measures to take into account the worst possible interdependent effects. The relationship between the magnitude of dependencies and network-wide effects is non-linear. The stronger dependencies between infrastructure nodes lead to cascading effects of higher magnitude and geographical scale compared to a network in which there are weaker dependencies. The most-likely estimates of system performance lie between the best-case and worst-case values. The most-likely estimates of gas storage/terminals are between 37% and 43% with a mean value of 41%.

Considering only the interdependent effects, the gas nodes are also affected in similar magnitudes. According to the best case distribution, the mean degraded performance in gas nodes could be between 91% and 97% (3% to 9% performance loss due to interdependencies) with a mean value of 95%. The estimated mean

performance of gas nodes based on the worst-case distribution is between 58% and 90% (10% to 42% performance loss due to interdependencies) with a mean of 80%.

With regard to the individual nodes belonging to each network, there are variations in the performance loss due to network topology, including the effect of redundancies in the network. Figure 2.6 shows the performance loss estimates (due to interdependent effects) in gas and electricity network components based on the best-, worst-, and most-likely distributions, capturing the uncertainties in the linguistic dependency values with which the network was modeled.

2.4.2.3 Effect of uncertainty reduction in network performance estimates

Though best-, worst-, and most-likely case estimates of infrastructure system vulnerability are extremely helpful in risk-based and risk-informed decision making, those estimates are based on imprecise dependency values constructed using expert judgments and opinions. Over time, such dependency distributions are expected to be improved with more data collection and expert judgment elicitation efforts. This will lead to a reduction in the uncertainty over dependency parameters in the model. In order to check how the three estimates of interdependent effects are sensitive to the epistemic uncertainty of dependencies, three levels of uncertainty reduction in dependency parameters were considered for testing. To implement this in the model, simulations to develop the best-, worst-, and most-likely distributions were repeated by setting the maximum support width of fuzzy dependency values to be 0.1 and 0.05 (against 0.2 in the base model) assuming that the true dependency is w_{jk}.

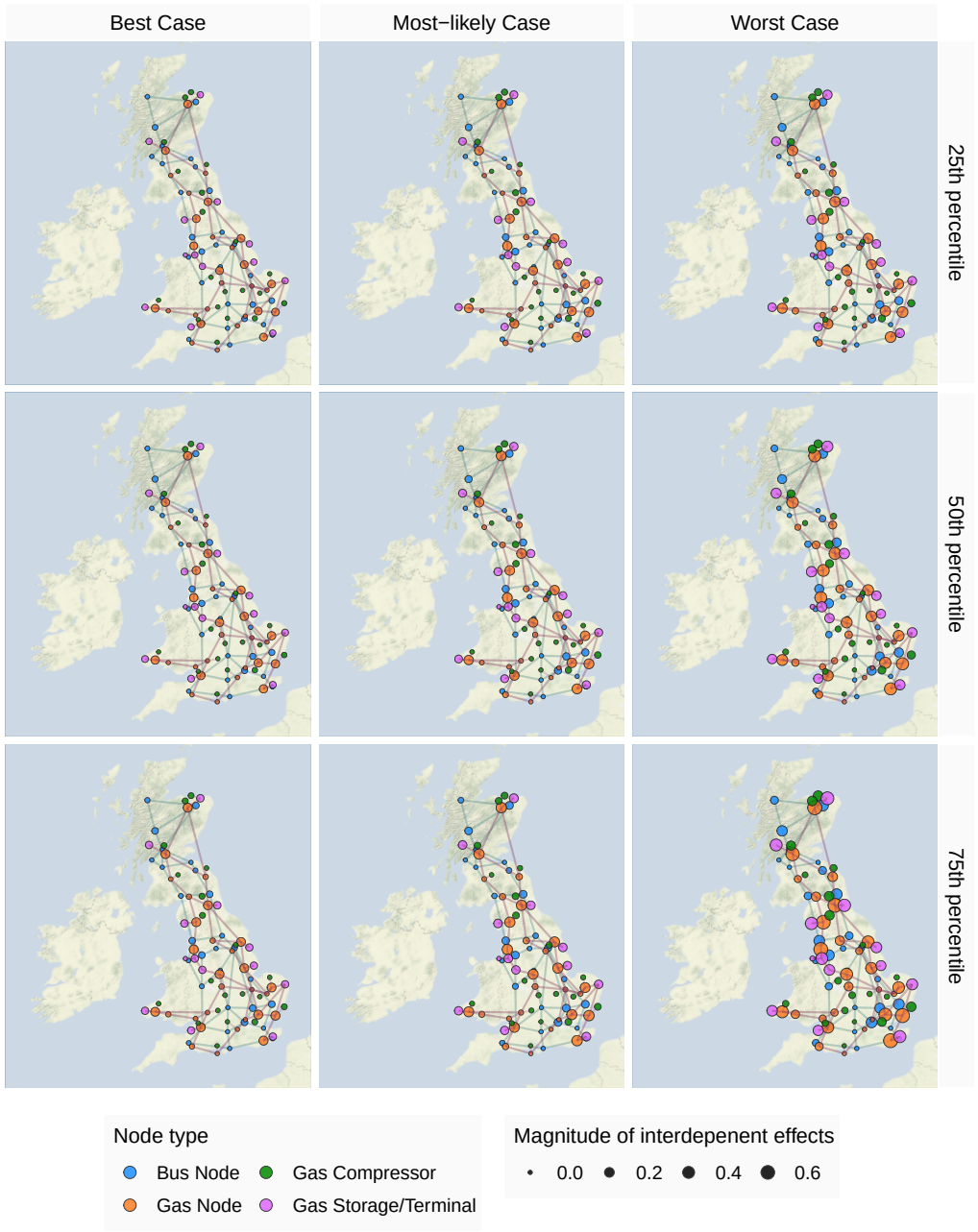

Figure 2.6: The 25th-, 50th-, and 75th percentile performance loss estimates on different infrastructure nodes based on the best-, worst- and most-likely distribution (Only interdependent effects considered)

$$\underline{w_{jk}}^{\lambda} = \underline{w_{jk}} + \lambda(w_{jk} - \underline{w_{jk}})$$
$$\overline{w_{jk}}^{\lambda} = \overline{w_{jk}} - \lambda(\overline{w_{jk}} - w_{jk}) \tag{2.22}$$

where $\underline{w_{jk}^{\lambda}}$ and $\overline{w_{jk}^{\lambda}}$ are the lower and upper bounds of the support of the fuzzy number when uncertainty is reduced by a fraction of λ.

The simulation results using dependencies with various levels of uncertainties are presented in Figure 2.7. The colors represent the best-, worst-, and most-likely cases, and the linetypes correspond to the various levels of uncertainty considered. The simulation results indicate that the reduction in epistemic uncertainty associated with dependencies considerably influences the mean performance distributions in all three scenarios. Also, by reducing the epistemic uncertainties, tighter

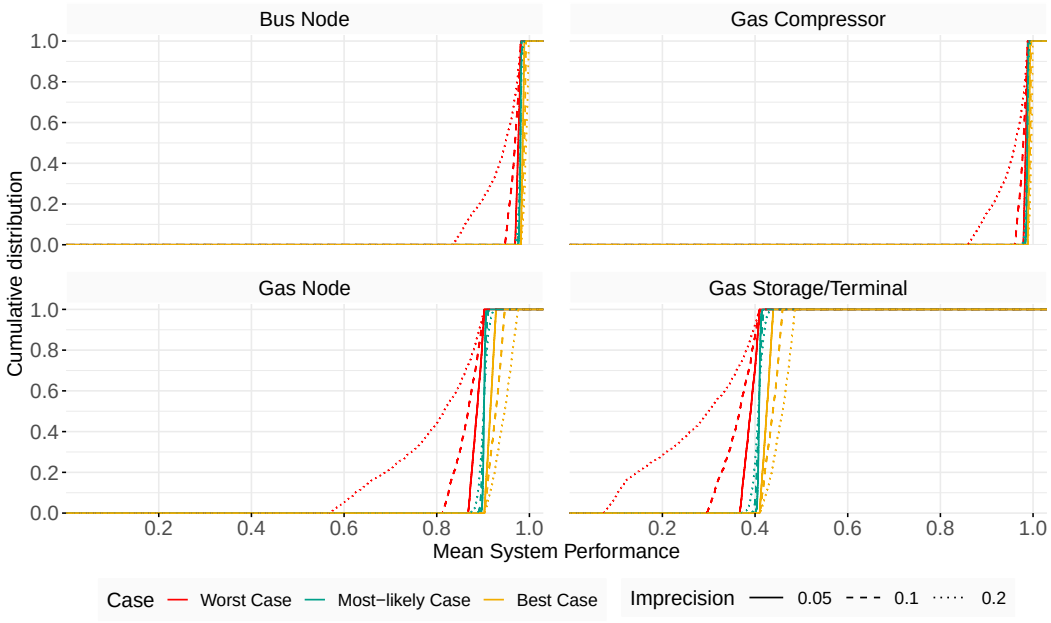

Figure 2.7: Effect of reduction in epistemic uncertainty of linguistic dependencies on the precision of performance estimates

bounds (best- and worst-case distributions) are obtained for vulnerability distributions. As the epistemic uncertainties are reduced, there is a significant reduction in the uncertainty over the performance loss estimates. This stresses the need for data collection efforts to accurately capture the dependencies among infrastructure systems and their combined effects on system performance. Underestimating epistemic uncertainties in infrastructure interdependency models could lead to conservative estimates of network-wide impacts of extreme events, and may adversely affect the effectiveness of policy interventions for resilience enhancements.

2.5 Conclusion

This chapter presented a methodological framework to model the propagation of interdependent effects of localized failures on large-scale interdependent infrastructure network with its focus on using imprecise dependency information. Linguistic dependency data are comparatively easier to obtain and more cost-effective than conventional flow-based dependency data. The linguistic data, which can be elicited from subject-matter experts, are often the only way to understand the dependencies and/or interdependencies in large-scale infrastructure networks in many cities either due to the unavailability or the absence of quantitative dependency data. This chapter also presented a simulation technique based on probability theory and possibility theory to deal with the epistemic uncertainties intrinsic to imprecise linguistic data. The interdependent risk estimates generated by the proposed methodology are characterized by a pair of bounds for mean system performance distributions along with a most-likely distribution rather than a single distribution,

providing decision-makers with a better understanding of the risks.

The best-, worst-, and most-likely case distributions of interdependent effects are simulated on a simplified infrastructure network with many underlying assumptions. Hence, the numerical results of the case study are only a reflection of the interdependent characteristics of the network being employed, but not a representation of the geographical area based on which the analysis network was built. In addition, the redistribution of resource flows due to infrastructure failures may not be accurately captured as in typical flow-based infrastructure models, requiring further modifications in the presented method. Nevertheless, the trends obtained reveal the general physics behind the functioning of interdependent infrastructure networks, which may be of interest to stakeholders of infrastructure resilience. The results quantitatively suggest that risk assessment of infrastructure systems requires adequate attention to the uncertainties related to infrastructure dependencies along with the potential threats to various infrastructure system components in the network. The infrastructure network vulnerability model developed based on the topological characteristics and the expert judgments could be considered as a preliminary form of an expert system. As more empirical or engineering data of the specific network, with different levels of accuracy and sources of uncertainty, become available, the expert system is capable of incorporating them. The agent-based framework, which forms the back end of the model, is capable of incorporating such sophisticated infrastructure-specific modeling components and empirical evidence from historical events.

Chapter 3

Development of a Resilience Enhancement Scheme Using the Hybrid Risk Measure: Introducing Criticality and Susceptibility Indicators[1]

3.1 Introduction

Ensuring the resilience of infrastructure networks not only minimizes direct losses from extreme events but also plays a vital role in the recovery and mitigation of urban communities and economic hotspots (Orabi, Senouci, El-Rayes, & Al-Derham, 2010). However, traditional infrastructure management practices adopt a reliability-based life-cycle cost minimization approach for maintaining infrastructure systems at an acceptable level of performance (Frangopol & Liu, 2007), while overlooking the resilience of networks to extreme events. Because of the rising risks from conventional and emerging threats and the fact that infrastructure systems are becoming more interdependent, incorporating resilience priorities in current management practices has become a necessity rather than a choice. Several studies have identified disaster risk reduction as one of the most important criteria in project prioritization and selection (Thekdi & Lambert, 2014)

[1]based on Balakrishnan, S. and Z. Zhang (2020), Criticality and Susceptibility Indexes for Resilience-Based Ranking and Prioritization of Components in Interdependent Infrastructure Networks, American Society of Civil Engineers. *Journal of Management in Engineering*, https://doi.org/10.1061/(ASCE)ME.1943-5479.0000769.

Like any other resource allocation problem, infrastructure-related resilience investments are dependent on budgetary constraints. Common optimization methods for enhancing resilience could be computationally expensive or insufficient due to the presence of complex interdependencies in the network and the unique operational characteristics of the component systems. A more actionable approach is to prioritize the infrastructure components for implementing resilience enhancement programs so that the desired level of network resilience can be achieved under the given constraints. While resilience metrics specific to certain infrastructure systems have been developed in the past, the development of indicators for measuring resilience improvements in large-scale interdependent infrastructure networks remains a sparsely researched domain. Hence, the primary objective of this chapter is to introduce two generic resilience indexes for characterizing and quantifying the resilience of interdependent infrastructure networks. Two indexes, namely, the criticality index and the susceptibility index for ranking infrastructure nodes are proposed in this chapter.

This study employs the inoperability input-output model (IIM), a widely adopted approach for quantifying interdependent effects of infrastructure failures (Y. Haimes & Jiang, 2001; Y. Y. Haimes et al., 2005), to compute the criticality and susceptibility indexes of infrastructure systems. The IIM simplifies infrastructure systems into a bidirected weighted graph, where nodes represent the origins and destinations of utility service flow, whereas, the links represent the degree of dependency between individual infrastructure nodes. The proposed indexes take both the topological and the generic functional characteristics of infrastructure net-

works into consideration. Later, this chapter also demonstrates the application of the resilience indexes to rank and prioritize infrastructure network components for resilience-oriented investments and for evaluating the resultant improvements.

This chapter is organized as follows: the Background section discusses the major resilience indicators for evaluating resilience in various types of infrastructure networks; the Methodology section discusses the development of the proposed indexes and their application for prioritizing infrastructure components; the Experiment Simulation section presents how the indexes are used for prioritizing infrastructure components in a simplified network; and the Conclusion section summarizes the findings from the study.

3.2 Literature Review

Several definitions have been proposed for system resilience with a focus on the specific aspects of the resilience problem being handled (Francis & Bekera, 2014; Hosseini, Barker, & Ramirez-Marquez, 2016). In the context of infrastructure systems, The White House (2013) defined resilience as the ability of infrastructure systems or components to endure potential external shocks and to recover quickly and adapt to changing external conditions. Bruneau et al. (2003) suggested that infrastructure resilience can be characterized using the following four dimensions (properties): (a) robustness, which refers to the ability of a system or a component to endure a given level of stress, shock or demand without consequences on its level of functioning; (b) redundancy, which is the ability of the system to satisfy its functional requirements and achieve stated goals by substituting its elements of the

system itself in the event of a disruption, degradation, or loss of functionality; (c) resourcefulness, which is defined as the ability of the system to recognize failures in the system, prioritize restoration activities, and mobilize resources during conditions that threaten to disrupt the functions of the system; and (d) rapidity, which is the capacity of the system to recognize problems and mobilize resources to contain and avoid further losses due to external stress in a timely manner.

The resilience of the infrastructure system can be enhanced by improving any of the above four dimensions of resilience. While some of these aspects of resilience overlap with that of reliability (for example, the robustness of infrastructure systems can be improved by traditional maintenance and rehabilitation efforts (Rydzak, Magnuszewski, Sendzimir, & Chlebus, 2006)), the other three aspects also require adequate attention for achieving optimal resilience. This highlights the need for dedicated resource allocation programs for managing the resilience of infrastructure systems.

For devising optimal resource allocation strategies, identifying those infrastructure systems and components whose resilience is crucial for the whole system is necessary. Appropriate resilience indicators can not only be used for ranking and prioritization but also be effectively used for measuring and evaluating resilience of infrastructure systems Henry and Emmanuel Ramirez-Marquez (2012); Nan and Sansavini (2017); K. Zhao et al. (2011). The survey of the literature suggests that the available resilience indicators can be broadly classified into three: (a) performance-based indicators; (b) topology-based indicators; and (c) hybrid indicators. Each category of metrics can be further subclassified into those developed for

generic interdependent infrastructure networks and those for specific infrastructure systems. The scope of the review was limited to the quantitative methods, though qualitative indicators based on subjective information are also available.

3.2.1 Performance-based indicators

Performance-based indicators are developed using metrics that represent the operational and physical characteristics of a system pertaining to its resilience. Comparison of performance indicators under normal- and extreme conditions can be used to understand a system's vulnerability to extreme events. Such indicators can be used to rank components based on their relevance to the overall resilience of the system. For reliable estimation of resilience, simulating the stresses on the system due to the extreme event and the resultant response by the system is essential (Tran, Balchanos, Domerçant, & Mavris, 2017). Alternatively, historical disaster data can be used to characterize system response to specific events (Ouyang, 2014). In both approaches, extensive data related to the system as well as the disruptive event are needed.

The initial attempt to quantify resilience in generic infrastructure networks was made by Bruneau et al. (2003) by introducing the concept of the "resilience triangle". The resilience triangle represents the performance timeline of the infrastructure system after it is impacted by external stress. The area of the triangle above the timeline is called the area of loss of resilience. In reality, this metric represents the cumulative loss of functionality (in terms of an appropriate measure of performance) in the infrastructure system which is subject to the external stresses

and shocks. The significance of this metric is that it is simple, intuitive, and relates to the four resilience dimensions. Many modified resilience metrics based on the resilience triangle have been proposed in subsequent studies to address various technical issues intrinsic to the original resilience triangle, such as its incapability to distinguish fast and slow recovery processes (Bocchini & Frangopol, 2012) and its incapability to distinguish between various time scales (Frangopol & Bocchini, 2011).

Based on the concept of the resilience triangle, several studies attempted to quantify the resilience of specific infrastructure systems using relevant performance indicators. Bagchi, Sprintson, and Singh (2013) developed the load loss damage index (LLDI) based on the resilience triangle concept to assess the resilience of electrical distribution networks to urban fire hazards. LLDI represents the cumulative load lost in the network caused due to a fire event. Similarly, for assessing the resilience of transportation networks, Ganin et al. (2017) used the concept of efficiency, computed as the average commuter delays induced by simulated random traffic disruptions in the network, to quantify the network resilience of 40 cities in the United States. Similar indicators have also been used in other infrastructure networks such as water distribution networks (Jeong, Wicaksono, & Kang, 2017; Todini, 2003), communication networks (Ibrahim, 2018; Kwasinski, 2015), etc. In addition to the direct functional losses, some studies also considered the socioeconomic losses as well to quantify resilience. For instance, Cimellaro et al. (2016) used the total number of households affected by water outage along with other performance measures to develop resilience indicators for water distribution network

components.

3.2.2 Topology-based indicators

Using network theory, infrastructure networks can be represented as complex graphs in which the nodes represent the infrastructure system components and the links represent the dependencies among them (Dunn et al., 2013). The topological characteristics of a network could be indicative of the ability of different infrastructure systems and components to respond to extreme events by reorienting themselves to minimize the aggregate functional loss to the whole system. The topology-based indicators, which reflect these characteristics, can be used to rank the nodes and links in the network which are most vulnerable to the direct and indirect effects of extreme events (Grubesic, Matisziw, Murray, & Snediker, 2008). The general methodology to assess the resilience of infrastructure networks using network theory is to identify the components whose removal from the network would lead to the loss of specific properties relevant to network resilience (Sudakov & Vu, 2008). The topology-based indicators are generally independent of any specific extreme event, simplifying the analysis.

As far as the generic interdependent infrastructure systems are concerned, there have been a few attempts to assess resilience using topological factors. Centrality (Pinnaka, Yarlagadda, & Çetinkaya, 2015) and prestige measures are commonly used as topological measures for ranking infrastructure nodes based on their importance. Topology-based indicators are also developed for individual infrastructure systems with consideration of their unique network characteristics. For

example, Wyss, Mühlemeier, and Binder (2018) used path length, degree centrality, modularity, technological variety, balance, and disparity in energy distribution networks to characterize resilience in different network topologies. Herrera, Abraham, and Stoianov (2016) used the number of water sources and energy loss along various paths to quantify the resilience in water distribution networks. Rohrer, Jabbar, and Sterbenz (2009) used path diversity to assess the resilience of communication networks. Topology-based resilience indicators are less accurate than the performance-based indicators as the former do not reflect the real-world operational relationships among the components of the infrastructure systems.

3.2.3 Hybrid indicators

Hybrid indicators combine the advantages of performance-based indicators and topology-based indicators. They can be used for representing both the generic and the event-specific resilience of infrastructure systems. Modern infrastructure networks, being highly interdependent and heterogeneous, are often considered as edge-weighted bidirected graphs (Y. Haimes & Jiang, 2001), where the weight of the links represents the degree of dependency in the form of resource or service, and the direction of the links indicates its direction of flow. The first effort to rank infrastructure systems based on their resilience using the hybrid approach was made by Oliva et al. (2011) where the authors introduced two measures, namely, influence gain and dependency index, to denote the concepts of criticality and susceptibility of nodes. However, these measures did not consider the higher-order interdependent effects of infrastructure disruptions. Recently, a biased-*PageRank* measure was

developed by C. Zhao, Li, and Fang (2018) for interdependent infrastructure networks integrating both the topological and the functional characteristics of nodes. Some studies also combined performance and network properties with social indicators such as the number of consumers affected by infrastructure disruptions to rank critical infrastructure components (Pant, Zorn, Thacker, & Hall, 2018).

Hybrid resilience indicators are widely used for analyzing the resilience of individual infrastructure systems as well. Bompard, Napoli, and Xue (2010) evaluated the resilience of energy distribution networks by a resilience indicator combining net availability (a functional characteristic) and path redundancy (a graph characteristic). Ulusoy, Stoianov, and Chazerain (2018) combined the random walk betweenness centrality of pipe nodes with energy loss in pipelines to evaluate the resilience of water distribution networks. Heaslip, Louisell, Collura, and Serulle (2010) used network availability, network accessibility, traveler perception, and transportation cost to assess the resilience of transportation networks.

Table 3.1 enlists a few examples of the various categories of resilience indicators discussed above along with the details of the performance- and topological factors used in their development.

3.2.4 Gaps in the literature

The review of the literature revealed that there has been a considerable number of studies that explored the use of both performance- and topology-related factors for evaluating the resilience of infrastructure systems and their components Henry and Emmanuel Ramirez-Marquez (2012); Nan and Sansavini (2017);

Table 3.1: Examples of infrastructure resilience indicators

Infrastructure system	Study	Type of resilience indicator	Factors determining resilience
Energy networks	Ilbeigi and Dilkina (2018)	Performance-based	Cumulative decrease in production (petroleum infrastructure).
	Brancucci Martínez-Anido et al. (2012)	Performance-based	Energy not supplied, total loss of power and restoration time.
	Wyss et al. (2018)	Topology-based	Path length, degree centrality, modularity, technological variety, balance and disparity.
	Bompard et al. (2010)	Hybrid	Net ability and path redundancy.
Water networks	Jeong et al. (2017)	Performance-based	Input energy, required energy and surplus energy.
	Cimellaro et al. (2016)	Performance-based	Number of households affected by water outage, tank water level and water quality.
	Todini (2003)	Performance-based	Surplus power (energy per unit time) at each node.
	Pandit and Crittenden (2016)	Topology-based	Graph diameter, characteristic path length, central point dominance, critical ratio of defragmentation, algebraic connectivity, and meshed coefficient.
	Herrera et al. (2016)	Topology-based	Number of water sources and energy loss along various paths.
	Aydin (2018)	Hybrid	Algebraic connectivity, meshedness coefficient, entropic degree.
	Ulusoy et al. (2018)	Hybrid	Random walk betweenness and pipe energy loss.
Communications/ Cyber-systems	Ibrahim (2018)	Performance-based	Percentage of traffic dropped, reduction in quality of service, recovery time.
	Kwasinski (2015)	Performance-based	Ratio of down time to total time.
	Alenazi and Sterbenz (2015)	Topology-based	Centrality measures, path diversity, centrality-based robustness, spectral robustness, etc.
	Rohrer et al. (2009)	Topology-based	Path diversity.
	Rosenkrantz, Goel, Ravi, and Gangolly (2005)	Topology-based	Node and edge resilience based on number of failed nodes or links.
Transportation networks	Ganin et al. (2017)	Performance-based	Change in delays with respect to stress
	Chan and Schofer (2016)	Performance-based	Lost service days of rail transit systems.
	X. Zhang, Miller-Hooks, and Denny (2015)	Topology-based	Throughput, connectivity and compactness.
	Tu, Yang, and Chen (2013)	Topology-based	Number of minicuts of cardinality.
	Chen and Miller-Hooks (2012)	Hybrid	Ratio of post-disaster capacity to pre-disaster capacity
	Heaslip et al. (2010)	Hybrid	Network availability, network accessibility, traveler perception, and transportation cost.
Generic infrastructure networks	Bruneau et al. (2003)	Performance-based	Cumulative loss in operational performance
	Pinnaka et al. (2015)	Topology-based	Centrality measures
	C. Zhao et al. (2018)	Hybrid	Biased PageRank, functional characteristics

K. Zhao et al. (2011). While performance-based and topology-based resilience indicators are commonly used, hybrid indicators have recently emerged as an alternative. It was observed that the majority of indicators are developed for individual infrastructure systems with less focus on the cascading effects of infrastructure disruptions. Available indicators for evaluating the resilience of generic large-scale interdependent infrastructure networks are limited.

3.3 Methodology

This section presents the methodology adopted for developing the resilience indexes introduced in this chapter, namely criticality and susceptibility indexes. The indexes are computed using an agent-based approach with inoperability input-output model (IIM) determining the characteristics of the agents and their interrelationships. Later the indexes are used to identify the most important infrastructure nodes from the perspective of system resilience. A heuristic algorithm based on the proposed resilience indexes is also presented to systematically identify critical links and improve the resilience of infrastructure networks by introducing redundancies.

3.3.1 Infrastructure interdependency model

Several methods have been proposed in the past to quantify the interdependent effects of external hazards in infrastructure networks (Table 3.2). In this chapter, the methodology for developing the criticality and susceptibility indexes is derived from the static IIM proposed by Y. Haimes and Jiang (2001). The IIM is a simple model used for quantifying the effects of an infrastructure failure on an

Table 3.2: Major categories of infrastructure interdependency models (Ouyang, 2014)

Model category	Key features	Examples
Empirical models	• Use data related to historical infrastructure failure and consequences. • Identify frequency of failures. • Quantify strength of interdependencies between systems.	Luiijf et al. (2009); Mendonça and Wallace (2006)
System dynamics-based models	• Apply theory of nonlinear dynamics and feedback loops to define system. • Feedback controls capture relationships between events and components. • Stocks and flows capture flow of resources and information.	Pasqualini and Witkowski (2005); Powell et al. (2008); Santella et al. (2009)
Economic theory-based models	• Based on the well-known input-output models used for quantifying the impacts of fluctuations in economic sectors.	Y. Haimes and Jiang (2001); Y. Y. Haimes et al. (2005)
Network-based models	• Based on the concepts of graph theory. • a system is viewed as a set of nodes and (weighted) links. • captures spatial and functional aspects of large-scale networks.	Dunn et al. (2013); Svendsen and Wolthusen (2007)
Agent-based models	• bottom-up approaches in which systems components are modeled as agents interacting with each other under a set of rules. • capable of incorporating the behavior of decision maker; can be used to model any level of complexity.	Nilsson and Darley (2006); Tesfatsion (2003); Oliva et al. (2010)

interdependent infrastructure network. The IIM was adapted from the well-known input-output model (I-O model) used in economics for estimating the effect of disruptions to economic sectors to the national economy (Leontief, 1986). Several

extensions of IIM such as dynamic IIM (Y. Y. Haimes et al., 2005; Oliva et al., 2010) and fuzzy dynamic IIM (Oliva et al., 2011) also consider the temporal dynamic behavior of infrastructure networks affected by extreme effects.

Similar to Chapter 2, an agent-based static IIM (Oliva et al., 2010) is adopted to simulate the interdependent effects of infrastructure node failures. The agent-based IIM models the interdependent infrastructure network as a weighted bidirected graph in which nodes represent infrastructure components that either produce or consume some type of infrastructure service or resource. The flow of resources/services (dependency) is captured by the weights assigned to the directed links on a scale of 0 to 1. For example, a weight of 0.2 for a link from node$A$ to node B suggests that if A fails, the performance level of B will decrease by 20%.

The agent-based IIM can incorporate minute details about interdependencies and infrastructure components to imitate real-world operational characteristics. Agent-based IIM can also efficiently capture the diffusion of effects of failure of infrastructure components on large-scale networks with minimal computational requirements. These factors make IIM a good choice for developing indicators intended to quantify resilience of infrastructure networks and evaluate the implications of resilience enhancement strategies.

The IIM assumes that the degree of failure of any node in the network is dependent on the following two factors:

1. the extent of failure caused by the direct impact of the event

2. the degree of failure of the nodes on which the node depends on (dependee nodes) for functioning.

Similar to a node, the failure of its dependee nodes can also occur due to the above set of factors. In addition, it is also important to take the redundancies in the network into consideration. If a node receives same resource from two independent dependee nodes, then even if one of those nodes fails, the dependent node is not affected as the redundant dependee node continues to provide the same resource. Therefore, the performance of a node is determined by the dependee node with the highest performance level among the set of nodes supplying the same service. Taking these factors into account, the propagation of failure of a node i on an infrastructure network is modeled as follows (Equation 3.1):

$$P_j^i(t) = \max\left(0, P_j^i(0) - \left[\sum_{k^* \in K_j^*(t)} \left(P_{k^*}^i(0) - P_{k^*}^i(t-\Delta t)\right) w_{jk^*}\right] - \rho_j \iota_j^H\right) : 0 \leq P_j^i(t) \leq 1, \tag{3.1}$$

where $P_j^i(t)$ is the performance of node j at time t after node i fails, $P_j^i(0)$ is the performance of j before the failure of i due to extreme event H, Δt is the time-step in the simulation, $K_j^*(t)$ is the set of dependee nodes of i with the highest performance level corresponding to each infrastructure system $r \in R$ in the previous iteration, i.e., $K_j^*(t) = \left\{\arg\max_{k \in K_j^r} P_k^i(t-\Delta t) : r \in R\right\}$ where K_j^r is the set of all nodes belonging to $r \in R$ providing resources to i, w_{jk^*} is the dependency of node j on node k^*, ρ_j is an indicator variable determining if the node j is directly impacted by event H, and ι_j^H is the degree of impact of extreme event H on node j.

3.3.2 Development of criticality and susceptibility indexes

For this chapter, two factors for node ranking and prioritization are considered. The first factor is the criticality of nodes, which is a term introduced to indicate the importance of a node for the functioning of other nodes in the network. The second factor is the susceptibility of nodes, which is introduced to denote the exposure of a node to the failure of other nodes in the network. While the failure of the most-critical nodes may cause large-scale disruptions in infrastructure networks and they often may become the primary targets of intentional attacks, such as the acts of terrorism or cyber-attacks, the most-susceptible nodes are more likely to fail or be affected by the cascading effects triggered by the failure of other nodes in the network. Critical nodes require initiatives to protect the nodes from extreme events, whereas, susceptible nodes require capacity enhancement to reduce the impacts of cascading effects on them. Similarly, the links connected to the critical nodes are also of high criticality, as their failure would trigger large-scale cascading effects in the network.

Table 3.3 lists the major functional aspects determining the criticality and susceptibility of nodes in an infrastructure network. These factors are identified based on the principles of agent-based interdependency models presented by Oliva et al. (2010). While the criticality of a node is largely determined by the criticality of its dependent nodes, its susceptibility is dependent on the susceptibility of those nodes on which it is dependent on for functioning (dependee nodes).

Along with the functional characteristics of a network, the computation of criticality and susceptibility of the constituent nodes is also dependent on the topol-

Table 3.3: Major factors influencing criticality and susceptibility of a node in an infrastructure network

Factors affecting node criticality	Factors affecting node susceptibility
The number of nodes to which the node provides resources or services.	The number of nodes to which the node is dependent on for critical resources or services.
The type of nodes to which the node provides resources or services.	The type of nodes on which the node is dependent.
The criticality of the nodes to which the node provides resources or services.	The susceptibility of the nodes which provide resource or services to the node.

ogy of the network; more specifically, on how the infrastructure nodes are dependent on each other. Infrastructure networks can be broadly classified into three categories based on the presence of dependencies and interdependencies, as illustrated in Figure 3.1.

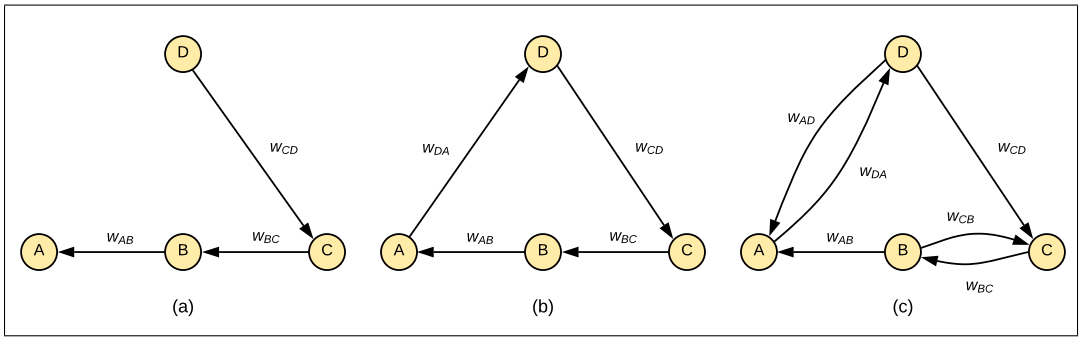

Figure 3.1: Basic infrastructure network topologies based on the presence of dependencies and interdependencies: (a) network with only dependencies; (b) network with dependencies and indirect interdependencies; (c) network with direct and indirect interdependencies

1. *Network with only dependencies*: There are no directed cycles in the network. For example, in Figure 3.1a, between any pair of nodes, there are only unidirectional dependencies and directed cycles are absent. Any disturbance in

the functioning of node B will only impact its dependent node A, and not the latter's dependee node C.

2. *Network with indirect interdependencies*: There are no bidirectional dependencies between any pair of nodes, but the network consists of at least one n-cycle ($n \geq 3$). Hence, disturbance in any node in the cycle can cause further disturbance to its functioning as the initial disturbance can return to the node through the directed cycle. In Figure 3.1b, the partial failure of node A will indirectly impact itself through nodes D, C, and B as those nodes form a directed 4-cycle in the network.
3. *Network with direct interdependencies*: There is at least one pair of infrastructure nodes that are interdependent; i.e., the network consists of at least one 2-cycle. Hence, disturbance on one such node would cause a disturbance on itself through the other nodes in the cycle. In Figure 3.1c, nodes A and D, as well as nodes B and C are interdependent.

The presence of cycles in the network gives rise to interdependent effects, leading to gradual degradation of performance of the whole network over time. Therefore, criticality and susceptibility indexes must also take into account of the higher-order interdependent effects.

Consider $\psi_{ij} \in \Psi$ and $\chi_{ij} \in \mathrm{X}$, where ψ_{ij} is the criticality value of node i with respect to node j, which can be interpreted as the degree of failure of j induced by a complete failure of i (including interdependent effects), and χ_{ij} is the susceptibility of node i with respect to j, which can be interpreted as the degree of failure of i given j fails. Comparing the definitions of the two concepts presented above, the

following relationship can be obtained between criticality and susceptibility values.

$$\psi_{ij} = \chi_{ji} \tag{3.2}$$

The agent-based method presented in this chapter attempts to compute the individual effects of each node failure on other nodes in the network and aggregate them appropriately to develop the criticality and susceptibility indexes. As in any agent-based model, the computation is done by implementing a recursive procedure.

Consider that a node i fails completely due to an extreme event at time $t = 0$. At that time, only the functioning of that node in the network is affected, and other nodes in the network remain unaffected (as evident in the interdependency model in Equation 3.1). Hence, the individual criticality values of node i with respect to every other node in the network remains zero at $t = 0$.

$$\psi_{ij}(t = 0) = 0, \ \forall i, j \in N, j \neq i, \tag{3.3}$$

where N is the set of all nodes in the network. In the next time-step $t = 1$, the effect of failure of node i is reflected in the functioning of dependent nodes of i and is proportional to the dependency of dependent nodes on node i. That is, if the dependency of node j on i is w_{ji}, then the performance of node j will be reduced by $P_i(0) \times w_{ji}$. Hence, the criticality values for any node at time-step $t = 1$ is given by,

$$\psi_{ij}(t = 1) = \begin{cases} P_i(0) \times w_{ji} & \text{if } \exists (i, j) \\ 0 & \text{otherwise} \end{cases} \tag{3.4}$$

where $(i, j) \in D$ represents the dependency of j on i.

Using the above two initial conditions (Equations 3.3 and 3.4), the criticality values of all the nodes can be simulated. In the subsequent iterations, the criticality of i for other nodes which are indirectly dependent on it needs to be reflected in i's criticality values. Also, any higher-order interdependent effects of failure of node i on other nodes (due to the presence of directed cycles in the network) needs to be taken into account. The interdependency model presented in Equation 3.1 can be adapted to compute the criticality values. Based on the definition, the general function to derive criticality values of nodes at any time-step $t \geq 1$ in the simulation is given by the following equation.

$$\psi_{ij} = \lim_{t \to \infty} P_j^i(0) - P_j^i(t) \tag{3.5}$$

where $P_j^i(0)$ is the performance of j before i is set to fail and $P_j^i(t)$ is the performance of j at the time-step t after i is set to fail ($t \geq 1$). Now, substituting for $P_j^i(t)$ in Equation 3.5,

$$\psi_{ij} = \lim_{t \to \infty} P_j^i(0) - \max\left(0,\ P_j^i(0) - \left[\sum_{k^* \in K_j^*(t)} \left(P_{k^*}^i(0) - P_{k^*}^i(t - \Delta t)\right) w_{jk^*}\right] - \rho_j\right) \tag{3.6}$$

where $K_j^*(t)$ is the set of dependee nodes of i with the highest performance level corresponding to each infrastructure system $r \in R$ in the previous iteration, ρ_j is an indicator variable with value 1 if $j = i$ and 0 otherwise to denote the complete

failure of node i in the simulation. Equation 3.6 can be further reduced as follows:

$$\begin{aligned}\psi_{ij} &= \lim_{t\to\infty} \min\left(P_j^i(0), \left[\sum_{k^*\in K_j^*(t)} \left(P_{k^*}^i(0) - P_{k^*}^i(t-\Delta t)\right) w_{jk^*}\right] + \rho_j\right) \\ &= \lim_{t\to\infty} \min\left(P_j^i(0), \left[\sum_{k\in K} \psi_{ik^*}(t-\Delta t) \times w_{jk^*}\right] + \rho_j\right)\end{aligned} \tag{3.7}$$

Equation 3.7 provides a simulation framework for computing the criticality values of i for other nodes in the network. Simulation is continued until all interdependent effects are reflected in the criticality values of the all nodes $i \in N$, where N is the set of all nodes in the network. The final critical values are represented by ψ_{ij}.

For homogeneous networks, where all the nodes belong to a particular infrastructure system, the node criticality index of i can be obtained by aggregating the individual criticality values corresponding to i, ψ_{ij}, except for $j = i$ (since criticality value of a node with respect to itself is meaningless).

$$\psi_i = \sum_{j\neq i} \psi_{ij} : \ 0 \leq \psi_i \leq n-1 \tag{3.8}$$

Similarly, the node susceptibility index of node i is obtained by aggregating the susceptibility values corresponding to i as follows:

$$\chi_i = \sum_{j\neq i} \chi_{ij} = \sum_{j\neq i} \psi_{ji} : \ 0 \leq \chi_i \leq n-1 \tag{3.9}$$

In heterogeneous networks, which consists of multiple infrastructure systems, it may be practically more useful to denote the criticality and susceptibility

indexes of each node in the form of vectors as follows:

$$\psi_i = \left\{ \sum_{j \neq i} \delta_j^r \psi_{ij} : r \in R \right\} = \{\psi_i^r : r \in R\} \tag{3.10}$$

$$\chi_i = \left\{ \sum_{j \neq i} \delta_j^r \chi_{ij} : r \in R \right\} = \{\chi_i^r : r \in R\} \tag{3.11}$$

where δ_j^r is an indicator vector with value 1 if j belongs to the infrastructure system type $r \in R$, and 0 otherwise. Each element in the criticality index vector of a node can be interpreted as the equivalent number of node failures in the corresponding infrastructure system triggered by the failure of that node. Similarly, each element in the susceptibility index vector of a node represents the equivalent number of nodes belonging to an infrastructure system that would trigger the failure of that node. As an alternative, the criticality and susceptibility values of a node can also be visualized as distributions which could give a better picture of network conditions due to node failures as follows:

$$F_{\psi_{ij}^r}(x) = P\left(\delta_j^r \psi_{ij} \leq x\right) : 0 \leq x \leq 1 \tag{3.12}$$

$$F_{\chi_{ij}^r}(x) = P\left(\delta_j^r \chi_{ij} \leq x\right) : 0 \leq x \leq 1 \tag{3.13}$$

where $F_{\psi_{ij}^r}(\cdot)$ and $F_{\chi_{ij}^r}(\cdot)$ are the cumulative distributions of criticality and susceptibility values of i corresponding to the infrastructure system $r \in R$, respectively. Finally, the network criticality indicator ψ and network susceptibility indicator χ, which represents the aggregate criticality and susceptibility of a network, are expressed as follows (Equation 3.14):

$$\psi = \sum_i \psi_i = \sum_i \sum_{j \neq i} \psi_{ij};\ \chi = \sum_i \chi_i = \sum_i \sum_{j \neq i} \psi_{ji} \tag{3.14}$$

The network criticality indicator or susceptibility indicator (both being equal) essentially reflects the cumulative cascading failures induced by each node in the network on other constituent nodes. Thus, they can be treated as a measure for the resilience of the network and can be used for evaluating the effectiveness of resilience measures, especially those measures intended to improve the robustness and redundancy dimensions. The resilience-oriented investments should essentially reduce the value of network criticality and susceptibility as they are intended to reduce the extent of the cascading failures in the network.

3.3.3 Prioritization of infrastructure nodes

The criticality index and the susceptibility index reflect the two important aspects of resilience of components in interdependent infrastructure networks. Sometimes, in order to prioritize nodes within a system for resilience enhancement programs, both criticality and susceptibility of nodes may need to be considered. A node that is more susceptible as well as critical must be allocated more resources than nodes that are less susceptible and critical. A combined index is proposed for this purpose and is defined as the weighted Euclidean distance between the criticality index and susceptibility index of a node (Equation 3.15).

$$\varphi_i = \sqrt{\left(\sum_k m^k \psi_i^k\right)^2 + \left(\sum_k \chi_i^k\right)^2}, \tag{3.15}$$

where φ_i is the combined index of node i and m^k is the weight factor corresponding to infrastructure k. The weight factors for criticality indexes allow the combined index to take the difference in the strategic and economic importance of various

infrastructure systems into consideration. Since susceptibility indexes reflect the effect of other node failures on a node, weight factors are equal and need not be included explicitly.

For resilience-oriented investments focusing on hazards with historical data, the probability of the occurrence of hazards at the geographical location of each node may also be needed to be considered in the computation of criticality and susceptibility indexes of nodes. Different nodes may experience different hazard probabilities which could influence the criticality and susceptibility of other nodes in the network. In such cases, criticality and susceptibility indexes can be computed as follows:

$$\psi_i = p_H^i \times \sum_{j \neq i} \psi_{ij};\ \chi_i = \sum_{j \neq i} p_H^j \times \psi_{ji} \tag{3.16}$$

where p_H^i is probability of hazard H affecting node i in a given time frame.

The nodes can be prioritized using criticality index, susceptibility index or combined index based on the type of the planned resilience investment program.

3.3.4 Prioritization of infrastructure links

Like nodes, links between infrastructure nodes are also equally important as far as resilience is concerned. Failure of infrastructure links may delay production node operations and result in network-wide disruptions. Using criticality and susceptibility indexes, one can identify important links in the network and plan strategies for improving their resilience. The most critical infrastructure link is the one whose failure would cause the highest cascading failures in the network. The

criticality of each link (i, j) can be calculated as $\psi_{(i,j)} = w_{ji}\psi_j : 0 \leq \psi_{(i,j)} \leq n-1$. Then, the most critical link (p, q) is given by $(p, q) \leftarrow \arg\max_{(i,j)\in D} \psi_{(i,j)}$.

Once the most-critical link is identified, several resilience interventions can be made. Among these, the most commonly adopted strategy is to create an alternate source for the service provided by node p to node q. This can be done by building a redundant link (s, q) where s belongs to the same infrastructure type as that of p. A heuristic algorithm for selecting the redundant link (s, q) is presented below.

Step 1: Run the agent-based IIM and update the node criticality and susceptibility values.

Step 2: Identify the most-critical link (p, q) from D, where D is the set of all links.

Step 3: Identify the type of infrastructure system $k \in K$ of the node p and all the nodes belonging to k except p. Let the set of nodes be S.

Step 4: Select the node $s \in S$ with lowest susceptibility index as follows: $s \leftarrow \arg\min_{i\in S} \chi_i$. If (s, q) exists, set $D \leftarrow D - \{(p, q)\}$ and go to Step 2. Selection of s could also consider other factors, such as the geographical proximity to q and the exposure and vulnerability of s to major hazards in the region.

Step 5: Construct (s, q) and update criticality and susceptibility values by rerunning the agent-based IIM. Set $D \leftarrow D + \{(s, q)\}$ and go to step 1.

Selecting the least-susceptible nodes for constructing redundant links would ensure that the new links are less likely to fail due to interdependent effects in the network compared to other possible redundant links of the same type.

The above algorithm does not consider the capacity limitations of the nodes while developing the redundancy enhancement scheme. However, this limitation can be easily overcome by adding a capacity constraint condition in the above algorithm. After allocating a redundant link, the capacity residual of each node can be updated in the algorithm so that unless there is enough capacity, further redundant links will not be assigned from those nodes. Interestingly, the above algorithm, although does not consider node capacity constraints, can be used to identify those infrastructure nodes whose capacity needs to be increased while constructing redundant dependencies for improving the overall network resilience.

3.4 Experiment Simulation

3.4.1 Description of infrastructure network

The infrastructure network and the dependency model used in this chapter are adopted from Balakrishnan and Zhang (2018). It is a simplified infrastructure network based in Austin, Texas consisting of nine power plants (four outside the region), 62 substations, two electrical maintenance centers, 40 hospitals, three water treatment plants (WTPs), and four wastewater treatment plants (WWTPs). The dependencies between infrastructure nodes are determined using the distance criterion where service area data was not available (each infrastructure node is connected to the nearest nodes belonging to other infrastructure systems) and system redundancy is assumed to be absent (each node is connected to only one node for a particular infrastructure service). In addition, nodes are assumed to have no capacity to negate the effects of cascading failures arising from infrastructure disruptions.

These assumptions make the network hypothetical, and the numerical results presented henceforth do not reflect the conditions of the actual infrastructure network that the network used in this study is based off. The network used in this study is presented in Figure 3.2. The dependency matrix used in the infrastructure network is presented in Table 3.4. The definition of the dependency values is in accordance with the interdependency model presented in Equation 3.1.

Table 3.4: Degree of dependencies between infrastructure nodes Balakrishnan and Zhang (2018)

		Consumer					
		Substation	Electrical Service	Hospital	Power Plant	WTP	WWTP
Producer	Substation	0	0.3	0.4	0.05	0.5	0.5
	Electrical Service	0.1	0	0.1	0.1	0.1	0.1
	Hospital	0.05	0.05	0	0.05	0.05	0.05
	Power Plant	0.9	0	0	0	0	0
	WTP	0.1	0.3	0.3	0.05	0	0.3
	WWTP	0.1	0.2	0.3	0.05	0.2	0

3.4.2 Agent-based IIM simulation for computing criticality values

The simulation framework presented in Equation 3.7 to compute criticality and susceptibility indexes of nodes is implemented in the simplified infrastructure network using the agent-based IIM. The agent-based model consists of two types of agents, namely a disaster initiator and subpopulations of infrastructure nodes belonging to the six infrastructure systems constituting the network. In each simulation, the failure of a specific infrastructure agent is triggered and the effects on other infrastructure nodes are computed. The behavior and actions of the infras-

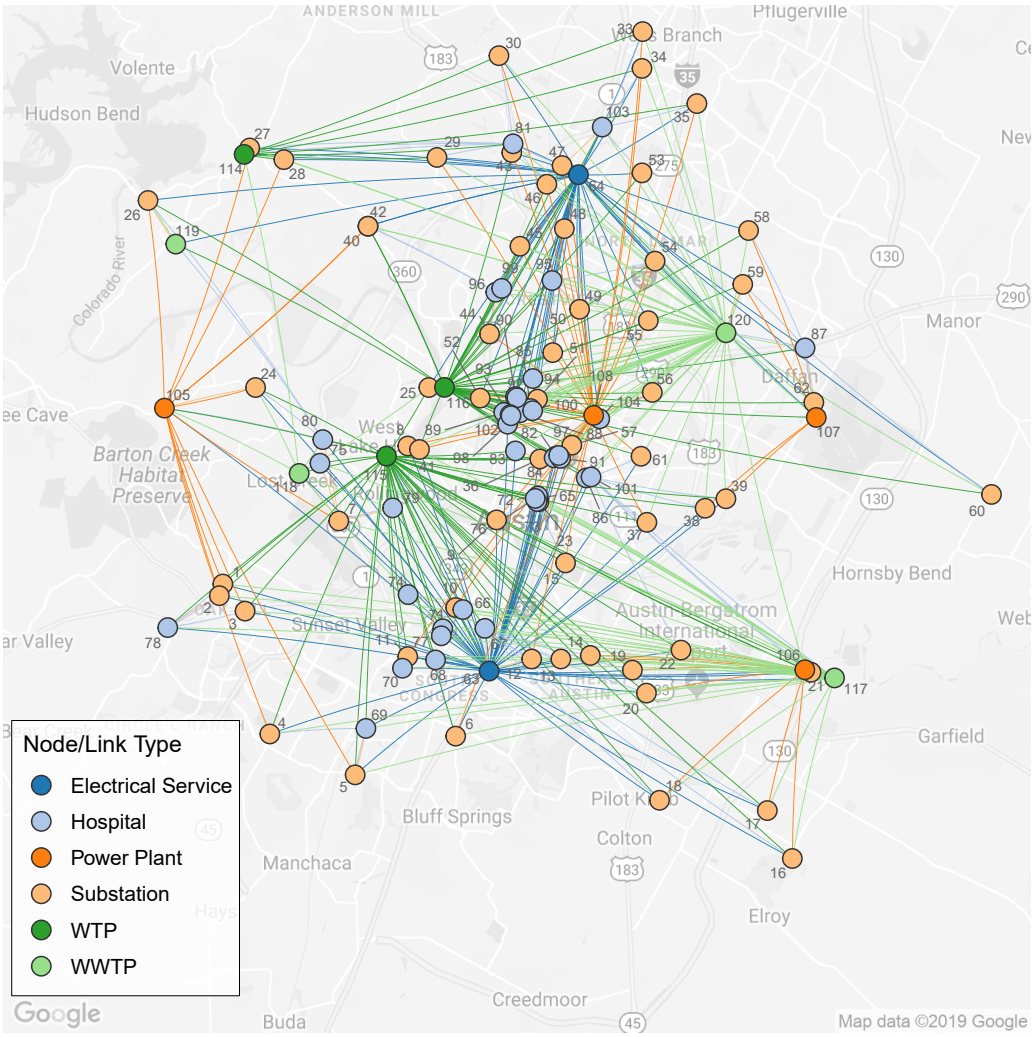

Figure 3.2: Simplified infrastructure network (The link colors represent the type of resource/service flow between two links instead of arrows to reduce the complexity of the network representation. For example, if the link color between two nodes is dark green, one of the nodes is a water treatment plant (WTP) which is the producer node and the other node is the consumer node)

tructure agents are defined using an agent state chart as shown in Figure 3.3. In the model, each infrastructure agent is assigned with a state at every time-step of the

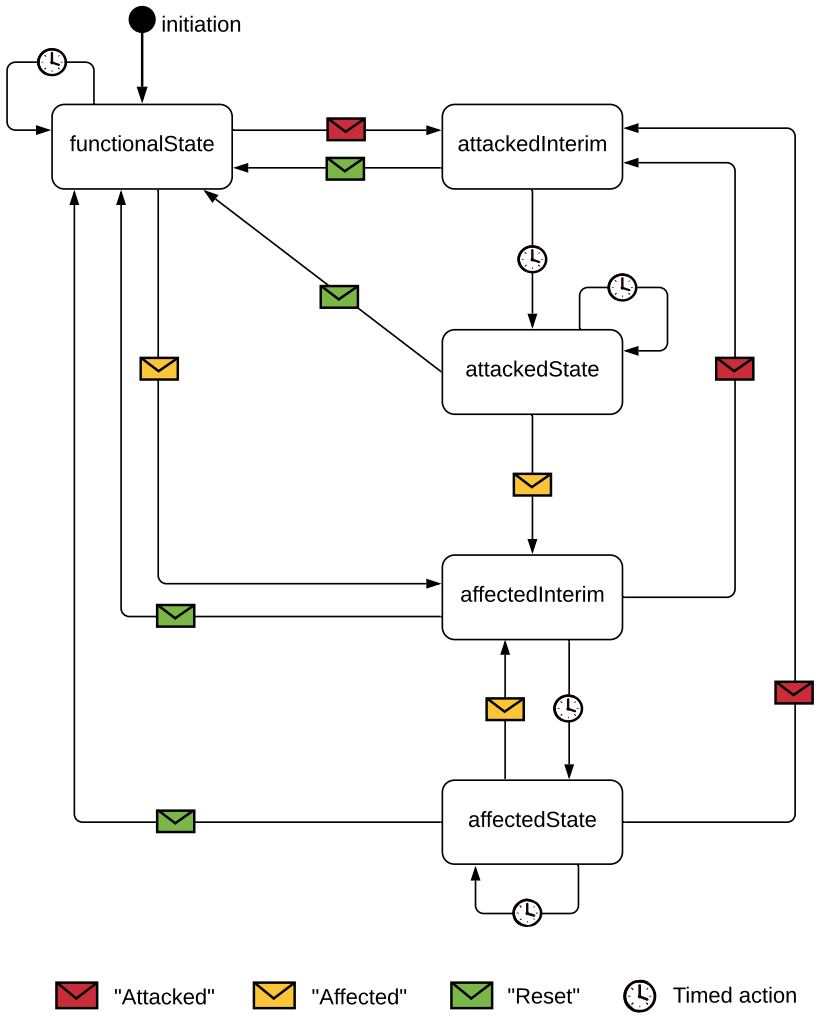

Figure 3.3: State chart used in the agent-based IIM illustrating how the behavior of infrastructure agents are modeled

simulation, which decides the behavior and actions of the agents. Each simulation is elapsed for 15 time-steps excluding the initiation. When the model is initiated, all the infrastructure agent parameters are set to their default values, and the state is set to "*functionalState*", which denotes a performance level of 1 (fully func-

tional). At the first time-step of every simulation, the disaster initiator identifies an infrastructure agent which is to be failed and sends the message "*Attacked*" to that agent. Consequently, the state of the agent changes to "*attackedInterim*" where it updates the performance level using Equation . In the next time-step (timed action), the agent switches to "*attackedState*" state where it sends the message "*Affected*" to all its dependent infrastructure agents. The agents which receive the message "*Affected*" would change their state to "*affectedInterim*", which prompts them to update their performance level to reflect the changes in the performance level of their dependee agents. In the next time-step, these agents would shift to "*affected-State*" (timed action), in which the agents will send the message "*Affected*" to all their dependent nodes and update the performance level. Additional state changes would be triggered based on the dependencies between infrastructure agents in subsequent time-steps until the final time-step in the simulation, where the disaster trigger agent would collect the latest performance levels of all infrastructure agents. Subsequently, the disaster initiator agent would also send the message "*Reset*" to all infrastructure agents, marking the termination of the simulation. The disaster trigger would also convert the collected performance level data into criticality values using Equation 3.5.

The above simulation is repeated for quantifying the network-wide effects of failure of each infrastructure agent using an iterative loop that updates the initial node to be "attacked".

3.4.3 Node criticality and susceptibility values and indexes

Figure 3.4 shows the criticality and susceptibility indexes of all nodes in the network. Since the network is heterogeneous, the criticality and susceptibility indexes are presented as vectors.

Figure 3.4a presents the criticality indexes of all the nodes in the network. Each of the stacked bars in the radial bar chart represents the criticality index vector of a node in the network. The node IDs of all nodes with a criticality index greater than five are also marked adjacent to the bars. The colored segments in each bar represent the node's criticality index components corresponding to various affected infrastructure systems (based on Equation 3.10). The infrastructure family of each node is represented by the color-coded baseline.

The results suggest that there is a significant variation in the criticality of nodes in the network. The most-critical nodes have a high chance of targeted attacks compared to other nodes. The power plants are found to be most-critical (except for a few which are outside the region under consideration) for the network, followed by WTPs, electrical maintenance centers, WWTPs, and substations. The criticality indexes of hospital nodes are comparatively lower, owing to its limited role in providing services to other infrastructure systems as evident in the dependency matrix (Table 3.4). In addition to the cross-system variations, there are variations in criticality indexes among nodes belonging to specific infrastructure systems as well. This is dominantly due to the geographical distribution of nodes and the network structure. Though each of these nodes provides the same resource or service to other infrastructure nodes, the number of dependent nodes varies. In addition,

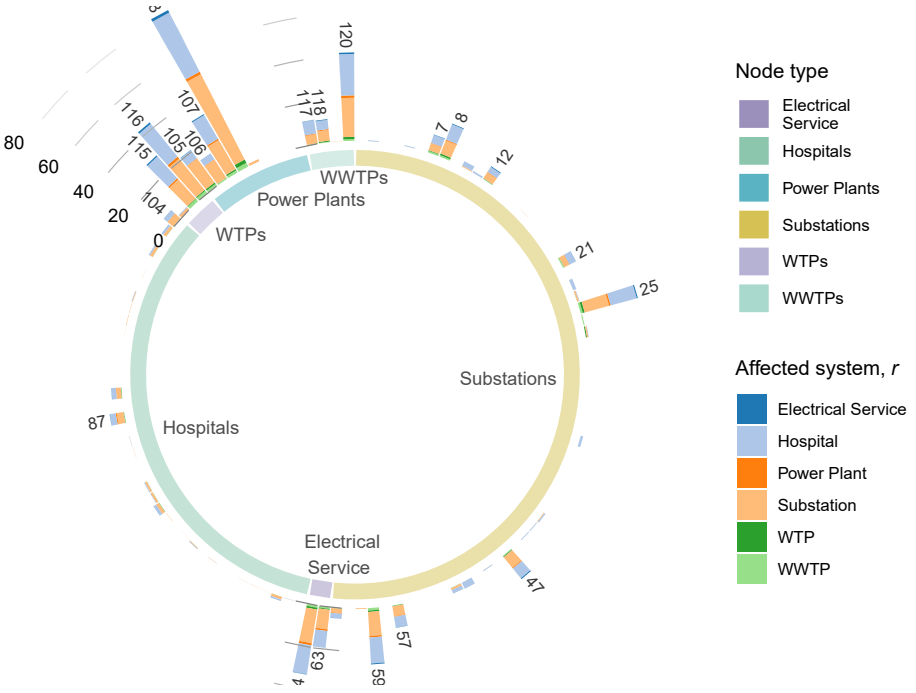

(a) Criticality index of nodes

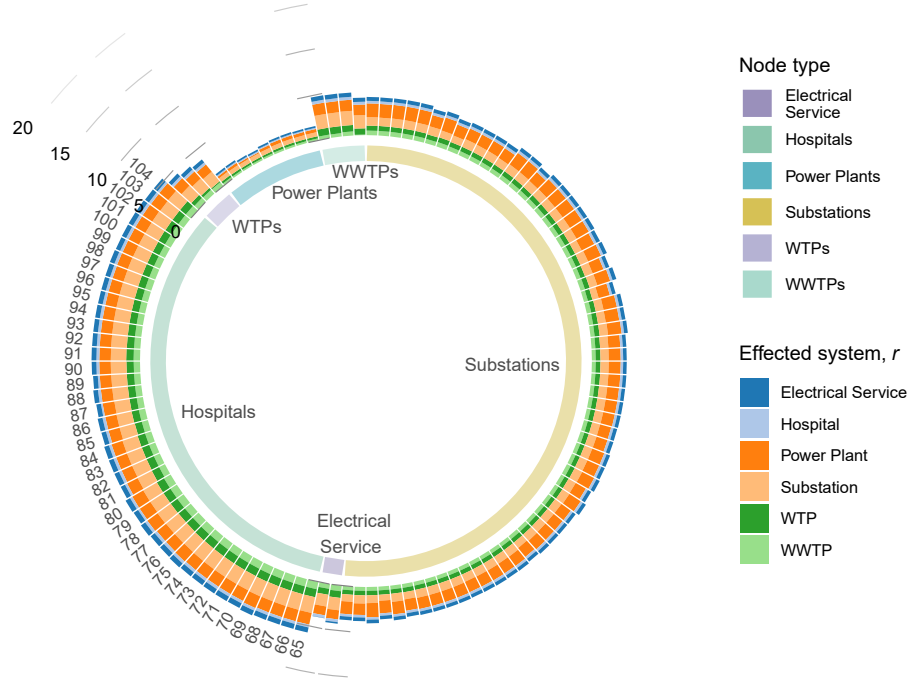

(b) Susceptibility index of nodes

Figure 3.4: Criticality and susceptibility indexes of nodes in the infrastructure network

some nodes may not provide resources to all types of nodes due to their location characteristics. These factors lead to within-system variations in criticality indexes.

Similarly, Figure 3.4b illustrates the susceptibility index vectors of various infrastructure nodes (based on Equation 3.11). The most-susceptible nodes have a higher chance of being affected by cascading failures. The results from the analysis indicate that compared to the criticality indexes, susceptibility indexes are much lower, implying that only a few nodes (mostly, the dependee nodes) can cause significant performance reductions in every infrastructure system. The cross-system variation in susceptibility indexes is more significant than the within-system variations. The most important reason for cross-system variations is the difference in the strength of dependency with different infrastructure systems. For example, the susceptibility indexes of all power plants are comparatively lower because power plants are less dependent on other infrastructure systems (according to the dependency matrix in Table 3.4). Meanwhile, with regard to the topology of the network, each node is dependent on the nearest nodes corresponding to other infrastructure systems for certain resources or services. Therefore, the number of dependee nodes for each node in the network remains the same. Hence, the major contributors to a node's susceptibility index are the dependee nodes, though some other nodes can indirectly affect its performance. Susceptibility indexes may vary if there are system redundancies.

Alternatively, criticality and susceptibility values can also be represented as cumulative distribution curves (based on Equations 3.12 and 3.13), which provide a better picture of the network conditions affecting criticality and susceptibility of

nodes. Figure 3.5 provides the cumulative distributions of criticality and susceptibility values of the most-critical and the most-susceptible infrastructure nodes in the network.

In Figure 3.5a, each subfigure corresponds to the most-critical node belonging to one of the six infrastructure systems in the network. Each curve represents the cumulative distribution of criticality values of the node with respect to an affected infrastructure in the network. Color codes are used to differentiate among various infrastructure systems. The curves can also be interpreted as the distribution of interdependent effects on each infrastructure system induced by the failure of the node. For example, the cumulative distributions corresponding to the most-critical power plant node are shown in the "Power Plant" subfigure in Figure 6a. It can be seen that the distribution curves corresponding to the power plant node are the most diverging from the origin, indicating that the failure of that node will have significantly more effect on the network compared to the failure of the most-critical nodes belonging to other infrastructure systems. The most-critical hospital node ("Hospital" subfigure in Figure 6a) is the least critical node among the given nodes.

Similarly, Figure 3.5b shows the susceptibility distribution curves of the most susceptible nodes belonging to each infrastructure system. Distribution curves presented in each subfigure can be interpreted as the cumulative distributions of interdependent effects induced by the failure of nodes belonging to various infrastructure systems on the most susceptible node shown. For example, in "Substation" subfigure in Figure 3.5b, the bright green curve represents the distribution of interdependent effects of WTP node failures on the most-susceptible substation

(a) Cumulative distribution of criticality values of the most critical nodes

“

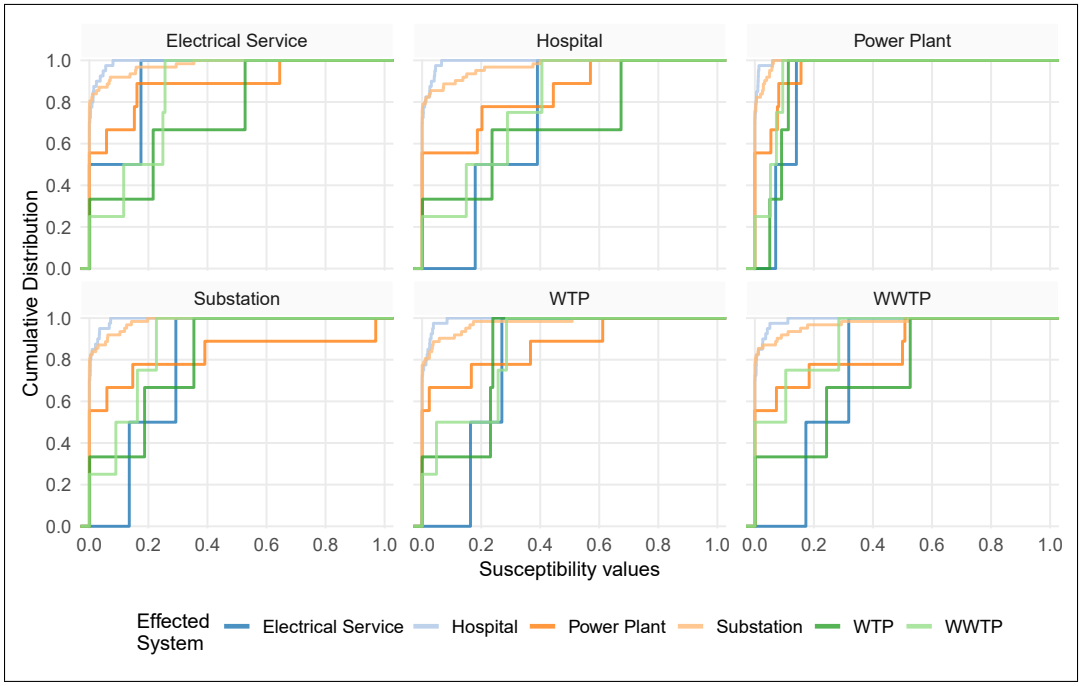

(b) Cumulative distribution of susceptibility values of the most susceptible nodes

Figure 3.5: Cumulative distributions of criticality values of most critical nodes and susceptibility values of most susceptible nodes

node. The power plant node ("Power Plant" subfigure in Figure 3.5b) is the least-susceptible among all the given nodes, as its susceptibility distribution curves are the least divergent among all the most-susceptible nodes. On the contrary, the most-susceptible node is the hospital node ("Hospital" subfigure in Figure 3.5b) as it has the most divergent susceptibility distribution curves among all the nodes.

3.4.4 Combining criticality and susceptibility indexes

The combined index of each node, which is indicative of the combined criticality and susceptibility is calculated using Equation 3.15. The weight factors for criticality indexes corresponding to all infrastructure systems were assumed to be equal. Figure 3.6 presents the combined indexes of nodes in the network. Since the susceptibility indexes of nodes are much lower than the criticality indexes, it can be seen that combined indexes are mostly determined by the criticality indexes of nodes. The power plant with the highest criticality value has the highest combined index, whereas, hospitals have the least combined index along with some substations, WTPs, power plants (which are located outside the region), and WWTPs. The combined index could be used to rank nodes within infrastructure systems for allocating resources for resilience enhancement.

3.4.5 Development of a redundancy enhancement plan for improving network resilience

Building redundant links in the network is one of the methods often chosen by utility companies and other infrastructure agencies to improve the resilience of respective systems. The algorithm presented in this chapter for identifying re-

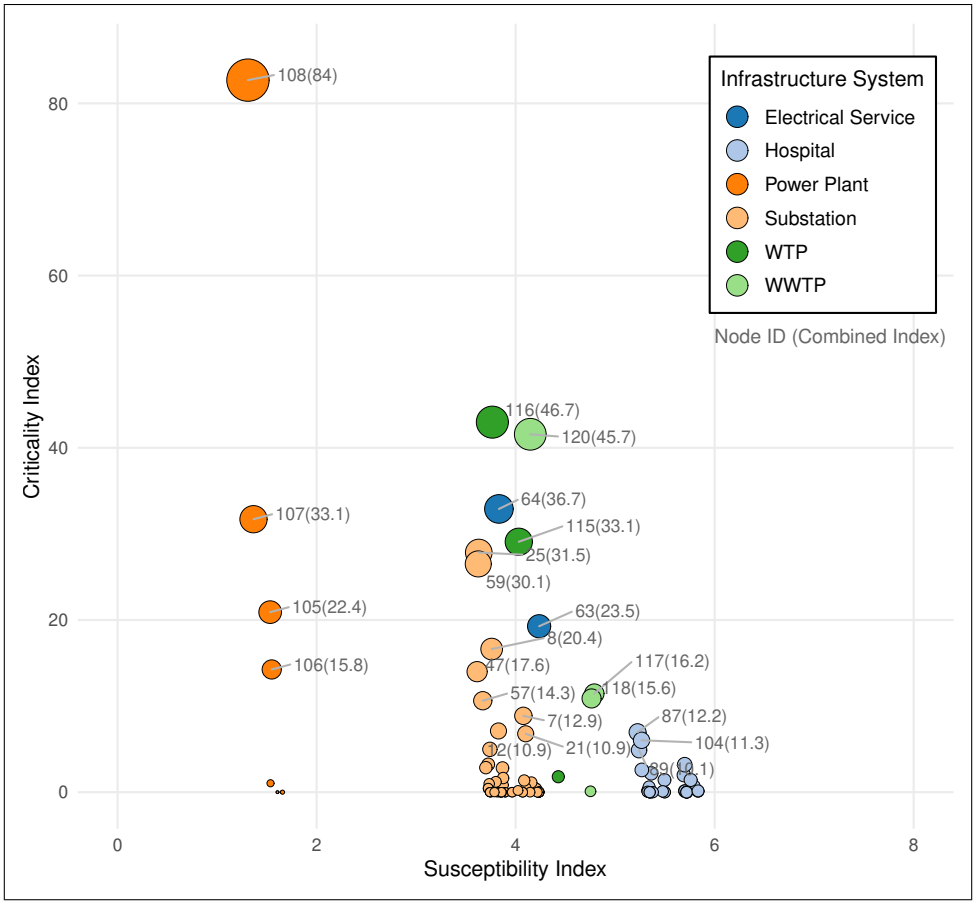

Figure 3.6: Combined index of nodes in the infrastructure network

dundant links to be built into the infrastructure networks can effectively be used for developing a resilience-enhancement plan. The algorithm was used to identify the first twenty redundant links to be built in the simplified Austin network to improve the resilience of the entire network. The effect of the sequential addition of the prioritized redundant links on network criticality and susceptibility is illustrated in Figure 3.7. The network criticality and susceptibility indicators are normalized by that corresponding to the base network for the convenience of comparison of

improvements. The redundant links are represented by the node pair.

As evident in Figure 3.7, the values of the network criticality and the network susceptibility indicators drastically reduce with the initial additions of redundant links and then slow down with further redundancy improvements. With the addition of only 20 redundant links (among $n(n-1)-|D| = 120 \times 119 - 551 = 13,729$ possible links), the network criticality (and susceptibility) was reduced by more than 57% compared to that in the base network with no redundant links. This suggests that the overall chance of cascading effects as well as the overall degree of exposure of constituent nodes to cascading effects in the network were reduced by more than a half due to the addition of the selected redundant links. The figure also illustrates how the system-level criticality and susceptibility also reduces with the addition of each of the redundant links.

An important point to note is that the reduction in the values of the network criticality or susceptibility indicators is not smooth. This is because these indicators are based on the cumulative sum of individual cascading effects across all node pairs with links between them. Cascading failures of several nodes may overlap, and therefore the improvement due to the addition of redundant links is not strictly monotonous; nevertheless, the values of network criticality and susceptibility shall reach zero when all nodes have redundant links for each of the infrastructure service needed for functioning.

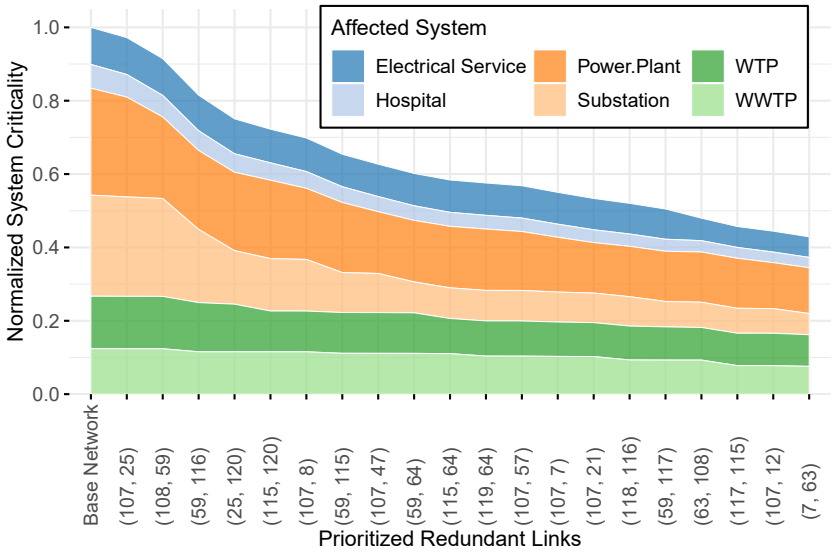

(a) Reduction in criticality

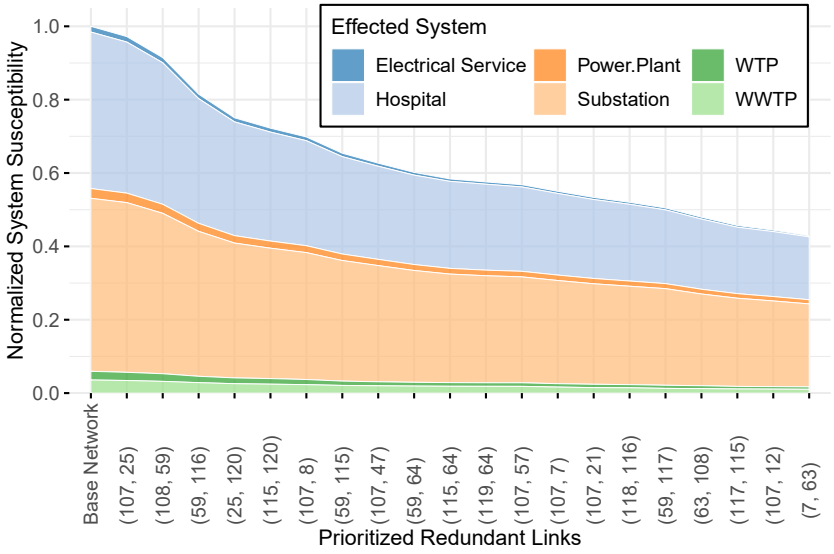

(b) Reduction in susceptibility

Figure 3.7: Network-level and system-level reduction in criticality and susceptibility metrics as a result of the implementation of the redundancy enhancement program

3.5 Conclusion

In this chapter, the authors presented two generic resilience indicators to rank and prioritize infrastructure nodes (and thereby links) in terms of two aspects related to cascading failures in infrastructure networks: (a) their necessity to operate for the functioning of the whole network (criticality); and (b) their exposure to cascading effects arising from disruptions in other components (susceptibility). The indexes introduced in this chapter to measure the above two properties of infrastructure nodes can be used to identify the nodes (and links) which require resources for protection from the direct impact of external hazards as well as the nodes which require capacity enhancement to isolate them from cascading effects. This chapter also presented a heuristic algorithm based on the developed indexes to identify the most-critical links and build redundancies to reduce the network's dependence on them. This chapter also implemented the methodology on a simplified network to demonstrate the computation of the resilience indexes and their application to develop a redundancy scheme to enhance resilience against cascading failures in the network. It must be noted that the case study was conducted based on several assumptions with respect to the interdependencies in the network and the intrinsic resilience of infrastructure nodes. Therefore, the results are not indicative of the conditions of the real network. However, the methodological framework and process can be adapted to conduct similar analyses with real data when available.

There are several key advantages of using the indexes from the perspective of infrastructure resilience management:

1. The indexes are not dependent on the specific model used for estimating the

interdependent impacts of infrastructure failures (though IIM was used in this chapter). The indexes are equally appropriate even if an interdependent infrastructure model which captures the real-world operational characteristics of the component infrastructure systems are used to model the network.

2. The indexes are well-suited for capturing the resilience improvements in the network due to resilience interventions based on robustness and redundancy, which are crucial to pre-disaster preparedness.
3. The indexes are easy to comprehend and could be easily communicated with domain experts as well as the public.
4. The indexes can be combined with vulnerability metrics related to component infrastructure systems to develop resilience indicators for specific external hazards.

The key limitations of the proposed resilience indexes include:

1. The indexes do not take into account the social, economic, and ecological significance of infrastructure network components. A node that has a low criticality index in the given network may be significantly important for residing communities or economic systems. Similarly, a node that has a low susceptibility index in the network may still be vulnerable to changes in the socio-economic landscape.
2. The indexes do not incorporate the rapidity and resourcefulness dimensions of system resilience. Rapidity and, to an extent, resourcefulness are properties that are more crucial in immediate restoration of a disrupted system and the recovery afterward, as the main objective during these phases is to op-

timize network performance in the shortest possible time with the available resources. However, the inclusion of rapidity and resourcefulness in the resilience indexes presented in this study requires additional information on the amount of resources required for restoring various components and the speed at which they could be restored/recovered. Nevertheless, the current form of the indexes for prioritization of infrastructure components would still work well for prioritizing post-disaster interventions, given there are no resource constraints during restoration and recovery phases of disaster management.

3. The risk of failure of infrastructure links (direct or interdependent) due to an extreme event is not considered in the present study. This may be relevant in the case of physical infrastructure interconnections such as pipelines, electricity grids, or transportation networks. If the physical links also need to be considered, the current agent-based IIM may be modified by including "link" agents so that the impact of external effects on them can also be quantified. However, this would neither change the basic definition of the resilience indexes presented in this study, nor the way they are calculated.

The methodology has several potential applications in the area of infrastructure resilience management. During the planning phase of infrastructure systems, the framework can be used to evaluate the best topological design for resilience infrastructure networks in new cities. In the case of existing cities, the framework can be used to identify the most-critical and most-susceptible infrastructure components and can devise appropriate resilience enhancement programs. In addition, the framework can also be used to incorporate the resilience criterion in current

infrastructure management practices which mostly focus only on infrastructure performance criterion and do not account for failures due to extreme events where infrastructure interdependencies are of vital importance. To summarize, this chapter provides an organized approach to planning, designing, and implementing projects for resilience enhancement, especially in urban and rural settings where accurate infrastructure interdependency data are either unavailable or non-existent.

Finally, though the resilience indexes are presented in the context of infrastructure networks, it can also be used for generic resilience evaluation of other weighted bidirected networks with similar functional characteristics, such as certain economic networks, global trade networks, etc.

Chapter 4

Application of the Hybrid Risk Measure to Prioritize Vulnerable Communities and Economic Centers for Emergency Planning[1]

4.1 Introduction

Today, cities constitute the most critical element of the social and economic development of nations. The two most important components of cities are the infrastructure network and the communities. The mutual dependence of these two components has resulted in efficient and constantly evolving cities. However, this integral nexus, while being an opportunity, is also a challenge for urban planners, because disturbances on either of these two components by any external incident will have far-reaching consequences in the other, and has the potential to bring a city to halt. Due to the networked structure of urban infrastructure systems, failure of a system could further trigger the failure of dependent systems in the network, and consequently cause widespread disruptions in public utility services. This has been evident in many past incidents like the World Trade Center attack in 2001, the Northeast blackout in 2003, the Indian Ocean earthquake in 2004, etc. These

[1]based on Balakrishnan, S., and Z. Zhang. (2018). Developing Priority Index for Managing Utility Disruptions in Urban Areas with Focus on Cascading and Interdependent Effects. *Transportation Research Record: Journal of the Transportation Research Board.* 2672(1), 101–112, https://doi.org/10.1177/0361198118774239

events were unforeseen, and their consequences on infrastructure systems were aggravated by the complex and interdependent structure of the urban infrastructure network. Thus, during such disasters, urban communities are susceptible not only to the direct impacts of the disaster but also to prolonged utility disruptions resulting from the inability of infrastructure systems to function at satisfactory performance levels. At present, there are vulnerability assessment tools to predict the direct impact of disasters on communities. However, there is a lack of models to evaluate the indirect impacts, such as large-scale utility disruptions. In this chapter, the authors present a framework and modified measure called Priority Index (PI) to prioritize relief operations during emergencies that would simultaneously augment the infrastructure and community resilience of a city.

The rest of this chapter is organized as follows: the Literature Review section presents a review of existing literature pertaining to this chapter; the Methodology section elaborates on the framework adopted for developing PI; the Case Study section demonstrates the implementation of the methodological framework; and the Conclusion section lists the findings.

4.2 Literature Review

The characteristics of a city are largely dependent on its infrastructure systems, such as utility services, economic institutions, and transportation infrastructure. Infrastructure systems are critical for ensuring an adequate supply of resources and services to communities, economic sectors, and other social institutions in a city. In addition, several studies in the past have validated the constructive role of

urban infrastructure in stimulating the social and economic development of cities and nations. Some of the areas in which infrastructure development made significant improvements are economic development (Kumari & Sharma, 2017), poverty alleviation (Ogun, 2010), social equity (Calderon & Serven, 2010), and agricultural and regional development (Pinstrup-Andersen & Shimokawa, 2007).

A modern urban infrastructure network can be considered as a complex and dynamic system of interconnected and interdependent infrastructures. Rinaldi et al. (2001) classified the interdependencies existing among infrastructure systems into four categories, namely, physical, geographic, cyber, and logical interdependencies. Physical interdependency is linked to material flows, whereas, cyber interdependency pertains to information flows. Geographic interdependency relates to physical proximity, and finally, logical interdependency encompasses all other types of interdependencies. In an interconnected network, the performance of an infrastructure system is influenced not only by its functional capability but also by the performance of its dependee systems. Though the interdependent nature of urban infrastructure ensures the operational efficiency of component systems, it can also increase system vulnerability (Ouyang & Wang, 2015). A disruptive event that affects an infrastructure system could trigger cascading and interdependent effects on its dependent systems, degrading their functional efficiency. The ability of communities to endure such disruptions depends on their socio-economic characteristics. However, major social and economic disparities among urban communities are commonplace in cities. Hence, from an emergency management perspective, the disaster risks arising due to such interdependencies on infrastructure systems

and communities need to be assessed using an integrated approach. The first step in the process of evaluating the vulnerability in an infrastructure network is to quantify the consequences arising due to interdependencies.

4.2.1 Methods for quantifying interdependent effects of hazards

Ouyang (2014) identified and classified various methods for quantifying the interdependent effects in networked infrastructures into five categories, namely, empirical-, agent based-, system dynamics based-, economic theory based-, and network based approaches. In the empirical approach, the interdependencies are quantified based on historical failure patterns and expert experience (Chang, McDaniels, Mikawoz, & Peterson, 2007). Agent-based models consider each component of a complex infrastructure network as an autonomous agent whose functions are decided by a set of well-described rules. This is a bottom-up approach which can be used to simulate the interdependent effects in large-scale urban systems (Dudenhoeffer, Permann, & Manic, 2006). Studies like the one by Brown et al. (2004) used principles of system dynamics to evaluate the potential risks to critical systems arising from the interdependencies in infrastructure networks. Another important approach is the inoperability input-output model (IIM) derived from the Leontief Input-Output economic model used for assessing the stability of economic systems (Y. Haimes & Jiang, 2001). This approach has been used in several hybrid models for evaluation of infrastructure interdependencies. Recent studies have focused more on models based on network theory (Svendsen & Wolthusen, 2007). An infrastructure system can be treated as a graph, where nodes represent infrastructure

components and links represent interdependent relationships.

4.2.2 Methods for evaluating social vulnerability to hazards

The approaches summarized in the previous section have been used for evaluating the effect of interdependencies in aggravating the risks on infrastructure networks arising from unanticipated events. The authors also conducted another phase of the literature review to understand how hazard risks on urban communities are evaluated, and whether interdependent effects are considered in the evaluation.

Social vulnerability indicates how sensitive communities are to hazards, and their ability to respond during such events. The metrics to evaluate the vulnerability of communities to hazards can be broadly classified into two categories: generic vulnerability measures and event-specific vulnerability measures. The generic vulnerability measures use surrogate socio-economic, built-environment, and demographic variables to identify the most vulnerable communities. Cutter, Boruff, and Shirley (2003) constructed a Social Vulnerability Index (SoVI) for evaluating the social vulnerability of communities to environmental hazards. The researchers identified 42 relevant variables from US Census data to develop SoVI for the counties in the United States. In a similar effort, Flanagan, Gregory, Hallisey, Heitgerd, and Lewis (2011) developed another generic social vulnerability index (SVI) for the Agency for Toxic Substances and Disease Registry using 15 census variables pertaining to socio-economic status, household characteristics, demographic characteristics, and housing characteristics. SVI is an ordinal measure that indicates the percentile rank of census tracts based on the variables. Though the index provides

the vulnerability ranks of census tracts, relative comparisons about the magnitude of vulnerability are not possible. Huang and London (2012) developed a census block level social vulnerability index as a measure of the health challenges posed by hazards, based on six variables, namely, proximity to health care facilities, poverty rate, education, linguistic isolation, race/ethnicity, and age. The advantages of this index are that it is a normalized value between 0 and 1, and that it can be used for relative vulnerability comparisons.

Event- or hazard-specific social vulnerability measures, along with generic vulnerability factors, also account for the factors or policies that can augment the community's response to that hazard. For example, Chakraborty, Tobin, and Montz (2005) combined generic vulnerability index and geophysical risk index (an index based on vulnerability to floods) to prioritize evacuation assistance needs in Florida. Schmidtlein, Shafer, Berry, and Cutter (2011) simulated the potential earthquake losses in South Carolina using the HAZUS-MH software (developed by the Federal Emergency Management Agency) and assessed the correlations with SoVI values. The study also identified the most significant census variables that are correlated with losses to earthquakes. Rygel, O'sullivan, and Yarnal (2006) developed a social vulnerability indicator for assessing the impact of storm surges resulting from hurricanes. The researchers performed the principal component analysis to identify the most relevant set of factors affecting vulnerability to the hazard under consideration.

4.2.3 Gaps in the literature

The review revealed that literature is scarce when it comes to evaluating the vulnerability of communities to widespread utility service outages resulting from various types of hazards. The direct impacts of disasters on communities, such as health hazards and physical harm, may be limited to the location of occurrence. However, the indirect impacts, such as prolonged utility service disruptions arising from infrastructure system failures during a disaster, are more likely to affect communities in other regions of cities, as well. This warrants the need for a framework to assess and prioritize communities that are most vulnerable to the indirect impacts of disasters resulting from the interdependent nature of infrastructure systems.

4.3 Methodology

Figure 4.1 presents the methodological framework adopted for developing the Priority Index (PI). The index is designed to rank census tracts based on their vulnerability to utility disruptions resulting from an unanticipated event. The framework consists of two independent components. The first component is the quantification of impacts of the event on the performance of various utility systems in the infrastructure network (from which a community's exposure to such disruptions can be quantified) using agent-based modeling (ABM) approach. The exposure would depend on the structure of the infrastructure network, and the interdependent relationships existing among its various components. The second component is the evaluation of the social vulnerability of communities residing in the affected regions from publicly available American Community Survey (ACS) data. Social

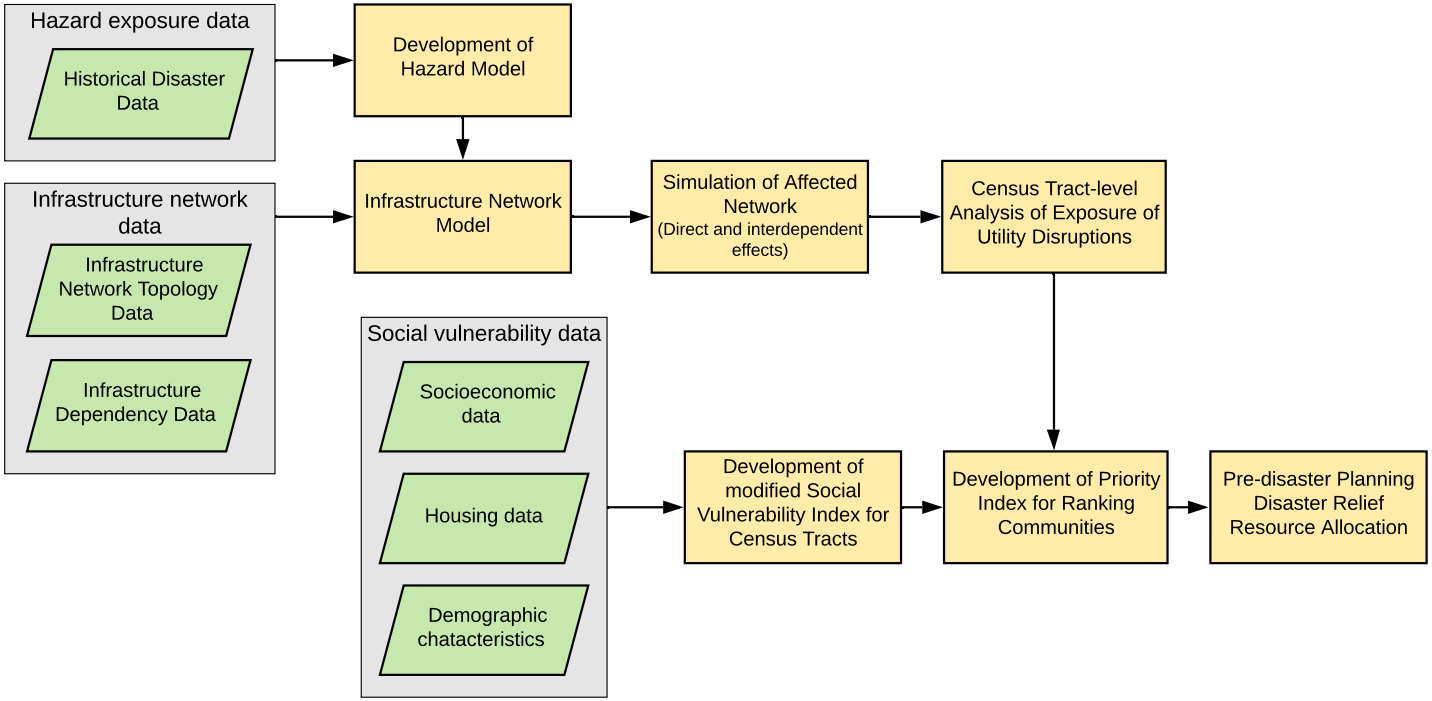

Figure 4.1: Methodological framework for developing Priority Index

vulnerability variables could be used as surrogate measures to evaluate the capability of communities in a census tract to endure prolonged utility disruptions. Once the exposure and social vulnerability are quantified, they are combined to develop the PI. In the rest of the section, the various stages in the development of PI are elaborated.

4.3.1 Simulation of disruptive event and evaluation of post-event performance of infrastructure network

Every urban infrastructure network consists of numerous interconnected and interdependent infrastructure systems (or utility services) such as electricity grid, water supply system, sewage disposal system, and so on. Though each of these infrastructure systems is established independently, they depend on other infrastructure systems for their proper functioning. The degree of dependency of an infrastructure system on another is affected by various factors, including the resources and services required by the former, the resources and services produced by the latter, geographical proximity, etc. Any degree of performance drop in one infrastructure node in the network could trigger further performance drops in its dependent nodes in the presence of such dependencies and or interdependencies. This may disrupt the normal supply of multiple utility services in the affected regions.

As mentioned before, the first stage in the process of developing PI is to analyze and estimate the network level performance drop in various utilities which might occur due to the disruptive event. The network-wide effects of utility disruptions are simulated using the agent-based model presented in Chapter 2 as shown

in Equation 4.1. Note that instead of fuzzy interdependency values, deterministic values are used in the simulation model for this study.

$$P_j(t) = \max\left(0, P_j(0) - \left[\sum_{k^* \in K_j^*(t)} \left(P_{k^*}(0) - P_{k^*}(t - \Delta t)\right) \tilde{w}_{jk^*}\right] - \rho_j \iota_j^H\right) : 0 \leq P_j(t) \leq 1, \tag{4.1}$$

where $P_j(t)$ is the performance of node j at time t, $P_j(0)$ is the performance of j before the occurrence of the extreme event H Δt is the time step in the simulation, $K_j^*(t)$ is the set of dependee nodes of j with the highest performance level corresponding to each infrastructure system $r \in R$ in the previous iteration, $\tilde{w}_{jk^*}$ is the dependency of node j on node k^*, ρ_j is the indicator variable with value 1 if $t - T > \frac{\ell_{jp}}{\nu}$, and 0 otherwise, and ι_j^H is the degree of impact of extreme event H on node j. The performance loss of a node j at any time t is given by $P_j(0) - P_j(t)$.

4.3.2 Spatial analysis of hazard exposure and social vulnerability of communities

Once the post-event expected performance of utility services is estimated, the analysis must identify how the disruptions affect the communities. For this purpose, the following steps are adopted:

1. Create an adequate sample of buildings that are dependent on the disrupted utility services based on the actual spatial distribution of building footprint in the study area.

2. Identify and map the dependent utility service nodes to each building in the

sample and their corresponding post-event performance levels.

3. Identify and map the buildings to the corresponding census tract to which they belong.

4. Evaluate the distribution of utility service disruptions in each census tract from the building data. This provides information about the exposure of each census tract to the utility service disruptions resulting from the reduced performance levels of the infrastructure nodes.

Next, the generic social vulnerability characteristics of communities are analyzed. The underlying assumption is that those populations with higher social vulnerability to disasters are more likely to be affected than their counterparts with lower social vulnerability during a disaster or disruptive event. Data from censuses and related updates can be used to obtain relevant information about the demography, infrastructure, and socio-economic characteristics of communities residing in the city. In the United States, the Census Bureau conducts the American Community Survey (ACS) to collect data regarding communities at various geographic levels every year. Based on the ACS data, the Agency for Toxic Substances and Disease Registry (Flanagan et al., 2011) has developed a Social Vulnerability Index (SVI) for each of the census tracts using 15 social factors that describe a community's social vulnerability (Table 4.1). However, the limitation of SVI is that it is an ordinal measure and hence does not convey the magnitude of relative differences in vulnerability across regions. Hence, a modified Social Vulnerability Index (mSVI) is developed based on the same set of variables, which also accounts for the relative

difference in social vulnerabilities. An approach like the one suggested by Huang and London (2012) is adopted for developing mSVI.

Table 4.1: Social factors considered in developing Social Vulnerability Index (Source: Agency for Toxic Substances and Disease Registry)

Category	Variables
Socio-economic status	• % of population below poverty • % population unemployed • per capita income† • % population without high school diploma
Household composition & disability	• % population older than 65 years of age • % population younger than 17 years of age • % civilians with disability • % single parent household
Minority status and language	• % population belonging to minority communities • % population speaking English "less than well"
Housing and transportation	• % multi-units structures • % mobile homes • % housing units with more people than rooms • % households with no vehicle • % persons in institutionalized group quarters

†During the calculation of mSVI, per capita income (pci) is converted into a percentage variable which is equivalent to the ratio of the difference between the highest tract-level pci in the region and that in the current census tract to the same highest tract-level pci.

Consider a census tract, m, with the social factors listed in Table 4.1 denoted by a set, S. The corresponding mSVI is given by Equation 4.2.

$$mSVI_m = \frac{\sum_{s \in S} s_m}{15 \times 100} \tag{4.2}$$

In order to convert $mSVI_m$ to its normalized form, Equation 4.3 is employed.

$$mSVI_{m,norm} = \frac{mSVI_m}{\max(mSVI_m)} : 0 \leq mSVI_{m,norm} \leq 1 \tag{4.3}$$

4.3.3 Development of Priority Indexe

The final step is to combine the exposure and social vulnerability of census tracts to develop the Priority Index. If the expected performance of utility service K in census tract m is denoted by P_K^m, then the weighted exposure in census tract, E_m is given by Equation 4.4.

$$E_m = \sum_K (1 - P_K^m) \times \omega_K^m : 0 \leq E_m \leq 1, \tag{4.4}$$

where ω_K^m is the weight for utility service K in census tract m. PI of a census tract for a given disruptive event, PI_m, is defined as the product of weighted exposure (E_m), and normalized social vulnerability index ($mSVI_{m,norm}$) corresponding to m.

$$PI_m = E_m \times mSVI_{m,norm} : 0 \leq PI_m \leq 1 \tag{4.5}$$

If a census tract has a high social vulnerability and high exposure to the event, the PI will be close to 1. Conversely, if the census tract has a low social vulnerability and is subjected to low exposure, the PI will be close to 0. Thus, the PI could be used to identify those census tracts that require immediate attention after a hazard occurs in the infrastructure network. This would help in making decisions that ensure the rational utilization of available resources during emergencies.

4.4 Case Study

4.4.1 Description of infrastructure network

Similar to Chapter 3, the city of Austin, Texas is chosen for the case study. The primary goal of this chapter is to present a methodology to prioritize urban

regions for managing utility service disruptions during a hazard or disruptive event, rather than the accurate quantification of interdependent risks. Hence, the author created a semi-realistic network by limiting the number of utility services and adopting hypothetical values for interdependencies. The infrastructure systems chosen for the study are power plants, substations, electricity maintenance services, water treatment plants, and sewage treatment plants. The location details of the infrastructure nodes are obtained from public data and reports published by the City of Austin (2009, 2017), and are presented in Figure 4.2. For the simplicity of the network, it is assumed that each of the infrastructure units has a unique service area, which does not overlap with each other. The details regarding the service areas of water treatment plants, sewage treatment plants, and electrical maintenance service stations are obtained from respective utility websites and official reports published by the City of Austin. For those infrastructure systems such as substations and power plants (for which the service area details are not available), the service area is decided by the distance criterion, *i.e.*, all other utilities and buildings under study depend on the nearest substation and every substation depends on the nearest power plant for its functioning. In addition to the locations of infrastructure nodes and their respective service areas, information regarding dependencies is also required for simulating the indirect impacts of the disruptive event on the network. Since this information was not available, appropriate values are assumed and are presented in Figure 4.3. The values represent the reduction in performance at the consumer node if the producer node, which it is dependent on, is completely failed.

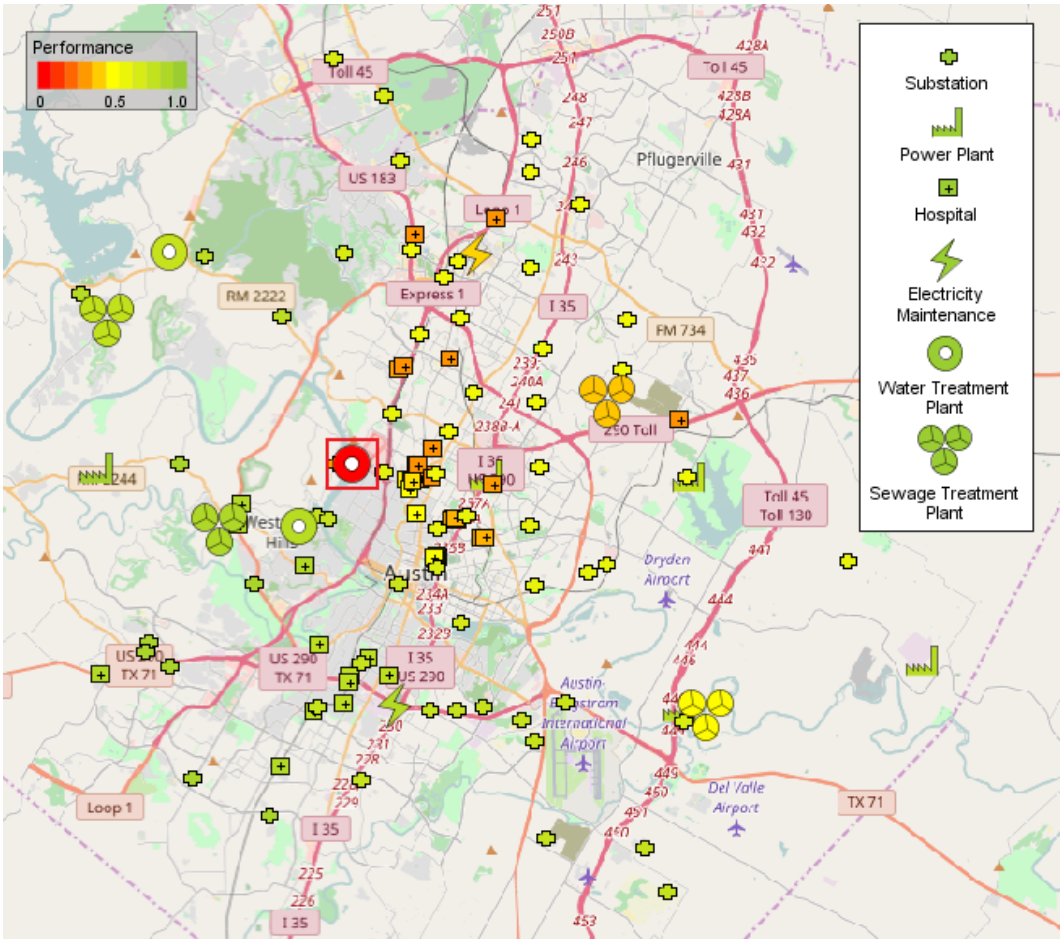

Figure 4.2: Semi-realistic infrastructure network and impacts of the failure event: The initial failure occurs in the water treatment plant (marked in red line). Due to the interdependencies, the effect propagates to other infrastructure systems. The color of the infrastructure nodes represents their performance level after the event occurs (red indicates that the node failed, and green indicates that the node is still functioning).

4.4.2 Simulation results

As discussed earlier in this chapter, the agent-based modeling approach is used to simulate the propagation of cascading and interdependent effects on the

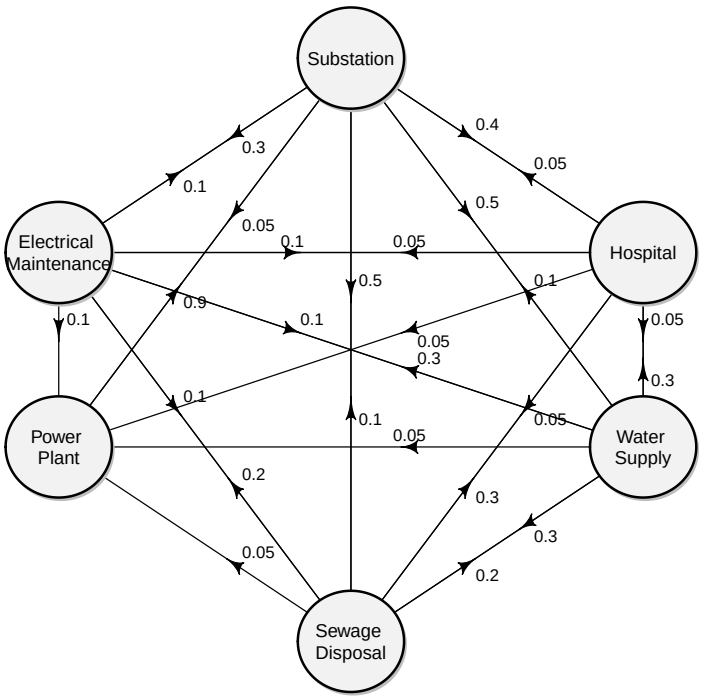

Figure 4.3: Assumed dependencies among infrastructure systems: Every edge represents dependency, and the direction of the arrows represents the direction of dependency (flow of resource or service). The number adjacent to each arrow represents the degree of dependency. For example, a dependency of 0.3 from the water supply node to the sewage disposal node suggests that if the water supply completely fails, the percentage of performance reduction in the sewage disposal system dependent on it is 30%. An edge with arrows in both directions represents interdependency.

infrastructure network. To demonstrate this, an artificial disruptive event is generated which caused a water treatment plant to stop functioning entirely as shown in Figure 4.2 (denoted by the red rectangle). It is assumed that all the infrastructure nodes in the network function at maximum performance levels prior to the event. The Anylogic® software package (The Anylogic Company, 2017) is used to con-

struct the infrastructure network model and simulate the impact of the event on the network. A step size of 1 minute is used for the simulation.

Figure 4.4 presents the simulated progression of expected system performance of various utility services after the disruptive event is generated. The failure of the water treatment due to the initial event is reflected in the expected performance of utility services such as health care, electricity, and sewage disposal, due to the existing interdependencies in the network. As can be seen in the figure, the initial reductions in expected performance (lower order) in all utility systems are abrupt compared to the subsequent reductions. The initial reductions result from the direct and cascading impacts caused by dependencies. The comparatively smaller, and higher-order reductions in expected performance in the later stages could be attributed to indirect and interdependent effects. Once the higher-order effects become negligible, the affected utility systems stabilize and attain a new equilibrium,

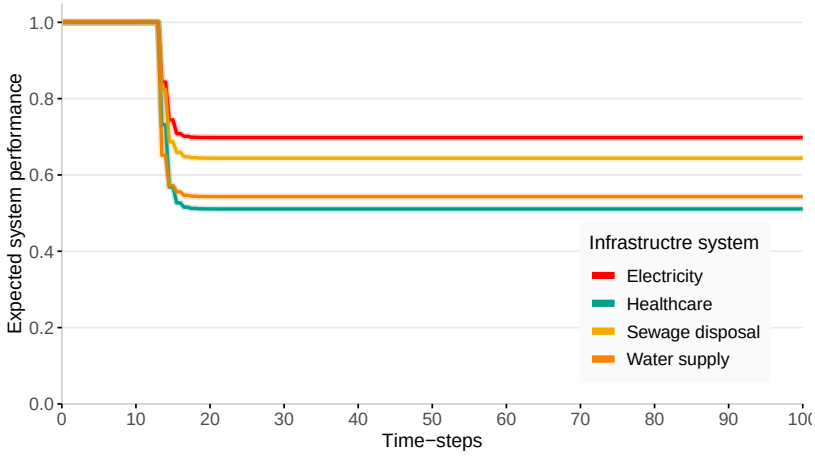

Figure 4.4: Simulated impact of the disruptive event on the expected performance of infrastructure network

but with reduced performance levels.

Figure 4.5 presents the distribution of the expected performance levels of utility services in various census tracts. The expected performance level of electricity supply in various census tracts after the event ranges from 35 percent to 92 percent with an average of 70 percent (Figure 4.5a).

Similarly, the expected service level of hospitals ranges from 28 percent to 87 percent with an average of 52 percent (Figure 4.5b). The expected performance of water supply service ranges between 0 percent and 84 percent with an average of 54 percent (Figure 4.5c), and that of sewage treatment service ranges between 39 percent and 89 percent with an average of 45 percent (Figure 4.5d).

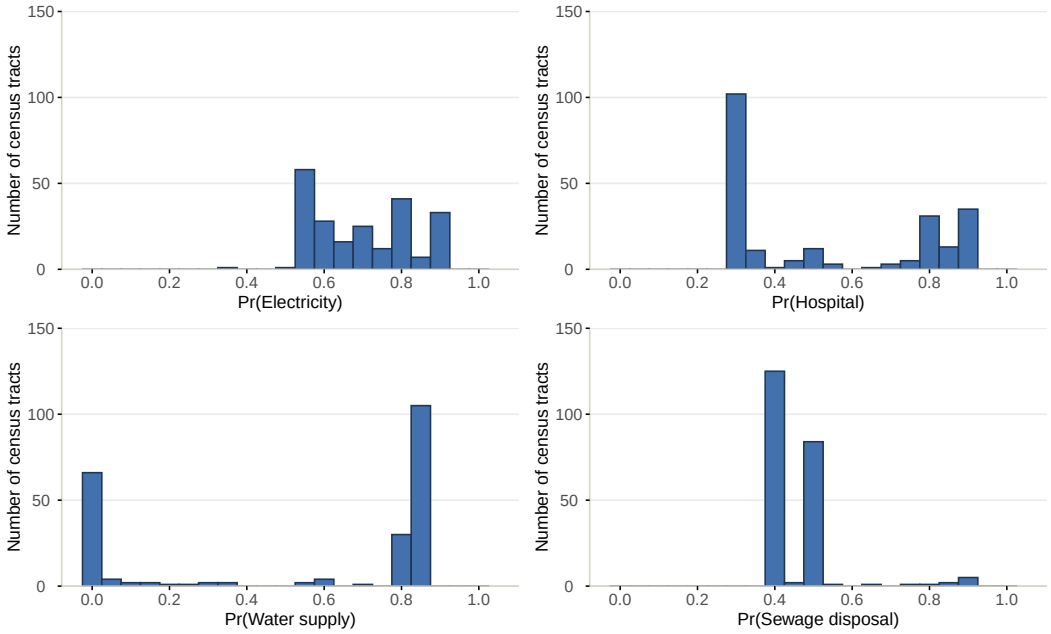

Figure 4.5: Distribution of expected utility service levels in census tracts after the event: a) Electricity; b) Health Care; c) Water Supply; d) Sewage Disposal

Though Figures 4.4 and 4.5 provide an overall idea about the post-event expected network performance, this is of insignificant use from a decision maker's perspective unless the spatial distributions of the utility services disruption levels are understood. For this purpose, a random sample of 10,925 buildings (approximately 2% of total building footprint) distributed in the study area is selected. The buildings are then classified according to the respective utility nodes they depend on for their functioning (electricity, health care, water supply, and sewage treatment), and corresponding performance levels are identified. The buildings are then mapped to the census tracts to which they belong. In this way, the distribution of utility disruptions in all the 222 census tracts under study is obtained. The expected levels of utility disruptions in each of the census tracts are presented in Figure 4.6.

Figure 4.6a shows the levels of electricity supply in the study area after the occurrence of the event. It can be observed that electricity supply disruptions are more likely to occur in census tracts in the northeastern and southeastern parts as shown in Figure 4.2. Similarly, Figure 4.6b shows that the functioning of hospitals in the north and northeastern parts are more likely to be disrupted. This suggests that a significant fraction of the communities will have access to no or less efficient health care. In addition, Figures 4.6c and 4.6d illustrate how the failure of the water treatment plant could affect the water supply and sewage treatment services in different parts of the city, respectively.

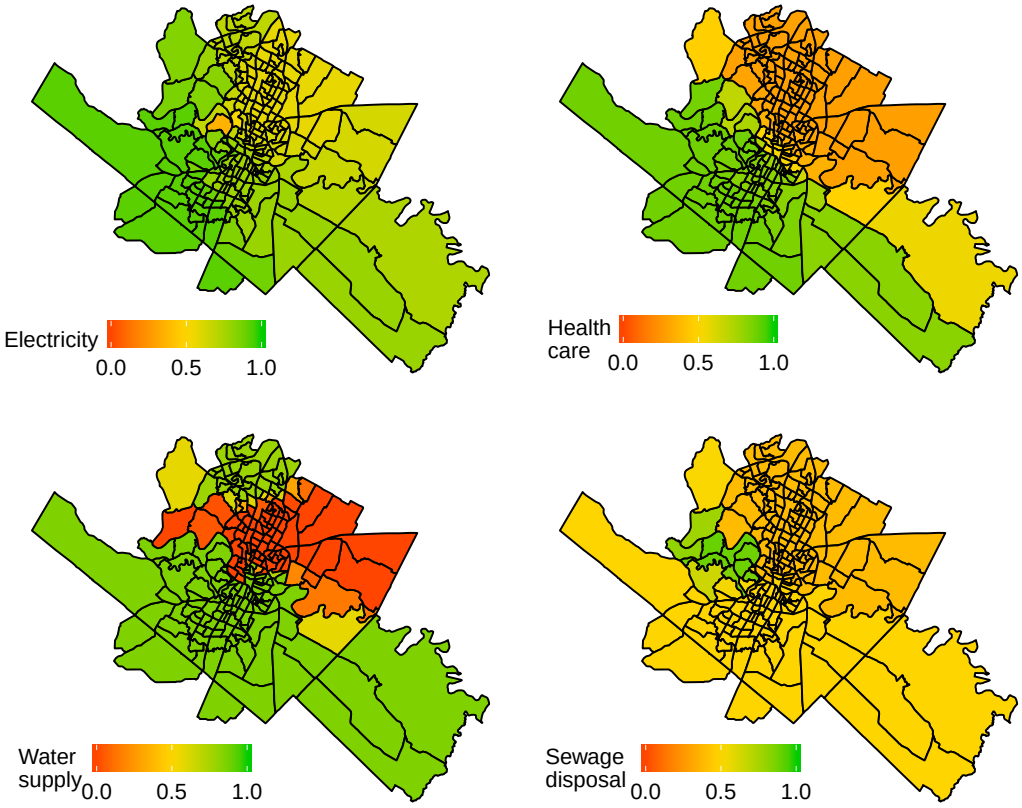

Figure 4.6: Spatial distribution of utility disruptions based on census tracts: (a) electricity; (b) health care; (c) water supply; and (d) sewage disposal

4.4.3 Estimation of weighted exposure and social vulnerability

Analyzing the spatial distribution of the performance of utility services, it is evident that the degree of utility disruptions differs significantly across census tracts. For example, in the northeastern parts of the city, the simulation results predict that there will be almost no water supply and a considerable reduction in the performance of health care and sewage disposal services. However, in the census tracts in the southwest, the probability of disruptions in sewage disposal service

is high, whereas, other utility services are expected to function satisfactorily. To identify the most affected census tracts due to the disruption in utility services, a weighted performance measure is calculated. In reality, the dependency of buildings and communities on utility services differ from one region to another, depending on socio-economic factors. In such scenarios, the decision-maker can provide actual weights for the utilities to obtain the weighted exposure on the urban region. For this case study, the weighted exposure is obtained by assuming a weight factor of 0.25 for all the four utility services. The weighted exposure values of census tracts are presented in Figure 4.7a.

In addition to the geographical distribution of exposure to the disruptive event, it is also important to analyze the generic socio-economic, demographic, and housing characteristics of the census tracts. To estimate the vulnerability of the communities, normalized social vulnerability indexes ($mSVI_{norm}$) of census tracts were computed from the 2014 ACS data, based on the methodology explained in the methodology section. The $mSVI_{norm}$ values are presented in Figure 4.7b. The results show that the communities residing in the eastern part of the city are comparatively more vulnerable to disasters and service disruptions than those in the western part. This can be directly linked to the socio-economic disparities existing between the communities residing in the eastern and western sides of Interstate-35, which runs north-south of Austin.

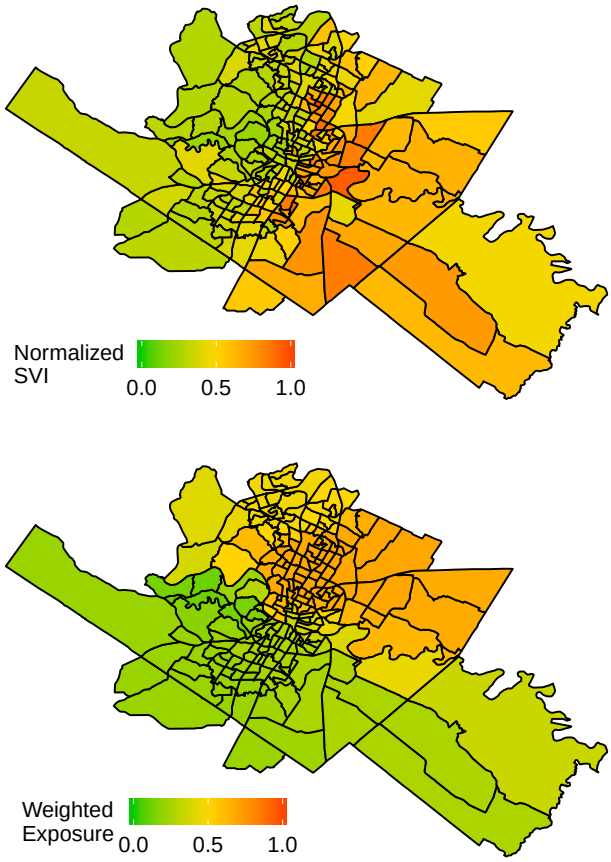

Figure 4.7: Normalized social vulnerability index and weighted exposure of the disruptive event (a) Normalized mSVI values of census tracts; (b) weighted exposure of the combined effect of the disruptive event on communities

4.4.4 Calculation of Priority Index

The Priority Indexes for the census tracts are calculated using Equation 4.5. The results are presented in Figure 4.8. The results show that the northeastern regions of the city have high index values, indicating that those regions are more likely to be affected by the given water treatment plant failure. Communities in the

southwestern region are the least likely to be affected by the same hazard. More importantly, it is possible from the figure to easily identify the census tracts that require immediate attention, and those do not. This property of PI makes it an easy and efficient tool for managing utility disruptions.

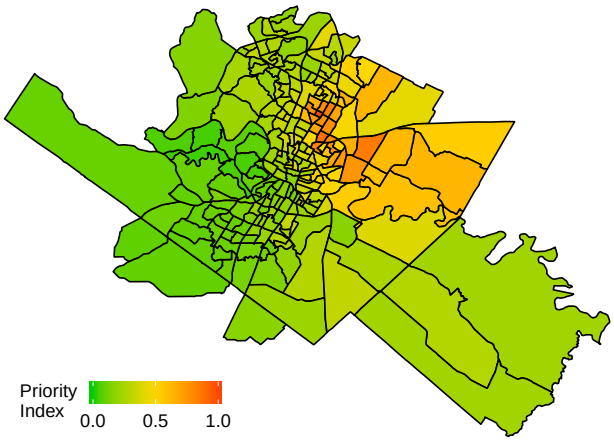

Figure 4.8: Priority Index values of census tracts under study for the simulated disruptive event (PI = 1: highly susceptible; PI = 0: not susceptible)

4.5 Conclusion

In the present chapter, a ratio-scale measure, Priority Index (PI), is proposed to evaluate the susceptibility of communities to unanticipated events and the resultant utility disruptions. The advantage of PI is that it is equally dependent on the generic social vulnerability of communities, as well as the degree of exposure to a given disruption on the network, enabling it to reflect the real conditions of communities in various parts of the urban region during utility disruptions and hazards.

In addition, it enables comparison of the susceptibility of two census tracts using a linear scale. The performance drop in the infrastructure network is evaluated by giving due consideration to both the direct and indirect impacts of hazards arising from its interdependent structure.

The framework could be employed for emergency planning and disaster risk assessment, as well as for managing immediate relief operations, such as the distribution of food, and water during a disaster. The framework could find potential applications in cities where backup mechanisms to withstand prolonged and uncertain utility service disruptions are unreliable or absent. The results from this chapter underscore the importance of proper management of interdependent infrastructure systems to ensure the well-being of urban communities.

A key limitation of the present chapter is that it has not accounted for the ability of the infrastructure network to minimize the impacts of utility service failures through resource redistribution and backup systems. These factors warrant due consideration while implementing the framework.

Chapter 5

Evaluation of the Functional and Economic Risks Posed by Natural Hazards to Infrastructure Systems: A Case Study of the Texas Ports[1]

5.1 Introduction

Ports are critical infrastructure facilities with economic, social, and strategic significance. Ports act as major multimodal transportation hubs and are responsible for connecting inland and maritime transport with other modes of land transport, such as road, rail, and pipelines. For a nation's economy, ports are critical links in both domestic and international supply chains, integrating local businesses with national and international markets. For example, in the U.S., ports facilitated US$5.4 trillion in economic activity in 2018, accounting for approximately 26% of the national gross domestic product. U.S. ports also generated approximately US$378 billion of tax revenue in the same year (Martin Associates, 2019).

Apart from their importance in the national economy, studies have dominantly shown that port facilities attract port-dependent industries in the long-term, driving economic growth and social development in the region (Bottasso, Conti,

[1]based on Balakrishnan, S., T. Lim, and Z. Zhang. A Framework to Predict Economic Risks of Hurricane-caused Disruptions to Port Operations. submitted to *Transportation Research Part A: Policy and Practice*.

Ferrari, & Tei, 2014; Bryan, Munday, Pickernell, & Roberts, 2006; L. Song & van Geenhuizen, 2014), though a few studies presented mixed evidence for the role of ports in shaping up regional urban dynamics (Ducruet & Lee, 2006; B.-m. Jung, 2011). In addition to this, port activity in the U.S. generated more than 3 million jobs in total, out of which approximately 652,000 are directly created by the port sector (Martin Associates, 2019). With trade globalization, the increasing reliance of domestic businesses on overseas commodities for production has also increased and further strengthened the role of ports as enablers of regional and national growth.

This increasing dependence of the economy on port operations has also become a concern in recent decades. Maritime transportation systems are identified as one of the vital infrastructure systems by the Presidential Policy Directive 21 (The White House, 2013) that are critical for security, national economic security, and national public health or safety. Extreme-weather events pose severe threats to ports and associated infrastructure due to their proximity to the oceans and rivers. In the U.S., hurricanes and the resultant storms and winds are the most frequent causes for a shutdown of port operations. While physical damages may lead to operational shutdowns when ports are directly impacted by hurricanes, most frequently, the uncertainties associated with hurricanes and their intensity also play a crucial role in such decisions. The scale of indirect economic impacts of natural disaster-related damages to infrastructure systems is found to be larger than the cost of physical damages and increases with the intensity of the disasters (National Research Council, 1999).

Each port is unique in the range of commodities and the quantities that are handled. There are also seasonal fluctuations and long-term trend changes in port activity. Therefore, the extent of economic impacts and the economic sectors that are affected by port disruptions vary across ports and must be studied with due consideration to the hurricane risks and the significance of such disruptions to the U.S. economy. Understanding the economic impacts of port shutdowns is critical in making risk-informed decisions on resilience enhancement investments in a port system.

Through this chapter, the authors attempt to achieve the following three objectives.

1. Introduce a risk analysis methodology for predicting the duration of port shutdown using hurricane-related factors with due consideration to the associated aleatory uncertainties.
2. Present a methodology to estimate the port-specific economic loss due to hurricane-related shutdowns using the International Trade Inoperability Input-Output Model (IT-IIM) factoring in the inconsistencies between port trade data and I-O tables.
3. Link the above two methodologies to estimate the economic risks of port shutdowns caused by hurricanes of various frequencies.

The hurricane-related risks to port shutdown and the resultant economic impacts are characterized using the concept of return periods. In this study, the return

period is defined as “the average time elapsing between two successive realizations of the event itself” (Salvadori & De Michele, 2004)

The rest of this chapter is organized as follows: the Literature Review presents an overview of existing methods for analyzing the operational and economic impacts of natural disasters on port facilities; the Methodology discusses the stages in the proposed study methodology; the Model Application presents the findings from a case study for quantifying the economic risks of the hurricane-related shutdown of ports along Texas coast on the U.S. economy; Implications of the Methodology highlights some of the potential applications of the methodology; and the Conclusion summarizes the major findings.

5.2 Literature Review

Unlike other critical infrastructure systems, ports do not specifically denote a set of physical installations; rather it is defined as a geographic region with facilities for transferring commodities from a vessel to the land and vice versa. Key infrastructure components at a port include berths, waterside access, channel, terminal, loading and unloading equipment, modal connections, and cargo/container storage and depots (Bureau of Transportation Statistics, 2017). The design and construction of port structures and the channel are largely dependent on several factors, such as the type and size of cargo and vessels handled at the port.

5.2.1 Port disruptions and causes

Delays and disruptions have been identified as two of the major sources of uncertainties in supply chain management (Sanchez-Rodrigues, Potter, & Naim, 2010; Sunil & ManMohan, 2004). Given ports' role as inevitable links in any supply chain that relies on waterborne transport, the vulnerability of ports to natural disasters significantly contributes to business uncertainties and economic losses (Chhetri, Jayatilleke, Gekara, Manzoni, & Corbitt, 2016; J. S. L. Lam & Lassa, 2017; Ng, Chen, Cahoon, Brooks, & Yang, 2013). Identifying the vulnerabilities and evaluating the risks, therefore, are crucial for adopting mitigation measures to ensure operational continuity of ports (J. S. L. Lam & Su, 2015; Ng et al., 2013) as well as to incorporate resilience in individual supply chains (Loh & Van Thai, 2014).

Øyvind, Rice, and Bjørn (2011), from an operations standpoint, suggested that port functionality could be considerably affected by the failure of the following six components of ports– port supplies, financial flows, transportation, communication, internal operations, or capacity, and human resources. J. S. L. Lam and Su (2015) identified major port disruption incidents in Asian nations between 2001 and 2011 and classified their causes into three categories, namely, natural disasters (earthquakes, hurricanes, tsunami, and extreme winter conditions), man-made accidents (oil spill and ship collisions), and port strikes. A recent study by John, Yang, Riahi, and Wang (2016) conducted a holistic review of external port disruption risks pertaining to the functional and management aspects and classified them into five categories– operational risks, security risks, technical risks, organizational

risks, and natural risks. The other major sources of port disruptions discussed in the literature include port congestion (Lewis, Erera, Nowak, & White, 2013), inadaptability to the introduction of new port equipment, and management systems (Lun, Lai, & Cheng, 2010), and governmental regulations (Nze & Onyemechi, 2018).

5.2.2 Common methods for disaster-related economic impact analysis

There are several methods that could be used for quantifying economic losses resulting from various disasters and extreme events. Okuyama Okuyama (2009) classified those methods into four categories, namely, input-output methods (I-O), social accountability matrices (SAM), computable general equilibrium models (CGE), and econometric methods. Table 5.1 presents the major advantages and limitations of these models along with examples of their applications. Models, such as social accountability matrices, computable equilibrium models, and hypothetical extraction methods, are generalized or extended versions of the input-output model to resolve specific limitations of the latter. Koks and Thissen suggested that among the aforementioned models, input-output models and computable general equilibrium models are the most common and well-documented approaches as far as economic impacts of disasters are concerned Koks and Thissen (2016). These models differ in the extent of flexibility in making assumptions, data requirements, and accuracy of estimates. Several studies have shown that input-output models are suitable for analyzing short-horizon disruptions whereas computable equilibrium models are suitable for analyzing the long-horizon effects of disruptions. Galbusera and Giannopoulos (2018); Oosterhaven and Bouwmeester (2016).

Table 5.1: Major disaster-related economic impact estimation methods

Model category	Description	Advantages	Limitations	Example applications
Input-output models	Model for analyzing the initial and higher-order effects of an economic perturbation on various sectors using linear inter-industry relationships	• Simple structure. • Well-structured inter-industry relationships. • Ease of application. • Suitable for short-horizon predictions.	• Assumption of linear relationships. • Rigid coefficients. • No supply constraints. • Overestimation of impacts.	Great Hanshin Earthquake (Okuyama, 2004), Hurricane Katrina (Hallegatte, 2008), Climate change induced drought in Spain (Jenkins, 2013)
Social accountability matrices	Generalized version of input-output models which considers transactions and transfers between production activities, factors of production, and institutions	• More extensive than I-O tables. • Ease of application.	• Assumption of linear relationships. • Rigid coefficients. • No supply constraints. • Extensive data collection efforts.	Hypothetical pipeline failure (Cole, 1995)
Computable general equilibrium models	A more flexible approach in which the variation in prices, output, policy-related economic welfare, etc. can be analyzed based on established mathematical relationships	• Non-linear structure. • Accommodates the effects of price changes. • Handles supply capacity constraints. • Suitable for long-horizon predictions.	• More unrestricted, hence more expertise required. • Immense data collection and model calibration efforts. • Underestimates economic impacts.	Electric grid failure (Rose & Guha, 2004), Niigata-Chuetsu earthquake (Tatano & Tsuchiya, 2008), Water service disruption (Rose & Liao, 2005)
Econometric models	Statistical models which use historical data to develop inter-industry relationships and analyze the effects.	• Statistically rigorous. • Ability to forecast changes.	• Immense data collection efforts. • Not suitable for extreme event analysis if similar historical events are not reflected in the data.	Fiscal impact of hurricanes in Floria (French, Lee, & Anderson, 2010), Effect on built environment due to earthquakes (Wu et al., 2019)

However, these methods mostly focus specifically on the domestic demand- and supply-side disruptions (e.g., bottlenecks/damages in the industry supply chains, fall in consumption due to security concerns, etc.) resulting from domestic disruptive events; they do not give much attention to disruptions in the total international trade (comprising of imports and exports), which is the focus of the current study.

5.2.3 Port disruption-related economic impacts

Economic vulnerability and associated risks highly influence a port's competitiveness, which is a measure of the port's ability to provide operational functions (Yuen, Zhang, & Cheung, 2012). Studies on economic risks of ports can be broadly classified into two: (a) those which analyze port disruptions from the perspective of a single- or a group of supply chain(s) with a focus on a specific economic sector (J. S. L. Lam & Su, 2015); and (b) those which analyze port disruptions from the perspective of a port agency or a government, with an emphasis on the overall economic impacts to a region or a country, and with or without identifying sector-wise losses (Y. Zhang & Lam, 2015). The mitigation strategies that are developed in these two sets of studies are divergent; while the industry/supply chain-specific studies aim at minimizing the cumulative delays/losses incurred by that industry due to a port shutdown, the system-level analysis evaluates mitigation strategies that are aimed at reducing the total duration of shutdowns by improving the resilience of ports and related infrastructure. Table 5.2 enlists some examples of studies that belong to the above two categories along with the specific evaluation methodologies used.

Table 5.2: Examples of port-centric and supply chain-centric studies focusing on economic impacts of port disruptions

Type	Study	Shutdown reason	Method for analysis	Economic impacts analyzed
Port-centric studies	Y. Zhang and Lam (2015)	Extreme wind events	• Regression model for predicting cyclic and trend components of terminal throughput. • Historical climate data to identify port shutdown days.	Direct loss to reputation, shippers, carrier, and port.
	Pant, Barker, and Landers (2015)	Generic	• Direct delays using discrete-event queuing model. • Interdependent effects using Multi-regional input-output model.	Port-level and industry-specific economic loss
	Rose and Wei (2013)	Generic	• Input-output model. • Various resilience strategies evaluated assuming 90-days shutdown.	Port-level (direct) and economic (indirect) losses
	J. Jung, Santos, and Haimes (2009)	Labor dispute	• International-Trade Inoperability Input-Output Model.	Impact on U.S. gross trade economy and domestic output
	Rosoff and Von Winterfeldt (2007)	Simulated terrorist attacks	• Scenario generation and pruning, project risk analysis, direct consequence modeling and indirect economic impact assessment.	Human health and direct economic costs.
Supply chain-centric studies	Y. Zhang and Lam (2016)	Generic	• Petrinet models to model supply chains. • Evaluated effect of mitigation strategies (optimal inventory control) using simulations.	Sector-wise economic loss of industry clusters.
	Loh and Thai (2015)	Supply chain disruptions like port strikes and congestion	• Simulations using additive models	Supply chain management costs including production costs, warehousing cost, and transportation costs.
	Lewis, Erera, and White (2006)	Generic	• Markov Decision Process	Increase in costs for supply chain management.

The most widely used frameworks for quantifying system-level economic impacts of port shutdowns are input-output models, gravity models, and computable equilibrium models (J. S. L. Lam & Su, 2015). With regard to the methods that focus on individual supply chain disruptions, multi-agent simulations, and network models like Petri nets and Bayesian networks are commonly adopted.

Recently, Wei et al. Wei, Chen, Rose, Banks, and Miller (2017) presented a detailed framework for evaluating the economic losses of port disruptions. Though the study mainly focused on the petroleum industry, the methodology can be extended to other industries that are dependent on ports. The framework broadly classified the economic risks under two heads, namely, microeconomic and macroeconomic risks. Microeconomic impacts mainly deal with the cost incurred by port agencies and dependent industries due to revenue losses, cargo damages, import/export delays, etc. Macroeconomic costs are much more extensive and are related to the fall in commodity production, raw material, intermediate commodity shortage, etc.

5.2.4 Gaps in the literature

The review of the literature revealed that extensive research has been carried out with regard to estimating the economic risks of port shutdowns (J. S. L. Lam & Lassa, 2017; Loh & Van Thai, 2014; Wendler-Bosco & Nicholson, 2019). However, a majority of studies focus on the economic losses incurred by economic sectors and individual supply chains due to a given historical event. While quantification of port shutdown consequences is integral for holistic risk evaluation, it must be

highlighted that there have been very few attempts made in the past for developing relationships between disaster characteristics and the extent of port shutdowns and disruptions. The authors believe that these relationships are crucial in predicting port-related economic risks arising from future natural disasters, such as hurricanes. The current chapter intends to bridge the above gap in the literature and introduce a detailed framework to predict the operational and economic risks to ports posed by hurricanes with the support of appropriate statistical methods. The methodology would also allow different stakeholders to analyze the different types of economic impacts resulting from a given hypothetical hurricane event.

5.3 Methodology

Figure 6.1 summarizes the framework developed in this study for evaluating the operational- and associated economic risks posed by hurricanes to ports. The framework consists of four stages. In the first stage, prediction models are developed for estimating the expected duration of hurricane-related port shutdowns. In the second stage, the models are applied to simulated hurricanes to estimate the port shutdown risks from potential future hurricanes of various intensities. In the third stage, International Trade Inoperability Input-Output models are used to estimate the economic impacts of a single-day shutdown of ports. In the final stage, port shutdown risks are combined with the single-day shutdown loss estimates to quantify the economic risks (to the overall economy as well as to the constituent industrial sectors) resulting from hurricane-related port shutdowns. The detailed methodology adopted in each of the above stages is discussed in the rest of the

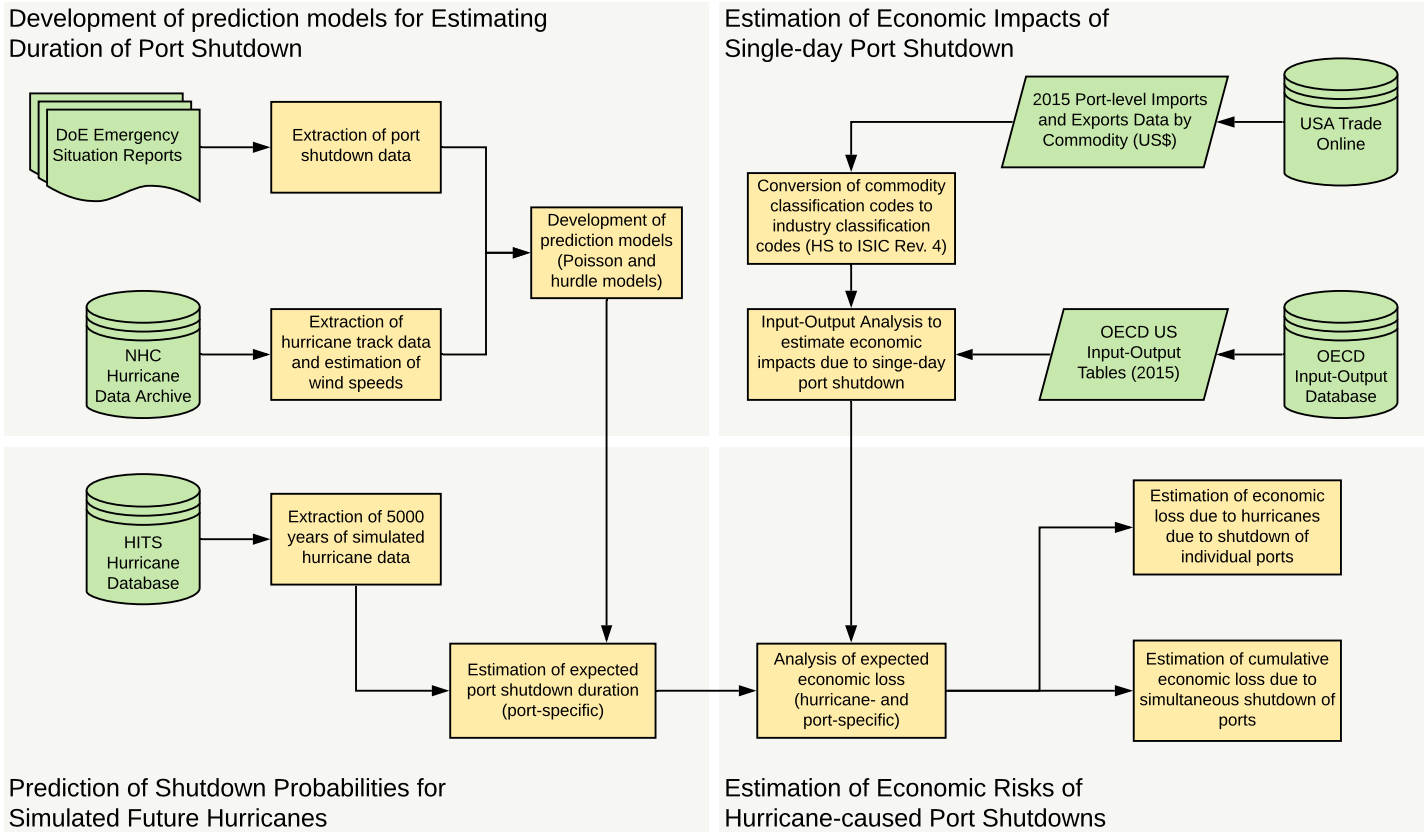

Figure 5.1: Proposed methodology for analyzing economic risks of hurricane-related port shutdowns

section.

5.3.1 Development of prediction models based on historical port shutdown data

In addition to the direct damage inflicted by hurricanes on port infrastructure, a number of other factors also lead to port shutdowns. Some of these factors include: whether the port is along the predicted course of the hurricane, how far is the eye of a hurricane from the location of the port, and the intensity and duration of hurricane-related winds and storms, etc. The directive for a shutdown of port operations is issued in such circumstances by the Captain of the Port (COPT) who is responsible for maintaining a port's safety and security (U.S. Coast Guard, 2018). Since direct data on port shutdowns were not readily available, the authors developed a port shutdown data set based on surrogate data that reflected port shutdown duration.

5.3.1.1 Extraction of port shutdown data

In recent years, the U.S. Department of Energy (DoE) (Office of Cybersecurity Energy Security and Emergency Response, 2019) began publishing detailed situation reports with updates over the condition of major critical infrastructure systems during extreme events like hurricanes. Among the various infrastructure conditions, the operational statuses of major ports along the course of the hurricane, as declared by respective COPTs, are also reported. The port statuses are reported in four conditions, namely, Zulu, Yankee, X-Ray, and Whiskey, providing relevant information on the port operations during hurricanes (Table 5.3). Among

Table 5.3: U.S. Coast Guard system of port conditions and their definitions Legal Information Institute (2015)

Port condition	Criteria for directive	Port regulations
Zulu	The landfall with sustained gale wind forces of magnitude 39-54 mph within 12 hours is expected to occur at the port.	All port waterfront operations are suspended, except final preparations to ensure safety of port facilities.
Yankee	The landfall with sustained gale wind forces of magnitude 39-54 mph within 24 hours is expected to occur at the port.	Port is closed to incoming vessels.
X-Ray	The landfall with sustained gale wind forces of magnitude 39-54 mph within 48 hours is expected to occur at the port.	Port is functional with a few restrictions on vessel movement.
Whiskey	The landfall with sustained gale wind forces of magnitude 39-54 mph within 72 hours is expected to occur at the port.	Port is functional with a very few restrictions on vessel movement.

these conditions, Zulu refers to a complete shutdown and Yankee refers to a partial regulation of port operations. Port condition Zulu may be brought into effect as part of pre-hurricane preparation and post-hurricane mitigation.

For this chapter, the authors compiled the information regarding the number of days in which affected ports were in Zulu condition from the DoE emergency situation reports that were published during nine major hurricanes that affected the states along East Coast and Gulf Coast between 2012 and 2019. The hurricanes are, namely, Barry (2019), Dorian (2019), Nate (2019), Florence (2018), Michael (2018), Harvey (2017), Irma (2017), Matthew (2016), and Sandy (2012). Port shutdown information related to 46 unique U.S. ports along the Atlantic- and Gulf Coasts were compiled in this exercise (Figure 5.2).

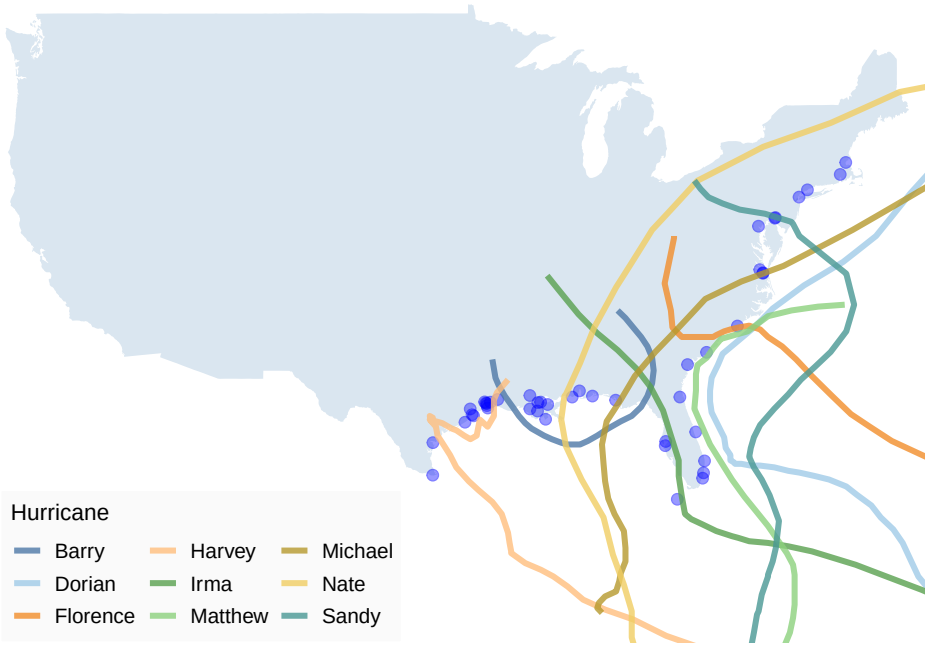

Figure 5.2: Hurricanes and ports included in the port shutdown data set (blue circles denote the port locations)

5.3.1.2 Extraction of hurricane- and port-related data

In the next step, the port-specific characteristics that could potentially influence the extent of shutdowns were analyzed. For this purpose, various factors related to those ports (such as, geographic location, port type, harbor type and size, and depth of channel) and their interaction with the hurricanes (such as, distance from port to hurricane eye, distance from port to nearest landfall, and wind speed and duration at the ports) were extracted. For collecting information on port-hurricane interactions, the hurricane characteristics were to be analyzed. The best tracks of the nine hurricanes were obtained from the National Hurricane Center (NHC) Hurricane Data Archive (National Hurricane Center, 2019). The informa-

tion such as the nearest distance from affected ports to the eye of hurricane and landfall location (if any) were manually measured using a Geographic Information System (GIS) software package (Figure 5.3).

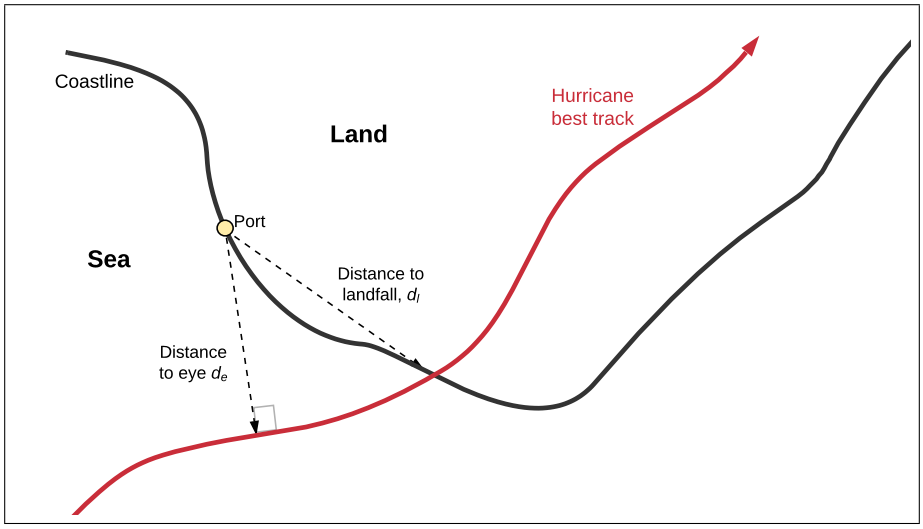

Figure 5.3: Definition of distance to landfall (d_l) and distance to eye (d_e) variables

The hurricane wind-related historical data was not readily available. Therefore, the wind speed and duration information (maximum sustained wind and gust speeds, duration of gusts and sustained winds) were computed using the hurricane wind model proposed by Willoughby, Darling, and Rahn (2006). The full hurricane wind profile in this study is modeled as follows:

$$w\left(\frac{R_{max}-R_1}{R_2-R_1}\right)=\frac{\frac{\partial V_i}{\partial r}}{\frac{\partial V_i}{\partial r}-\frac{\partial V_o}{\partial r}}=\frac{nX_1}{nX_1+R_{max}} \tag{5.1}$$

where w is a weighing function, V_i and V_o are the tangential wind component in the hurricane eye and beyond the transition zone, R_{max} is the radius at which the maximum wind speed occurs, X_1 is the exponential decay length in the outer vortex of

the hurricane and n is the exponent for the power-law function inside the hurricane eye. The transition zone limits are denoted by radii $r = R_1$ and $r = R_2$.

The computation of the wind variables was done using the `stormwindmodel` package in R-statistical software (Anderson et al., 2018). The model is capable of estimating the wind-related variables for each county in the U.S. using the hurricane track information in North Atlantic Hurricane Databases (HURDAT) format (Jarvinen & Caso, 1984) as the input. The counties were later matched with the geographical locations of ports to derive the wind speed and duration at ports.

5.3.1.3 Model specification and construction

In this study, the duration of port shutdowns due to simulated hurricanes are predicted using regression models. While the duration of shutdown is a non-negative continuous variable, in this study, it is modeled as a count variable (non-negative integer). This is because the available information on shutdown duration reported in DoE emergency situation reports can be easily converted into days of shutdown. Poisson regression and its variants are most widely used for modeling count data (Colin & Pravin, 2013).

For the current study, the following two regression models were developed based on the relative positions of the hurricane and the port.

1. Landfall model (L-model): Regression model developed to predict the expected days of ports shutdown due to hurricanes that make landfall before approaching the port; and

2. No landfall model (NL-model): Regression model developed to predict the expected days of port shutdowns due to hurricanes that make landfall after passing a port.

In order to identify the most relevant hurricane- and port-related variables for constructing the regression models, a correlation analysis of the dependent and independent variables was conducted (Figure 5.4).

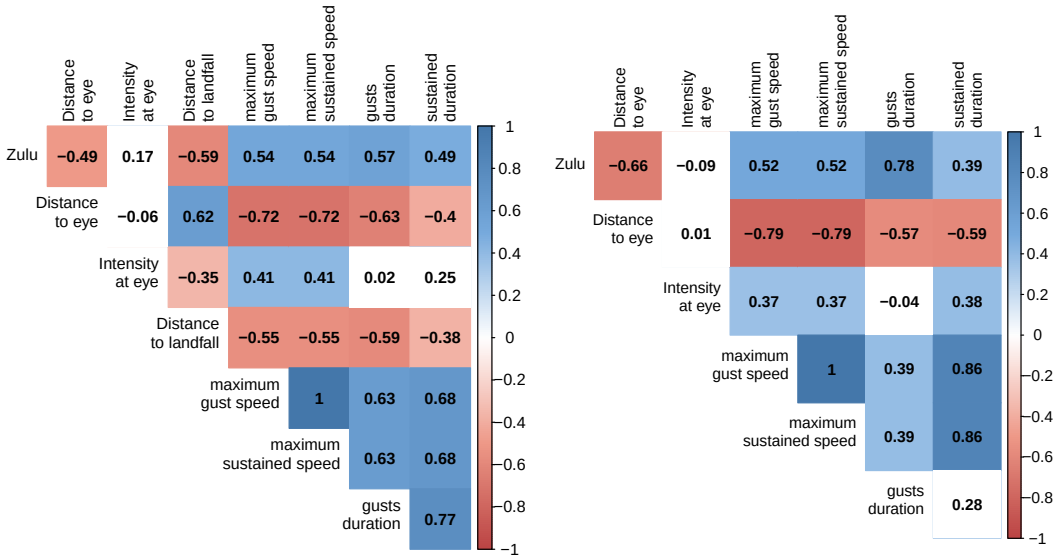

(a) Landfall condition

(b) No landfall condition

Figure 5.4: Estimated Pearson's correlation coefficients from the correlation analysis of port- and hurricane-related factors based on historical data

The results show that for L-model, the most relevant covariates are the distance to landfall (d_l) and length of time in minutes of surface-level wind gusts with intensity greater than 18 m/s at the port (t_{18}) at the port. In the case of NL-model, the most relevant covariates are the distance to the hurricane eye (d_e) and length of

time in minutes of surface-level wind gusts with intensity greater than 18 m/s at the port (t_{18}).

In order to select the type of Poisson regression model to be developed for landfall and no landfall conditions, further analysis of the dependent variable (days of shutdown) was conducted.

It was found that though shutdown duration in both cases follows a Poisson distribution, the proportion of events with zero days of the shutdown was considerably higher in the landfall condition ($\sim 37\%$). In this case, a hurdle count model was used for modeling the duration of port shutdown assuming that whether a port is shut down and the duration of the shutdown are determined by two different processes. In the model, a binary logit model with the distance between the landfall location and the port (d_l) as predictor variable governs if the port will be shut down due to a given hurricane, and a truncated-at-zero Poisson regression model with the duration of wind gusts greater than 18m/s (t_{18}) as the predictor is used to model the number of shutdown days given the port is predicted to shut down. Based on the above hurdle model, the probability mass function of days of shutdown k is given as follows (McDowell, 2003):

$$\Pr(K = k) = \begin{cases} \pi & \text{if } k = 0 \\ (1-\pi)\,\frac{\lambda^k}{\left(e^{\lambda}-1\right)k!} & \text{if } 1.2.3.\ldots \end{cases} \tag{5.2}$$

where π is the Binomial distribution parameter and λ is the Poisson distribution parameter.

Consequently, the log-likelihood of ith observation can be written as:

$$\ln L(\pi_i, \lambda_i; k_i) = \begin{cases} \ln \pi_i & \text{if } k_i = 0 \\ \ln \left[(1 - \pi_i) \frac{\lambda^{k_i}}{\left(e^{\lambda} - 1\right) k_i!} \right] & \text{if } k_i = 1, 2, 3, \ldots \end{cases} \tag{5.3}$$

Now using a logit link function $\left(\pi_i = \frac{e^{\mathbf{x_i}\beta_1}}{1+e^{\mathbf{x_i}\beta_1}}\right)$ for explaining the binomial process and a log link function $\left(\lambda_i = e^{\mathbf{x_i}\beta_2}\right)$ for the Poisson process, the log-likelihood function can be constructed using Equation 5.3. Incorporating the link functions along with the pertinent predictor variables and simplifying Equation 5.3, the log-likelihood function for the hurdle model used in the present chapter can be written as follows:

$$\begin{aligned} \ln L(\pi_i, \lambda_i; k_i) &= \ln \left\{ \left(\prod_{i=1}^{n_0} \frac{e^{\beta_{10} + \beta_{11} d_l}}{1 + e^{\beta_{10} + \beta_{11} d_l}} \right) \prod_{i=1}^{n_1} \left(1 \right. \right. \\ &\qquad \left. \left. - \frac{e^{\beta_{10} + \beta_{11} d_l}}{1 + e^{\beta_{10} + \beta_{11} d_l}} \right) \prod_{i=1}^{n_1} \left(\frac{e^{k_i (\beta_{20} + \beta_{21} (t_{18})^p)}}{\left(e^{\beta_{20} + \beta_{21} (t_{18})^p} - 1\right) k_i!} \right) \right\} \\ &= \sum_{i=1}^{n_0} \ln \left(\frac{e^{\beta_{10} + \beta_{11} d_l}}{1 + e^{\beta_{10} + \beta_{11} d_l}} \right) + \sum_{i=1}^{n_1} \ln \left(1 - \frac{e^{\beta_{10} + \beta_{11} d_l}}{1 + e^{\beta_{10} + \beta_{11} d_l}} \right) \\ &\quad + \sum_{i=1}^{n_1} k_i \left(\beta_{20} + \beta_{21} (t_{18})^p \right) + \sum_{i=1}^{n_1} \ln \left(e^{\beta_{20} + \beta_{21} (t_{18})^p} - 1 \right) \\ &\quad - \sum_{i=1}^{n_1} \ln \left(k_i! \right) \end{aligned} \tag{5.4}$$

where n_0 and n_1 are the number of observations with zero and more than zero days of shutdown, β_{1j} and β_{2j} are model parameters corresponding to the Binomial submodel and the Poisson submodel, respectively. p is the exponent of t_{18} which captures the nonlinear relationship with the duration of the port shutdown.

The value of p was computed by applying an iterative loop on the log-likelihood function. As evident in Equation 5.4, the log-likelihood of the hurdle model is the product of log-likelihood values of the binomial and Poisson submodels.

In the case of no landfall model (NL-model), since there is no abnormally high number of events with zero days of shutdown, a Poisson regression model was chosen. The probability mass function of days of shutdown k, if assumed to follow a Poisson distribution, is given by Equation 5.5.

$$\Pr(K = k) = \frac{\lambda^k e^{-\lambda k}}{k!} \quad k = 0, 1, 2, \ldots \tag{5.5}$$

Now, the log-likelihood function can be written as follows:

$$\ln L(\lambda_i; k_i) = \ln \left\{ \prod_{i=i}^{n} \frac{\lambda^{k_i} e^{-\lambda}}{k_i!} \right\} \tag{5.6}$$

Now, using a log link function ($\lambda_i = e^{\mathbf{x_i}\beta_3}$) using the predictor variables d_e and t_{18} and simplifying, the log-likelihood function can be rewritten in the following form.

$$\begin{aligned} \ln L(\lambda_i; k_i) &= \ln \left(\prod_{i=i}^{n} \frac{e^{(\beta_{30}+\beta_{31}d_e+\beta_{32}(t_{18})^q)k_i} \times e^{-(e^{\beta_{30}+\beta_{31}d_e+\beta_{32}(t_{18})^q})}}{k_i!} \right) \\ &= \sum_{i=1}^{n} k_i(\beta_{30}+\beta_{31}d_e+\beta_{32}(t_{18})^q) - \sum_{i=1}^{n} e^{(\beta_{30}+\beta_{31}d_e+\beta_{32}(t_{18})^q))} - \sum_{i=1}^{n} \ln k_i! \end{aligned} \tag{5.7}$$

where q is the exponent of t_{18} to capture its nonlinear relationship with the duration of the port shutdown. The value of q was computed by applying an iterative loop on the log-likelihood function.

By maximizing the log-likelihood functions, the model parameters are obtained. Further, the probability mass function of the shutdown duration at each port due to a given hurricane can be derived.

5.3.2 Prediction of expected port shutdown duration for simulated hurricanes

Once the shutdown duration models were developed, the port shutdown risks due to future hurricanes were to be evaluated. Hurricane Interactive Track Simulator (HITS) for North Atlantic Basin is a non-parametric stochastic model, based on the principle of non-homogeneous hidden Markov renewal model, developed by Nakamura, Lall, Kushnir, and Rajagopalan (2015) for simulation of tropical cyclone tracks. The hurricane seasons are simulated based on the historical best-track North Atlantic Hurricane Databases (HURDAT). Currently, 60,000 years of simulated hurricane seasons are available in the HITS database. For the current study, the authors extracted the first 5000 years of simulated hurricane seasons (consisting of 76,577 unique hurricane tracks with non-empty observations) from the HITS database[2]. The HITS hurricane tracks consist of the geographic coordinates and wind intensity details of the eye of the simulated hurricanes at a frequency of two hours throughout their life-cycle. For each of the hurricane in the database, an algorithm, as illustrated in Figure 5.5, was used to compute the distance and wind speed variables corresponding to the ports (d_e, d_l, and t_{18}) and determine the regression model (L-model or NL-model) for predicting the expected

[2] `http://rainbow.ldeo.columbia.edu/~jennie/HITS/`

duration of port shutdowns.

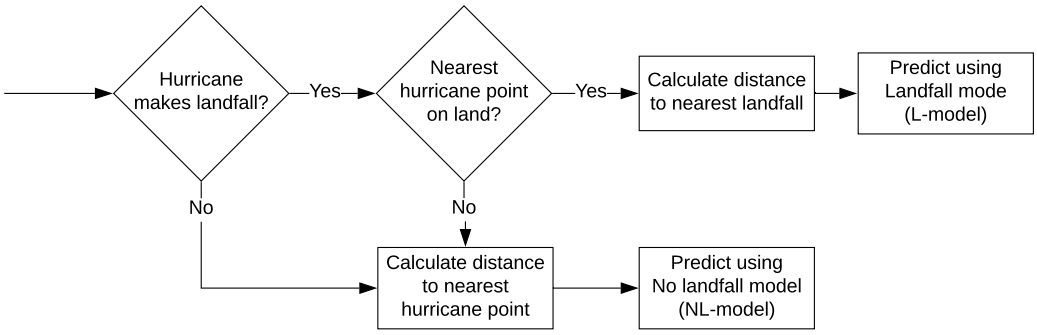

Figure 5.5: Algorithm used for determining the prediction model for estimating port shutdown risks

The expected values of port shutdown durations corresponding to the simulated hurricanes were used to identify the hurricanes of various return periods for each port under consideration. Return period is a concept closely linked to the probability or chance of an event's occurrence and is defined as "*the average time elapsing between two successive realizations of the event itself*" (Salvadori & De Michele, 2004). The return period is used as the criteria in the current study to estimate the severity of hurricanes based on the extent of port shutdowns and associated economic impacts. The following steps were implemented to identify the hurricanes of various intensities in terms of the duration of the port shutdown.

Step 1: Estimate the expected days of the shutdown of a port $r \in \mathbf{R}$ due to hurricane $h \in \mathbf{H}$ using the appropriate prediction model. This value is denoted by $\bar{k}_r^h$.

Step 2: Sort the N simulated hurricanes in the descending order of the expected

days of shutdown and assign them a rank m_h such that the most severe hurricane gets rank 1.

Step 3: Calculate the return periods in years T_r^h of N simulated hurricanes as follows:

$$T_r^h = \frac{N+1}{m_h \tilde{N}} \tag{5.8}$$

where $\tilde{N} = N/5000$ is the average number of hurricanes in a simulated season.

Step 4: Identify the hurricanes with the return period estimates closest to the return periods of interest (10-year, 20-year, 50-year, 100-year, 200-year, 500-year, and 1000-year hurricanes).

Step 5: Repeat Steps 1–4 for all the ports for which the analysis is to be done.

5.3.3 Estimation of economic impacts of single-day port shutdown

In this study, the economic impact of port disruptions refers to the direct and indirect economic losses incurred to the U.S. economy due to the shutdown of port operations. The economic loss consists of the impacts on the gross domestic product (due to forward- and backward linkage effects) and the disruptions to exports and imports during the port shutdown. For the current study, the International Trade Inoperability Input-Output Model (IT-IIM) was used for quantifying the economic impact of a single-day port shutdown (J. Jung et al., 2009). The Input-Output Model proposed by Leontief (1986) and its extensions, including IT-IIM, are systems of linear equations representing the relationships between various economic sectors in a region of interest. The input-output data are maintained and regularly updated by

federal governments and international trade organizations.

The traditional IIM adopts Gross Domestic Product (GDP), which represents the total market value of all the final goods and services produced within a country, as a measure of economic impact. The application of traditional IIM is, therefore, limited to the analysis of perturbations in domestic infrastructure sectors and their ripple effects on other sectors. The IIM is not capable of analyzing the effects of disruptions to imports and exports of commodities.

The IT-IIM was specifically developed to investigate the effect of disruptions on imports and exports at ports-of-entries on national and regional economies using Gross Trade Economy (GTE) as a measure for quantifying economic impacts. The GTE is the combined value of GDP and imports and is expressed as in Equation 5.9.

$$\begin{aligned} GTE &= GDP + M \\ &= DD + X + M \end{aligned} \tag{5.9}$$

where M is the imports, DD is the domestic products for domestic use, and X is the exports. By replacing GDP with the concept of the GTE in the input-output framework, all imports can be treated as if they were produced domestically. The IT-IIM enables a more comprehensive evaluation of the importance of total international trade to a nation's economy, supplementing the traditional GDP perspective for evaluating economic impacts.

The IT-IIM comprises two configurations (Case A and Case B) based on the assumptions on how imports are used in the economy. The Case A model assumes that all imports are used exclusively by domestic industries as intermediary goods.

Therefore, the economic loss estimated by Case A model also reflects the interdependent effects induced in domestic production due to disruptions in the import of intermediary goods. On the other hand, the Case B model assumes that all the imports are used for final consumption as a fall in imports will not have any impact on domestic production.

In reality, a fraction of imports are used for domestic production, and the rest is consumed as final products. Therefore, the economic impact estimates provided by Case A and Case B models can be considered as the upper- and lower bounds, respectively. A detailed methodology of IT-IIM can be found in the study by J. Jung et al. (2009).

The overall economic impacts incurred by a single-day closure of a port r according to IT-IIM models are computed using the following equations.

$$C_{r,A} = \sum_{i \in I} \left[\bar{x}_i^{TO} - \tilde{x}_i^{TO} \right] \tag{5.10}$$

$$C_{r,B} = \sum_{i \in I} \left[\left(\bar{x}_i^{TO} - |\bar{m}_i| \right) - \left(\tilde{x}_i^{TO} - |\tilde{m}_i| \right) \right] \tag{5.11}$$

where $C_{r,A}$ and $C_{r,B}$ are the overall economic impacts calculated using IT-IIM Case A and Case B models, $\bar{x}_i^{TO}$ and $|\bar{m}_i|$ are the output value and import value corresponding to industry i during normal port operating conditions (baseline values), and $\tilde{x}_i^{TO}$ and $|\tilde{m}_i|$ are the output value and import value corresponding to industry i during port disruptions (degraded values), respectively. Considering the actual economic loss lies between $C_{r,A}$ and $C_{r,B}$, the two estimates, and their average value were used for calculating the economic risks of a port shutdown in this study.

The IT-IIM requires two types of data: (a) the demand-based interdependency table (input-output table) consisting of the details of the flow of goods and services among different industries within a national economy; and (b) the demand-based perturbation vector. Typically, industry input-output data can be retrieved from several sources depending on the regions of interest. For instance, the Organization for Economic Co-operation and Development (OECD) publishes the national input-output tables for all OECD countries and 28 non-member countries, covering the years 2005 through 2015. As the purpose of this case study was to investigate the economic impacts of port shutdowns in Texas on the U.S. economy, the 2015 U.S. input-output table published by Organization for Economic Cooperation and Development (2019) was used. The OECD input-output table contains information on the inter-industrial flow of goods and services among 36 industry clusters based on the International Standard Industrial Classification of All Economic Activities (ISIC Rev.4). The industry clusters that constitute the U.S. economy and the corresponding ISIC Rev. 4 codes are presented in Table 5.4.

For constructing the perturbation vector, the 2015 port-level monthly exports and imports data for the ports in Texas during the hurricane season were extracted from USA Trade Online (U.S. Census Bureau, 2019). The port-specific data related to imports and exports are available in terms of their monetary values (U.S. Dollars) and are classified into 6,093 different product groups using the 6-digit Harmonized System (HS). The single-day shutdown perturbation vector was constructed by calculating the average daily values of imports and exports during the hurricane season for port and each industry cluster. In the U.S., the official

Table 5.4: Industry classification according to the ISIC Rev. 4 format

ISIC Rev. 4 industry cluster	Code	Industry	ISIC Rev. 4 industry cluster	Code	Industry
1	TTL_01T03	Agriculture, forestry and fishing	19	TTL_30	Other transport equipment
2	TTL_05T06	Mining and extraction of energy producing products	20	TTL_31T33	Other manufacturing; repair and installation of machinery and equipment
3	TTL_07T08	Mining and quarrying of non-energy producing products	21	TTL_35T39	Electricity, gas, water supply, sewerage, waste and remediation services
4	TTL_09	Mining support service activities	22	TTL_41T43	Construction
5	TTL_10T12	Food products, beverages and tobacco	23	TTL_45T47	Wholesale and retail trade; repair of motor vehicles
6	TTL_13T15	Textiles, wearing apparel, leather and related products	24	TTL_49T53	Transportation and storage
7	TTL_16	Wood and of products of wood and cork (except furniture)	25	TTL_55T56	Accomodation and food services
8	TTL_17T18	Paper products and printing	26	TTL_58T60	Publishing, audiovisual and broadcasting activities
9	TTL_19	Coke and refined petroleum products	27	TTL_61	Telecommunications
10	TTL_20T21	Chemicals and pharmaceutical products	28	TTL_62T63	IT and other information services
11	TTL_22	Rubber and plastics products	29	TTL_64T66	Financial and insurance activities
12	TTL_23	Other non-metallic mineral products	30	TTL_68	Real estate activities
13	TTL_24	Manufacture of basic metals	31	TTL_69T82	Other business sector services
14	TTL_25	Fabricated metal products, except machinery and equipment	32	TTL_84	Public administration and defence; compulsory social security
15	TTL_26	Computer, electronic and optical products	33	TTL_85	Education
16	TTL_27	Electrical equipment	34	TTL_86T88	Human health and social work
17	TTL_28	Machinery and equipment n.e.c.	35	TTL_90T96	Arts, entertainment, recreation and other service activities
18	TTL_29	Motor vehicles, trailers and semi-trailers	36	TTL_97T98	Private households with employed persons

Atlantic hurricane season begins on June 1 and ends on November 30.

In order to conduct the input-output analyses, the inconsistency between the classification systems based on which the input-output table (ISIC Rev. 4) and the port perturbation vector (HS) were to be rectified. While HS is based on industry products, ISIC Rev. 4 is based on economic activity. For this purpose, the port perturbation vector in HS format was converted into the ISIC Rev.4 format using the concordance table developed by OECD ([Dataset] Directorate for Science Technology and Innovation, 2019). By doing so, the import and export loss for different product types resulting from port shutdown could be properly reflected in the final uses of each industry sector defined in the input-output table.

5.3.4 Estimation of economic risks of hurricane-related port shutdown

Once the hurricanes corresponding to the return periods based on the shutdown duration were identified, the corresponding expected days of the port shutdowns and the port-specific economic impacts due to a single-day shutdown were combined to calculate the expected economic risks. Additional analyses were also carried out to identify the major industry clusters directly and indirectly affected by the port disruptions. The economic risks to various industrial clusters as well as to the overall economy were quantified.

In order to evaluate the economic risks of hurricane-related port disruptions, two types of analyses were carried out. In the first analysis, the expected economic impact of port shutdown corresponding to each port due to each hurricane in the HITS database was calculated using Equation 5.12. Then, using the port-specific

economic impacts as the criteria, the hurricanes were ranked and the economic impacts of various return periods were calculated using Steps 2–4 in Subsection 5.3.2.

$$\bar{C}_r^h = \bar{k}_r^h \times C_r \tag{5.12}$$

where $\bar{C}_r^h$ is the expected economic loss if a port r is affected by hurricane h, and C_r is the total economic impact of single-day shutdown of port r, calculated using the IT-IIM models.

In the second analysis, each hurricane in the HITS database was investigated and the cumulative economic impacts of a simultaneous shutdown of ports in Texas were quantified using Equation 5.13.

$$\bar{C}^h = \sum_{r \in \mathbf{R}} \bar{C}_r^h \tag{5.13}$$

where $\bar{C}^h$ is the cumulative economic impact of port shutdowns due to hurricane h (calculated using either IT-IIM Case A or Case B models).

The cumulative economic impact estimates were used to rank hurricanes and the cumulative economic impact values corresponding to various return periods were identified. For this, a similar procedure as the one used for determining port-specific economic impacts of different return periods was used; however, the ranking was done based on the cumulative economic impacts of each simulated hurricane using Equation 5.13.

5.4 Model Application on Texas Port System

In this section, the analysis results from the application of the economic risks analysis methodology on the Texas port system are discussed. The Texas port

system consists of 11 commercial deep-draft ports and five commercial shallow-draft ports. The system is augmented by waterways and intermodal surface transportation connectors. Texas ports have a significant role in the regional and national economy as Texas is the largest exporting state in the U.S. Texas ports handled more than 28% of total U.S. export tonnage in 2015. Texas ports also import commodities, such as crude oil and chemicals, which are important intermediary goods for domestic industries. In the current chapter, the deep-draft ports (except Port of Sabine Pass) were considered for analysis as they handle most of the commodities being exported and imported through the Texas Coast (Figure 5.6).

Texas Coast is highly prone to hurricanes and hence the ports are susceptible to hurricane-related shutdowns. For example, Hurricane Harvey, a Category 4 hurricane that affected the Houston region in 2017, disrupted the operations of Port of Houston completely for a week, resulting in considerable economic loss. The proposed methodology was implemented on the Texas Port System and the hurricane-related disruptions and associated economic risks were evaluated.

5.4.1 Estimated model parameters for predicting port shutdown duration in the North Atlantic Basin

Table 5.5 presents the estimated coefficients and model performance statistics corresponding to L-model and NL-model. The model estimates were computed using R-statistical software. In order to estimate the values of the exponents of t_{18} (p and q), the respective models were iterated by varying those parameters and the models with the lowest value of Akaike information criterion (AIC) were chosen.

Figure 5.6: Major deep-draft ports in Texas and their locations along Texas Coast (Source: Texas Department of Transportation)

The landfall model (L-model) consists of two components. The first component is a zero hurdle model which calculates the probability that a port will be closed due to a given hurricane. The model uses the distance between landfall and the port in miles (d_l) to predict the probability. The model suggests that the expected duration of a port being closed due to a hurricane decreases by 6.67% ($= (e^{-0.006721} - 1) \times 10$ miles $\times\ 100\%$) for every 10 miles (16.1 km) increase in the distance between the point of landfall and the port. According to the landfall model, the probability of a port shutdown exceeds 50% when the distance between

Table 5.5: Landfall and No Landfall models for prediction of port shutdown duration

Model	Submodel	Model statistics				
		Parameter	Estimate	Std. Error	z-value	p-value
L-Model	Zero Hurdle Model	Constant	2.1381	0.5913	3.6160	0.0003
		d_l	-0.0067	0.00207	-3.2410	0.0012
	Zero-truncated Poisson Model	Constant	0.5487	0.2354	2.3310	0.0198
		$[t_{18}]^{0.67}$	0.0047	0.0018	2.6900	0.0071
		n	51			
		AIC†	160.02			
		LR χ^2	22.694			
		Pr($> \chi^2_{crit}$)	0.000018			
		pseudo R^2	0.434			
NL-Model	Poisson Model	Constant	0.1644	0.4809	0.3420	0.7324
		d_e	-0.0074	0.0028	-2.6220	0.0086
		$[t_{18}]^{0.5}$	0.0331	0.0081	4.080	0.0000
		n	40			
		AIC	129.750			
		LR χ^2	47.047			
		Pr($> \chi^2_{crit}$)	0.00000			
		pseudo R^2	0.815			

the port and the location of landfall is less than 318.1 miles (511.8 km).

The second component of the landfall model is a zero-truncated Poisson model which calculates the conditional probabilities (and therefore the conditional expected value) of various days of port shutdown, given the port is predicted to be shut down. The duration of the port shutdown in the landfall model is determined by the power function of the duration of wind gusts (in minutes) of intensity greater than 18 m/s experienced by the port due to a hurricane ($[t_{18}]^{0.67}$). The model statistics suggest that the expected duration of shutdown increases by 0.47% (=$(e^{0.0047} - 1) \times 100\%$) for every one unit increase in the value of $[t_{18}]^{0.67}$. Longer

duration of high-intensity winds leads to longer port shutdowns either as a precaution or due to direct physical damage.

For the no-landfall model (NL-model), a Poisson regression model was constructed using d_e and $[t_{18}]^{0.5}$ as the variables. The model suggests that the expected number of days of shutdown decreases by 7.37% ($= (e^{-0.0074} - 1) \times 10$ miles $\times$ 100%) for every 10 miles increase in the distance between the port and the closest location of the eye of the hurricane. At the same time, the expected days of port shutdown increases by 3.37% ($= (e^{0.0331} - 1) \times 100\%$) for every one unit increase in the value of $[t_{18}]^{0.5}$, indicating a positive relationship between the days of shutdown and the duration of wind gusts.

Log-likelihood ratio tests (LR tests) were employed to check the statistical significance of both models fits. For the landfall model and no-landfall model, the $p-$values obtained from the LR-tests were below 0.05, confirming that both models are statistically significant. The models were validated using the k-folds cross-validation method (with 10 folds). The average Root Means Squared Error (RMSE) for the landfall model was 0.939 days, whereas the average RMSE for the no-landfall model was 1.21 days. Furthermore, the goodness of fit of the models was evaluated using rootograms and residual distributions (Figure 5.7). Rootograms are graphical tools which compare the predicted and actual distributions of the count variable, instead of directly comparing the predicted values with the actual counts **?**. The red line represents the distribution fitted by the model, whereas the hanging bars show the actual frequency (square-root) of shutdown days from the data set. It can be seen that the models fit fairly well with a few discrepancies which are

random across the shutdown duration. To add to this, it can be observed that the residuals follow a normal distribution.

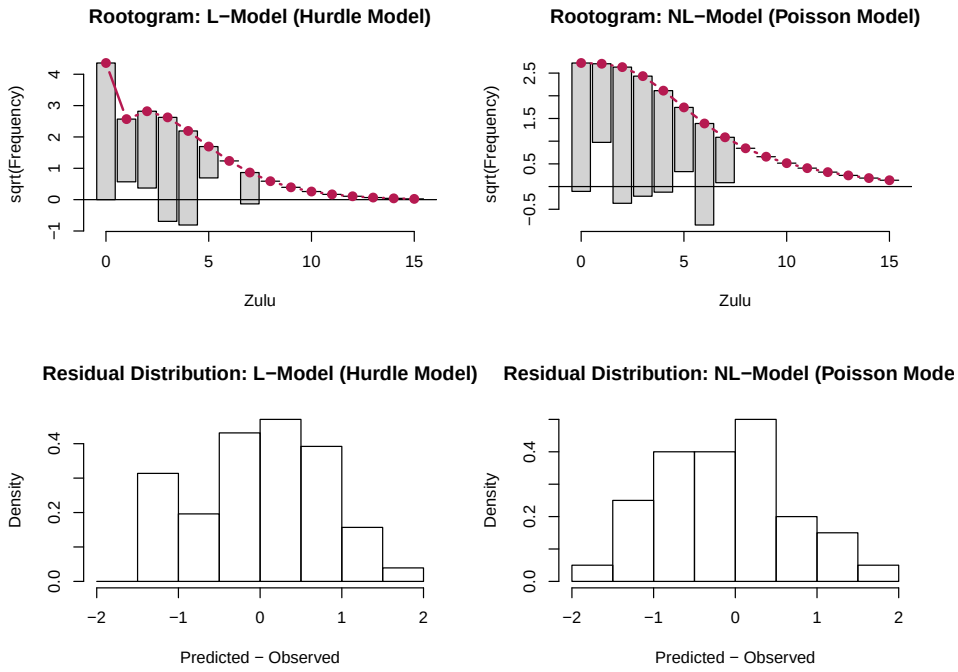

Figure 5.7: Rootograms and residual distributions for evaluating model fit

5.4.2 Hurricane-related port shutdown risks to the Texas Port System

The prediction model (L-model or NL-model) for calculating the probabilities and the expected values of shutdown durations are determined using the algorithm presented in Figure 5.5. Based on the expected days of shutdowns of each port, the simulated hurricanes corresponding to various return periods (10-, 20-, 50-, 100-, 200-, 500-, and 1000-years) were identified. Figure 5.8 presents the expected shutdown durations corresponding to the hurricanes identified. For each

port, the expected duration of shutdown increases as the severity of the hurricanes increases. For example, the expected duration of the shutdown of Port Houston due to a 1 in 10-year hurricane is estimated to be 3.0 days, whereas, the same due to a 1 in 1000-year hurricane is 8.6 days.

Figure 5.8: Expected duration of hurricane-related port shutdowns of various return periods

The results indicate that the operational risks posed by low-intensity hurricanes (characterized by low return periods) to all ports in Texas are relatively uniform. For example, the expected number of days of shutdown due to 1 in 10-year hurricanes on all ports is between three and four days. However, due to the geographical characteristics of locations, there is a large variation in the expected days of shutdown resulting from low-probability high-intensity hurricanes in those regions. For example, the duration of port shutdowns due to 1 in 500-year hurricanes

range between 5.9 and 9.7 days. The ports that have very high risks to hurricane-related port shutdowns are Texas City, Galveston, and Freeport. The higher risks to the above ports are dominantly due to two reasons as follows:

1. The above ports are located along the coastal regions of Texas that are susceptible to more severe hurricanes.
2. The ports located close to the coast have higher exposure to severe hurricanes than those situated on bays or rivers.

The ports with the lowest shutdown risks from hurricanes are Orange, Beaumont, Port Arthur, and Brownsville, which are located at regions with relatively lower hurricane risks.

It must be noted that the above predictions are made using models that are developed based on historical port shutdown data set with limited shutdown information about low-probability high-intensity hurricanes. Therefore, several of the port shutdown duration predictions presented in Table 5.8 corresponding to larger return periods (for example, 1 in 1000-year events) are extrapolated values using the developed models with predictor values outside the range of the model data set. Therefore, those estimates are susceptible to errors and this fact must be taken into account while drawing any inference about the operational and economic risks of hurricanes events of very low probability.

5.4.3 Predicted economic impacts of single-day shutdown of ports in Texas Port System

The economic impacts of single-day port shutdowns were quantified by employing the IT-IIM (Case A and Case B) on port data retrieved from U.S. Trade Online (U.S. Census Bureau, 2019) and the OECD U.S. input-output tables (Organization for Economic Cooperation and Development, 2019) for the year 2015 (Equations 5.10 and 5.11). The economic impacts of a single-day shutdown of each port in the Texas port system on the U.S. economy, in terms of Gross Trade Economy (GTE) (J. Jung et al., 2009), are presented in Table 5.6. Along with the economic impacts on the overall economy, the direct and indirect impacts on various industrial clusters were also evaluated. The directly impacted industry clusters are those immediately affected by the shutdown due to import and export delays or disruptions resulting from port shutdown. The indirectly impacted industries do not necessarily depend on the disrupted ports for imports and exports; however, they could also be affected due to forward and backward linkage effects in the economy.

From the estimated values, it is evident that single day disruption to Port Houston will have the largest overall impact on the U.S. economy compared to other ports in Texas. The overall economic impact due to a single-day shutdown of Port Houston in 2015 estimated using IT-IIM Case A model (which assumes all the imported are used as intermediary goods by domestic industries) was $706.5M, whereas, the same estimated using IT-IIM Case B model (which assumes all imports are used for direct domestic consumption) was $554.3M. The industry cluster that could be most impacted by disruptions in imports due to a single-day shut-

Table 5.6: Predicted economic impacts of single-day shutdown and the three most-affected industry clusters

Port	Estimated economic impact†			Industries clusters most directly affected†		Industries clusters most indirectly affected†	
	Case A	Case B	Mean	In terms of imports	In terms of exports	Case A	Case B
Corpus Christi	82.73	70.71	76.72	Cluster 2 (10.591) Cluster 9 (5.107) Cluster 17 (1.408)	Cluster 9 (14.348) Cluster 2 (6.146) Cluster 10 (3.483)	Cluster 9 (38.21) Cluster 2 (23.063) Cluster 10 (7.174)	Cluster 9 (33.287) Cluster 2 (19.06) Cluster 10 (6.961)
Freeport	40.66	34.41	37.53	Cluster 2 (7.639) Cluster 10 (0.675) Cluster 17 (0.644)	Cluster 18 (5.644) Cluster 10 (3.272) Cluster 2 (0.698)	Cluster 18 (15.321) Cluster 2 (11.489) Cluster 10 (7.628)	Cluster 18 (14.731) Cluster 2 (8.601) Cluster 10 (6.999)
Galveston	25.04	17.11	21.08	Cluster 17 (4.323) Cluster 10 (0.573) Cluster 1 (0.522)	Cluster 17 (1.632) Cluster 1 (0.821) Cluster 10 (0.809)	Cluster 17 (13.249) Cluster 18 (2.909) Cluster 1 (2.832)	Cluster 17 (7.953) Cluster 1 (2.253) Cluster 18 (2.205)
Houston	706.50	554.31	630.41	Cluster 2 (23.058) Cluster 10 (18.818) Cluster 17 (18.283)	Cluster 10 (62.798) Cluster 9 (61.111) Cluster 17 (32.689)	Cluster 10 (157.764) Cluster 9 (144.806) Cluster 17 (113.413)	Cluster 10 (140.207) Cluster 9 (132.641) Cluster 17 (91.016)
Port Lavaca	4.61	3.73	4.17	Cluster 10 (0.578) Cluster 3 (0.395) Cluster 14 (0.057)	Cluster 10 (1.373) Cluster 9 (0.013) Cluster 1 (0)	Cluster 10 (3.772) Cluster 3 (0.633) Cluster 14 (0.128)	Cluster 10 (3.233) Cluster 3 (0.395) Cluster 14 (0.057)
Texas City	49.48	45.30	47.39	Cluster 2 (9.015) Cluster 10 (0.476) Cluster 9 (0.331)	Cluster 9 (14.144) Cluster 10 (3.702) Cluster 2 (0.348)	Cluster 9 (28.429) Cluster 2 (12.902) Cluster 10 (8.075)	Cluster 9 (28.11) Cluster 2 (9.494) Cluster 10 (7.631)
Brownsville	6.86	4.38	5.62	Cluster 9 (0.822) Cluster 17 (0.42) Cluster 16 (0.305)	Cluster 2 (0.746) Cluster 9 (0.258) Cluster 15 (0.065)	Cluster 9 (2.12) Cluster 2 (1.028) Cluster 17 (0.983)	Cluster 9 (1.328) Cluster 2 (1.028) Cluster 17 (0.468)
Beaumont	42.72	39.02	40.87	Cluster 2 (3.389) Cluster 9 (0.637) Cluster 17 (0.513)	Cluster 9 (13.281) Cluster 10 (2.046) Cluster 1 (1.21)	Cluster 9 (27.336) Cluster 2 (4.67) Cluster 10 (4.621)	Cluster 9 (26.722) Cluster 10 (4.3) Cluster 2 (3.389)
Orange	0.0007	0.0007	0.0007	NA‡	Cluster 10 (0.0004)	Cluster 10 (0.0007)	Cluster 10 (0.0007)
Port Arthur	75.78	62.49	69.13	Cluster 2 (26.923) Cluster 9 (2.145) Cluster 8 (0.4)	Cluster 9 (13.883) Cluster 2 (1.885) Cluster 10 (0.992)	Cluster 2 (39.698) Cluster 9 (31.479) Cluster 10 (2.007)	Cluster 2 (29.521) Cluster 9 (29.411) Cluster 10 (1.964)

†All loss estimates in million US$. All values correspond to the year 2015.
‡No import data was reported during the analysis period.

down of Port Houston is the Cluster 2 (mining and extraction of energy-producing products) with an estimated loss of $23.1M, whereas the industry cluster that could be most impacted by a delay in exports is the Cluster 10 (chemicals and pharmaceutical products) with an estimated loss of $62.8M. As far as the industry-specific impacts are concerned (taking into account of both the direct and indirect economic impacts), the industry cluster most affected is Cluster 10 (chemicals and pharmaceutical products) with an estimated economic impact of $157.8M according to IT-IIM Case A model and $140.2M according to IT-IIM Case B model.

5.4.4 Predicted economic risks of hurricane-related shutdown of ports in Texas

5.4.4.1 Economic impacts of individual port shutdowns

In order to estimate the port-specific economic risks, the estimates of economic impacts due to the single-day port shutdown were combined with the expected number of port shutdown days of various return periods. The expected port-specific economic impacts corresponding to various return periods is presented in Figure 5.9.

In the figure, the maximum and minimum values of error bars denote the economic impacts estimated by IT-IIM Case A and Case B models respectively, whereas, the bar heights represent the mean economic impact. Evidently, as the intensity of hurricanes increases, there is a substantial increase in the economic risks due to prolonged port shutdowns. Port Houston faces the highest economic risks due to hurricane-related port shutdowns with an estimated mean economic impact of $2.28 billion due to a 1 in 10-year hurricane and an estimated mean economic

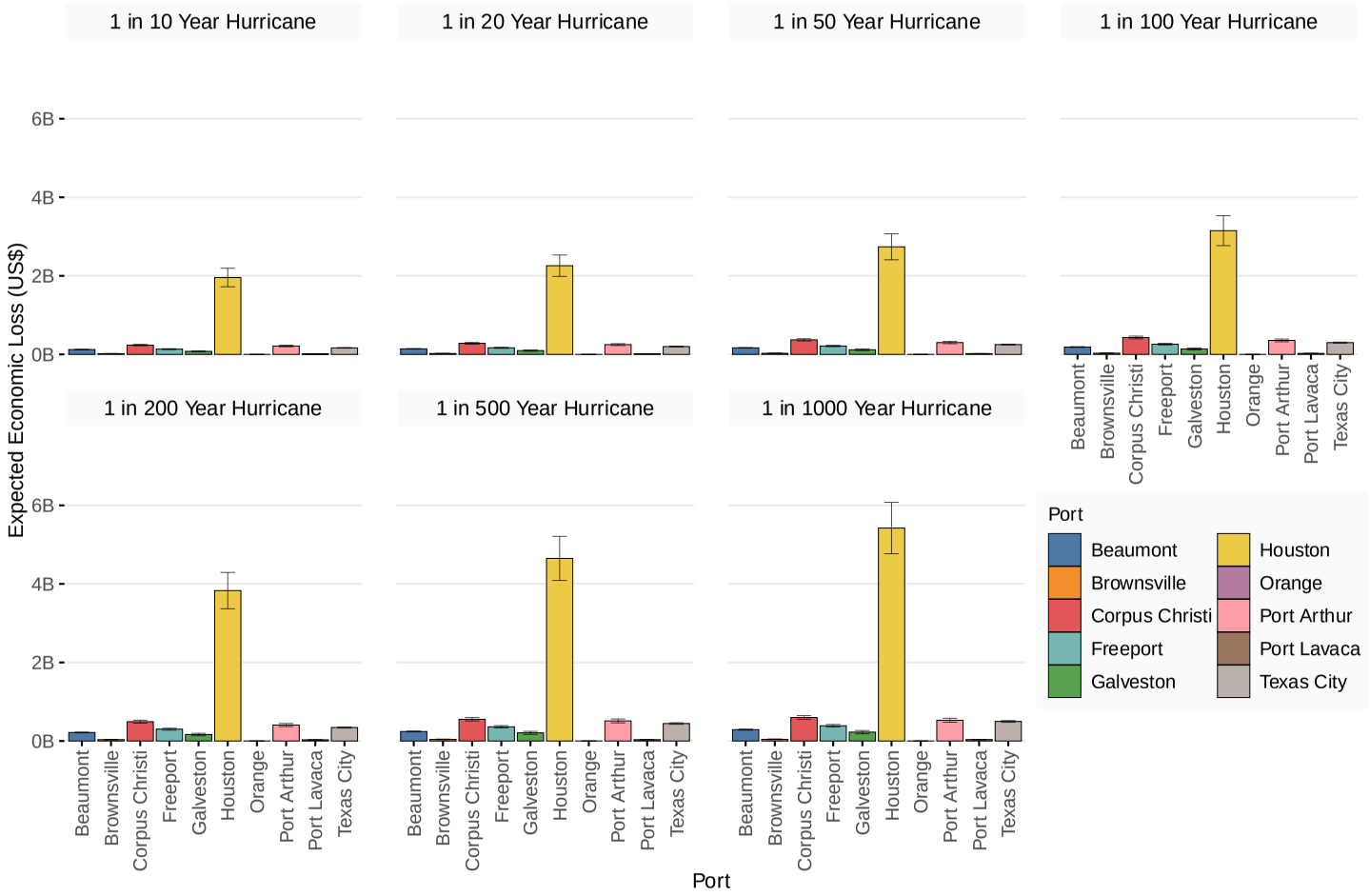

Figure 5.9: Estimated mean economic loss incurred to U.S. economy due to hurricane-related individual port shutdowns in Texas

impact of $4.3 billion.

5.4.4.2 Economic impacts of simultaneous shutdown of ports

While understanding the economic impacts of the hurricane-related shutdowns of each port in a port system is extremely useful in devising mitigation measures, an equally important aspect to investigate is the cumulative economic impacts of a simultaneous shutdown of multiple ports resulting from a single hurricane event. For this purpose, the cumulative economic impacts of port shutdowns in Texas resulting from each hurricane in the HITS database were calculated and the cumulative economic impacts of various return periods were estimated.

Table 5.7 presents the cumulative economic impact due to hurricane-related simultaneous shutdown of Texas ports considering various return periods. For a return period of 10-years, the expected cumulative economic impact is estimated to be $2.80 billion ($3.11 billion according to IT-IIM Case A model and $2.49 billion based on Case B model). Similarly, for a 500-year return period, the expected cumulative economic impact is $6.20 billion ($6.88 billion based on IT-IIM Case A model and $5.52 billion according to Case B model).

The hurricane tracks corresponding to various return periods based on cumulative impacts of simultaneous port shutdowns were identified from the HITS database and are illustrated in Figure 5.10. The expected days of shutdown of Texas ports due to each of the hurricanes are also presented for comparison. It is observed that the cumulative economic impacts are largely the consequence of the simultaneous shutdown of ports in the Houston and Beaumont regions. Due to

Table 5.7: Hurricanes of various return periods based on cumulative economic impact due to simultaneous shutdown of ports

Return Period*	Cumulative economic impact†			Top three most-affected ports in terms of economic impacts†		
	Case A	Case B	Mean	I	II	III
10	3.107	2.494	2.800	Houston (1.980)	Port Arthur (0.190)	Texas City (0.160)
20	3.578	2.857	3.218	Houston (2.482)	Port Arthur (0.198)	Texas City (0.159)
50	4.326	3.475	3.900	Houston (2.577)	Port Arthur (0.401)	Beaumont (0.219)
100	4.958	3.981	4.469	Houston (3.143)	Port Arthur (0.31)	Corpus Christi (0.26)
200	5.470	4.665	5.256	Houston (4.103)	Corpus Christi (0.287)	Port Arthur (0.218)
500	6.883	5.515	6.199	Houston (4.543)	Texas City (0.414)	Port Arthur (0.364)
1000	8.412	6.708	7.560	Houston (5.928)	Texas City (0.469)	Port Arthur (0.406)

*Return periods in years.
†All loss estimates in billion US$. All values correspond to the year 2015.

the geographical proximity of the ports in the above two port-clusters, a hurricane that affects these regions could lead to the shutdown of multiple ports and result in significant economic impacts on the U.S. economy. The possibility of the simultaneous shutdown of ports in these clusters must be taken into consideration while developing mitigation plans, such as rerouting or cargo capacity enhancement.

5.5 Implications of the Methodology on Port- and Supply Chain Resilience Management

The presented methodology may be of interest to a wide range of port stakeholders, including port authorities, private port operators, port-dependent industries,

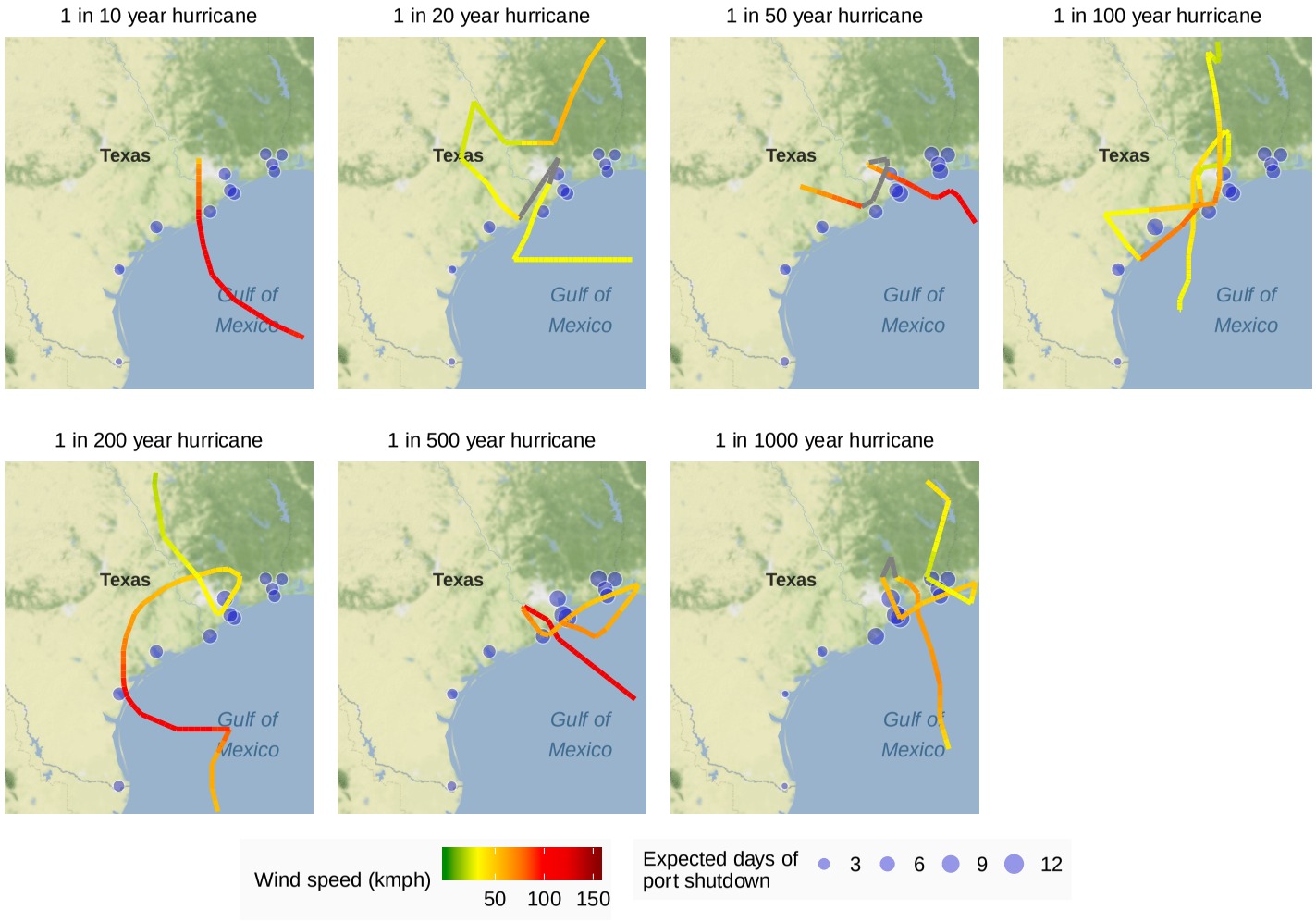

Figure 5.10: Simulated hurricanes of various intensities identified from HITS database based on the combined economic impacts due to simultaneous shutdown of Texas ports (Grey-colored line segments indicate the hurricane track segments with no wind speed details)

and different levels of governments. Given how critical the operational continuity of ports are for the regional and national economies, the economic risks could be integrated into decision-making processes related to port investments and management. To be specific, the aleatory uncertainties associated with hurricane-related shutdowns and resultant economic risks are characterized using return periods, a widely adopted measure to represent the probability of occurrence of natural disasters in a given year. For example, the expected economic impact on the U.S. economy due to simultaneous shutdown of ports in Texas resulting from a 1 in 10-year hurricane is approximately \$280 millions $(1/10 \times \$2.8$ billion) according to Table 5.7, which is higher than the expected cumulative impacts due to hurricanes of higher return periods. Such information could be of extreme importance for the port agencies and various levels of governments to make decisions related to annual spending on resilience interventions in the Texas port system. Similar methods can be adopted by other port stakeholders to improve their capabilities to minimize economic risks due to hurricane-related port shutdowns. Table 5.8 lists some of the potential applications of the proposed methodology from the perspective of various stakeholders responsible for the management of ports.

5.6 Conclusion

In this chapter, a methodology is presented for evaluating the operational and associated economic risks posed by hurricanes to ports. As part of the study, port shutdown prediction models were developed using the hurricane- and port-related data based on historical port shutdown events. The prediction models were

Table 5.8: Potential applications of proposed methodology for port resilience management from the perspective of different stakeholders

Stakeholders	Role in ports	Resilience improvement strategies	Application of proposed methodology
Port authorities and private port operators	Port investments and management	Port expansions	Compare disruption risks to various alternatives
		Port infrastructure design	Determine facility requirements based on hurricane intensities
Industries and logistics companies	Dependent on ports for imports/exports	Inventory management and contingency logistics	Estimate the value of commodities at risk for import disruptions
		Alternative routing strategy	Identify ports which have the least probability of simultaneous shutdown
Governments and public agencies	Formulation of policies and port development	Resilience investment decisions related to ports and port systems	Estimate overall impact on regional or national economy due to port shutdowns

later employed for estimating the future operational risks to Texas Port System due to hurricanes using simulated hurricane tracks. The operational risks of ports were combined with port-specific economic impact due to single-day shutdowns in order to predict the direct and indirect economic risks of port closures in Texas. In the process, the most critical ports in Texas and dependent industries were identified. The economic risks of simultaneous port closures in Texas were also evaluated. It was found that even though Port Houston has relatively lower shutdown risks compared to many other ports in Texas, such as Freeport and Galveston, the significantly large quantity of commodities being handled by Port Houston makes it the port in Texas which has the highest impact on U.S. economy.

It must be emphasized that port shutdowns occur not only due to the phys-

ical impacts of hurricanes, but are also ordered as a precautionary measure and to prepare ports against any impending threat from hurricanes. In such cases, reducing the port shutdown duration may not be always possible. Nevertheless, for a port authority, the proposed framework offers a systematic methodology to quantify the economic risks of port shutdowns and make informed decisions on future resilience enhancement investments which could significantly reduce the hurricane damages and improve restoration capabilities. However, deciding the type of investments needs further investigation with due consideration to the technical, operational, geographical, and organizational aspects of the port. From the perspective of port-dependent industries, understanding the shutdown risks could aid in planning and implementing mitigation measures to reduce the supply chain disruptions by adopting measures, such as making alternative arrangements for transportation of commodities and optimizing inventories.

While highlighting the numerous advantages of the methodology, there are a few limitations that provide directions for further research.

- As discussed before, the port shutdown duration prediction models are based on a very small number of recent hurricane events for which port shutdown information is available. The current attempt is expected to highlight the need for more extensive and systematic data collection efforts with regard to infrastructure system disruptions due to extreme weather events which could assist stakeholders to make risk-informed decisions for resilience enhancement.

- The number of high-intensity hurricanes in the port shutdown data set is lim-

ited and therefore the predictions using the developed models corresponding to low-probability, high-intensity hurricanes may be susceptible to large variations.

- Additionally, the scope of the prediction models could be expanded by incorporating the specific resilience capabilities of the ports that could significantly reduce the shutdown duration.
- Moreover, the current methodology could also be improved by considering the potential changes in hurricane intensity and frequency that may result from climate change.

Chapter 6

Mapping Resilience of Infrastructure Systems Using Historical Data: A Case Study of Houston Freeway Network During Hurricane Harvey [1]

6.1 Introduction

Severe natural disasters, such as hurricanes, floods, and earthquakes, can severely impact critical infrastructure systems (CIS) leading to large-scale functional disruptions in the dependent urban systems. As far as disaster management is concerned, among the major critical infrastructure systems, road networks are of utmost importance as they play a crucial role in evacuation, emergency response and logistics, restoration of essential facilities, and recovery in affected areas. However, road networks are highly vulnerable to hazards due to their vast geographical scale and direct exposure to the environment. Apropos hurricanes, transportation infrastructure (such as bridges and pavements) are subjected not only to the direct damage inflicted by the intense rainfall and powerful, sustained winds and wind gusts but also to the resultant flooding and debris formation. In addition, traffic signals, illumination, and Intelligent Transportation Systems (ITS) message signs

[1] based on Balakrishnan, S., Z. Zhang, R. Machemehl, M. Murphy. 2020, Mapping resilience of Houston freeway network during Hurricane Harvey using extreme travel time metrics, *International Journal of Disaster Risk Reduction*, https://doi.org/10.1016/j.ijdrr.2020.101565

may be disrupted, due to fallen transmission lines resulting in loss of electrical power, communications, and other services. Such incidents heavily influence traffic flow characteristics in cities before-, during- and immediately after hurricanes. It is therefore of utmost importance to understand how traffic conditions vary due to hurricanes and identify road segments which could be the worst-affected to make improvements in existing disaster management practices. In addition, from a resilience point of view, understanding the extent and types of impacts and how the traffic network recovered to normal conditions is extremely important to document and understand (O'Rourke, 2007).

In this study, an attempt is made to understand the traffic variations on the freeway network in the Houston region, Texas caused by Hurricane Harvey using link-level travel times collected using *Bluetooth*® sensors. Instead of using conventional travel time reliability measures, the metrics for measuring the effect of the hurricane on the traffic conditions are developed based on extreme travel time observations. An extreme travel time observation, in this study, is defined as one that considerably deviates from normal travel times trends based on non-hurricane travel time data. The underlying assumption is that the frequency and magnitude of extreme travel time observations are correlated to the hurricane impacts on the traffic network and driver travel choices. Time series analysis techniques combined with anomaly detection algorithms were used to identify links that experienced extreme travel times and to identify the worst-affected freeway links. For this purpose, three transportation resilience metrics based on extreme travel time observations were introduced and the hurricane-effects on the traffic and subse-

quent recovery on freeway links were quantified. An alternative representation for measuring the resilience of traffic networks, analogous to the well-known resilience triangle (Bruneau et al., 2003), is also presented. While fluctuations in travel times are the result of a combination of several potential causes, including high water over a roadway or bridge and changes in traffic movements, the results provide considerable insight into the extent of the impact on the freeway network and its recovery to pre-disaster conditions.

The rest of this chapter is organized as follows: the Literature Review section presents an overview of existing methods for analyzing transportation system resilience; the Methodology section discusses the stages in the study methodology; the Discussion of Results section presents an application of the methodology for quantifying traffic impacts of Hurricane Harvey on the Houston freeway network; and the Conclusion section summarizes major findings.

6.2 Literature Review

Disruption to transportation infrastructure is a major source of social and economic loss during disasters. Therefore, the extent of such disruptions (physical and socio-economic) and the rapidity with which the affected transportation infrastructure can be restored to pre-disaster conditions are crucial factors determining urban resilience (Chang, 2003). While the rapid restoration of disrupted road links and efficient real-time traffic management are top priorities of emergency management in urban regions, it requires identification of the most vulnerable links based on the physical and traffic impacts caused by historical extreme events in the region

and the availability of alternate routes. Quantification of the effects on various links can also be used to assess the effectiveness of existing emergency management practices in order to make improvements to enhance preparedness and response during future extreme events (Faturechi & Miller-Hooks, 2015).

6.2.1 Quantification of disaster-induced effects in transportation systems

Quantification of physical effects of extreme events on transportation systems is conducted by employing relevant performance measures that reflect the functional- or road network characteristics. The effects of external stresses or incidents on traffic networks are estimated by calculating the loss in functionality experienced during the extreme event in terms of one or several performance indicators. Faturechi and Miller-Hooks (2015) classified such measures of effectiveness into five categories- travel time/distance-based, throughput/capacity-based, accessibility-based, economic measures, and topology-based measures, among which the first four are commonly used for evaluating direct and indirect effects of historical disasters. The performance measures are used to study a wide range of traffic- and behavior-changing patterns, such as route choice, mode choice, and extent of congestion, caused by extreme events. For example, Ganin et al. (2017) evaluated the resilience of road networks in forty major urban areas in the U.S. by simulating random failure of road links and estimating the resultant cumulative increase in network delays due to vehicle rerouting. In another study, Zhu, Levinson, Liu, and Harder (2010) investigated the changes in traffic and travel behavior patterns in Minneapolis, Minnesota caused by the I-35W Mississippi River bridge collapse

by conducting before-after comparisons of several indicators, such as traffic counts on adjacent bridges, mode choice, departure and arrival times of commuter, and total commute time. A study by Giuliano and Golob (1998) based in Los Angeles evaluated the long-term effects of failure of two major highway corridors after the Northbridge earthquake in 1994 on commuter mode choice, route choice, work trip times, and home and work locations. In an attempt to quantify the effects of potential targeted attacks on transportation networks, Murray-Tuite and Fei (2010) employed performance indicators, such as adjacent and opposing direction capacity reduction, bridge capacity reduction, and total and average trip times, to compare the pre- and post-attack traffic conditions on a sample network based in the Northern Virginia area.

6.2.2 Methods for evaluation of transportation system resilience

Along with quantifying the network-wide extreme event effects, another crucial factor determining the mitigation strategies is the resilience of the network components. With regard to the transportation infrastructure systems, Sun, Bocchini, and Davison (2018) defined a resilient system as the one which "should have a small probability of failure, redundant connectivity, minimal time of full recovery, and limited propagations of the effects." Methods developed for evaluating transportation system resilience could be broadly classified into two categories: (a) functionality-based methods, and (b) socioeconomic methods.

Two approaches are commonly adopted in functionality-based methods. In the first set of methods, the functionality measures, such as throughput or travel

time, are compared before and after the occurrence of the disaster. In the second set of methods, resilience is calculated as a function of the aggregate loss of functionality of the network starting from the time of extreme event occurrence until the network recovers to the normal state. Most of these methods are adapted from the concept of the "resilience triangle" introduced by Bruneau et al. (2003) for characterizing resilience in generic infrastructure networks. Mudigonda, Ozbay, and Bartin (2018) extended the application of the resilience triangle for comparing the resilience and vulnerability of public transit networks (rail, subway, and bus transit networks) in New Jersey during Hurricane Sandy. In another study, D'Lima and Medda (2015) developed resilience triangles based on passenger counts to quantify the resilience of the London Underground rail network against simulated Poisson shocks. As an alternative to resilience triangles, some studies introduced resilience indices to represent system resilience as a single normalized value. The delay-based metric developed by Ganin et al. (2017) for quantifying the resilience of major road networks in the U.S. and the metric based on total lost service days developed by Chan and Schofer (2016) for evaluating the resilience of transit systems in New York against hurricanes are relevant examples. The functionality-based resilience indices are also used for testing the effectiveness of disaster management strategies, such as transportation system component restoration after disasters (Aydin, 2018; Hu, Yeung, Yang, Wang, & Zeng, 2016).

Given the fact that transportation infrastructure plays a crucial role in the community- and economic resilience, several studies have also considered the socioeconomic impacts of disruptions while evaluating transportation system resilience.

Cox, Prager, and Rose (2011) adapted the concept of direct static economic resilience (DSER) to estimate the impacts of the 2005 London subway and bus bombings on commuting choices in the city. Similarly, Franchin and Cavalieri (2015) introduced a community resilience metric based on the proportion of population displaced to quantify the resilience of civil infrastructure systems such as transportation networks. In addition, community-based resilience indices have also been applied for prioritizing disaster affected regions for emergency logistics with a focus on interdependencies among various infrastructure systems (Balakrishnan & Zhang, 2018; Choi, Naderpajouh, Yu, & Hastak, 2019).

6.2.3 Gaps in the literature

The review of the literature revealed that there has been extensive research in the area of transportation system resilience (Faturechi & Miller-Hooks, 2015; Sun et al., 2018). With regard to the effects of extreme events on traffic conditions, the most widely used metrics are based on traffic performance, such as travel time and traffic counts. Several of these studies compare the values of traffic performance measures during the extreme event with that in the pre-event scenario to quantify the impacts and thereby the network resilience. However, the author thinks that this might not be the best approach as the absolute traffic performance indicators like travel times are also influenced by seasonal factors including time of the day and day of the week, holidays, and less than severe weather events. The most-affected links must be determined based on the true effects of extreme events on the traffic, which requires further processing of observed performance indicators.

In addition, performance measures like travel times alone may not be adequate for evaluating traffic conditions as a significant number of roads get flooded or damaged, preventing vehicle movements. Therefore, an alternative methodology is needed for evaluating disaster effects as well as for quantifying network resilience.

6.3 Methodology

Figure 6.1 illustrates the methodology proposed in the study. While the methodology was developed and implemented for analyzing the traffic fluctuations induced by Hurricane Harvey on the Houston freeway network, it can also be generalized for any other natural disaster. During natural disasters, irrespective of the type and magnitude of the disaster, their effects on traffic networks are caused by both the direct and indirect consequences (Figure 6.2). Direct effects include physical damages to the transportation infrastructure, whereas, the road closures and the evacuation-based trip decisions are the indirect consequences that determine the immediate traffic conditions. Such generality among natural disaster effects makes the current methodology flexible enough to study the traffic impacts caused by any natural disaster.

For the convenience of demonstrating the application of the methodology, the scope of the study was restricted to the freeway corridors in the Houston region which were flooded by heavy rainfall during Hurricane Harvey.

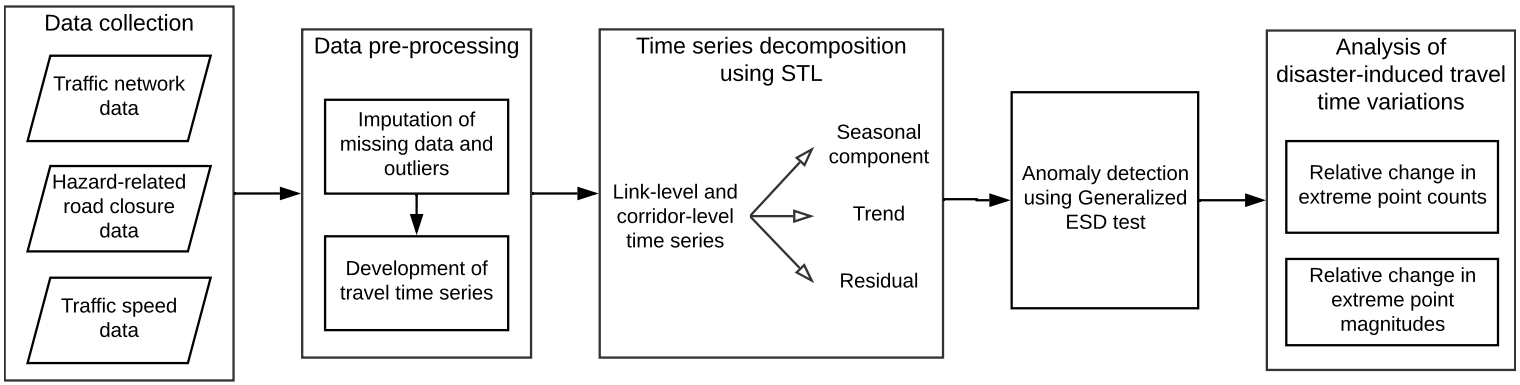

Figure 6.1: Methodology adopted in the study for investigating the changes in traffic conditions caused by natural disasters using extreme travel time metrics

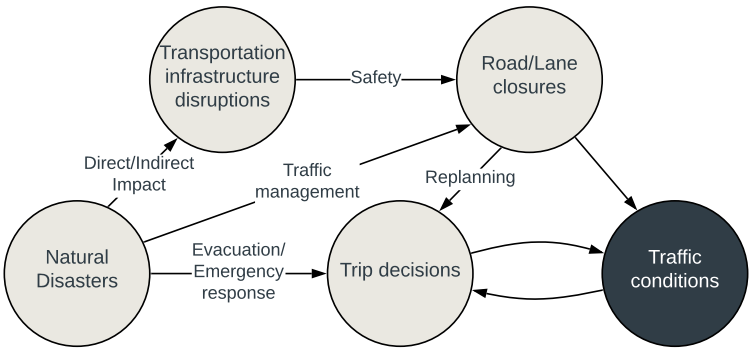

Figure 6.2: Effects of natural disasters on traffic conditions in affected regions

6.3.1 Data collection and pre-processing

For the study, three major data sets were used: (a) the Houston freeway network; (b) historical speed data before-, during-, and after Hurricane Harvey; and (c) road closure data during- and immediately after the hurricane event.

6.3.1.1 The Houston freeway network

The Houston freeway network considered in the study (Figure 6.3) consists of 485 freeway links including those belonging to IH-10, IH-45, IH-610, US-59, US-290, US-90, Beltway-8, Spur-330, SH-288 and SH-99. The data pertaining to the links such as the location of start and end intersections/interchanges, length, traffic direction, and geographic coordinates of the links were retrieved from the traffic maps available in the Houston Transtar website ([Dataset] Houston Transtar, 2019). A major share of the corridors in the freeway network is designated as hurricane evacuation routes (approximately 589 centerline miles out of the total 1,107 centerline miles in the network) by the Houston-Galveston Area Council ([Dataset]

Figure 6.3: Houston freeway network considered in the study (Map tiles by Stamen Design, under CC BY 3.0. Data by OpenStreetMap, under ODbL)

Houston-Galveston Area Council, 2017). Since the Gulf Coast is located South-East of Houston, the direction of all evacuation routes is generally from the South-East of Houston (coastal regions) to the West (toward San Antonio and Austin) and to the North (toward Dallas).

6.3.1.2 Traffic speeds

Traffic speeds or travel times can be used to track the performance of freeway corridors and links. Unlike traffic density and flow parameters, speed/travel time data is comparatively easier to obtain. Temporal variations in travel times or speeds in the traffic networks have been widely used to detect incidents like crashes (Abdel-Aty & Pande, 2007) or quantify the impact of special events (Jiann-Shiou Yang, 2005).

For the current study, traffic speed data was obtained from the Houston Transtar speed map archive. Houston Transtar has maintained a database consisting of 15-minute average speeds of 485 freeway links in Houston since January 2009 ([Dataset] Houston Transtar, 2019). Houston Transtar employs Anonymous Wireless Address Matching (AWAM) technology to detect Bluetooth enabled networking devices such as cellular phones, mobile GPS systems, telephone headsets, in-vehicle navigation, and hands-free systems. The time and location of the Bluetooth enabled devices are recorded by roadside AWAM readers and are later processed to estimate vehicle speeds and travel times. With prior permission from Houston Transtar, the traffic speed data pertaining to all the 485 links from June 16, 2017 (Friday) through September 28, 2017, was extracted from the web archive. The 15-minute average link speeds were later converted to 15-minute average link travel times. Figure 6.4 shows the historical travel times from one of the links in the Houston freeway network.

Once the travel times were computed, pre-processing of the data was performed to eliminate issues associated with missing observations from the travel

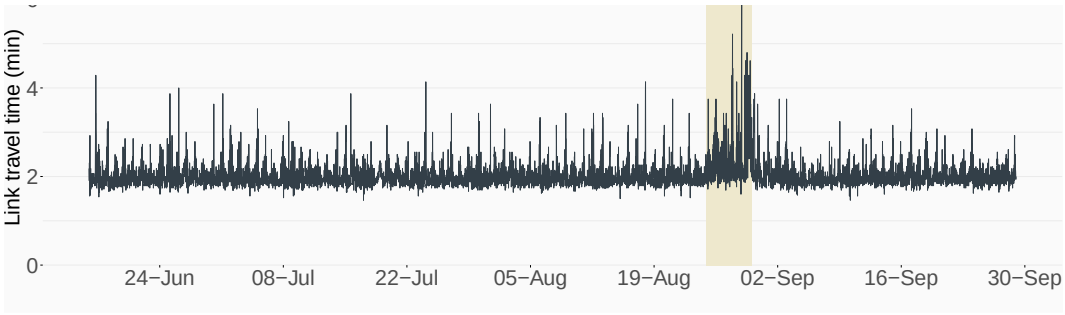

Figure 6.4: 15-minute travel times between June 16, 2017 and September 30, 2017 on Beltway 8-South Eastbound (from Hillcroft to South Post Oak) derived from historical 15-minute speed observations

time data sets. There were four major categories of missing data observations. The details, such as potential causes for the missing data, the corresponding imputation method used for each category of the missing data, and the amount of data affected, are tabulated in Table 6.1.

The 15th percentile travel time (corresponding to the 85th percentile speed) on the day of the missing data observation was chosen for imputing the periodic missing data to reflect the roadway and weather conditions on that day. The periodic missing data observations (due to ideal free-flow conditions) were imputed before the random missing data observations were imputed. This was done to prevent the imputation algorithm from introducing unnecessary seasonality in imputed values corresponding to the periodic missing data.

6.3.1.3 Road closure data

During natural disasters like hurricanes, roads are often closed due to traffic rerouting, high water, emergency response, debris removal, and previously es-

Table 6.1: Types of missing observations in the travel time data and imputation methods used

Type of missing data	Potential causes	Imputation method used	Quantity of data affected
No data (link-specific)	• Permanently dysfunctional roadside sensors. • Permanent closure of road links.	Remove links from further analysis.	7 out of 485 links had no reported travel time observations (∼1.5% of links removed).
Periodic missing data (link-specific)	• No vehicles on some links during off-peak hours.	Impute using free-flow travel time (15th percentile travel time on the link on that day).	24 out of 485 links affected (∼3.5% observations imputed.)
Random missing data (across all links)	• Temporary technical glitches in the data management system.	Impute using interpolated values obtained from fitted seasonal models (`forecast` package in R-statistical software).	478 out of 485 links affected (∼0.9% observations imputed.)
Random missing data (link-specific)	• Temporary technical glitches in some roadside sensors, road closure events, or special events.	Impute using interpolated values obtained from fitted seasonal models (`forecast` package in R-statistical software).	476 out of 485 links affected (∼1.4% observations imputed).

tablished work zones for maintenance and construction. Road closures may significantly affect vehicle movement on the affected lanes. Therefore, these events should also be considered while analyzing variations in travel times.

Since the road closure events related to Hurricane Harvey are relevant to the present study, the data pertaining to the road closure events in the Houston region between August 20, 2017, and September 10, 2017, was obtained from TxDOT Houston District Office. The data was later manually matched with the freeway links in the Houston network considered in the study. Out of the 218 events recorded in the region, 98 were located on the Houston freeway network. Figure 6.5 shows the various categories of road closure events (Figure 6.5a), the distribution of duration of closure events (Figure 6.5b) and the corresponding time and duration of occurrence (Figure 6.5c).

As evident, the duration and frequency of road closure events increased during and after the hurricane. These road closure events are dominated by high water, construction and unknown/NA reasons. Given the association of these road closures to the time of occurrence of the hurricane, these events are most-likely related to the hurricane and resultant rainfall and must be taken into account in the analysis of travel time fluctuations.

6.3.2 Time series decomposition and extraction of extreme link travel times

The hurricane-induced effects on the traffic network could last for several days or weeks. However, the travel times also fluctuate based on the time-of-the-day and day-of-the-week traffic flow variations. In addition, travel times on freeway

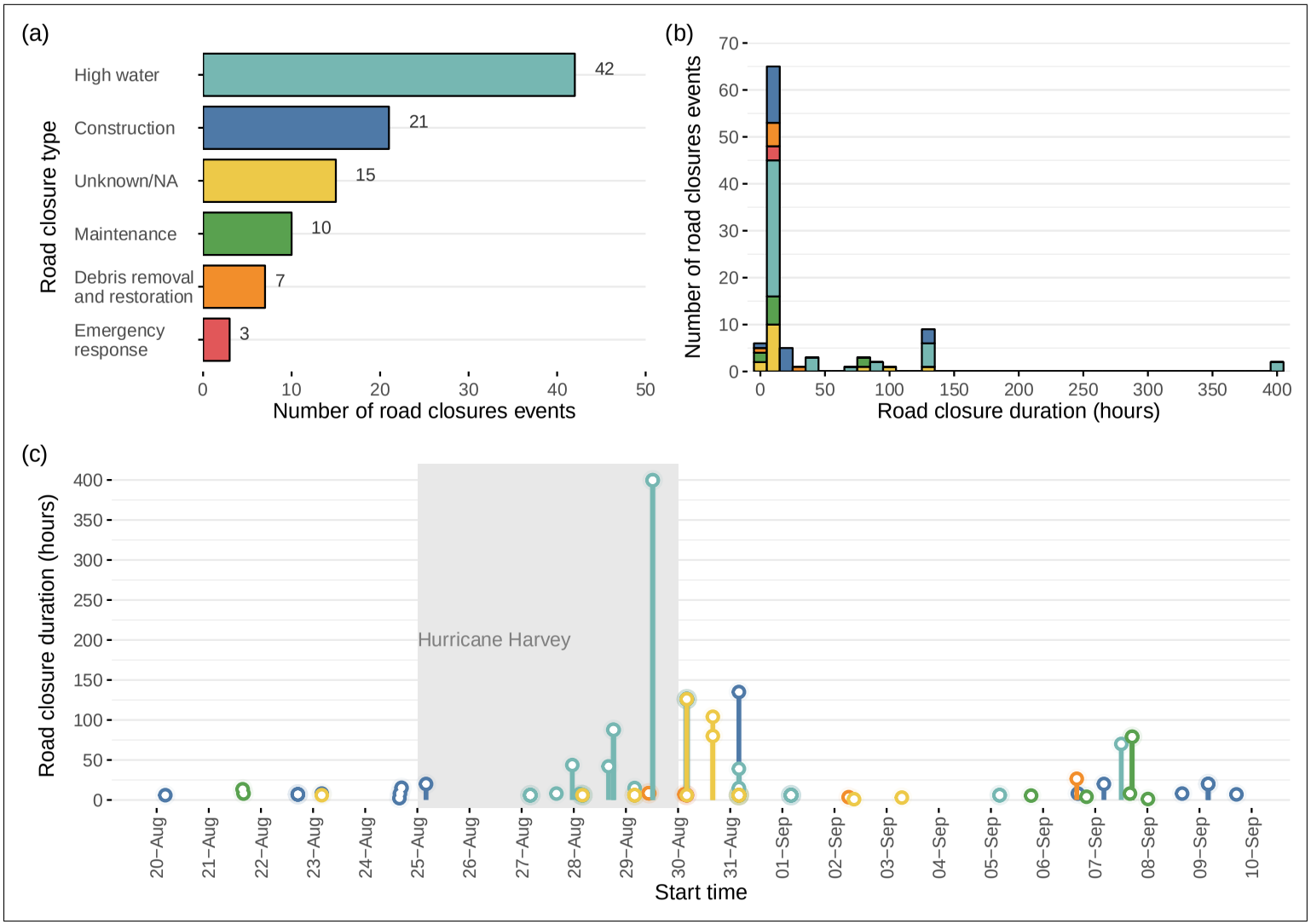

Figure 6.5: Road closure events in Houston freeway network between August 20, 2017 and September 10, 2017: (a) Road closure categories; (b) Road closure duration; and (c) Individual road closure start time and duration (Data source: Safety Office, TxDOT Houston District)

segments are also influenced by long-term and gradual land use changes in adjacent regions as well as new transportation projects. Time series decomposition offers an effective way to separate the seasonal variations and long-term trends from the observed travel times so that hurricane effects can be quantified. Since the present study focuses more on deviations from normal traffic behavior on links due to hurricanes, the traffic fluctuations were measured in terms of extreme travel time observations. An extreme travel time observation in this study is defined as a 15-minute observation in the link travel time data sets that deviates significantly from what is expected to be the normal travel time for a given time of the day and day of the week or overlaps with a hurricane-related road closure event. In this study, an anomaly detection algorithm was used to segregate unusual travel time observations (extreme observations) from the data sets. Anomaly detection techniques find applications in a wide range of domains, such as cybersecurity (Kumar, 2005; Ten, Hong, & Liu, 2011), social media analytics (Savage, Zhang, Yu, Chou, & Wang, 2014), and natural language processing (Gao, Kuo, Pieraccini, Quinn, & Wu, 2007), to identify unusual behavior in spatiotemporal data (Jiang, Yuan, Tsaftaris, & Katsaggelos, 2011).

6.3.2.1 Decomposition of travel time using Seasonal-Trend Decomposition using Loess method

Time series decomposition is the process of separating a time series into three components, namely, the trend component, seasonality component and the remainder component. This can be mathematically represented using Equation 6.1.

$$y_t = T_t + S_t + R_t \tag{6.1}$$

where y_t, T_t, S_t and R_t are the observed time series, the trend component, the seasonal component, and the remainder component, respectively, at time $0 \leq t \leq \tau$.

There are several time-series decomposition techniques available such as classical decomposition, Box-Cox transforms, ARMA errors, Trend, and Seasonal components (BATS), X11 decomposition, Seasonal Extraction in ARIMA Time Series (SEATS) and Seasonal-Trend Decomposition using Loess (STL). In this study, the STL technique was used for travel time decomposition because of its greater flexibility in choosing seasonality characteristics and the ability to handle series with missing data. Moreover, STL also allows controlling the degree of robustness against outliers (Cleveland, Cleveland, McRae, & Terpenning, 1990; Hyndman & Athanasopoulos, 2018), which makes it appropriate for identifying the abnormal variations in travel times due to external perturbations.

In STL decomposition, loess regression, which is a non-parametric smoothing technique using neighborhood weights, is used to fit a polynomial curve over the time series corresponding to the link travel time data of different links. The weights used in loess regression reduce the effect of outliers, and the non-parametric nature makes it an effective technique for detecting non-linear patterns in the time series. The STL decomposition was applied to the travel time data sets using the algorithm presented by Cleveland et al. (1990). The algorithm consists of two nested loops. In

the outer loop, a set of robustness weights is applied to each set of time-series observations to reduce the effect of outliers. The inner loop is used to iteratively update the seasonal and trend components from the observed data. To be specific, within the second loop, the time series is split into cycle-subseries to extract seasonal variations. The cycles are smoothed using the loess function and are passed through a low-pass filter. The seasonal components are obtained by subtracting the output of the low-pass filter from the loess-smoothed cycle sub-series. This is followed by subtracting the seasonal components from the actual time series and smoothing it. The resultant series is again loess smoothed to obtain the trend component. Finally, the remainder is obtained by subtracting the seasonal and trend components from the original series.

As far as time series of travel times are concerned, the trend usually denotes the long-term gradual change in travel times due to increases or decreases in traffic demand. The seasonal component of travel times captures the time of the day and day of the week variations in the travel times. The remainder (residual) component captures other random fluctuations in the travel times, mostly induced by traffic incidents such as crashes and special events. Since STL offers the flexibility to choose the rate of change over time, it can capture the periodic variations in travel times. For this study, the seasonal duration parameter in STL algorithm was set to 672 observations ([60 minutes/15-minute data observation interval = 4] $\times$ 24 hours $\times$ 7 days) so that the long-term trends, seasonal (weekly) variations, and the residual components can be separated from the observed travel times.

6.3.2.2 Identification of extreme 15-minute intervals using Generalized Extreme Studentized Deviate test

Once decomposition of travel time data sets using the STL method was carried out, the next step in the analysis was to develop metrics for quantifying the hurricane-effects on the network traffic conditions and subsequent recovery. In this process, the worst-affected links in the network during the various stages of recovery were also identified.

In this study, the worst-affected link is defined as the link which experienced extreme travel times for the longest period during the hurricane both in terms of magnitude and frequency. The number of extreme travel time observations is a metric reflecting the duration for which the link experienced travel times that were unexpectedly lower or higher than the normal link travel time (each point in the time series is an aggregated 15-minute average link travel time observation). The number of extreme travel times on a link is generally expected to be higher if a perturbation in the traffic is induced by an external hazard like a hurricane. On some links, the number of extreme observations may be lower than usual due to a decrease in traffic flows.

In order to identify the extreme observations in the travel time data sets, Generalized Extreme Studentized Deviate tests (Generalized ESD tests) were conducted on the remainder components of the link-wise travel time data sets obtained in the STL method. The Generalized ESD test is used to identify one or more outliers in a univariate normal data set (Rosner, 1983). Since the remainder component obtained from the STL analysis is relatively normal, the Generalized ESD test

is an appropriate test for identifying travel time observations that have considerable deviation from those during normal traffic conditions.

The Generalized ESD test checks if there are up to r outliers in a data set against the null hypothesis that there are no outliers at all. The test statistic for each observation in a sample of size n is given in Equation 6.2 where x_i is the ith observation in the sample; $\bar{x}$ is the mean and s is the standard deviation of the sample.

$$R_i = \frac{\max_i |x_i - \bar{x}|}{s} \tag{6.2}$$

Next, the observation maximizing the test statistic R_i is removed from the sample and the test statistic for the remaining observations is recomputed. This process is repeated until r observations (potential outliers) are removed. Next, corresponding to the r test statistics computed, r test critical values are calculated using Equation 6.3.

$$\lambda_i = \frac{(n-i)t_{p,n-i-1}}{\sqrt{(n-i-1+t^2_{p,n-i-1})(n-i-1)}};\ i = 1, 2, \ldots r \tag{6.3}$$

where $t_{p,n-i-1}$ is the value in the t-distribution corresponding to $100p$ percentage value and $(n-i-1)$ degrees of freedom. The value of p is calculated as in Equation 6.4:

$$p = 1 - \frac{\alpha}{2(n-i+1)} \tag{6.4}$$

where α is the confidence level. The number of outliers in the sample is determined by the largest i such that $R_i > \lambda_i$. In the current study, the value of r was set as 20% of the total number of travel time observations on a link, and α was set to 0.05. Selecting a relatively higher value for r would prevent any outliers from being not identified at the chosen confidence level.

Figure 6.6 demonstrates how the STL method followed by anomaly detection using the Generalized ESD test is applied to identify extreme travel time observations (15-minute intervals) on a link in the Houston freeway network between June 16, 2017, and September 28, 2017. The first subfigure shows the observed travel times, the second one shows the long-term trend (since the time frame considered is short, this is a flat line implying no gradual changes in travel time patterns), the third one is the seasonal component, and the last one is the remainder travel time component. As expected, the seasonal component repeats every week (Friday through Thursday). The concentration and magnitude of extreme observations abruptly increase between August 25, 2017, and September 01, 2017, when Hurricane Harvey struck the Houston-Galveston region (marked in light green). This suggests that the two characteristics, namely, magnitude and frequency of extreme observations, could be used for estimating the hurricane effects on network link travel times.

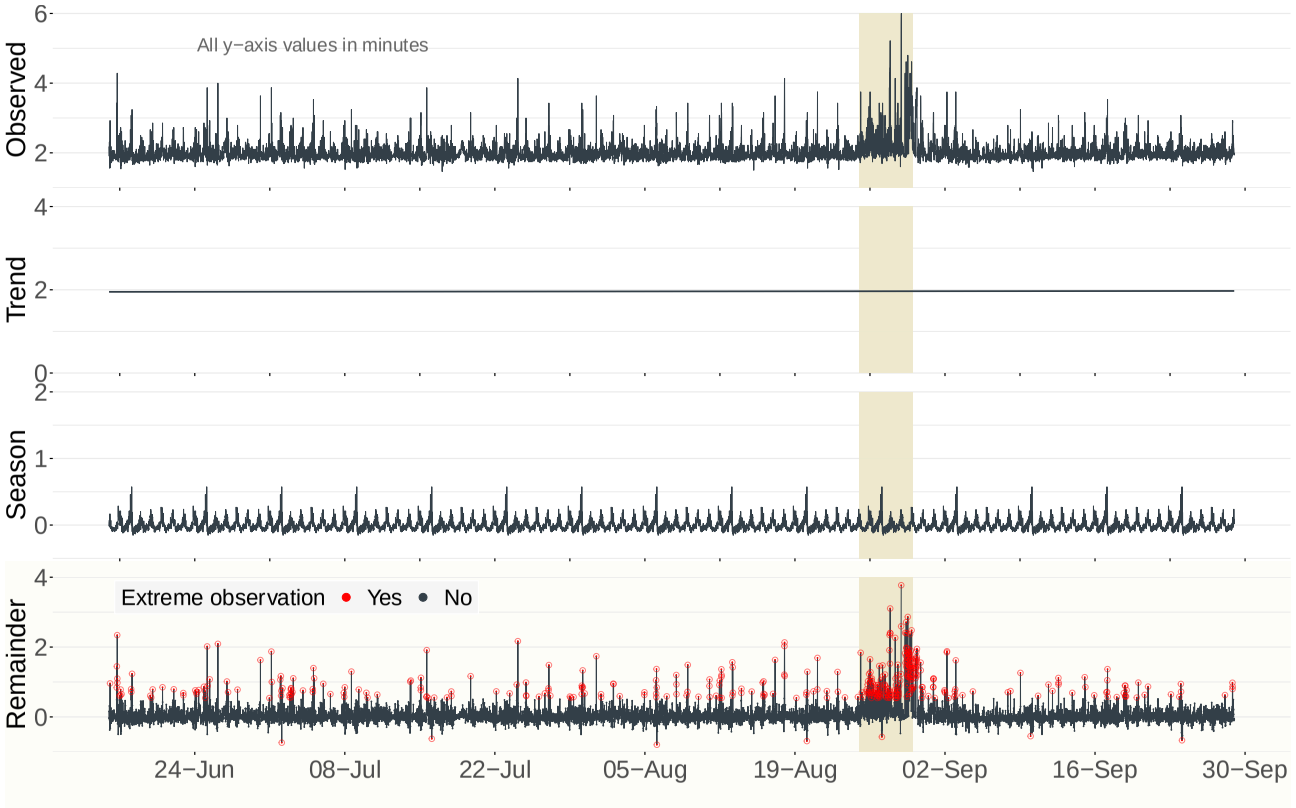

Figure 6.6: Detection of extreme 15-minute travel time observations (in minutes) between June 16, 2017, and September 30, 2017, on Beltway 8-South Eastbound (from Hillcroft to South Post Oak) using STL method followed by Generalized ESD test ($r \leq 20\%$ and $\alpha = 0.05$)

6.3.3 Analysis of hurricane-Induced travel time variations

6.3.3.1 Extreme observation-based metrics

For the ease of analysis of the hurricane-induced travel time variations described by mean and variance and to identify the worst-affected links, the travel times were categorized weekly (however, the analysis could be also done for shorter time spans to obtain more disaggregate traffic variations, even though it could be computationally expensive). Since the rainfall associated with Hurricane Harvey started on August 25, 2017, every week in this study begins on Friday and ends on the subsequent Thursday. With the objectives of capturing the travel time variations and thereby to understand the network impacts and recovery patterns, two link metrics were introduced.

1. Relative change in number of extreme travel time observations:

$$\Delta n_w^i = n_w^i - \text{med}\{N_{historical}^i\} \tag{6.5}$$

where Δn_w^i is the relative change in number of extreme observations in week w on link i; n_w^i is the absolute count of extreme observations obtained in week w; and med$\{N_{historical}^i\}$ is the historical median weekly count of extreme observations on that link. Choosing the median historical values for representing normal conditions would eliminate the effect of any abrupt travel time fluctuations that occurred due to unknown reasons.

2. Relative change in mean size of extreme travel time observations:

$$\Delta y_w^i = \bar{y}_w^i - \text{med}\{Y_{historical}^i\} \tag{6.6}$$

where Δy_w^i is the relative shift in mean size of the remainder component of extreme observations in week w on link i, $\bar{y}_w^i$ is the absolute mean size of the remainder components of the extreme observations and is obtained as the average of residual components of all the n_w^i extreme observations reported in week w excluding those corresponding to road closures (travel times during road closures are undefined); and $\text{med}\{Y_{historical}^i\}$ is the historical median of the weekly average size of the remainder components of the extreme observations.

The set of historical weekly values $N_{historical}^i$ and $Y_{historical}^i$ were obtained from the remainder components of the travel time data between June 16, 2017 (Friday) and August 10, 2017 (Thursday). From a driver's perspective, the above two metrics capture two distinct types of uncertainties: (a) Δn_w^i indicates the change in probability by which a driver could experience an extreme travel time on a link in a hurricane-affected week, and (b) Δy_w^i indicates how much worse or better the experienced travel time would be if a driver has to make a trip on the link during an extreme 15-minute interval compared to that in a normal week.

The above two link metrics can be calculated using extreme travel time observations with either positive remainder components or negative remainder components separately, depending upon the objective of the analysis. Metrics based on

extreme travel time observations with the positive remainder ($\Delta n^i_{w,+}$ and $\Delta y^i_{w,+}$) may be used to identify those freeway links whose traffic conditions are worsened during and after the hurricane (or any other natural disaster). On the other hand, metrics developed based on extreme travel time observations with the negative remainder ($\Delta n^i_{w,-}$ and $\Delta y^i_{w,-}$) could identify those links which witnessed a reduction in traffic flows due to the disaster. Since the focus of the present study is to evaluate how worse the traffic network was affected, only extreme observations with positive remainder were considered for computing the above two link metrics.

6.3.3.2 Mapping network disruptions and identification of the worst affected links and corridors

In this study, worst-affected links are defined as those links which experienced abnormal increases in travel times due to the hurricane. For identifying such links, the extreme observation-based metrics (developed using travel time observations with positive remainder component) were combined to develop a relative deviation in delay metric as in Equation 6.7.

$$\Delta k^i_w = \frac{1}{m \times l^i} \times \left(n^i_{w,+} \times \bar{y}^i_{w,+} - \text{med}\{N^i_{historical,+}\} \times \text{med}\{Y^i_{historical,+}\} \right) \quad (6.7)$$

where Δk^i_w is the metric combining both magnitude and frequency of extreme observations; m is the number of travel time observations in a week in the original series (692 observations); l^i is the length of the link i, $n^i_{w,+}$ and $\bar{y}^i_{w,+}$ are the weekly count and mean size of positive remainder components of extreme observations,

respectively; and $N^i_{historical,+}$ and $Y^i_{historical,+}$ are the corresponding historical values, respectively. The normalization of the metric based on the link length enables comparison among links/corridors. The metric can be interpreted as the average deviation in travel time delay experienced by a driver while traversing 1 km on a link during a random 15-minute interval compared to that in a normal week.

Conversely, the metric can also be used to find the links which experienced the highest reduction in travel times by considering only the negative remainder components of extreme observations in Equation 6.7.

6.4 Discussion of Results

The hurricane analysis was focused on the six weeks between August 11, 2017, and September 21, 2017 – two weeks prior to hurricane (Week -2 and Week -1), the hurricane week (Week 0), and three weeks after the hurricane (Week 1 through Week 3). Since road closures (hurricane-related) would have significantly impacted the traffic conditions, the travel time observations during those events on corresponding links were considered as extreme observations.

6.4.1 Network-wide traffic effects of Hurricane Harvey

Figure 6.7 shows the spatial and temporal distribution of absolute counts of extreme travel time observations recorded on various links during the analysis period. The extreme travel times and their frequency during the hurricane weeks are indicative of significant slowing down or complete disruption of traffic movement on a link due to the hurricane or associated reasons listed in Figure 6.5. Each of

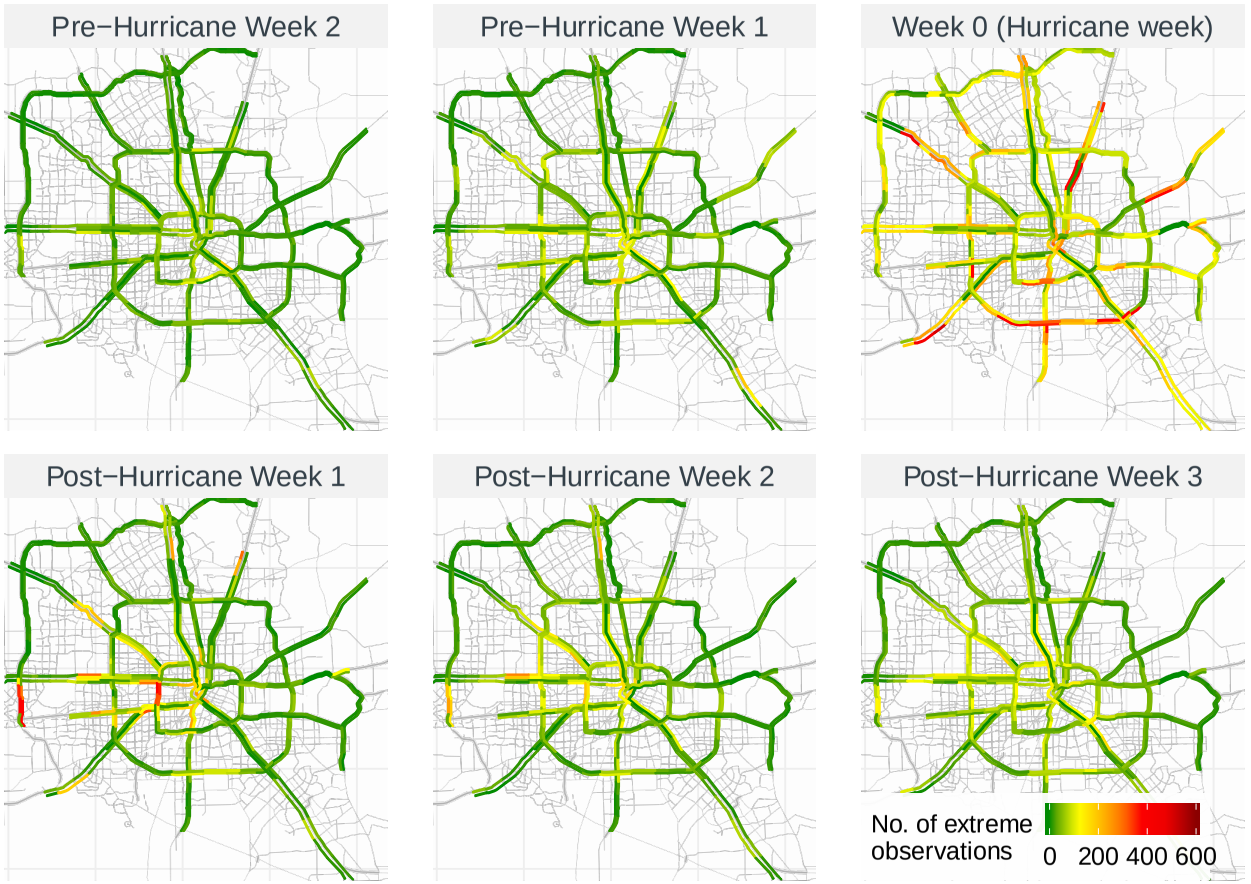

Figure 6.7: Link-wise absolute counts of extreme 15-minute intervals (n_w^i) during the analysis period weeks obtained using Generalized ESD Test (Map tiles by Stamen Design, under CC BY 3.0. Data by OpenStreetMap, under ODbL)

the subfigures corresponds to a specific week in the analysis period. The subfigures capture the traffic impact caused by Hurricane Harvey and the gradual recovery of the network once the hurricane effects subsided. The maximum impact in terms of duration of extreme traffic conditions (represented by the extreme travel time observation counts) in the network was recorded during the hurricane week (Week 0). Further analysis revealed that most of these extreme observations correspond to an abrupt reduction in the magnitudes of travel times. This was due to reduced traffic on freeway links as a large number of urban streets in the Houston region were flooded Lazo, Powers, and Hasley III (2017). On the other hand, the high concentration of road closures (Figure 6.5) in Week 0 could have contributed to slowing down the traffic on several freeway segments which reported positive extreme observations. In the post-hurricane week (Week 1), most of the links returned to normalcy. However, on some links, the extreme traffic conditions still existed, indicating damages caused by the hurricane and related incidents. From Week 1 through Week 3, the duration of extreme traffic conditions gradually decreased, indicated by the decreasing numbers of extreme observations. However, the results show that even in Week 3, many of the links still experienced longer durations of extreme traffic conditions compared to that in a 'normal' week.

Similarly, the variations in the magnitude of extreme travel time observations were also analyzed (Figure 6.8). It was found that the highest average size of extreme observation was observed during Week 1 and Week 2, after the hurricane, though the number of such links was small. This might be indicating extensive damage to some links and the return of evacuated populations back into the city.

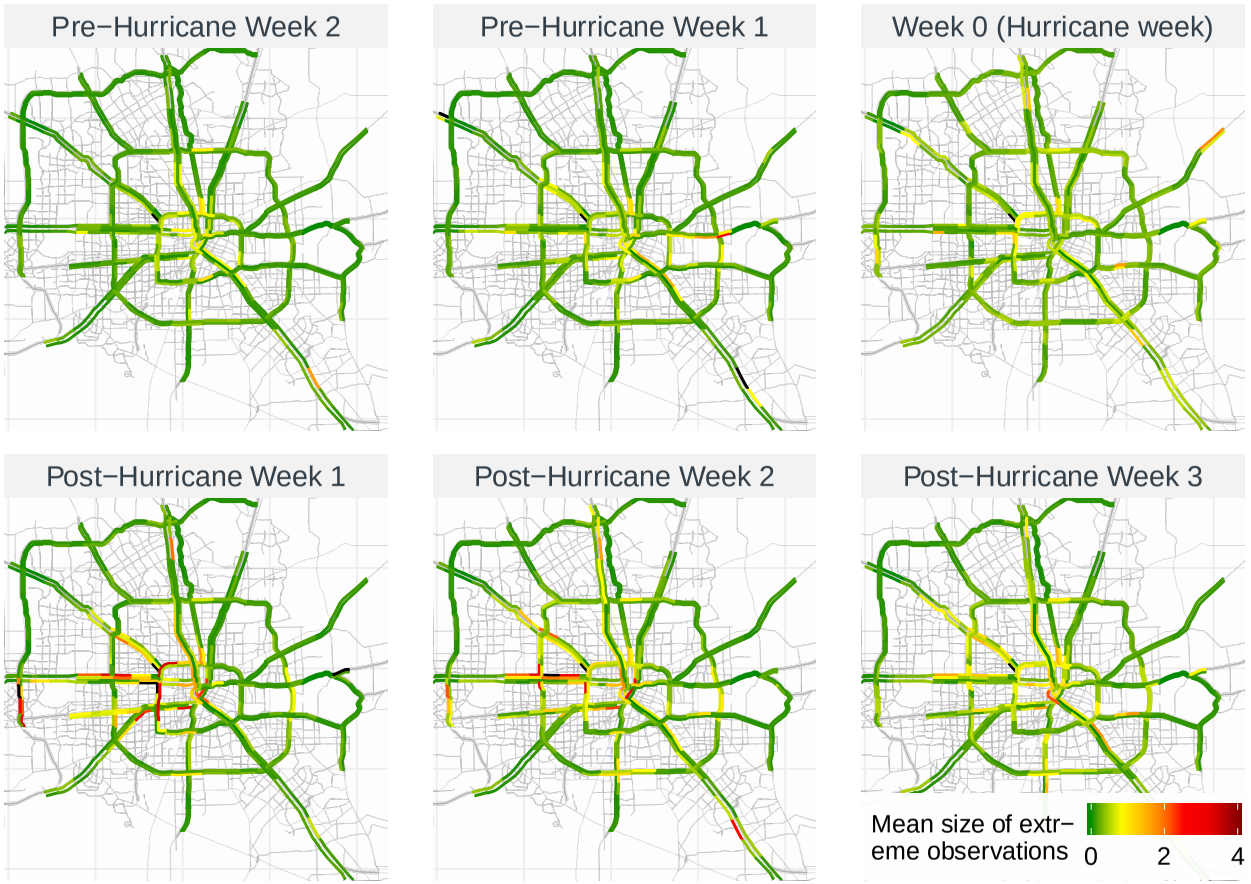

Figure 6.8: Link-wise absolute mean size of extreme 15-minute intervals in minutes (y_w^i, only positive observations considered) during the analysis period weeks obtained using Generalized ESD Test (Map tiles by Stamen Design, under CC BY 3.0. Data by OpenStreetMap, under ODbL)

It was also reported that floodwaters persisted for weeks in some of the road links, slowing down the traffic on those links considerably.

6.4.2 Application of extreme observation metrics to quantify network impacts and recovery

Findings from the analysis of frequency and size of extreme travel time observations reiterate that the metrics discussed in Equations 6.5 and 6.6 can be effectively used to capture spatiotemporal variations in traffic, such as the initial network impact and the subsequent recovery to normal conditions. In this manner, the metrics can also be used to quantify the resilience of the traffic network against Hurricane Harvey. The extreme observation metrics were combined to depict the network impact and recovery as shown in Figure 6.9.

The figure shows the moderate change in link metrics in Week -1, most-likely indicating evacuation and related fluctuations in traffic conditions, the sudden change in the network in Week 0 when the hurricane struck the region, and the gradual recovery of the network to the pre-disaster state from Week 1 through Week 3. The largest impact of the hurricane on traffic conditions are observed during Week 1 (post-hurricane week), with several major links having an average additional delay (Δk_w^i) more than one minute relative to that in a normal week (It must be noted that one minute is the average over the entire week including off-peak hours). The above representation is analogous to the resilience triangle metric introduced by Bruneau et al. (2003) for characterizing system resilience. However, the representation generalizes the concept of resilience triangle by capturing the

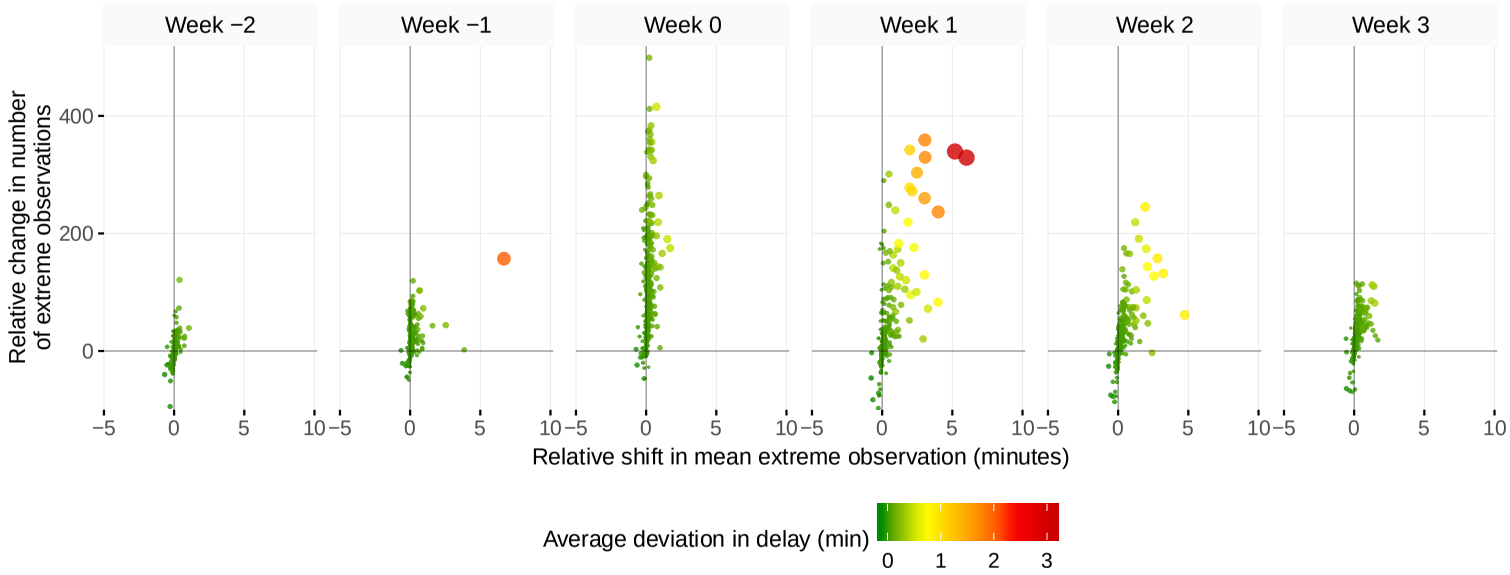

Figure 6.9: Extreme observation-based link metrics to quantify hurricane impact and subsequent recovery on Houston freeway network (Size of the points indicates the magnitude of average deviation in link delay Δk_w^i

multi-dimensional aspects of resilience of system of systems (SoS), such as traffic networks, and provides details regarding the overall system/network resilience as well as component-level resilience.

Statistical analyses were performed to understand the difference in the distribution of the link metrics across weeks. The trends obtained by the analyses of the extreme observation metrics are presented in Figure 6.10. The lines represent the mean value of the extreme observation metric in a week, whereas, the ribbon denotes the standard deviation of the same metric.

The results confirm the abrupt changes that occurred in the Houston freeway network due to the hurricane and the slow recovery that followed. The highest mean and the largest standard deviation of the number of extreme travel time observations were reported in Week 0 (hurricane week), reflecting the reduction in traffic on the freeways as a large part of the city was flooded during the hurricane. The highest increases in magnitudes of extreme travel times were observed in Week 1 (post-hurricane week) (indicating Week 1 experienced the worst traffic conditions among all the six weeks under consideration). This sudden change is a result of the combined effect of a spike in local and inbound traffic post-hurricane once the hurricane subsided, even though several of the links were still recovering from floodwaters Begley (2017). It is worth mentioning that the standard deviation of relative change in the size of extreme travel time observations ($\Delta y^i_{w,+}$) significantly increased in Week -1 (pre-hurricane week), while the increase in mean of the metric remained almost the same as that in Week -2. This is indicative of the fluctuations in the traffic conditions triggered by pre-hurricane evacuations and associated travel

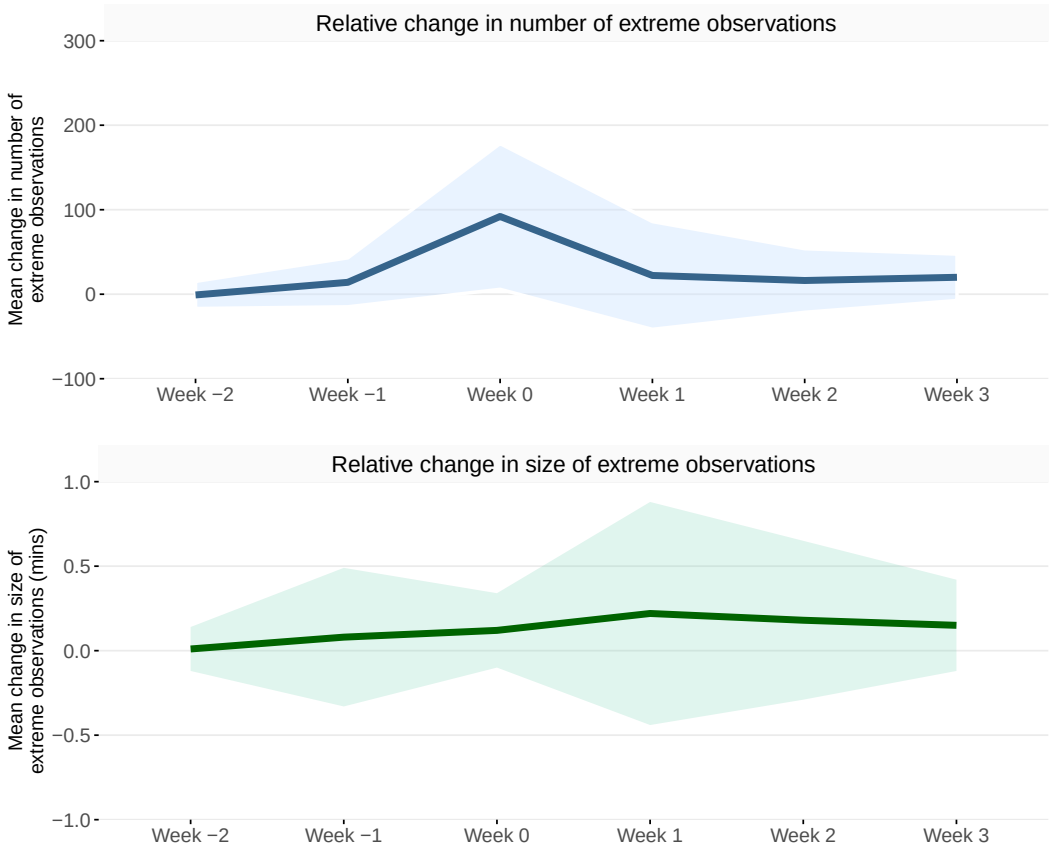

Figure 6.10: Results of statistical tests to compare extreme observation-based link metrics corresponding to Week -1 through Week 3 with that in Week -2

pattern changes. The sudden fall in the standard deviation of the mean change in the size of extreme observations in Week 0 (while the mean change in size continue to increase in the same week) points at the combined effect of high rainfall and reduction in traffic due to the hurricane. It can also be seen that the mean and standard deviation of link-wise extreme observation metrics, though gradually reduced after the hurricane week, were still significantly higher in Week 3 compared to that in

pre-hurricane Week -2, indicating that several links were still recovering to normal traffic conditions even three weeks after the hurricane.

6.4.3 Identification of worst-affected hurricane evacuation corridors

In order to understand the hurricane-induced impacts on evacuation routes (Figure 6.3), the extreme observation metrics were calculated for various constituent corridors. The analysis was also carried out for the six weeks to analyze the hurricane effects on traffic conditions along the hurricane evacuation routes. In the majority of the corridors, the impact and recovery patterns followed the general trend shown in Figure 6.9; i.e., the number of extreme travel time observations abruptly increased in the hurricane week (Week 0), whereas the largest deviations in travel times compared to that under normal conditions were observed during the week after the hurricane subsided (Week 1). As expected, the extent to which the frequency and magnitude of extreme travel time observations fluctuated was unique to the evacuation corridors, indicating the differential impact of the hurricane on various corridors.

In the next stage of analysis, the worst-affected evacuation corridors were identified. First, the extreme observation metrics for all links that are part of those routes were calculated from Week -2 through Week 3. Then, the worst-affected corridors in each week were identified by ranking them based on the mean values of the extreme travel time metrics corresponding to each corridor. The worst-affected links were identified in terms of the relative change in the number of extreme observations $\Delta n^i_{w,+}$ (Equation 6.5), relative change in mean size of extreme observations,

$\Delta y^i_{w,+}$ (Equation 6.6), and additional weekly unexpected link travel time per km, Δk^i_w (Equation 6.7) along with the value of the corresponding metric. Table 6.2 presents the worst-affected three corridors from Week -1 through Week 3.

The results suggest that the worst-affected corridor in terms of relative change in the number of extreme travel times was US-59 Southwest Northbound with an additional 455 extreme observations (approximately 114 hours of unusual traffic conditions) in the hurricane week (Week 0). With respect to the relative change in the mean size of positive extreme observations, IH-10 East Westbound was the worst-affected with drivers experiencing an additional travel time of 1.36 minutes if they made a trip during the extreme 15-minute intervals in Week 1. Lastly, the worst-affected corridor according to the relative increase in delay was the SH-99 Lanier Parkway-West Southbound with an average increase of 0.44 minutes of unexpected travel time for traversing 1 km in a random 15-minute interval in Week 1. It can be observed that the identified worst-affected corridors are different with respect to each of the three metrics. This is because of the unique characteristics of the traffic fluctuations that are captured by the three metrics as discussed in the subsection 6.3.3.

The worst-affected corridors (as presented in Table 6.2) are illustrated in Figure 6.11

6.5 Conclusion

In this study, the traffic impacts of Hurricane Harvey on the Houston freeway network were analyzed. The application of time series decomposition along

Table 6.2: Worst-affected evacuation corridors in different weeks during Hurricane Harvey (Only links with increase in travel times relative to normal conditions are considered)

Rank	Week -2	Week -1	Week 0	Week 1	Week 2	Week 3
Based on relative change in number of extreme observations, $\Delta n^i_{w,+}$						
1	Beltway 8-North WB (12.92)	US-59 Eastex SB (60.67)	US-59 Southwest NB (455.5)	US-59 Southwest NB (178)	IH-10 Katy Managed Lanes WB (133.5)	IH-10 Katy Managed Lanes WB (60)
2	Beltway 8-South WB (12.89)	US-59 Southwest NB (53.5)	Beltway 8-South EB (229.17)	US-59 Eastex SB (162.33)	Beltway 8-West SB (61.82)	Beltway 8-West SB (58.64)
3	IH-10 Katy Managed Lanes WB (7)	IH-45 Gulf NB (43.27)	SH-288 NB (214)	IH-10 Katy Managed Lanes WB (95)	IH-10 Katy WB (45.22)	Beltway 8-West NB (45.73)
Based on relative change in mean size of extreme observations in minutes, $\Delta y^i_{w,+}$						
1	IH-45 Gulf NB (0.1)	IH-10 East EB (0.86)	IH-10 Katy WB (0.3)	IH-10 East WB (1.36)	IH-10 Katy Managed Lanes WB (0.9)	IH-10 Katy Managed Lanes WB (0.51)
2	IH-10 Katy Managed Lanes EB (0.06)	IH-45 Gulf NB (0.68)	IH-45 Gulf SB (0.28)	IH-10 Katy Managed Lanes WB (0.88)	IH-10 Katy WB (0.61)	SH-288 NB (0.46)
3	Beltway 8-North WB (0.06)	US-290 Northwest WB (0.53)	IH-10 East WB (0.24)	SH-99 Lanier Parkway-West SB (0.86)	Beltway 8-West SB (0.5)	IH-45 Gulf NB (0.35)
Based on relative change in unexpected travel time per km, Δk^i_w						
1	IH-45 Gulf NB (0.02)	IH-45 Gulf NB (0.2)	US-59 Southwest NB (0.19)	SH-99 Lanier Parkway-West SB (0.44)	IH-10 Katy Managed Lanes WB (0.23)	IH-45 Gulf NB (0.08)
2	Beltway 8-North WB (0.02)	IH-10 East EB (0.08)	Beltway 8-South EB (0.13)	SH-99 Lanier Parkway-West NB (0.28)	IH-10 Katy WB (0.19)	IH-10 Katy Managed Lanes WB (0.08)
3	IH-45 North NB (0.01)	IH-10 Katy EB (0.04)	Beltway 8-South WB (0.11)	IH-10 East WB (0.25)	SH-99 Lanier Parkway-West SB (0.09)	IH-10 Katy WB (0.06)

(a) NB: Northbound, SB: Southbound, EB: Eastbound, WB: WestBound
(b) Values in parentheses denote the value of the corresponding link metric

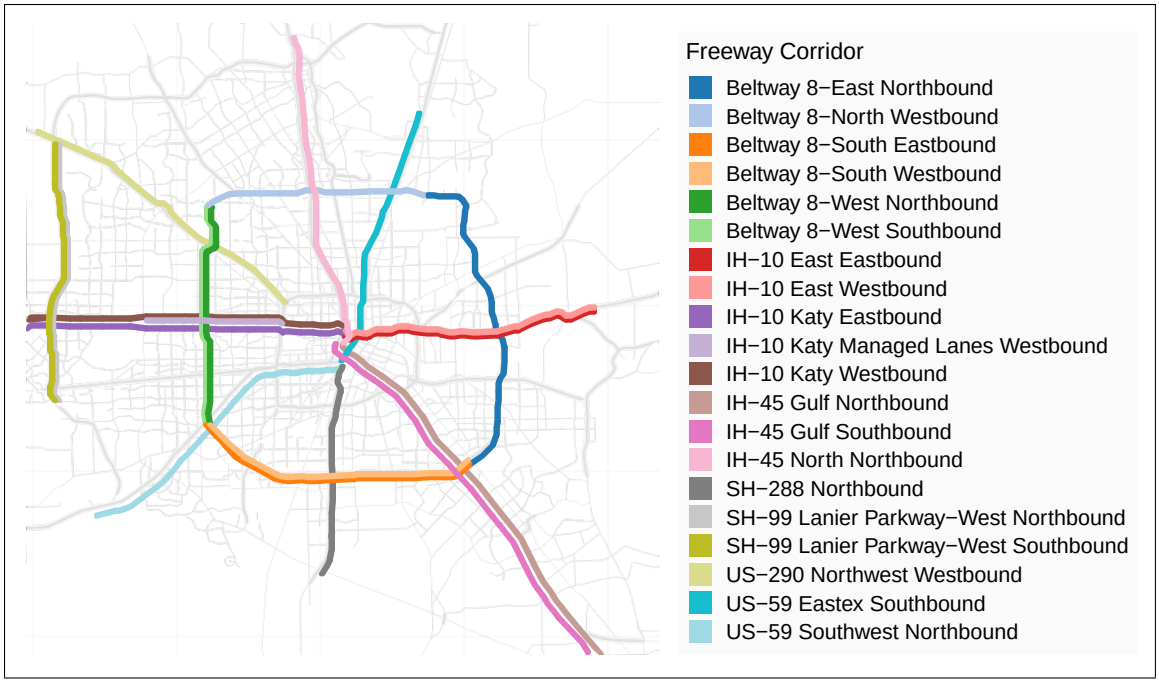

Figure 6.11: Locations of the most-affected freeway corridors presented in Table 6.2.

with anomaly detection algorithms proved to be an effective method to identify the hurricane-induced effects from the observed travel time data. Instead of conventional travel time reliability methods, the study employed metrics based on extreme travel time observations to quantify the traffic effects of the hurricane. It was found that the proposed metrics are not only effective in capturing the traffic variations, but also offer a practical method to represent, quantify, and evaluate the resilience of large-scale traffic networks. A majority of links experienced longer durations of extreme travel times during the hurricane and the analysis of their characteristics provided very useful information on the traffic performance of network links and corridors.

The study found that the extreme travel time observations were concentrated more in the week of the hurricane (on an average, approximately 92 additional extreme observations, equivalent to 23 hours of "unusual" traffic conditions), whereas, the largest magnitudes of extreme observations were recorded in the weeks that followed its occurrence (with an average increase of 0.22 minutes in extreme travel time on links in Week 1) (Figure 6.10). Combining the metrics based on the extreme observation characteristics, the overall impact of the hurricane on the network, and the gradual recovery of traffic to pre-hurricane conditions were captured. It was found that even three weeks after the hurricane, several links were experiencing higher travel times, indicating the extensive pavement damage or prevalent flooding. While the higher magnitude and frequency of extreme travel times may be due to a vast range of events, such as high water, fluctuations in traffic flow, and egress and ingress of affected populations, the findings provide insights into the potential impacts on the network traffic conditions in the case of a similar hurricane in the future.

The primary application of the metrics is in the quantification of the spatial and temporal changes in network- and link-level traffic conditions induced by natural disasters as well as other traffic incidents. However, the proposed framework and metrics could be extended to several applications in disaster management, including improving existing evacuation plans and enhancing traffic management strategies for first-responders and rescue personnel during and immediately after similar natural disasters. A few of the potential applications (and associated limitations) are listed below:

1. Further analysis of traffic flows along the worst-affected corridors identified using the extreme travel time metrics could potentially help to determine locations for pre-staging essential supplies and setting up temporary fuel supply stations during future disaster events. Inadequate emergency supplies along heavily used corridors during past hurricane evacuations had forced drivers to abandon their vehicles in the midway leading to extreme congestion.

2. While the current methodology is not designed for predicting the disaster impacts, its application on past hurricane events (or any other recurring natural disasters) in a region could be used to identify major traffic segments that are repeatedly disrupted (due to high-water, traffic congestion, etc.). Such information could be used for re-planning evacuation routes and modify existing emergency traffic management plans. However, uncertainties over the extent of traffic impact may still persist as the model is not able to predict the impacts based on the characteristics of the extreme event.

3. The metrics can be effectively used for evaluating the overall effectiveness of any mitigation- or adaptive strategies that were implemented for improving the traffic network performance prior to extreme events.

A major challenge in the implementation of the proposed methodology is that many cities currently lack the technology to collect, process, and store traffic performance information related to major urban corridors, including arterial roads. However, there has been a greater emphasis on the adoption of intelligent transportation systems for monitoring traffic performance in major cities globally. In

other cities, the applicability of data from alternative sources, including smartphone navigation applications, could be explored.

Chapter 7

Conclusions

Increasing risks from unanticipated events, including natural disasters and targeted threats, have prompted decision-makers to adopt various strategies to enhance the resilience of infrastructure networks. In this dissertation, five indicator-based methodological frameworks for evaluating infrastructure risks and resilience and identifying vulnerable and critical infrastructure components were proposed. Extensions of current methods to incorporate societal and economic impacts of infrastructure failures for infrastructure prioritization and selection were introduced. The methodologies can be easily incorporated into the existing frameworks and decision support systems related to infrastructure development and management to improve the resilience of critical infrastructure networks. This chapter summarizes the major findings and conclusions from various studies done as part of this dissertation research and provides recommendations for the application of the proposed methodological frameworks. In addition, directions for potential future research are also presented.

7.1 Research Contributions

The primary objective of the research was to introduce methodological frameworks to develop and apply network-based and performance-based indicators that are reflective of the resilience characteristics of infrastructure systems. The efforts were intended to address the gaps in the literature pertaining to the evaluation of infrastructure network resilience under several constraints, such as a lack of interdependency data and varying levels of technology adoption among component systems. The dissertation focused on two broad categories of indicators for evaluating the risks and resilience in large-scale interdependent infrastructure networks, namely, graph-based methods and empirical methods.

The key findings and recommendations of the dissertation are as follows:

- Globally, infrastructure resilience has gained considerable attention due to the increased disaster risks in recent decades. This trend has been further accelerated by the emergence of new threats, such as cyber-attacks, acts of terrorism, and climate crisis. With urban infrastructure systems becoming more interdependent and technology-reliant, substantial changes in the manner in which disaster risks are incorporated in the current infrastructure development and management practices will be required.

- The first part of the dissertation introduced a hybrid risk measure developed based on the principles of Inoperability Input-Output Model (IIM) to quantify the network-wide effects of infrastructure failures. For developing the risk measure, the use of linguistic descriptions of dependencies instead of

quantitative infrastructure interdependency data was investigated. Linguistic dependency data were comparatively easier to obtain and more cost-effective than conventional flow-based dependency data. The dissertation proposed that the network-wide impacts of extreme events can be better communicated by combining a pair of extreme probability distributions (derived using possibility theory) and a most-likely distribution (derived using probability theory). The infrastructure network vulnerability model developed based on the topological characteristics and the expert judgments could be considered as a preliminary form of an expert system. As more empirical or engineering data of the specific network, with different levels of accuracy and sources of uncertainty, become available, the expert system is capable of incorporating them. The agent-based framework, which forms the back end of the model, is capable of incorporating such sophisticated infrastructure-specific modeling components and empirical evidence from historical events.

- The hybrid risk measure was extended to develop two generic resilience indicators to rank and prioritize infrastructure nodes (and thereby links) in terms of two aspects related to cascading failures in infrastructure networks: (a) their necessity to operate for the functioning of the whole network (criticality); and (b) their exposure to cascading effects arising from disruptions in other components (susceptibility). Later, simulation-based algorithms were proposed to rank and prioritize infrastructure nodes and links based on the resilience indicators. The indexes can support decision-making for designing and managing resilience in interdependent infrastructure networks before a

disaster, for identifying the infrastructure components which warrant immediate restoration during or after a disaster, and for devising additional resilience strategies to handle enhanced disaster risks during recovery. The indexes are not dependent on the specific model used for estimating the interdependent effects of infrastructure failures (though IIM was used). The indexes are equally appropriate even if an interdependent infrastructure model that captures the real-world operational characteristics of the component infrastructure systems is used to model the network. The indexes are well-suited for capturing the resilience improvements in the network due to resilience interventions based on robustness and redundancy, which are crucial to pre-disaster preparedness.

- The dissertation also proposed a socioeconomic indicator (Priority Index) to evaluate the susceptibility of communities to unanticipated events and the resultant utility disruptions. The Priority Index was developed by combining the generic social vulnerability of communities with the interdependent effects of utility failures. In order to quantify the network-wide impacts of utility failures, the hybrid risk measure proposed in the dissertation was used. The methodology enables the comparison of the susceptibility of two census tracts using a linear scale. The performance drop in the infrastructure network was evaluated by giving due consideration to both the direct and indirect impacts of hazards arising from its interdependent structure. The framework could be employed for emergency planning and disaster risk assessment, as well as for managing immediate relief operations, such as the distribution of

food, and water during a disaster. The framework could find potential applications in cities where backup mechanisms to withstand prolonged and uncertain utility service disruptions are unreliable or absent.

- In the later part of the dissertation, a data-driven methodology to analyze the economic risks of such hurricane-related shutdowns using hurricane- and port-related determinants was introduced. The risks of shutdowns were modeled using regression analysis based on historical port shutdown data and are combined with extensions of the well-known input-output model to predict the operational and economic risks of ports to hurricanes. The application of the methodology was demonstrated by conducting a case study based on the Texas Port System to evaluate the economic risks of hurricane-related port disruptions on the U.S. economy. The presented methodology may be of interest to a wide range of port stakeholders, including port authorities, private port operators, port-dependent industries, and different levels of governments. Given how critical the operational continuity of ports are for the regional and national economies, the economic risks could be integrated into decision-making processes related to port investments and management. While the data-driven methodological framework was developed specifically for port systems, it can be generalized for any other infrastructure system, enabling decision-makers to evaluate the effects of resilience interventions in monetary terms leading to more cost-effective solutions.

- In addition, a methodological framework was presented for identifying the traffic fluctuations induced by natural disasters on the urban traffic networks

using historical disaster data. The dissertation relied on time series decomposition and anomaly detection algorithms to investigate the spatiotemporal effects of the hurricane on the traffic conditions. The results of a case study based on the Houston traffic network during Hurricane Harvey suggested that the metrics developed are effective in quantifying the resilience of traffic networks against natural disasters by capturing both the initial impact and recovery. The primary application of the metrics is in the quantification of the spatial and temporal changes in network- and link-level traffic conditions induced by natural disasters as well as other traffic incidents. However, the proposed framework and metrics could be extended to several applications in disaster management, including improving existing evacuation plans and enhancing traffic management strategies for first-responders and rescue personnel during and immediately after similar natural disasters.

While infrastructure agencies have given attention to disaster resilience of individual infrastructure systems, the resilience of urban infrastructure networks as a whole is still in the conceptual stage. As infrastructure systems become more interdependent, implementing reactive and uncoordinated measures to restore failed infrastructure systems during and after disasters may not produce desired improvements in the overall resilience of cities. It requires proper planning and implementation of resilience strategies to ensure that the disaster risks are minimized. The methodologies presented in this dissertation research should provide directions for evaluating the risks and resilience of large-scale infrastructure networks under various data and modeling constraints and provide useful insights for prioritizing

infrastructure system components.

7.2 Future Research

This dissertation research contributes to the existing body of knowledge in the quantification of disaster risks on infrastructure networks and the prioritization of infrastructure components for resilience enhancement. However, each study is based on several assumptions and has a few limitations, which provide directions for future research. The following are some of the potential areas for further investigation.

- The methodological frameworks presented in the dissertation do not incorporate the rapidity and resourcefulness dimensions of system resilience. Rapidity and, to an extent, resourcefulness are properties that are more crucial in immediate restoration of a disrupted system and the recovery afterward, as the main objective during these phases is to optimize network performance in the shortest possible time with the available resources. However, the inclusion of rapidity and resourcefulness in frameworks requires additional information on the amount of resources required for restoring various components and the speed at which they could be restored/recovered. More research efforts in this direction could improve the applicability of the presented methodologies.

- The hybrid risk measure and associated methodological frameworks developed for quantifying interdependent are based on the Inoperability Input-Output Model (IIM) which does not consider the redistribution of resource

flows which might occur after infrastructure failures. A flow-based interdependent infrastructure model may capture the network-wide effects of infrastructure failures more accurately. However, this requires additional data regarding resource exchanges among component infrastructure systems.

- Empirical approach is a powerful tool for understanding the aggregate disaster impacts on infrastructure networks, communities, and economies. For empirical modeling and estimation of infrastructure risks and resilience, adequate and reliable historical data is required. However, the systematic recording of disaster impacts has started only very recently. More data collection efforts are required to develop critical infrastructure disruption databases for furthering research in urban infrastructure resilience.

References

Abdel-Aty, M., & Pande, A. (2007). Crash Data Analysis: Collective vs. Individual Crash Level Approach. *Journal of Safety Research*, *38*(5), 581-587.

Alderson, D. L., Brown, G. G., & Carlyle, W. M. (2015). Operational Models of Infrastructure Resilience. *Risk Analysis*, *35*(4), 562–586. Retrieved from `http://doi.wiley.com/10.1111/risa.12333`

Alenazi, M. J., & Sterbenz, J. P. (2015). Comprehensive Comparison and Accuracy of Graph Metrics in Predicting Network Resilience. In *2015 11th International Conference on the Design of Reliable Communication Networks (DRCN)* (pp. 157–164). IEEE.

Ameli, H., Qadrdan, M., & Strbac, G. (2017). Value of Gas Network Infrastructure Flexibility in Supporting Cost Effective Operation of Power Systems. *Applied Energy*, *202*, 571–580.

Anderson, B., Schumacher, A., Guikema, S., Quiring, S., Ferreri, J., Staid, A., ... Zhu, L. (2018). 'stormwindmodel': Model Tropical Cyclone Wind Speeds [Computer software manual]. CRAN. Retrieved from `https://github.com/geanders/stormwindmodel` (R package version 0.1.1)

Apostolakis, G. E., & Lemon, D. M. (2005). A Screening Methodology for the Identification and Ranking of Infrastructure Vulnerabilities Due to Terrorism. *Risk Analysis*, *25*(2), 361–376.

Aydin, N. Y. (2018). Measuring Topological and Operational Resilience and Recovery of Water Networks for Planning and Management. In *World Environmental and Water Resources Congress 2018* (pp. 370–379). Minneapolis, Minnesota: American Society of Civil Engineers.

Bagchi, A., Sprintson, A., & Singh, C. (2013). Modeling the Impact of Fire Spread on an Electrical Distribution Network. *Electric Power Systems Research*, *100*, 15–24.

Balakrishnan, S., & Zhang, Z. (2018). Developing Priority Index for Managing Utility Disruptions in Urban Areas with Focus on Cascading and Interdependent Effects. *Transportation Research Record: Journal of the Transportation Research Board*, *2672*(1), 101–112.

Beer, M., Ferson, S., & Kreinovich, V. (2013). Imprecise Probabilities in Engineering Analyses. *Mechanical Systems and Signal Processing*, *37*(1-2), 4–29.

Begley, D. (2017). *After Harvey, A Flood of Cars and Trucks Ties Up Traffic.* Houston, TX. (Newspaper Article, https://www.chron.com/news/transportation/article/Houston-freeways-flooded-again-this-time-with-12174163.php, Accessed July 28, 2019)

Benson, C., Myers, M., & Twigg, J. (2001). NGO Initiatives in Risk Reduction: An Overview. *Disasters*, *25*(3), 199–215.

Bocchini, P., & Frangopol, D. M. (2012). Optimal Resilience- and Cost-Based Post-disaster Intervention Prioritization for Bridges along a Highway Segment. *Journal of Bridge Engineering*, *17*(1), 117–129.

Boin, A., & Smith, D. (2006). Terrorism and Critical Infrastructures: Implications for Public-Private Crisis Management. *Public Money and Management*, *26*(5), 295–304.

Bompard, E., Napoli, R., & Xue, F. (2010). Extended Topological Approach for the Assessment of Structural Vulnerability in Transmission Networks. *IET Generation, Transmission & Distribution*, *4*(6), 716.

Boole, G. (1854). *An Investigation of the Laws of Thought: On Which are Founded the Mathematical Theories of Logic and Probabilities*. Dover Publications.

Bottasso, A., Conti, M., Ferrari, C., & Tei, A. (2014). Ports and Regional Development: A Spatial Analysis on a Panel of European Regions. *Transportation Research Part A: Policy and Practice*, *65*, 44–55.

Brancucci Martínez-Anido, C., Bolado, R., De Vries, L., Fulli, G., Vandenbergh, M., & Masera, M. (2012). European Power Grid Reliability Indicators, What Do They Really Tell? *Electric Power Systems Research*, *90*, 79–84.

Brown, T., Beyeler, W., & Barton, D. (2004). Assessing Infrastructure Interdependencies: The Challenge of Risk Analysis for Complex Adaptive Systems. *International Journal of Critical Infrastructures*, *1*(1), 108–117.

Bruneau, M., Chang, S. E., Eguchi, R. T., Lee, G. C., O'Rourke, T. D., Reinhorn, A. M., ... Von Winterfeldt, D. (2003). A Framework to Quantitatively Assess and Enhance the Seismic Resilience of Communities. *Earthquake Spectra*, *19*(4), 733–752.

Bryan, J., Munday, M., Pickernell, D., & Roberts, A. (2006). Assessing the Economic Significance of Port Activity: Evidence from ABP Operations in Industrial South Wales. *Maritime Policy & Management*, *33*(4), 371–386.

Bukhsh, W. A., & McKinnon, K. (2013). *Network Data of Real Transmission Networks.* Retrieved from https://www.maths.ed.ac.uk/optenergy/NetworkData/introduction.html

Bureau of Transportation Statistics. (2017). *Port Performance Freight Statistics*

Program: Annual Report to Congress 2017 (Tech. Rep.). Washington D. C.: U.S. Department of Transportation.

Calderon, C., & Serven, L. (2010). Infrastructure and Economic Development in Sub-Saharan Africa. *Journal of African Economies*, *19*, i13–i87.

Camagni, R., Gibelli, M. C., & Rigamonti, P. (2002). Urban Mobility and Urban Form: The Social and Environmental Costs of Different Patterns of Urban Expansion. *Ecological Economics*, *40*(2), 199–216.

Cardenas, A., Amin, S., Sinopoli, B., Giani, A., Perrig, A., Sastry, S., & Others. (2009). Challenges for Securing Cyber Physical Systems. In *Workshop on Future Directions in Cyber-Physical Systems Security* (Vol. 5). Newark, NJ.

Cardona, O.-D., van Aalst, M., Birkmann, J., Fordham, M., McGregor, G., Perez, R., ... Dahe, Q. (2012). *Managing the Risks of Extreme Events and Disasters to Advance Climate Change Adaptation: Special Report of the Intergovernmental Panel on Climate Change*. Cambridge: Cambridge University Press. Retrieved from `https://www.ipcc.ch/pdf/special-reports/srex/SREX-Chap2{_}FINAL.pdf`

Castillo, A. (2014). Risk Analysis and Management in Power Outage and Restoration: A Literature Survey. *Electric Power Systems Research*, *107*, 9 - 15.

Cavdaroglu, B., Hammel, E., Mitchell, J. E., Sharkey, T. C., & Wallace, W. A. (2013, 01). Integrating Restoration and Scheduling Decisions for Disrupted Interdependent Infrastructure Systems. *Annals of Operations Research*, *203*(1), 279–294.

Chakraborty, J., Tobin, G. A., & Montz, B. E. (2005). Population Evacuation: Assessing Spatial Variability in Geophysical Risk and Social Vulnerability to Natural Hazards. *Natural Hazards Review*, *6*(1), 23–33.

Chan, R., & Schofer, J. L. (2016). Measuring Transportation System Resilience: Response of Rail Transit to Weather Disruptions. *Natural Hazards Review*, *17*(1), 05015004.

Chandra, A., & Thompson, E. (2000). Does Public Infrastructure Affect Economic Activity? Evidence from the Rural Interstate Highway System. *Regional Science and Urban Economics*, *30*(4), 457–490.

Chang, S. E. (2003). Transportation Planning for Disasters: An Accessibility Approach. *Environment and Planning A: Economy and Space*, *35*(6), 1051-1072.

Chang, S. E. (2016). Socioeconomic Impacts of Infrastructure Disruptions. *Oxford Research Encyclopedia of Natural Hazard Science*. Retrieved from `http://naturalhazardscience.oxfordre.com/view/10.1093/acrefore/`

9780199389407.001.0001/acrefore-9780199389407-e-66

Chang, S. E., McDaniels, T. L., Mikawoz, J., & Peterson, K. (2007). Infrastructure Failure Interdependencies in Extreme Events: Power Outage Consequences in the 1998 Ice Storm. *Natural Hazards*, *41*(2), 337–358.

Chen, L., & Miller-Hooks, E. (2012). Resilience: An Indicator of Recovery Capability in Intermodal Freight Transport. *Transportation Science*, *46*(1), 109–123.

Cheng, C. B. (2004). Group Opinion Aggregation Based on a Grading Process: A Method for Constructing Triangular Fuzzy Numbers. *Computers and Mathematics with Applications*, *48*(10-11), 1619–1632.

Chhetri, P., Jayatilleke, G. B., Gekara, V. O., Manzoni, A., & Corbitt, B. (2016). Container Terminal Operations Simulator (CTOS) – Simulating the Impact of Extreme Weather Events on Port Operation. *European Journal of Transport and Infrastructure Research*, *16*(1), 195–213.

Chmutina, K., Ganor, T., & Bosher, L. (2014). Role of Urban Design and Planning in Disaster Risk Reduction. *Proceedings of the Institution of Civil Engineers: Urban Design and Planning*, *167*(3), 125–135. Retrieved from http://www.icevirtuallibrary.com/doi/10.1680/udap.13.00011

Choi, J., Naderpajouh, N., Yu, D. J., & Hastak, M. (2019). Capacity Building for an Infrastructure System in Case of Disaster Using the System's Associated Social and Technical Components. *Journal of Management in Engineering*, *35*(4).

Chou, C.-C., & Tseng, S.-M. (2010). Collection and Analysis of Critical Infrastructure Interdependency Relationships. *Journal of Computing in Civil Engineering*, *24*(6), 539–547.

Cimellaro, G. P., Tinebra, A., Renschler, C., & Fragiadakis, M. (2016). New Resilience Index for Urban Water Distribution Networks. *Journal of Structural Engineering*, *142*(8), C4015014. Retrieved from http://ascelibrary.org/doi/10.1061/{%}28ASCE{%}29ST.1943-541X.0001433

City of Austin. (2009). *Community inventory report draft: Public utilities* (Tech. Rep.). Austin: City of Austin. Retrieved July 21, 2017, from ftp://ftp.ci.austin.tx.us/GIS-Data/planning/compplan/8-community_inventory_PublicUtilities_v3.pdf

City of Austin. (2017). *Open Data Portal.* Retrieved July 21, 2017, from https://data.austintexas.gov

Cleveland, R. B., Cleveland, W. S., McRae, J. E., & Terpenning, I. (1990). STL: A Seasonal-Trend Decomposition Procedure Based on Loess. *Journal of Of-*

ficial Statistics, *6*(1), 3–73.

Cole, S. (1995). Lifelines and Livelihood: a Social Accounting Matrix Approach to Calamity Preparedness. *Journal of Contingencies and Crisis Management*, *3*(4), 228–246. Retrieved from http://doi.wiley.com/10.1111/j.1468-5973.1995.tb00102.x

Colin, C. A., & Pravin, T. (2013). *Regression Analysis of Count Data, Second edition*. Cambridge University Press.

Cooke, R. M., & Goossens, L. H. J. (2004). Expert Judgement Elicitation for Risk Assessments of Critical Infrastructures. *Journal of Risk Research*, *7*(6), 643–656.

Cox, A., Prager, F., & Rose, A. (2011). Transportation Security and the Role of Resilience: A Foundation for Operational Metrics. *Transport Policy*, *18*(2), 307-317.

Cruz, A. M., Kajitani, Y., & Tatano, H. (2015). Natech Disaster Risk Reduction: Can Integrated Risk Governance Help? In *Risk Governance* (pp. 441–462). Dordrecht: Springer Netherlands.

Cui, Y., & Sun, Y. (2019). Social Benefit of Urban Infrastructure: An Empirical Analysis of Four Chinese Autonomous Municipalities. *Utilities Policy*, *58*, 16–26.

Cutter, S. L., Boruff, B. J., & Shirley, W. L. (2003). Social Vulnerability to Environmental Hazards. *Social Science Quarterly*, *84*(2), 242–261.

[Dataset] Directorate for Science Technology and Innovation. (2019). *HS to ISIC to End-Use Conversion Key*. (Spreadsheet, URL https://www.oecd.org/sti/ind/ConversionKeyBTDIxE4PUB.xlsx, Accessed September 20, 2019)

[Dataset] Houston-Galveston Area Council. (2017). *Hurricane evacuation routes*. Houston, Texas: Houston-Galveston Area Council. (Webpage, http://houstontx.gov/oem/documents/evacuation-routes/routes-small.pdf, Accessed June 20, 2019.)

[Dataset] Houston Transtar. (2019). *Speed Map Archive*. Houston, Texas. (Webpage, https://traffic.houstontranstar.org/map_archive/, Accessed May 10, 2019)

Department of Homeland Security. (2016). *National Protection Framework* (Tech. Rep.). United States Department of Homeland Security. Retrieved from https://www.fema.gov/media-library-data/1466017309052-85051ed62fe595d4ad026edf4d85541e/National_Protection_Framework2nd.pdf

D'Lima, M., & Medda, F. (2015). A New Measure of Resilience: An Application to the London Underground. *Transportation Research Part A: Policy and Practice*, *81*, 35-46.

Dubois, D. (2006). Possibility Theory and Statistical Reasoning. *Computational Statistics and Data Analysis*, *51*(1), 47–69. Retrieved from https://www.sciencedirect.com/science/article/pii/S0167947306001149

Dubois, D., Kerre, E., Mesiar, R., & Prade, H. (2000). Fuzzy Interval Analysis. In *Fundamentals of Fuzzy Sets* (pp. 483–581). Boston, MA: Springer.

Ducruet, C., & Lee, S.-W. (2006). Frontline Soldiers of Globalisation: Port–city Evolution and Regional Competition. *GeoJournal*, *67*(2), 107–122.

Dudenhoeffer, D., Permann, M., & Manic, M. (2006). CIMS: A Framework for Infrastructure Interdependency Modeling and Analysis. In *Proceedings of the 2006 Winter Simulation Conference* (pp. 478–485). IEEE. Retrieved from http://ieeexplore.ieee.org/document/4117643/

Dunn, S., Fu, G., Wilkinson, S., & Dawson, R. (2013). Network Theory for Infrastructure Systems Modelling. In *Proceedings of the Institution of Civil Engineers - Engineering Sustainability* (Vol. 166, pp. 281–292). Thomas Telford Ltd.

European Network and Information Security Agency. (2010). *Measurement Frameworks and Metrics for Resilient Networks and Services: Challenges and Recommendations* (Tech. Rep.). Heraklion, Greece: European Network and Information Security Agency. Retrieved from https://www.enisa.europa.eu/publications/metrics-survey

Eusgeld, I., Nan, C., & Dietz, S. (2011). System-of-Systems Approach for Interdependent Critical Infrastructures. *Reliability Engineering & System Safety*, *96*(6), 679–686.

Faturechi, R., & Miller-Hooks, E. (2015). Measuring the Performance of Transportation Infrastructure Systems in Disasters: A Comprehensive Review. *Journal of Infrastructure Systems*, *21*(1), 04014025.

Fitzpatrick, T., & Molloy, J. (2014). The Role of NGOs in Building Sustainable Community Resilience. *International Journal of Disaster Resilience in the Built Environment*, *5*(3), 292–304.

Flanagan, B. E., Gregory, E. W., Hallisey, E. J., Heitgerd, J. L., & Lewis, B. (2011). A Social Vulnerability Index for Disaster Management. *Journal of Homeland Security and Emergency Management*, *8*(1).

Franchin, P., & Cavalieri, F. (2015). Probabilistic Assessment of Civil Infrastructure Resilience to Earthquakes. *Computer-Aided Civil and Infrastructure*

Engineering, *30*(7), 583-600.

Francis, R., & Bekera, B. (2014). A Metric and Frameworks for Resilience Analysis of Engineered and Infrastructure Systems. *Reliability Engineering & System Safety*, *121*, 90–103.

Frangopol, D. M., & Bocchini, P. (2011). Resilience As Optimization Criterion for the Rehabilitation of Bridges Belonging to a Transportation Network Subject to Earthquake. In *Structures Congress 2011* (pp. 2044–2055). Reston, VA: American Society of Civil Engineers.

Frangopol, D. M., & Liu, M. (2007). Maintenance and Management of Civil Infrastructure Based on Condition, Safety, Optimization, and Life-cycle Cost. *Structure and Infrastructure Engineering*, *3*(1), 29-41.

Franz, B., Leicht, R., Maslak, K., & Rinker, M. (2018). Framework for Assessing Resilience in the Communication Networks of AEC Teams. *The Engineering Project Organization Journal*, *8*.

French, S. P., Lee, D., & Anderson, K. (2010). Estimating the Social and Economic Consequences of Natural Hazards: Fiscal Impact Example. *Natural Hazards Review*, *11*(2), 49–57.

Galbusera, L., & Giannopoulos, G. (2018, sep). On Input-Output Economic Models in Disaster Impact Assessment. *International Journal of Disaster Risk Reduction*, *30*, 186–198.

Ganin, A. A., Kitsak, M., Marchese, D., Keisler, J. M., Seager, T., & Linkov, I. (2017). Resilience and Efficiency in Transportation Networks. *Science Advances*, *3*(12), e1701079.

Gao, Y., Kuo, H.-K., Pieraccini, R., Quinn, J., & Wu, C. (2007). *Method and Apparatus for Detecting Data Anomalies in Statistical Natural Language Applications.* Google Patents. (US Patent App. 11/179,789)

GFDRR. (2017). *Global Facility for Disaster Reduction and Recovery Annual Report 2017* (Tech. Rep. No. 2017). Washington D. C.: Global Facility for Disaster Reduction and Recovery. Retrieved from `https://www.gfdrr.org/sites/default/files/publication/GFDRR-Annual-Report-2017.pdf`

Giuliano, G., & Golob, J. (1998). Impacts of the Northridge Earthquake on Transit and Highway Use. *Journal of Transportation and Statistics*, *1*(2).

Grubesic, T. H., Matisziw, T. C., Murray, A. T., & Snediker, D. (2008). Comparative Approaches for Assessing Network Vulnerability. *International Regional Science Review*, *31*(1), 88–112.

Guild, R. L. (2000). Infrastructure Investment and Interregional Development:

Theory, Evidence, and Implications for Planning. *Public Works Management & Policy*, *4*(4), 274–285. Retrieved from http://journals.sagepub.com/doi/10.1177/1087724X0044002

Haimes, Y., & Jiang, P. (2001). Leontief-Based Model of Risk in Complex Interconnected Infrastructures. *Journal of Infrastructure Systems*, *7*(1), 1–12.

Haimes, Y. Y. (2009). On the Definition of Resilience in Systems. *Risk Analysis*, *29*(4), 498–501. Retrieved from https://onlinelibrary.wiley.com/doi/full/10.1111/j.1539-6924.2009.01216.x

Haimes, Y. Y., Horowitz, B. M., Lambert, J. H., Santos, J., Lian, C., & Crowther, K. (2005). Inoperability Input-Output Model for Interdependent Infrastructure Sectors. I: Theory and Methodology. *Journal of Infrastructure Systems*, *11*(2), 67–79.

Hallegatte, S. (2008). An Adaptive Regional Input-Output Model and its Application to the Assessment of the Economic Cost of Katrina. *Risk Analysis*, *28*(3), 779–799. Retrieved from http://doi.wiley.com/10.1111/j.1539-6924.2008.01046.x

Hallegatte, S., Rentschler, J., & Rozenberg, J. (2019). *Lifelines: The resilient infrastructure opportunity*. Washington D.C.: The World Bank.

Heaslip, K., Louisell, W., Collura, J., & Serulle, N. (2010). A Sketch Level Method for Assessing Transportation Network Resiliency to Natural Disasters and Man-Made Events. In *Proceedings of the 89th Transportation Research Board Annual Meeting*. Washington D. C..

Helbing, D., & Balietti, S. (2013). How to Do Agent-Based Simulations in the Future: From Modeling Social Mechanisms to Emergent Phenomena and Interactive Systems Design. In *Social Self-Organization* (pp. 25–70). Berlin, Germany.

Henderson, J. V. (2010). Cities and Development. *Journal of Regional Science*, *50*(1), 515–540.

Henry, D., & Emmanuel Ramirez-Marquez, J. (2012). Generic Metrics and Quantitative Approaches for System Resilience as a Function of Time. *Reliability Engineering & System Safety*, *99*, 114–122.

Herrera, M., Abraham, E., & Stoianov, I. (2016). A Graph-Theoretic Framework for Assessing the Resilience of Sectorised Water Distribution Networks. *Water Resources Management*, *30*(5), 1685–1699.

Hiles, A. (2010). *The Definitive Handbook of Business Continuity Management*. Wiley.

Holden, R., Val, D. V., Burkhard, R., & Nodwell, S. (2013). A Network Flow

Model for Interdependent Infrastructures at the Local Scale. *Safety Science*, *53*, 51–60.

Holling, C. S. (1973). Resilience and Stability of Ecological Systems. *Annual Review of Ecology and Systematics*, *4*(1), 1–23.

Hosseini, S., Barker, K., & Ramirez-Marquez, J. E. (2016). A Review of Definitions and Measures of System Resilience. *Reliability Engineering & System Safety*, *145*, 47–61.

Hsi-Mei Hsu, & Chen-Tung Chen. (1996). Aggregation of Fuzzy Opinions Under Group Decision Making. *Fuzzy Sets and Systems*, *79*(3), 279–285.

Hu, F., Yeung, C. H., Yang, S., Wang, W., & Zeng, A. (2016). Recovery of Infrastructure Networks After Localised Attacks. *Scientific Reports*, *6*, 24522.

Huang, G., & London, J. K. (2012). Cumulative Environmental Vulnerability and Environmental Justice in California's San Joaquin Valley. *International Journal of Environmental Research and Public Health*, *9*(5), 1593–1608.

Hyndman, R. J., & Athanasopoulos, G. (2018). *Forecasting: Principles and practice*. Melbourne, Australia: OTexts. Retrieved from `https://otexts.com/fpp2/` (Accessed October 2, 2019)

Ibrahim, M. W. (2018). Level of Resilience Measure for Communication Networks. *Journal of Infromation and Communication Technology*, *17*(1), 115–139.

Ilbeigi, M., & Dilkina, B. (2018). Statistical Approach to Quantifying the Destructive Impact of Natural Disasters on Petroleum Infrastructures. *Journal of Management in Engineering*, *34*(1).

Jarvinen, B. R., & Caso, E. L. (1984). *A Tropical Cyclone Data Tape for the North Atlantic Basin, 1886–1983: Contents, Limitations, and Uses* (Technical Memorandum No. NWS NHC 22). Miami, Florida: National Hurricane Center.

Jenkins, K. (2013). Indirect Economic Losses of Drought Under Future Projections of Climate Change: A Case Study for Spain. *Natural Hazards*, *69*(3), 1967–1986.

Jeong, G., Wicaksono, A., & Kang, D. (2017). Revisiting the Resilience Index for Water Distribution Networks. *Journal of Water Resources Planning and Management*, *143*(8), 04017035.

Jiang, F., Yuan, J., Tsaftaris, S. A., & Katsaggelos, A. K. (2011). Anomalous Video Event Detection Using Spatiotemporal Context. *Computer Vision and Image Understanding*, *115*(3), 323–333.

Jiann-Shiou Yang. (2005). Travel Time Prediction Using the GPS Test Vehicle and Kalman Filtering Techniques. In *Proceedings of the 2005, American Control*

Conference (p. 2128-2133 vol. 3).

John, A., Yang, Z., Riahi, R., & Wang, J. (2016). A Risk Assessment Approach to Improve the Resilience of a Seaport System Using Bayesian Networks. *Ocean Engineering*, *111*, 136–147.

Jung, B.-m. (2011). Economic Contribution of Ports to the Local Economies in Korea. *The Asian Journal of Shipping and Logistics*, *27*(1), 1–30.

Jung, J., Santos, J. R., & Haimes, Y. Y. (2009). International Trade Inoperability Input-Output Model (IT-IIM): Theory and Application. *Risk analysis : an official publication of the Society for Risk Analysis*, *29*(1), 137–54.

Koks, E. E., & Thissen, M. (2016). A Multiregional Impact Assessment Model for disaster analysis. *Economic Systems Research*, *28*(4), 429–449.

Kumar, V. (2005). Parallel and Distributed Computing for Cybersecurity. *IEEE Distributed Systems Online*, *6*(10), 1.

Kumari, A., & Sharma, A. (2017). Physical & Social Infrastructure in India and Its Relationship with Economic Development. *World Development Perspectives*, *5*, 30 - 33.

Kunreuther, H., Michel-Kerjan, E., & Tonn, G. (2016). *Insurance, Economic Incentives and other Policy Tools for Strengthening Critical Infrastructure Resilience: 20 Proposals for Action* (Tech. Rep.). Philadelphia, United States. Retrieved from `http://opim.wharton.upenn.edu/risk/library/WhartonRiskCenterReport.CIRI.Year1.Dec2016.pdf`

Kwasinski, A. (2015). Numerical Evaluation of Communication Networks Resilience with a Focus on Power Supply Performance During Natural Disasters. In *2015 IEEE International Telecommunications Energy Conference (INTELEC)* (pp. 1–6). IEEE.

Lam, J. S. L., & Lassa, J. A. (2017). Risk Assessment Framework for Exposure of Cargo and Ports to Natural Hazards and Climate Extremes. *Maritime Policy and Management*, *44*(1), 1–15.

Lam, J. S. L., & Su, S. (2015). Disruption Risks and Mitigation Strategies: An Analysis of Asian Ports. *Maritime Policy and Management*, *42*(5), 415–435.

Lam, W. (2002). Ensuring Business Continuity. *IT Professional*, *4*(3), 19-25.

Lazo, L., Powers, M., & Hasley III, A. (2017). *Transportation Remains at a Standstill Following Hurricane Harvey.* (Newspaper Article, `https://www.washingtonpost.com/news/dr-gridlock/wp/2017/08/28/houston-airports-struggle-to-return-to-service-following-hurricane-harvey/?utm_term=.2775812678c1`, Accessed July 28,

2019)

Legal Information Institute. (2015). *33 CFR § 165.781 - Safety Zone; Hurricanes and Other Disasters in Western Florida.* (Web page, URL `https://www.law.cornell.edu/cfr/text/33/165.781`, Accessed October 30, 2019)

Leontief, W. (1986). Input-Output Economics. *Scientific American*, *185*, 15–21.

Lewis, B. M., Erera, A. L., Nowak, M. A., & White, C. C. (2013). Managing Inventory in Global Supply Chains Facing Port-of-Entry Disruption Risks. *Transportation Science*, *47*(2), 162–180.

Lewis, B. M., Erera, A. L., & White, C. C. (2006). Impact of Temporary Seaport Closures on Freight Supply Chain Costs. *Transportation Research Record: Journal of the Transportation Research Board*, *1963*(1), 64–70.

Linnenluecke, M. K., Griffiths, A., & Winn, M. (2012). Extreme Weather Events and the Critical Importance of Anticipatory Adaptation and Organizational Resilience in Responding to Impacts. *Business Strategy and the Environment*, *21*(1), 17–32.

Liu, B., & Liu, Y.-K. (2002). Expected Value of Fuzzy Variable and Fuzzy Expected Value Models. *IEEE Transactions on Fuzzy Systems*, *10*(4), 445–450.

Lodwick, W. A. (2012). An Overview of Flexibility and Generalized Uncertainty in Optimization. *Computational & Applied Mathematics*, *31*(3), 569–589.

Loh, H. S., & Thai, V. V. (2015). Cost Consequences of a Port-Related Supply Chain Disruption. *Asian Journal of Shipping and Logistics*, *31*(3), 319–340.

Loh, H. S., & Van Thai, V. (2014). Managing Port-related Supply Chain Disruptions: A Conceptual Paper. *Asian Journal of Shipping and Logistics*, *30*(1), 97–116.

Luiijf, E., Nieuwenhuijs, A., Klaver, M., van Eeten, M., & Cruz, E. (2009). Empirical Findings on Critical Infrastructure Dependencies in Europe. In *Critical Information Infrastructure Security* (pp. 302–310). Springer, Berlin, Heidelberg.

Lun, Y., Lai, K.-H., & Cheng, T. (2010). Agile Port. In *Shipping and Logistics Management* (pp. 205–218). Springer London.

Malalgoda, C., Amaratunga, D., & Haigh, R. (2013). Creating a Disaster Resilient Built Environment in Urban Cities. *International Journal of Disaster Resilience in the Built Environment*, *4*(1), 72–94.

Martin Associates. (2019). *2018 National Economic Impact of the U.S. Coastal Port System* (Executive Summary). Lancaster, Pennsylvania: American Association of Port Authorities. (URL `http://aapa.files.cms-plus.com/`

Martin%20study_executive%20summary%202018%20US%20coastal%20port%20impacts%20final.docx, Accessed October 22, 2019)

McDaniels, T., Chang, S., Cole, D., Mikawoz, J., & Longstaff, H. (2008). Fostering Resilience to Extreme Events within Infrastructure Systems: Characterizing Decision Contexts for Mitigation and Adaptation. *Global Environmental Change*, *18*(2), 310 - 318.

McDowell, A. (2003). From the Help Desk: Hurdle Models. *The Stata Journal: Promoting Communications on Statistics and Stata*, *3*(2), 178–184.

Mendonça, D., & Wallace, W. A. (2006). Impacts of the 2001 World Trade Center Attack on New York City Critical Infrastructures. *Journal of Infrastructure Systems*, *12*(4), 260–270.

Minkel, J. (2008). The 2003 Northeast Blackout–Five Years Later. *Scientific American*, *13*. Retrieved from http://www.uvm.edu/~phines/media/sciam-blackout.pdf

Mostafavi, A. (2018). A System-of-systems Framework for Exploratory Analysis of Climate Change Impacts on Civil Infrastructure Resilience. *Sustainable and Resilient Infrastructure*, *3*(4), 175–192.

Mudigonda, S., Ozbay, K., & Bartin, B. (2018). Evaluating the Resilience and Recovery of Public Transit System Using Big Data: Case Study from New Jersey. *Journal of Transportation Safety & Security*, *11*(5), 491–519.

Murray-Tuite, P. M., & Fei, X. (2010). A Methodology for Assessing Transportation Network Terrorism Risk with Attacker and Defender Interactions. *Computer-Aided Civil and Infrastructure Engineering*, *25*(6), 396-410.

Nakamura, J., Lall, U., Kushnir, Y., & Rajagopalan, B. (2015). HITS: Hurricane Intensity and Track Simulator with North Atlantic Ocean Applications for Risk Assessment. *Journal of Applied Meteorology and Climatology*, *54*(7), 1620-1636.

Nan, C., & Sansavini, G. (2017). A Quantitative Method for Assessing Resilience of Interdependent Infrastructures. *Reliability Engineering & System Safety*, *157*, 35–53.

National Grid. (2014). *Electricity Ten Year Statement 2014: UK Electrictiy Transmission* (Tech. Rep.). London, UK: National Grid. Retrieved from https://www.nationalgrid.com/sites/default/files/documents/37790-ETYS2014.pdf

National Hurricane Center. (2019). *NHC Data Archive*. National Oceanic and Atmospheric Administration. (Web page, URL https://www.nhc.noaa.gov/data/, Accessed October 10, 2019)

National Infrastructure Advisory Council. (2010). *A Framework for Establishing Critical Infrastructure Resilience Goals: Final Report and Recommendations by the Council* (Tech. Rep.). Washington D.C.. Retrieved from https://www.dhs.gov/xlibrary/assets/niac/niac-a-framework-for-establishing-critical-infrastructure-resilience-goals-2010-10-19.pdf

National Research Council. (1999). *The Impacts of Natural Disasters*. Washington D. C.: National Academies Press.

Ng, A. K., Chen, S. L., Cahoon, S., Brooks, B., & Yang, Z. (2013). Climate Change and the Adaptation Strategies of Ports: The Australian Experiences. *Research in Transportation Business and Management*, *8*, 186–194.

Nicola, M., Alsafi, Z., Sohrabi, C., Kerwan, A., Al-Jabir, A., Iosifidis, C., ... Agha, R. (2020). *The Socio-economic Implications of the Coronavirus Pandemic (COVID-19): A Review* (Vol. 78). Elsevier Ltd.

Nilsson, F., & Darley, V. (2006). On Complex Adaptive Systems and Agent-based Modelling for Improving Decision-making in Manufacturing and Logistics Settings. *International Journal of Operations & Production Management*, *26*(12), 1351–1373.

Nze, I. C., & Onyemechi, C. (2018). Port Congestion Determinants and Impacts on Logistics and Supply Chain Network of Five African Ports. *Journal of Sustainable Development of Transport and Logistics*, *3*(1), 70–82.

Office of Cybersecurity Energy Security and Emergency Response. (2019). *Emergency Situation Reports.* U. S. Department of Energy. (Web page, URL https://www.energy.gov/ceser/activities/energy-security/monitoring-reporting-analysis/emergency-situation-reports, Accessed October 2, 2019)

Ogun, T. P. (2010, 01). Infrastructure and poverty reduction: Implications for urban development in nigeria. *Urban Forum*, *21*(3), 249–266.

Okuyama, Y. (2004). Modeling Spatial Economic Impacts of an Earthquake: Input-Output Approaches. *Disaster Prevention and Management: An International Journal*, *13*(4), 297–306.

Okuyama, Y. (2009). *Critical Review of Methodologies on Disaster Impact Estimation.* World Bank – UN Assessment on the Economics of Disaster Risk Reduction. Retrieved from http://onlineasdma.assam.gov.in/kmp/pdf/1491474441Okuyama{_}Critical{_}Review.pdf

Oliva, G., Panzieri, S., & Setola, R. (2010). Agent-based Input–Output Interdependency Model. *International Journal of Critical Infrastructure Protection*,

3(2), 76–82. Retrieved from http://www.sciencedirect.com/science/article/pii/S187454821000020X

Oliva, G., Panzieri, S., & Setola, R. (2011). Fuzzy Dynamic Input–Output Inoperability Model. *International Journal of Critical Infrastructure Protection*, *4*(3-4), 165–175. Retrieved from https://www.sciencedirect.com/science/article/pii/S1874548211000461

Oosterhaven, J., & Bouwmeester, M. C. (2016). A New Approach to Modeling the Impact of Disruptive Events. *Journal of Regional Science*, *56*(4), 583–595.

Orabi, W., Senouci, A. B., El-Rayes, K., & Al-Derham, H. (2010). Optimizing Resource Utilization During the Recovery of Civil Infrastructure Systems. *Journal of Management in Engineering*, *26*(4), 237–246.

Organization for Economic Cooperation and Development. (2019). *Input Output Tables 2018 Edition.* (Web page, URL https://stats.oecd.org/Index.aspx?DataSetCode=IOTSI4{_}2018, Accessed October 12, 2019)

O'Rourke, T. D. (2007). Critical Infrastructure, Interdependencies, and Resilience. *The Bridge-Linking Engineering and Society*, *37*(1), 22.

Ouyang, M. (2014). Review on Modeling and Simulation of Interdependent Critical Infrastructure Systems. *Reliability Engineering & System Safety*, *121*, 43–60.

Ouyang, M., & Wang, Z. (2015). Resilience Assessment of Interdependent Infrastructure Systems: With a Focus on Joint Restoration Modeling and Analysis. *Reliability Engineering & System Safety*, *141*, 74–82.

Øyvind, B., Rice, J. B., & Bjørn, E. A. (2011). Failure Modes in the Maritime Transportation System: A Functional Approach to Throughput Vulnerability. *Maritime Policy and Management*, *38*(6), 605–632.

Pandit, A., & Crittenden, J. C. (2016). Index of Network Resilience for Urban Water Distribution Systems. *International Journal of Critical Infrastructures*, *12*(1/2), 120.

Pant, R., Barker, K., & Landers, T. L. (2015). Dynamic Impacts of Commodity Flow Disruptions in Inland Waterway Networks. *Computers and Industrial Engineering*, *89*, 137–149.

Pant, R., Zorn, C., Thacker, S., & Hall, J. W. (2018). Systemic Resilience Metrics for Interdependent Infrastructure Networks. In *Sixth International Symposium on Reliability and Risk Management: Resilience and Sustainability of Urban Systems.* Research Publishing Services.

Panteli, M., & Mancarella, P. (2017). Modeling and Evaluating the Resilience of Critical Electrical Power Infrastructure to Extreme Weather Events. *IEEE Systems Journal*, *11*(3), 1733–1742.

Pasqualini, D., & Witkowski, M. (2005). System Dynamics Approach for Critical Infrastructure and Decision Support. A Model for a Potable Water System. In *American Geophysical Union Fall Meeting Abstracts.*

Patterson, S. A. (2005). *Identification of Critical Locations Across Multiple Infrastructures for Terrorist Actions* (Master's thesis, Massachusetts Institute of Technology). Retrieved from `https://dspace.mit.edu/handle/1721.1/34445`

Pinnaka, S., Yarlagadda, R., & Çetinkaya, E. K. (2015). Modelling robustness of critical infrastructure networks. In *2015 11th international conference on the design of reliable communication networks (drcn)* (p. 95-98). Kansas City.

Pinstrup-Andersen, P., & Shimokawa, S. (2007). Rural Infrastructure and Agricultural Development. In *Rethinking Infrastructure for Development* (pp. 175–203). Washington D. C.: The World Bank.

Powell, D. R., DeLand, S. M., & Samsa, M. E. (2008). Critical Infrastructure Protection Decision Making. In *Wiley Handbook of Science and Technology for Homeland Security* (pp. 1–15). Hoboken, NJ, USA: John Wiley & Sons, Inc.

Praks, P., Kopustinskas, V., & Masera, M. (2017). Monte-Carlo-based Reliability and Vulnerability Assessment of a Natural Gas Transmission System Due to Random Network Component Failures. *Sustainable and Resilient Infrastructure*, *2*(3), 97–107.

Qadrdan, M., Chaudry, M., Wu, J., Jenkins, N., & Ekanayake, J. (2010). Impact of a Large Penetration of Wind Generation on the GB Gas Network. *Energy Policy*, *38*(10), 5684–5695.

Rinaldi, S. M., Peerenboom, J. P., & Kelly, T. K. (2001). Identifying, Understanding, and Analyzing Critical Infrastructure Interdependencies. *IEEE Control Systems*, *21*(6), 11–25.

Ritchie, H., & Rose, M. (2018). *Urbanization.* Retrieved July 5, 2020, from `https://ourworldindata.org/urbanization`

Ritchie, H., & Roser, M. (2014). *Natural Disasters.* Retrieved June 27, 2020, from `https://ourworldindata.org/natural-disasters`

Rohrer, J. P., Jabbar, A., & Sterbenz, J. P. (2009). Path Diversification: A Multipath Resilience Mechanism. In *2009 7th International Workshop on Design of Reliable Communication Networks* (pp. 343–351). IEEE.

Rose, A., & Guha, G.-S. (2004). Computable General Equilibrium Modeling of Electric Utility Lifeline Losses from Earthquakes. In *Modeling Spatial and Economic Impacts of Disasters. Advances in Spatial Science* (pp. 119–141).

Springer, Berlin, Heidelberg.

Rose, A., & Liao, S.-Y. (2005, feb). Modeling Regional Economic Resilience to Disasters: A Computable General Equilibrium Analysis of Water Service Disruptions*. *Journal of Regional Science*, *45*(1), 75–112. Retrieved from http://doi.wiley.com/10.1111/j.0022-4146.2005.00365.x

Rose, A., & Wei, D. (2013). Estimating the Economic Consequences of a Port Shutdown: The Special Role of Resilience. *Economic Systems Research*, *25*(2), 212–232.

Rosenkrantz, D. J., Goel, S., Ravi, S. S., & Gangolly, J. (2005). Structure-Based Resilience Metrics for Service-Oriented Networks. In *EDCC 2005: Dependable Computing - EDCC 5. Lecture Notes in Computer Science* (pp. 345–362). Springer, Berlin, Heidelberg.

Rosner, B. (1983). Percentage Points for a Generalized ESD Many-Outlier Procedure. *Technometrics*, *25*(2), 165–172.

Rosoff, H., & Von Winterfeldt, D. (2007). A Risk and Economic Analysis of Dirty Bomb Attacks on the Ports of Los Angeles and Long Beach. *Risk Analysis*, *27*(3).

Rydzak, F., Magnuszewski, P., Sendzimir, J., & Chlebus, E. (2006). A concept of resilience in production systems. In *Proceedings of the 24th International Conference of the System Dynamics Society* (p. 1-26). Nijmegen : Radboud Universiteit Nijmegen.

Rygel, L., O'sullivan, D., & Yarnal, B. (2006). A method for constructing a social vulnerability index: An application to hurricane storm surges in a developed country. *Mitigation and Adaptation Strategies for Global Change*, *11*(3), 741–764.

Salvadori, G., & De Michele, C. (2004). Frequency Analysis via Copulas: Theoretical Aspects and Applications to Hydrological Events. *Water Resources Research*, *40*(12), 1–17.

Sanchez-Rodrigues, V., Potter, A., & Naim, M. M. (2010). Evaluating the Causes of Uncertainty in Logistics Operations. *International Journal of Logistics Management*, *21*(1), 45–64.

Santella, N., Steinberg, L. J., & Parks, K. (2009). Decision Making for Extreme Events: Modeling Critical Infrastructure Interdependencies to Aid Mitigation and Response Planning. *Review of Policy Research*, *26*(4), 409–422.

Satterthwaite, D., McGranahan, G., & Tacoli, C. (2010). Urbanization and its Implications for Food and Farming. In *Philosophical Transactions of the Royal Society B: Biological Sciences* (Vol. 365, pp. 2809–2820). Royal Society.

Saunders, W. S., & Kilvington, M. (2016). Innovative Land Use Planning for Natural Hazard Risk Reduction: A Consequence-driven Approach from New Zealand. *International Journal of Disaster Risk Reduction*, *18*, 244–255.

Savage, D., Zhang, X., Yu, X., Chou, P., & Wang, Q. (2014). Anomaly Detection in Online Social Networks. *Social Networks*, *39*, 62–70.

Schmidtlein, M. C., Shafer, J. M., Berry, M., & Cutter, S. L. (2011). Modeled earthquake losses and social vulnerability in charleston, south carolina. *Applied Geography*, *31*(1), 269–281.

Setola, R., De Porcellinis, S., & Sforna, M. (2009). Critical Infrastructure Dependency Assessment Using the Input-Output Inoperability Model. *International Journal of Critical Infrastructure Protection*, *2*(9), 170–178.

Shackelford, S. (2015). On Climate Change and Cyber Attacks: Leveraging Polycentric Governance to Mitigate Global Collective Action Problems. *SSRN Electronic Journal*, *18*. Retrieved from `https://heinonline.org/HOL/Page?handle=hein.journals/vanep18{&}id=677{&}div=28{&}collection=journals`

Smith, A. B., & Katz, R. W. (2013). US Billion-dollar Weather and Climate Disasters: Data Sources, Trends, Accuracy and Biases. *Natural Hazards*, *67*(2), 387–410.

Song, L., & van Geenhuizen, M. (2014). Port Infrastructure Investment and Regional Economic Growth in China: Panel Evidence in Port Regions and Provinces. *Transport Policy*, *36*, 173–183.

Song, Y. (2012). Infrastructure and Urban Development: Evidence from Chinese Cities. In G. K. Ingram & K. L. Brandt (Eds.), *Proceedings of the 2012 Land Policy Conference: Infrastructure and Land Policies* (pp. 21–60). Cambridge, Massachusetts: Lincoln Institute of Land Policy. Retrieved from `https://www.lincolninst.edu/sites/default/files/pubfiles/infrastructure-urban-development-chinese-cities{_}0.pdf`

Sudakov, B., & Vu, V. H. (2008). Local Resilience of Graphs. *Random Structures & Algorithms*, *33*(4), 409–433.

Sun, W., Bocchini, P., & Davison, B. D. (2018). Resilience Metrics and Measurement Methods for Transportation Infrastructure: The State of the Art. *Sustainable and Resilient Infrastructure*, 1-32.

Sunil, C., & ManMohan, S. (2004). Managing Risk to Avoid Supply-Chain Breakdown. *MIT Sloan Management Review*, 53–62. Retrieved from `https://sloanreview.mit.edu/article/managing-risk-to-avoid-supplychain-breakdown/`

Svendsen, N. K., & Wolthusen, S. D. (2007). Graph Models of Critical Infrastructure Interdependencies. In *AIMS 2007: Inter-Domain Management* (pp. 208–211). Berlin, Heidelberg: Springer Berlin Heidelberg.

Tatano, H., & Tsuchiya, S. (2008). A Framework for Economic Loss Estimation due to Seismic Transportation Network Disruption: A Spatial Computable General Equilibrium Approach. *Natural Hazards*, *44*(2), 253–265.

Ten, C. W., Hong, J., & Liu, C. C. (2011). Anomaly Detection for Cybersecurity of the Substations. *IEEE Transactions on Smart Grid*, *2*(4), 865–873.

Tesfatsion, L. (2003). Agent-based Computational Economics: Modeling Economies as Complex Adaptive Systems. *Information Sciences*, *149*(4), 262–268.

The Anylogic Company. (2017). *Anylogic®*. Chicago, Illinois. Retrieved from `https://www.anylogic.com` (Computer Software)

The White House. (2013). *Presidential Policy Directive 21: Critical Infrastructure Security and Resilience (PPD-21)* (Tech. Rep.). Washington D. C.: Office of the Press Secretary. Retrieved from `https://obamawhitehouse.archives.gov/the-press-office/2013/02/12/presidential-policy-directive-critical-infrastructure-security-and-resil` (Retrieved July 22, 2018)

The World Bank. (2009). *The Social Dimensions of Climate Change: Equity and Vulnerability in A Warming World* (A. N. Robin Mearns, Ed.). Washington D. C.: The World Bank. Retrieved from `http://hdl.handle.net/10986/2689`

The World Bank. (2015). *Investing in Urban Resilience: Protecting and Promoting in a Changing World* (Tech. Rep. No. 109431). Washington D. C.: World Bank Group. Retrieved from `https://www.gfdrr.org/sites/default/files/publication/UrbanResilienceFlagshipReportFINAL(101216).pdf`

Thekdi, S. A., & Lambert, J. H. (2014). Quantification of Scenarios and Stakeholders Influencing Priorities for Risk Mitigation in Infrastructure Systems. *Journal of Management in Engineering*, *30*(1), 32–40.

Todini, E. (2003). Looped Water Distribution Networks Design Using a Resilience Index Based Heuristic Approach. *Urban Water*, *2*(2), 115–122.

Tran, H. T., Balchanos, M., Domerçant, J. C., & Mavris, D. N. (2017). A framework for the quantitative assessment of performance-based system resilience. *Reliability Engineering & System Safety*, *158*, 73 - 84. (Special Sections : Reliability and Safety Certification of Software-Intensive Systems)

Tu, Y., Yang, C., & Chen, X. (2013). Road Network Topology Vulnerability Analysis and Application. *Proceedings of the Institution of Civil Engineers - Transport*(2), 95–104.

Turnquist, M., & Vugrin, E. (2013). Design for Resilience in Infrastructure Distribution Networks. *Environment Systems & Decisions*, *33*(1), 104–120. Retrieved from https://link.springer.com/article/10.1007/s10669-012-9428-z

Ulusoy, A.-J., Stoianov, I., & Chazerain, A. (2018). Hydraulically Informed Graph Theoretic Measure of Link Criticality for the Resilience Analysis of Water Distribution Networks. *Applied Network Science*, *3*(1), 31.

UNISDR. (2015). *Proposed Updated Terminology on Disaster Risk Reduction: A Technical Review* (Tech. Rep. No. August). Geneva. Retrieved from http://www.unisdr.org/files/45462_backgoundpaperonterminologyaugust20.pdf

U.S. Census Bureau. (2019). *USA Trade Online.* (Web page. URL https://usatrade.census.gov/, Accessed October 12, 2019)

U.S. Coast Guard. (2018). *The Coast Guard Journal of Safety and Security at Sea: Proceedings of the Marine Safety and Security Council* (Fall ed.; S. L. Quigley, D. Forbes, & L. C. Goodwin, Eds.). U.S. Coast Guard.

U.S. Department of Homeland Security. (2013). *Threat and Hazard Identification and Risk Assessment Guide* (Tech. Rep.). Retrieved from https://www.fema.gov/media-library-data/8ca0a9e54dc8b037a55b402b2a269e94/CPG201{_}htirag{_}2nd{_}edition.pdf

Usher, W., & Strachan, N. (2013). An Expert Elicitation of Climate, Energy and Economic Uncertainties. *Energy Policy*, *61*, 811–821.

Vugrin, E. D., Warren, D. E., & Ehlen, M. A. (2011). A Resilience Assessment Framework for Infrastructure and Economic Systems: Quantitative and Qualitative Resilience Analysis of Petrochemical Supply Chains to a Hurricane. *Process Safety Progress*, *30*(3), 280–290. Retrieved from https://aiche.onlinelibrary.wiley.com/doi/full/10.1002/prs.10437

Wang, J., Lin, Y., Glendinning, A., & Xu, Y. (2018). Land-use Changes and Land Policies Evolution in China's Urbanization Processes. *Land Use Policy*, *75*, 375–387.

Warner, M., & Gordon, W. (2009). Principles of Volcanic Risk Metrics: Theory and The Case Study of Mount Vesuvius and Campi Flegrei, Italy. *Journal of Geophysical Research: Solid Earth*, *114*(B3).

Wei, D., Chen, Z., Rose, A., Banks, J., & Miller, N. (2017). *Development and Application of an Economic Framework to Evaluate Resilience in Recovering from Major Port Disruptions* (Tech. Rep.). Sacremento, CA: California Department of Transportation. Retrieved from http://create.usc.edu/sites/default/files/metrans_port_disruption_final_report_revised_2_3_17b.pdf

Wendler-Bosco, V., & Nicholson, C. (2019). Port Disruption Impact on the Maritime Supply Chain: A Literature Review. *Sustainable and Resilient Infrastructure*, 1–17.

White, R., George, R., Boult, T., & Chow, C. E. (2016). Apples to Apples: RAMCAP and Emerging Threats to Lifeline Infrastructure. *Homeland Security Affairs*, *12*, 1–20. Retrieved from https://www.hsaj.org/articles/12012

Willis, H. H., Narayanan, A., Fischbach, J. R., Molina-Perez, E., Stelzner, C., Loa, K., & Kendrick, L. (2016). *Current and Future Exposure of Infrastructure in the United States to Natural Hazards*. RAND Corporation. Retrieved from http://www.jstor.org/stable/10.7249/j.ctt1d9np4s

Willoughby, H. E., Darling, R. W. R., & Rahn, M. E. (2006). Parametric Representation of the Primary Hurricane Vortex. Part II: A New Family of Sectionally Continuous Profiles. *Monthly Weather Review*, *134*(4), 1102-1120.

Wu, J., He, X., Li, Y., Shi, P., Ye, T., & Li, N. (2019). How Earthquake-induced Direct Economic Losses Change with Earthquake Magnitude, Asset Value, Residential Building Structural Type and Physical Environment: An Elasticity Perspective. *Journal of Environmental Management*, *231*, 321–328.

Wyss, R., Mühlemeier, S., & Binder, C. (2018). An Indicator-Based Approach for Analysing the Resilience of Transitions for Energy Regions. Part II: Empirical Application to the Case of Weiz-Gleisdorf, Austria. *Energies*, *11*(9), 2263.

Ye, T., Wang, Y., Wu, B., Shi, P., Wang, M., & Hu, X. (2016). Government Investment in Disaster Risk Reduction Based on a Probabilistic Risk Model: A Case Study of Typhoon Disasters in Shenzhen, China. *International Journal of Disaster Risk Science*, *7*(2), 123–137.

Yuen, C. L. A., Zhang, A., & Cheung, W. (2012). Port Competitiveness from the Users' Perspective: An Analysis of Major Container Ports in China and its Neighboring Countries. *Research in Transportation Economics*, *35*(1), 34–40.

Zadeh, L. (1965). Fuzzy Sets. *Information and Control*, *8*(3), 338–353.

Zadeh, L. (1999). Fuzzy Sets as a Basis For a Theory of Possibility. *Fuzzy Sets and Systems*, *100*, 9–34.

Zhang, X., Miller-Hooks, E., & Denny, K. (2015). Assessing the Role of Network Topology in Transportation Network Resilience. *Journal of Transport Geography*, *46*, 35–45.

Zhang, Y., & Lam, J. S. L. (2015). Estimating the Economic Losses of Port Disruption Due to Extreme Wind Events. *Ocean and Coastal Management*, *116*, 300–310.

Zhang, Y., & Lam, J. S. L. (2016). Estimating Economic Losses of Industry Clusters Due to Port Disruptions. *Transportation Research Part A: Policy and Practice*, *91*, 17–33.

Zhao, C., Li, N., & Fang, D. (2018). Criticality Assessment of Urban Interdependent Lifeline Systems Using a Biased PageRank Algorithm and a Multilayer Weighted Directed Network Model. *International Journal of Critical Infrastructure Protection*, *22*, 100–112.

Zhao, K., Kumar, A., Harrison, T. P., & Yen, J. (2011). Analyzing the Resilience of Complex Supply Network Topologies Against Random and Targeted Disruptions. *IEEE Systems Journal*, *5*(1), 28–39.

Zhu, S., Levinson, D., Liu, H. X., & Harder, K. (2010). The Traffic and Behavioral Effects of the I-35W Mississippi River Bridge Collapse. *Transportation Research Part A: Policy and Practice*, *44*(10), 771-784.

Zio, E. (2016). Challenges in the vulnerability and risk analysis of critical infrastructures. *Reliability Engineering and System Safety*, *152*, 137–150.

Zio, E., & Pedroni, N. (2013). *Literature Review of Methods for Representing Uncertainty*. Toulouse, France: Foundation for an Industrial Safety Culture.

Vita

Srijith hails from Palakkad, a small town located near the southern tip of India known for its paddy fields and iconic Palmyra palms. After completing his high school at his hometown in 2006, he moved to Kollam for his undergraduate studies. In 2012, he received his undergraduate degree in Civil Engineering from The University of Kerala. Later, he was admitted to the Indian Institute of Technology Madras (IIT Madras) for pursuing his graduate studies in transportation engineering. At IIT Madras, he was part of the Center of Excellence in Urban Transport, conducting studies in urban mobility. Upon completion of his graduate research in 2015, he moved to Singapore and joined the Sustainable Urban Mobility Research Laboratory at the Singapore University of Science and Technology as a Research Engineer, where he was involved in research projects related to freight transportation and emissions. In 2016, Srijith started his doctoral research at the Resilient Infrastructure and Smart Cities Lab (RISC) of The University of Texas at Austin under the supervision of Prof. Zhanmin Zhang.

Email: srijith@utexas.edu

This dissertation was typeset with LaTeX by the author.